НАУЧНО-ПРАКТИЧЕСКИЙ ЖУРНАЛ

БСМ

ISSN 1682-0363 (print)
ISSN 1819-3684 (online)

БЮЛЛЕТЕНЬ СИБИРСКОЙ МЕДИЦИНЫ

BULLETIN OF SIBERIAN MEDICINE

BSM

Том 22
№ 2. 2023

ЖУРНАЛ «БЮЛЛЕТЕНЬ СИБИРСКОЙ МЕДИЦИНЫ» ПРЕДСТАВЛЕН НА СЛЕДУЮЩИХ РЕСУРСАХ

Scopus	Крупнейшая в мире база данных рефератов и цитирований от компании Elzevier
DOAJ	DOAJ – это уникальный и обширный индекс разнообразных журналов открытого доступа со всего мира
НАУЧНАЯ ЭЛЕКТРОННАЯ БИБЛИОТЕКА eLIBRARY.RU	Национальная библиографическая база данных научного цитирования российских авторов
rnmj.ru	База российских научных медицинских журналов
CYBERLENINKA	КиберЛенинка – это научная электронная библиотека, построенная на парадигме открытой науки (Open Science)
AcademicKeys	AcademicKeys.com предоставляет ресурсы, которые объединяют и информируют академическое сообщество
ROAD	Международный центр ISSN
РОССИЙСКИЙ ИНДЕКС НАУЧНОГО ЦИТИРОВАНИЯ Science Index	Реферативно-библиографическая база данных научных публикаций российских учёных и индекс цитирования научных статей
znanium.com	Электронно-библиотечная система
LENS.ORG	Сервис предоставляет глобальный доступ к знаниям в области открытых инноваций
Mendeley	Платформа, предоставляющая сервисы совместной работы с библиографическими данными, которая была создана для построения социальной сети учёных на основе их публикаций
	Citations Open – независимая некоммерческая инфраструктурная организация, занимающаяся публикацией открытых библиографических данных и данных о цитировании с использованием технологий Semantic Web (связанных данных)

bulletin.ssmu.ru

BULLETIN OF SIBERIAN MEDICINE

Peer-reviewed scientific-practical journal
Issued quarterly

Volume 22, No. 2, 2023

ISSN 1682-0363 (print)
ISSN 1819-3684 (online)

FOUNDER AND PUBLISHER:
Siberian State Medical University, Ministry of Healthcare of the Russian Federation

Registered by the Ministry of Mass Media and Communications of the Russian Federation
Certificate of registration
No. 77-7366 of 26.03.2001

The journal "Bulletin of Siberian Medicine" is included in the list of peer-reviewed scientific journals and publications issued in the Russian Federation, which should publish main scientific results of doctoral and Candidate of Sciences theses

Bulletin of Siberian Medicine is indexed in:
Scopus
Web of Science (WoS (ESCI))
Science Index
RSCI
Ulrich's International Periodicals Directory
Cyberleninka
DOAS

Editorial Board Office:
107, Lenina Av., Tomsk, 634050, Russian Federation
Telephone: +7-(382-2)-51-41-53.
http://bulletin.ssmu.ru
E-mail: bulletin.tomsk@mail.ru

Publisher: Siberian State Medical University.
2, Moscow Trakt, Tomsk, 634050,
Russian Federation.
Editors: E.E. Stepanova, Yu.P. Gotfrid
Translators: M.E. Orlova, K.Yu.Skvortsova
Electronic makeup, cover design
L.D. Krivtsova

Printed in Litburo LLC,
4, Koroleva Str., Tomsk, 634055, Russian Federation

Signed to print on 29.06.2023
Format 60 × 84/8. Offset print.
Coated paper. Times font.
P.s. 23. C.p.s. 22,5.
500 copies. Order No. 315.

The price – free.
Date of publication 30.06.2023.

БЮЛЛЕТЕНЬ СИБИРСКОЙ МЕДИЦИНЫ

Научно-практический журнал
Выходит 4 раза в год

Том 22, № 2, 2023

ISSN 1682-0363 (print)
ISSN 1819-3684 (online)

УЧРЕДИТЕЛЬ И ИЗДАТЕЛЬ:
ФГБОУ ВО «Сибирский государственный медицинский университет» Минздрава России

Журнал основан в 2001 году
Зарегистрирован в Министерстве РФ по делам печати, телерадиовещания и средств массовых коммуникаций
Свидетельство регистрации ПИ № 77-7366 от 26.03.2001 г.

Журнал входит в Перечень ведущих рецензируемых научных журналов и изданий, выпускаемых в РФ, в которых должны быть опубликованы основные научные результаты диссертаций на соискание ученой степени доктора и кандидата наук

Индексация:
Scopus
Web of Science (WoS (ESCI))
РИНЦ (Science Index)
RSCI
Ulrich's International Periodicals Directory
Cyberleninka
DOAS

Редакция:
634050, г. Томск, пр. Ленина, 107.
Тел.: (382-2)-51-41-53.
http://bulletin.ssmu.ru
E-mail: bulletin.tomsk@mail.ru

Оригинал-макет:
Издательство СибГМУ.
634050, г. Томск, Московский тракт, 2.
Редакторы: Е.Е. Степанова, Ю.П. Готфрид
Перевод: М.Е. Орлова, Дж. Палацца
Электронная верстка, дизайн обложки Л.Д. Кривцова

Отпечатано в ООО «Литбюро»,
634055, г. Томск, ул. Королёва, 4.

Подписано в печать 29.06.2023 г.
Формат 60 × 84/8. Печать офсетная.
Бумага мелованная. Гарнитура «Times».
Печ. л. 23. Усл. печ. л. 22,5.
Тираж 500 экз. Заказ 315.

Цена – свободная.
Дата выхода в свет 30.06.2023.

СОДЕРЖАНИЕ

CONTENTS

УДК 615.212/.214:577.175.853
https://doi.org/10.20538/1682-0363-2023-2-6-13

Analgesic effect of a bradykinin antagonist – a 1,4-benzodiazepine-2-one derivative

Aliforenko A.E.[1, 2], Bykov V.V.[1, 2], Bykova A.V.[2], Motov V.S.[2], Stankevich S.A.[2], Pavlovsky V.I.[2, 3], Khazanov V.A.[2], Vengerovskii A.I.[1]

[1] *Siberian State Medical University*
2, Moscow Trakt, Tomsk, 634050, Russian Federation

[2] *Innovative Pharmacology Research LLC (IPHAR LLC)*
79/4, Elizarovykh Str., Tomsk, 634021, Russian Federation

[3] *National Research Tomsk Polytechnic University (TPU)*
30, Lenina Av., Tomsk, 634050, Russian Federation

ABSTRACT

Aim. To study the analgesic effect of a new 1,4-benzodiazepine-2-one derivative (codenamed PAV-0056) in pain models in mice, its anti-inflammatory effect in experimental exudative inflammation in rats, and its potential ulcerogenic effect.

Materials and methods. A 1,4-benzodiazepine-2-one derivative (codenamed PAV-0056) was orally administered in polyvinylpyrrolidone (PVP) solution to 192 CD-1 mice weighing 20–25 g and 140 Sprague – Dawley rats weighing 250–300 g. The analgesic effect of the PAV-0056 compound at a dose of 0.01, 0.1, and 1 mg / kg was studied in murine acute thermal pain models (hot plate test, hot water immersion tail-flick test), acute chemogenic pain models (formalin test), and visceral spasticity-related pain models (acetic acid-induced writhing test). The anti-inflammatory effect of PAV-0056 at doses of 0.01, 0.1, and 1 mg / kg was studied in an experimental rat model of inflammation induced by subplantar administration of bradykinin and histamine. The potential ulcerogenic effect was studied in intact rats, who were injected with PAV-0056 at doses of 1 and 50 mg / kg four times. The analgesic effect of the PAV-0056 compound was compared to that of diclofenac sodium at a dose of 10 mg / kg and tramadol at a dose of 20 mg / kg. Its anti-inflammatory and potential ulcerogenic effects were compared to those of diclofenac sodium at a dose of 10 mg / kg.

Results. In the hot plate test, the PAV-0056 compound at a dose of 0.1 mg / kg increased response latency in mice by 36%, and at a dose of 1 mg / kg, it increased response latency by 46% ($p < 0.05$). In the tail-flick test, the PAV-0056 compound at a dose of 1 mg / kg increased response latency to heat stimulation in mice by 46% ($p < 0.05$). After subplantar administration of formalin, PAV-0056 at doses of 0.01–1 mg / kg had a pronounced analgesic effect, as shown by a decrease in the number of pain responses by 39–55% ($p < 0.05$). When mice were intraperitoneally injected with an acetic acid solution, the PAV-0056 compound at doses of 0.1 and 1 mg / kg reduced the frequency of writhings by 46 and 57%, respectively; at a dose of 0.1 mg / kg, it delayed the onset of the first writhing by 21% ($p < 0.05$). In experiments on rats, the PAV-0056 compound prevented the development of exudative inflammation induced by subplantar administration of bradykinin and did not have an anti-inflammatory effect in histamine-induced inflammation. PAV-0056 did not cause formation of gastric ulcers and gastric mucosal bleeding.

Conclusion. A 1,4-benzodiazepine-2-one derivative, PAV-0056, has a pronounced analgesic effect in models of thermal, chemogenic, somatic, and visceral pain in a wide range of doses (0.01–1 mg / kg). Its analgesic effects are the same as those of diclofenac sodium at a dose of 10 mg / kg and tramadol at a dose of 20 mg / kg. The analgesic effect of the PAV-0056 compound is selective, depends little on suppression of inflammatory exudation, and is caused by bradykinin antagonism. This substance has low toxicity and does not damage the gastric mucosa.

Keywords: 1,4-benzodiazepine-2-one derivative, analgesic, anti-inflammatory, and potential ulcerogenic effects, mice, rats

✉ *Bykov Vladimir V.,* preclin5_dep@iphar.ru

Conflict of interest. The authors declare the absence of obvious and potential conflicts of interest related to the publication of this article.

Source of financing. The study was carried out with the financial support of Organica JSC (Novokuznetsk).

Conformity with the principles of ethics. The study was approved by the local Ethics Committee at IPHAR LLC (Protocol No. 77/2020 of 24.11.2020) and Siberian State Medical University (Protocol No. 8992 of 21.02.2022).

For citation: Aliforenko A.E., Bykov V.V., Bykova A.V., Motov V.S., Stankevich S.A., Pavlovsky V.I., Khazanov V.A., Vengerovskii A.I. Analgesic effect of a bradykinin antagonist – a 1,4-benzodiazepine-2-one derivative. *Bulletin of Siberian Medicine.* 2023;22(2):6–13. https://doi.org/10.20538/1682-0363-2023-2-6-13.

Анальгетическая активность антагониста брадикинина – производного 1,4-бензодиазепин-2-она

Алифоренко А.Е.[1, 2], Быков В.В.[1, 2], Быкова А.В.[2], Мотов В.С.[2], Станкевич С.А.[2], Павловский В.И.[2, 3], Хазанов В.А.[2], Венгеровский А.И.[1]

[1] Сибирский государственный медицинский университет (СибГМУ)
Россия, 634050, г. Томск, Московский тракт, 2

[2] ООО «Инновационные Фармакологические Разработки» (ООО «Ифар»)
Россия, 634021, г. Томск, ул. Елизаровых, 79/4

[3] Национальный исследовательский Томский политехнический университет (НИ ТПУ)
Россия, 634050, г. Томск, пр. Ленина, 30

РЕЗЮМЕ

Цель – изучить анальгетическую активность нового производного 1,4-бензодиазепин-2-она (шифр – PAV-0056) на моделях боли у мышей, противовоспалительное действие при экспериментальном экссудативном воспалении у крыс, а также его потенциальное ульцерогенное действие.

Материалы и методы. Производное 1,4-бензодиазепин-2-она, обозначенное шифром PAV-0056, вводили в растворе поливинилпирролидона в желудок 192 мышам стока CD-1 массой тела 20–25 г и 140 крысам стока Sprague Dawley массой тела 250–300 г. Анальгетическую активность соединения PAV-0056 в дозах 0,01; 0,1 и 1 мг/кг изучали у мышей на моделях острой термической боли (тесты «горячая пластина» и отдергивания хвоста при погружении в горячую воду), острой хемогенной боли (формалиновый тест) и висцеральной спастической боли (тест «уксусные корчи»). Противовоспалительное действие PAV-0056 в дозах 0,01; 0,1 и 1 мг/кг исследовали при экспериментальном воспалении, вызванном у крыс субплантарным введением брадикинина и гистамина. Потенциальное ульцерогенное влияние изучали у интактных крыс, которым вещество PAV-0056 в дозах 1 и 50 мг/кг вводили 4 раза. Анальгетический эффект соединения PAV-0056 сравнивали с действием диклофенака натрия в дозе 10 мг/кг и трамадола в дозе 20 мг/кг, противовоспалительное и возможное ульцерогенное действие – с влиянием диклофенака натрия в дозе 10 мг/кг.

Результаты. В тесте «горячая пластина» соединение PAV-0056 в дозе 0,1 мг/кг увеличивало у мышей время до появления первой болевой реакции на 36%, в дозе 1 мг/кг – на 46% ($p < 0,05$). В тесте отдергивания хвоста при погружении в горячую воду соединение PAV-0056 в дозе 1 мг/кг увеличивало латентное время наступления термической боли у мышей на 46% ($p < 0,05$). При субплантарном введении формалина соединение PAV-0056 в дозах 0,01–1 мг/кг оказывало выраженное анальгетическое действие, что проявлялось уменьшением на 39–55% количества болевых реакций ($p < 0,05$). При внутрибрюшинной инъекции мышам раствора уксусной кислоты соединение PAV-0056 в дозах 0,1 и 1 мг/кг уменьшало количество «корчей» на 46 и 57% соответственно, в дозе 0,1 мг/кг отдвигало наступление первой «корчи» на 21% ($p < 0,05$). В экспериментах на крысах соединение PAV-0056 препятствовало развитию экссудативного воспаления, вызванного субплантарным введением брадикинина, и не оказывало противовоспалительного эффекта при гистаминовом воспалении, не вызывало образования язв и кровоизлияний на слизистой оболочке желудка.

Заключение. Производное 1,4-бензодиазепин-2-она PAV-0056 в широком диапазоне доз (0,01–1 мг/кг) вызывает выраженную анальгезию на моделях термической, хемогенной, соматической и висцеральной боли, по анальгетической активности не уступает эффекту диклофенака натрия в дозе 10 мг/кг и трамадола в дозе 20 мг/кг. Анальгетическое действие соединения PAV-0056 является селективным, мало зависит

от подавления воспалительной экссудации и обусловлено антагонизмом с брадикинином. Это вещество малотоксично и не повреждает слизистую оболочку желудка.

Ключевые слова: производное 1,4-бензодиазепин-2-она, анальгетическое, противовоспалительное и потенциальное ульцерогенное действие, мыши, крысы

Конфликт интересов. Авторы декларируют отсутствие явных и потенциальных конфликтов интересов, связанных с публикацией настоящей статьи.

Источник финансирования. Исследование выполнено при финансовой поддержке АО «Органика» (г. Новокузнецк).

Соответствие принципам этики. Исследование одобрено локальными этическими комитетами ООО «Инновационные Фармакологические Разработки» (протокол № 77/2020 от 24.11.2020) и СибГМУ (протокол № 8992 от 21.02.2022).

Для цитирования: Алифоренко А.Е., Быков В.В., Быкова А.В., Мотов В.С., Станкевич С.А., Павловский В.И., Хазанов В.А., Венгеровский А.И. Анальгетическая активность антагониста брадикинина – производного 1,4-бензодиазепин-2-она. *Бюллетень сибирской медицины.* 2023;22(2):6–13. https://doi.org/10.20538/1682-0363-2023-2-6-13.

INTRODUCTION

Pain is a complex psycho-emotional sensation in response to the effect of nociceptive stimuli, characterized by impaired adaptation and deterioration in patients' quality of life [1]. To alleviate pain, opioid and non-opioid analgesics, as well as non-steroidal anti-inflammatory drugs (NSAIDs) are used. Opioid analgesics eliminate severe pain of any etiology, but depress the respiratory center and generate a risk of physical and psychological dependence and addiction [2]. NSAIDs are most effective for nociceptive pain at the inflammation site; their side effects include ulcerogenic and nephrotoxic effects, cardiovascular diseases, bronchospasm, and bleeding [3].

One of the modern strategies in the search for new analgesics is development of autacoid inhibitors (bradykinin, histamine, serotonin), which prevent their activating effects on the nociceptive system [4–6]. The nonapeptide bradykinin is generated during inflammation, allergies, and infections via cleavage of kininogen by the action of kallikrein and activates metabotropic B receptors [7]. Bradykinin directly irritates sensitive nerve endings and promotes secretion of other algogenic factors, such as substance P, neurokinin A, and calcitonin gene-related peptide. At the inflammation site, bradykinin dilates capillaries, disrupts cell – cell contacts, and increases exudation and migration of neutrophils, lymphocytes, and macrophages [8].

In clinical practice, there are no analgesics with anti-bradykinin action. Bradykinin B receptor is blocked by 1,4-benzodiazepine-2-one derivatives [9–12]; among them, the compound PAV-0056 has the greatest analgesic effect [13].

The aim of this work was to study the analgesic effect of a new 1,4-benzodiazepine-2-one derivative PAV-0056 in experimental models of pain and inflammation, as well as to evaluate its potential ulcerogenic effect.

MATERIALS AND METHODS

The PAV-0056 compound is methyl-2-(7-nitro-2-oxo-5-phenyl-3-propoxy-2,3-dihydro-1*H*-benzo[e][1,4]diazepine-1-yl)acetate (Fig.1). Derivatives of 1,4-benzodiazepine-2-ones were synthesized at IPHAR LLC based on molecular design and study of the relationship between the chemical structure and affinity to benzodiazepine receptors and analgesic effects [14]. Among this group of substances, the PAV-0056 compound has minimal toxicity, and its oral LD50 in mice and rats is over 2,000 mg / kg.

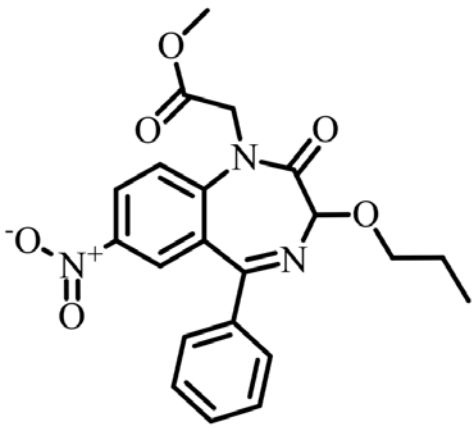

Fig. 1. Structural formula of the PAV-0056 compound

The experiments were carried out at the R&D center of IPHAR LLC in 192 pathogen-free male CD-1 mice weighing 20–25 g and 140 male Sprague – Dawley rats weighing 250–300 g. The animals were obtained from the Department of Laboratory Animals of the R&D center. They were kept in groups of 5–6 individuals each in plastic cages at 20–23 °C, relative humidity of no more than 50%, exhaust – supply ratio of 8 :10, in a 12 : 12 light /dark cycle.

The study was approved by the local Ethics Committees at IPHAR LLC (Protocol No. 77/2020 of 24.11.2020) and Siberian State Medical University (Protocol No. 8992 of 21.02.2022). It was conducted in accordance with the provisions of the European Convention for the Protection of Vertebrate Animals used for Experimental and Other Scientific Purposes (Strasbourg, 1986) and the principles and rules of Good Laboratory Practice (Decision of the Council of Eurasian Economic Commission No. 81 of 03.11.2016 and the National Standard of the Russian Federation (GOST) 33044-2014).

The PAV-0056 compound at doses of 0.01, 0.1, and 1 mg / kg or the reference listed drugs diclofenac sodium (Hemofarm, Serbia) at a dose of 10 mg / kg [15] and tramadol (Pharmaceuticals Formenti S.p.A., Italy) at a dose of 20 mg / kg [16] were orally administered to mice to assess the analgesic effect. All substances were dissolved in 0.5 ml of 1% aqueous solution of polyvinylpyrrolidone (PVP) (Plasdone S-630, Ashland Inc., USA). Control animals received the vehicle in an equivalent volume. Doses of the PAV-0056 compound were selected based on previous pilot studies. Analgesic effects were evaluated 60 min after the administration of the PAV-0056 compound, diclofenac sodium or tramadol, and compared with those in control animals. Each experimental group contained 6–10 animals.

Hot plate test. Mice (6 groups, n = 6 animals per group) were placed on a metal surface heated to a temperature of 55 ± 1 °C (thermal table HWT-75, Russia). We determined response latency, measured by paw withdrawal and licking. The mice were kept on the hot plate for no more than 1 min to avoid injury [4, 17].

Tail-flick test. The tails of mice (6 groups, n = 10 animals per group) were half immersed in water at a temperature of 45 ± 1 °C (Sakura 1450 water bath, Japan). We measured the time before the tail flicked to the side [4, 17].

Formalin test. Mice (6 groups, n = 10 animals per group) were injected with 0.02 ml of 0.5% formalin (Sigma-Aldrich, USA) into the plantar aponeurosis of the hind limb. A pain response was registered by the number of licks and shakes of the injured paw during 60 min. In the first 15 min (phase I), acute phase pain developed due to sensitization of peripheral structures of the nociceptive system, in the next 45 min (phase II), tonic pain developed, which was caused by activation of central mechanisms of the nociceptive system [17, 18].

Acetic acid-induced writhing test. Mice (6 groups, n = 6 animals per group) were intraperitoneally injected with 0.75% aqueous acetic acid solution (Sigma-Aldrich, USA) in a volume of 0.1 ml per 10 g of body weight. We assessed the number of abdominal muscle contractions (writhings) and time to the onset of the first writhing within 20 min [17, 18].

The anti-inflammatory effect of the PAV-0056 compound was studied in models of acute exudative inflammation. Rats (10 groups, n = 10 animals per group) were injected with 0.1 ml of 0.1% aqueous bradykinin solution (Sigma-Aldrich, USA) or 2% aqueous histamine solution (Sigma-Aldrich, USA) into the aponeurosis of the hind limb. The other hind limb of these animals was injected with 0.1 ml of sodium chloride (control). The PAV-0056 compound at doses of 0.01, 0.1, and 1 mg / kg or diclofenac sodium at a dose of 10 mg / kg [19] was injected 1 h before the injection of bradykinin or histamine. The limb volume was measured using a plethysmometer (UGO BASIL, Italy) 30 min after the injection of inflammatory mediators. The degree of edema reduction in the inflamed limb was expressed as a percentage of the control [4].

To study the potential ulcerogenic effect, intact rats (4 groups, n = 10 animals per group) were orally administered the PAV-0056 compound at doses of 1 and 50 mg / kg or diclofenac sodium at a dose of 10 mg / kg four times (with an interval of 24 h). The animals were withdrawn from the experiment in a CO_2 atmosphere 3 h after the last administration. The gastric mucosa was studied for erosions, ulcers, and hemorrhages using a stereoscopic microscope (Observational Instruments, Russia) at 10× magnification. We assessed the degree of damage according to a four-point scale: 0 – no damage; 0.5 – mucosal hyperemia; 1 – 1 or 2 punctate hemorrhages on the mucous membrane; 2 – single erosion and punctate hemorrhages on the mucous membrane; 3 – multiple erosions and hemorrhages on the mucous membrane; 4 – massive hemorrhages and ulcers throughout the mucous membrane [4].

The results were statistically processed using the Statistica v. 8.0 (StatSoft, USA) software package. The normality of trait distribution was assessed using the Shapiro – Wilk test. The data were presented as $M \pm m$, where M is the mean and m is the standard error of the mean. The differences between the groups were identified by the Student's t-test and considered statistically significant at $p < 0.05$.

RESULTS AND DISCUSSION

In the hot plate test, the 1,4-benzodiazepine-2-one derivative PAV-0056 at a dose of 0.1 mg / kg prolonged the response latency by 36 %, at a dose of 1 mg / kg – by 46 % compared to that in mice treated with PVP ($p < 0.05$). PAV-0056 had no analgesic effect at a dose of 0.01 mg / kg. Diclofenac sodium at a dose of 10 mg / kg and tramadol at a dose of 20 mg / kg increased the response latency by 64 and 82%, respectively ($p < 0.05$) (Fig. 2). The analgesic effect of PAV-0056 at a dose of 0.1 and 1 mg / kg was comparable to that of diclofenac sodium at a dose of 10 mg / kg ($p > 0.05$), but was not as great as that of tramadol at a dose of 20 mg / kg ($p < 0.05$).

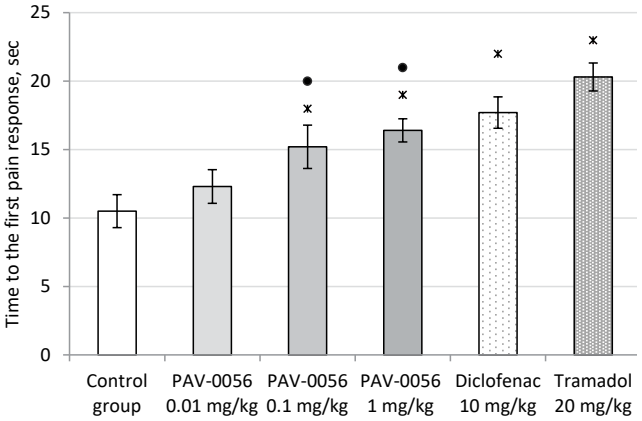

Fig. 2. Response latency in the hot plate test after the administration of PAV-0056, diclofenac sodium, and tramadol to mice: * differences with the control group, $p < 0.05$, • differences with the tramadol group, $p < 0.05$

PAV-0056 at a dose of 1 mg / kg prolonged the tail-flick latency by 46% in mice ($p < 0.05$), although it did not have an analgesic effect at doses of 0.1 and 0.01 mg / kg. Diclofenac sodium at a dose of 10 mg / kg increased the response latency by 46%, and tramadol at a dose of 20 mg / kg increased this parameter by 36%. The analgesic effect of tramadol was weak: the response latency did not differ from that in mice treated with PVP ($p > 0.05$) (Fig. 3).

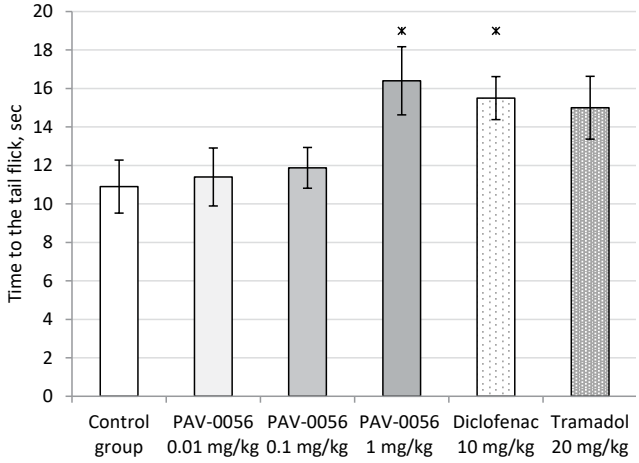

Fig. 3. Response latency in mice in the hot water immersion tail-flick test after the administration of PAV-0056, diclofenac sodium, and tramadol: * differences with the control group, $p < 0.05$

With subplantar formalin injection, PAV-0056 at a dose of 0.01–1 mg / kg reduced the number of pain responses in the acute and tonic pain phases ($p < 0.05$). Diclofenac sodium at a dose of 10 mg / kg and tramadol at a dose of 20 mg / kg also had an analgesic effect in both phases ($p < 0.05$). PAV-0056 at all studied doses had the same analgesic effects as diclofenac sodium and tramadol (Table 1).

PAV-0056 at a dose of 0.1 mg / kg reduced the frequency of writhings caused by the intraperitoneal injection of acetic acid by 46% and at a dose of 1 mg / kg – by 57%. At a dose of 0.1 mg / kg, it delayed the onset of the first writhing by 21% ($p < 0.05$). Diclofenac sodium and tramadol reduced the frequency of writhings by 49 and 68%, respectively and delayed the onset of the first writhing by 49 and 52%, respectively ($p < 0.05$). The analgesic effect of PAV-0056 at a dose of 0.1 and 1 mg / kg was the same as that of diclofenac sodium at a dose of 10 mg / kg; at a dose of 0.1 mg / kg, it was weaker than that of tramadol at a dose of 20 mg / kg (Table 2).

The contribution of the anti-inflammatory effect to the mechanism of the analgesic effect of PAV-0056 at doses of 0.01, 0.1, and 1 mg / kg was studied in rat models of exudative inflammation induced by the subplantar injection of bradykinin or histamine. The reference listed drug was diclofenac sodium at a dose of 10 mg / kg [19]. PAV-0056, administered 1 h before the injection of bradykinin, reduced limb edema by 33–58% ($p < 0.05$) (Table 3). The anti-inflammatory effect of PAV-0056 in histamine-induced edema was not significantly pronounced,

the volume of the limb decreased only by 6–16 % ($p > 0.05$). Diclofenac sodium prevented the development of paw edema by 43–54% in both models of inflammation ($p < 0.05$) (Table 4). The results of this experiment indicate bradykinin antagonism of PAV-0056 and a weak anti-histamine effect.

Table 1

Analgesic effect of PAV-0056, diclofenac sodium, and tramadol after administration to mice in the formalin test, *M* ± *m*

Number of responses	Control group, *n* = 10	PAV-0056 0.01 mg / kg, *n* = 10	PAV-0056 0.1 mg / kg, *n* = 10	PAV-0056 1 mg / kg, *n* = 10	Diclofenac 10 mg / kg, *n* = 10	Tramadol 20 mg / kg, *n* = 10
Phase I	31 ± 3	19 ± 1*	14 ± 1*	16 ± 1*	20 ± 4*	21 ± 3*
Phase II	15 ± 2	6 ± 1*	6 ± 2*	8 ± 3*#	7 ± 2*	9 ± 2*

* $p < 0.05$ compared to the controls (here and in Tables 2–4).
# One outlier was identified by the Smirnov – Grubbs test.

Table 2

Analgesic effect of PAV-0056, diclofenac sodium, and tramadol after administration to mice in the acetic acid-induced writhing test, *M* ± *m*

Parameter	Control group, *n* = 6	PAV-0056 0.01 mg / kg, *n* = 6	PAV-0056 0.1 mg / kg, *n* = 6	PAV-0056 1 mg / kg, *n* = 6	Diclofenac 10 mg / kg, *n* = 6	Tramadol 20 mg / kg, *n* = 6
Time before the first writhing, sec	258 ± 8	336 ± 66	312 ± 10*#	326 ± 59	385 ± 39*	393 ± 47*
Number of writhings	37 ± 1	29 ± 4	20 ± 2*	16 ± 2*	19 ± 4*	12 ± 3*

# $p < 0.05$ compared to the tramadol group.

Table 3

Anti-inflammatory effects of PAV-0056 and diclofenac sodium in the test with the subplantar injection of bradykinin in rats, *M* ± *m*

Parameter	Control group, *n* = 10	PAV-0056 0.01 mg / kg, *n* = 10	PAV-0056 0.1 mg / kg, *n* = 10	PAV-0056 1 mg / kg, *n* = 10	Diclofenac 10 mg / kg, *n* = 10
Volume of limb edema, ml	0.24 ± 0.02	0.16 ± 0.03*	0.08 ± 0.03*	0.10 ± 0.02*	0.11 ± 0.02*

Table 4

Anti-inflammatory effects of PAV-0056 and diclofenac sodium in the test with the subplantar injection of histamine in rats, *M* ± *m*

Parameter	Control group, *n* = 10	PAV-0056 0.01 mg / kg, *n* = 10	PAV-0056 0.1 mg / kg, *n* = 10	PAV-0056 1 mg / kg, *n* = 10	Diclofenac 10 mg / kg, *n* = 10
Volume of limb edema, ml	0.30 ± 0.8	0.32 ± 0.09	0.28 ± 0.11	0.25 ± 0.10	0.17 ± 0.05*

The 1,4-benzodiazepine-2-one derivative PAV-0056 at doses of 1 and 50 mg / kg, administered to the rats orally four times, did not have an ulcerogenic effect: there were no ulcers and hemorrhages in the gastric mucosa. Diclofenac sodium, administered four times at a dose of 10 mg / kg, caused multiple injuries, such as bleeding erosions and ulcers (3.5 points).

Thus, the 1,4-benzodiazepine-2-one derivative PAV-0056 exhibited analgesic effects in a wide dose range (0.01–1 mg / kg) which were the same as those of diclofenac sodium at a dose of 10 mg / kg and tramadol at a dose of 20 mg / kg. In the hot plate test, the PAV-0056 compound exerts a moderate analgesic effect because thermal somatic pain occurs with minimal involvement of inflammatory mediators, and thermoreceptors transmit pain information to the reticular formation in the midbrain and thalamus. In the tail-flick test, high-threshold mechanoreceptors are activated on a large surface of the thermal stimulation area; the pain signal through the polymodal C- and Aδ-fibers is carried mainly to the posterior horns of the spinal cord and then transmitted to the motor neurons of the anterior horns [20]. It can be assumed that the more pronounced analgesic effect of PAV-0056 in the hot plate test is associated with the activation of the antinociceptive system of the brain.

The PAV-0056 compound effectively alleviated chemogenic pain caused by formalin and acetic acid. Irritation of nociceptors at the damage site by bradykinin is of primary importance in the generation

of such pain. With the subplantar injection of formalin into the paw of the mice, PAV-0056 decreased the number of paw shakes more than the number of paw licks. This is due to the blockade of nociceptors and inhibition of the transmission of action potentials along afferent nerve fibers to the posterior horns of the spinal cord with suppression of the somatic reflex. The PAV-0056 compound has a weaker effect on the processing of pain signals in the cerebral cortex, so it interferes less with the formation of a conscious response to pain in the form of paw licking.

The PAV-0056 compound has analgesic and anti-inflammatory effects due to antagonism with bradykinin and is less effective in histamine-induced inflammation. The analgesic and anti-inflammatory effects of diclofenac sodium are caused by antagonism with prostaglandins, histamine and, to a lesser extent, with bradykinin. In a radioligand binding assay with Chinese hamster ovarian cytoreceptors, it was shown that some benzodiazepine derivatives, structurally similar to PAV-0056, block bradykinin B receptors at nanomolar concentrations [10].

An important advantage of the 1,4-benzodiazepine-2-one derivative PAV-0056 is the absence of an ulcerogenic effect. It is known that NSAIDs inhibiting cyclooxygenase-1 inhibit synthesis of gastroprotective prostaglandins and seriously damage the gastric mucosa [21]. In our experiment, diclofenac sodium resulted in the formation of numerous ulcers in the stomach, complicated by bleeding.

CONCLUSION

In the present study, the analgesic effect of a new 1,4-benzodiazepine-2-one derivative PAV-0056 was demonstrated for the first time in experimental models of thermal and chemogenic (somatic, visceral) pain. The PAV-0056 compound has a moderate anti-exudative effect in experimental inflammation induced by bradykinin. It does not damage the gastric mucosa. The analgesic effect of PAV-0056 is not weaker than that of diclofenac sodium and tramadol. The 1,4-benzodiazepine-2-one derivative is evaluated as a promising and safe drug with a selective analgesic effect.

REFERENCES

1. Kumar K.H., Elavarasi P., David C.M. Definition of pain and classification of pain disorders. *JCRI*. 2016;3:87–90. DOI: 10.15713/ ins.jcri.112.
2. Rizzi A., Ruzza C., Bianco S., Trapella C., Calo' G. Antinociceptive action of NOP and opioid receptor agonists in the mouse orofacial formalin test. *Peptides.* 2017;94:71–77. DOI: 10.1016/j.peptides.2017.07.002.
3. Lanas A., Chan F.K.L. Peptic ulcer disease. *Lancet.* 2017;390(10094):613–624. DOI: 10.1016/S0140-6736(16) 32404-7.
4. Mironov A.N. Guidelines on preclinical drug research. M.: Grif and K, 2013:944 (in Russ.).
5. Gonçalves E.C.D., Vieira G., Gonçalves T.R., Simões R.R., Brusco I., Oliveira S.M. et al. Bradykinin receptors play a critical role in the chronic postischaemia pain model. *Cell Mol. Neurobiol*. 2021;41(1):63–78. DOI: 10.1007/s10571-020-00832-3.
6. Litvitsky P.F. Inflammation. *Current Pediatrics.* 2006;5(4):75–81 (in Russ.).
7. Kaplan A.P., Joseph K., Silverberg M. Pathways for bradykinin formation and inflammatory disease. *J. Allergy Clin. Immunol.* 2002;109(2):195–209. DOI: 10.1067/mai.2002.121316.
8. Golias Ch., Charalabopoulos A., Stagikas D., Charalabopoulos K., Batistatou A. The kinin system – bradykinin: biological effects and clinical implications. Multiple role of the kinin system – bradykinin. *Hyppokratia*. 2007;11(3):124–128.
9. Dziadulewicz E.K., Brown M.C., Dunstan A.R., Lee W., Said N.B., Garratt P.J. The design of non-peptide human bradykinin B_2 receptor antagonists employing the benzodiazepine peptidomimetic scaffold. *Bioorg. Med. Chem. Lett.* 1999;9(3):463–468. DOI: 10.1016/s0960-894x(99)00015-3.
10. Wood M.R., Kim J.J., Han W., Dorsey B.D., Homnick C.F., DiPardo R.M. et al. Benzodiazepines as potent and selective bradykinin B1 antagonists. *J. Med. Chem.* 2003;46(10):1803–1806. DOI: 10.1021/jm034020y.
11. Pavlovsky V.I., Tsymbalyuk O.V., Martynyuk V.S., Kabanova T.A., Semenishyna E.A., Khalimova E.I. et al. Analgesic effects of 3-substituted derivatives of 1,4-benzodiazepines and their possible mechanisms. *Neurophysiology*. 2013;45:427–432. DOI: 10.1007/s11062-013-9389-y.
12. Pavlovsky V.I., Ushakov I.Yu., Kabanova T.A., Khalimova E.I., Kravtsov V.Kh, Andronati S.A. Synthesis and analgesic activity of 3-arylamino-1,2-dihydro-3н-1,4-benzodiazepin-2-ones. *Chemical and Pharmaceutical Journal*. 2015;49(9):22–27 (in Russ.). DOI: 10.30906/0023-1134-2015-49-9-22-27.
13. Pavlovsky V.I., Khazanov V.A., Stankevich S.A., inventors; Limited liability company "Innovative Pharmaceutical Developments" (IPHAR LLC), assignee. Derivatives of 1,4-benzodiazepin-2-one and their application. Russian Federation patent RU 2701557 C2. September 30, 2019. Russian Federation (in Russ.).
14. Virych P.A., Shelyuk O.V., Kabanova T.A., Khalimova E.I., Martynyuk V.S., Pavlovsky V.I. et al. Effect of 3-substituted 1,4-benzodiazepin-2-ones on bradykinin-induced smooth muscle contraction. *Ukr. Biochem. J.* 2017;89(1):31–37. DOI: 10.15407/ubj89.01.031.
15. Hasani A., Soljakova M., Jakupi M., Ustalar-Ozgen S. Preemptive analgesic effects of midazolam and diclofenac in rat model. *Bosn. J. Basic Med. Sci*. 2011;11(2):113–118. DOI: 10.17305/bjbms.2011.2593.
16. Bandapati S., Podila K.S., Yadala V.R. Comparative study of antinociceptive effect of venlafaxine with tramadol by tail-flick test in animal model of mice. *Natl. J. Physiol. Pharm. Pharmacol*. 2021;11(6):633–637. DOI: 10.5455/njppp.2021.11.11307202001022021.

17. Gregory N.S., Harris A.L., Robinson C.R., Dougherty P.M., Fuchs P.N., Sluka K.A. An overview of animal models of pain: disease models and outcome measures. *J. Pain*. 2013;14(11):1255–1269. DOI: 10.1016/j.jpain.2013.06.008.
18. Chayka A.V., Cheretaev I.V., Khusainov D.R. Methods of experimental preclinical testing of the analgesic effect of various factors in laboratory rats and mice. *Scientific Notes of V.I. Vernadsky Crimean Federal University*. 2015;1(67):161–173 (in Russ.).
19. Santos L.H., Feres C.A., Melo F.H., Coelho M.M., Nothenberg M.S., Oga S. et al. Anti-inflammatory, antinociceptive and ulcerogenic activity of a zinc-diclofenac complex in rats. *Braz. J. Med. Biol. Res.* 2004;37(8):1205–1213. DOI: 10.1590/S0100-879X2004000800011.
20. Bondarenko D.A., D›yachenko I.A., Skobtsov D.I., Murashev A.N. *In vivo* models for the study of analgesic activity. *Biomedicine*. 2011;2:84–94 (in Russ.).
21. Takeuchi K. Pathogenesis of NSAID-induced gastric damage: importance of cyclooxygenase inhibition and gastric hypermotility. *World J. Gastroenterol.* 2012;18(18):2147–2160. DOI: 10.3748/wjg.v18.i18.2147.

Authors' contribution

Aliforenko A.E., Bykov V.V., Bykova A.V., Motov V.S. – conception and design, carrying out of the experiment, analysis and interpretation of the data. Pavlovsky V.I. – chemical synthesis of the PAV-0056 compound. Khazanov V.A., Stankevich S.A. – justification of the manuscript, critical revision of the manuscript for important intellectual content. Vengerovskii A.I. – final approval of the manuscript for publication.

Authors' information

Aliforenko Anastasia E. – Post-Graduate Student, Pharmacology Division, Siberian State Medical University; Junior Researcher, IPHAR LLC, Tomsk, clin_dep2@iphar.ru, http://orcid.org/0000-0003-1656-8429

Bykov Vladimir V. – Cand. Sci. (Med.), Senior Lecturer, Pharmacology Division, Siberian State Medical University; Head of the Department of Pharmacological Research, IPHAR LLC, Tomsk, preclin5_dep@iphar.ru, http://orcid.org/0000-0002-5145-2184

Bykova Arina V. – Cand. Sci. (Biology), Senior Researcher, IPHAR LLC, Tomsk, preclin7_dep@iphar.ru, http://orcid.org/0000-0002-8495-8560

Motov Valery S. – Researcher, IPHAR LLC, Tomsk, preclin13_dep@iphar.ru, http://orcid.org/0000-0002-0197-7521

Stankevich Sergey A. – Cand. Sci. (Med.), Scientific Head of Preclinical Research, IPHAR LLC, Tomsk, project_dep@iphar.ru, http://orcid.org/0000-0003-1313-4967

Pavlovsky Victor I. — Dr. Sci. (Chemistry), Professor, Kizhner Research Center, Tomsk Polytechnic University; Leading Researcher, IPHAR LLC, Tomsk, med_chem@iphar.ru, http://orcid.org/0000-0002-4583-6245

Khazanov Veniamin A. – Dr. Sci. (Med.), Professor, Director General, IPHAR LLC, Tomsk, gen_dir@iphar.ru, http://orcid.org/0000-0002-8833-785X

Vengerovskii Alexander I. – Dr. Sci. (Med.), Professor, Pharmacology Division, Siberian State Medical University, Tomsk, pharm-sibgmu@rambler.ru, http://orcid.org/0000-0001-5094-3742

(✉) **Bykov Vladimir V.,** preclin5_dep@iphar.ru

Received 11.08.2022;
approved after peer review 05.09.2022;
accepted 08.12.2022

УДК 616.348-008.615:615.331]-092.9
https://doi.org/10.20538/1682-0363-2023-2-14-20

Effects of the $ACTH_{6-9}$-Pro-Gly-Pro peptide on the morphofunctional state of rat colon under conditions of chronic restraint stress

Vorvul A.O.[1], Bobyntsev I.I.[1], Mishina E.S.[1], Medvedeva O.A.[1], Andreeva L.A.[3], Myasoedov N.F.[2]

[1] *Kursk State Medical University (KSMU)*
3, K. Marksa Str., Kursk, 305041, Russian Federation

[2] *Institute of Molecular Genetics (IMG), Kurchatov Institute*
2, Academika Kurchatova Sq., Moscow, 123182, Russian Federation

ABSTRACT

Aim. To study the morphofunctional state of the colonic wall in rats when using the N–terminal analog of the adrenocorticotropic hormone (ACTH) $ACTH_{6-9}$-Pro-Gly-Pro ($ACTH_{6-9}$-PGP) peptide under chronic stress.

Materials and methods. The study was performed on 55 male Wistar rats, which were divided into 5 groups (n = 11): group 1 – control group (administration of saline solution without stress); group 2 – chronic restraint stress (CRS) + administration of saline solution; group 3 – CRS + administration of $ACTH_{6-9}$-PGP at a dose of 5 μg / kg; group 4 – administration of $ACTH_{6-9}$-PGP at a dose of 50 μg / kg; group 5 – administration of $ACTH_{6-9}$-PGP at a dose of 500 μg / kg. A histologic examination of the rat colon was performed. The histologic architecture of the colonic wall, the depth of crypts, and the number of goblet cells were assessed. Furthermore, the number of granulocytes, plasma cells, lymphocytes, macrophages, and mast cells was counted.

Results. The study demonstrated that chronic (14 days) restraint stress resulted in the development of inflammations in the colonic wall of the animals. Intraperitoneal administration of $ACTH_{6-9}$-PGP at doses of 50 and 500 μg / kg daily throughout the entire time of stress exposure prevented the development of stress-induced alterations observed in the control animals. At the same time, anti-inflammatory effects of the peptide in the colonic wall and a decrease in the level of corticosterone in the blood serum were noted.

Conclusion. The results of this work and data from other studies on the effects of N-terminal analogs of ACTH indicate the need for studying the mechanisms of their effect on inflammation and searching for targets of $ACTH_{6-9}$-PGP.

Keywords: $ACTH_{6-9}$-PGP, Wistar rats, chronic restraint stress, colon, inflammation

Conflict of interest. The authors declare the absence of obvious or potential conflicts of interest related to the publication of this article.

Source of financing. The authors state that they received no funding for the study.

Conformity with the principles of ethics. The study was approved by the Ethics Committee at KSMU (Protocol No. 3 of 16.11.2020).

For citation: Vorvul A.O., Bobyntsev I.I., Mishina E.S., Medvedeva O.A., Andreeva L.A., Myasoedov N.F. Effects of the $ACTH_{6-9}$-Pro-Gly-Pro peptide on the morphofunctional state of rat colon under conditions of chronic restraint stress. *Bulletin of Siberian Medicine.* 2023;22(2):14–20. https://doi.org/10.20538/1682-0363-2023-2-14-20.

✉ *Vorvul Anton O.,* vorvul1996@mail.ru

Влияние пептида АКТГ$_{6-9}$-Pro-Gly-Pro на морфофункциональное состояние толстой кишки крыс в условиях хронического иммобилизационного стресса

Ворвуль А.О.[1], Бобынцев И.И.[1], Мишина Е.С.[1], Медведева О.А.[1], Андреева Л.А.[2], Мясоедов Н.Ф.[2]

[1] *Курский государственный медицинский университет (КГМУ)*
Россия, 305041, г. Курск, ул. К. Маркса, 3

[2] *Институт молекулярной генетики (ИМГ), Национальный исследовательский центр (НИЦ) Курчатовский институт*
Россия, 123182, г. Москва, пл. Ак. Курчатова, 2

РЕЗЮМЕ

Цель – изучить морфофункциональное состояние стенки толстой кишки у крыс при применении N-концевого аналога адрекортикотропного гормона (АКТГ) пептида АКТГ$_{6-9}$-Pro-Gly-Pro (АКТГ$_{6-9}$-ПГП) в условиях хронического стресса.

Материалы и методы. Исследование выполнено на 55 самцах крыс линии Вистар, которые были разделены на пять групп (n = 11): 1 – контрольная группа (введение физиологического раствора без стрессирования); 2 – хронический иммобилизационный стресс (ХИС) + введение физиологического раствора; 3 – ХИС + введение АКТГ$_{6-9}$-ПГП в дозе 5 мкг/кг; 4 – 50 мкг/кг; 5 – 500 мкг/кг. Проводили гистологическое исследование толстой кишки крыс. Изучали гистоархитектонику стенки толстой кишки, глубину крипт, число бокаловидных клеток в них. Подсчитывали число гранулоцитов, плазмацитов, лимфоцитов, макрофагов и тучных клеток.

Результаты. Установлено, что хронический (14 сут) иммобилизационный стресс приводит к развитию воспалительных процессов в стенке толстой кишки животных. Внутрибрюшинное введение АКТГ$_{6-9}$-ПГП в дозах 50 и 500 мкг/кг 1 раз/сут на протяжении всего времени стрессорного воздействия препятствовало развитию наблюдавшихся у контрольных животных стресс-индуцированных сдвигов. При этом отмечались противовоспалительные эффекты пептида в стенке толстой кишки и снижение уровня кортикостерона в сыворотке крови.

Заключение. Результаты свидетельствуют о необходимости продолжения изучения механизмов их влияния на процессы воспаления и поиска мишеней АКТГ$_{6-9}$-ПГП.

Ключевые слова: АКТГ$_{6-9}$-ПГП, крысы линии Вистар, хронический иммобилизационный стресс, толстая кишка, воспаление

Конфликт интересов. Авторы декларируют отсутствие явных и потенциальных конфликтов интересов, связанных с публикацией настоящей статьи.

Источник финансирования. Авторы заявляют об отсутствии финансирования при проведении исследования.

Соответствие принципам этики. Исследование одобрено этическим комитетом КГМУ (протокол № 3 от 16.11.2020).

Для цитирования: Ворвуль А.О., Бобынцев И.И., Мишина Е.С., Медведева О.А., Андреева Л.А., Мясоедов Н.Ф. Влияние пептида АКТГ$_{6-9}$-Pro-Gly-Pro на морфофункциональное состояние толстой кишки крыс в условиях хронического иммобилизационного стресса. *Бюллетень сибирской медицины.* 2023;22(2):14–20. https://doi.org/10.20538/1682-0363-2023-2-14-20.

INTRODUCTION

It is known that N-terminal adrenocorticotropic hormone (ACTH) fragments have a wide spectrum of biological effects. Moreover, they are considered as perspective molecules for practical application as pharmacological agents [1, 2]. In particular, Semax created on the basis of the ACTH$_{4-7}$-Pro-Gly-Pro molecule is being used in medicine. Previously a range of its biological effects under conditions of chronic

restraint stress (CRS) was established [3–5] including the ones on the nervous system according to the modern concepts of functional interrelations in the gut – brain axis [6].

$ACTH_{6-9}$-Pro-Gly-Pro is structurally and functionally related to Semax. The His-Phe-Arg-Trp amino acid sequence, corresponding to the to the 6–9th amino acid residue of the ACTH molecule, is an active site of ACTH that interacts with all types of melanocortin receptors (MCR) except for MC2R [7]. Attachment of the Pro-Gly-Pro (PGP) tripeptide to the C-terminus of this molecule increases its sustainability against carboxypeptidases. $ACTH_{6-9}$-PGP has a wide range of neurotropic effects and, at comparable doses, demonstrated more pronounced effects in relation to anxiety-like and depression-like behaviours [8, 9], development and consolidation of conditioned reflexes [10], and pain sensitivity [11] than $ACTH_{4-7}$-PGP.

Previously, we established that $ACTH_{6-9}$-PGP had anxiolytic and antidepressant effects and prevented development of gut dysbiosis under conditions of CRS [12]. However, the studies on the mophofunctional state of the colon in the context of $ACTH_{6-9}$-PGP administration have not been conducted yet. Considering the proinflammatory effect of chronic stress and anti-inflammatory effects of $ACTH_{4-7}$-PGP [5], we carried out the study aimed at investigating the morphofunctional state of the rat colon when administering $ACTH_{6-9}$-PGP under conditions of CRS.

MATERIALS AND METHODS

The study was carried out on male Wistar rats (n = 55) weighing 280–300 g. The animals were obtained from the SPF vivarium at the Institute of Cytology and Genetics of SB RAS. The animals were kept at the temperature of 22 ± 2 °C, humidity of 60 ± 5%, and with the 12-hour light / dark cycle (light on from 8:00 to 20:00). The animals were provided with *ad libitum* access to food and water. The rats were divided into five groups (n = 11 animals per group): group 1 – control group (administration of saline solution without stress); group 2 – CRS + administration of saline solution; group 3 – CRS + administration of $ACTH_{6-9}$-PGP at a dose of 5 μg / kg; group 4 – CRP + administration of $ACTH_{6-9}$-PGP at a dose of 50 μg / kg; group 5 – CRS + administration of $ACTH_{6-9}$-PGP at a dose of 500 μg / kg.

CRS was modelled by placing the animals in tight transparent plastic boxes with ventilation holes. Their sizes were adjusted individually for each animal. The animals were subject to two-hour restraint stress (from 11:00 till 13:00) for 14 consecutive days.

The $ACTH_{6-9}$-PGP used in the study was synthesized at the Institute of Molecular Genetics, Kurchatov Institute. The peptide was dissolved in the saline solution and administered at doses of 5, 50, and 500 μg / kg (1 ml / kg) daily 15 min before restraint stress. The intact and control rats were injected daily with equivalent doses of saline.

Twenty-four hours after the final stress exposure, the rats were euthanized under ether anaesthesia by withdrawing 7.0–7.5 ml of blood from the right ventricle. The blood was centrifuged (1, 500g, 15 min), and the obtained serum was frozen for further research.

For a morphometric and histologic study, we isolated the colon, incised its middle third, and fixed it in the 10% neutral buffered formalin. The autopsy samples were then subject to standard histologic processing to obtain 5–7-μm thick paraffin sections which were stained with hematoxylin and eosin. To assess the morphofunctional changes in goblet and mast cells, the sections were stained with Schiff's reagent and counterstained with alcian blue.

A morphological study of the histologic colon specimens was carried out using the Nikon Eclipse Ci microscope (Nicon, Japan) with a standard digital camera. A morphometric examination was conducted by counting cells in the inflammatory infiltrate. We calculated their relative number and expressed it as a percentage. The cells were counted per 100 cells in 10 fields of view at ×400 magnification, or 502 mcm^2 (for reliable identification of karyocytological signs) on 5 sections of the examined autopsy samples [13].

To assess the intensity of the stress reaction, we quantified serum corticosterone concentration by enzyme-linked immunosorbent assay (ELISA) using the Corticosterone ELISA kit (ADI-900-097, Enzo Life Sciences, USA), the Varioskan Flash spectral scanning multimode reader (Thermo Fisher Scientific, USA), and the SkanIt software (Thermo Fisher Scientific, USA).

A statistical analysis was carried out using R v.4.1.0 in the integrated development environment RStudio Desktop v. 1.4.1717 (RStudio, PBC, USA; https://www.rstudio.com). The obtained data were assessed for normality of distribution using the Shapiro – Wilk test, for equality of variances – using the Levene's test. Quantitative variables were tested using the Wilcoxon – Mann – Whitney U-test for two groups and Kruskal – Wallis test with post-hoc Dunn's test for four groups. To minimize the effect of multiple

comparisons, the Benjamini – Hochberg false discovery rate procedure was applied. The data were presented as the median and the interquartile range Me [Q_1 ; Q_3]. The differences were considered significant at $p < 0.05$.

RESULTS

The histologic examination of the colon specimens obtained from the controls revealed no changes in all the membranes (Fig.1, *a*).

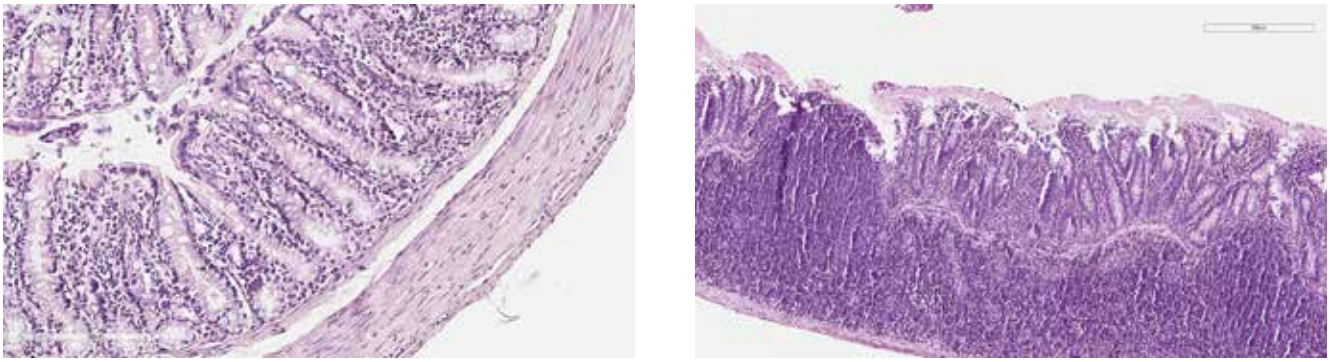

a *b*

Fig. 1. Fragment of the colon from the control group animal, ×100 (*a*), from the CRS group, ×40 (*b*). Here and in Fig. 2 – staining with hematoxylin and eosin

We found that CRS led to pronounced morphological changes in the colonic wall of the rats accompanied by disruptions of the mucosal architecture (Fig.1, *b*). The crypts were club-shaped, their depth decreased by 28.5% ($p = 0.00001$) (Table). The number of goblet cells decreased by 23.6% ($p = 0.0332$). There was a lot of mucus with destroyed cells in the lumen and on the colon surface. We noted focal epithelial desquamation and superficial necrosis of colonocytes. On the part of the mucosa-associated lymphoid tissue, we determined pronounced reactive changes. There were plenty of large lymphoid follicles with enlarged germinal centers compared to similar structures in the control animals. Pronounced diffuse polymorphic cellular infiltrate was visualized in all colonic membranes. Lymphocytes and granulocytes predominated among the cells. Their relative number increased by 6.8 times ($p = 0.00005$) and 1.5 times ($p = 0.00007$), respectively, compared to the controls. There was also a 3.8-fold increase in the number of mast cells in the colonic wall ($p = 0.00008$).

After administration of $ACTH_{6-9}$-PGP at a dose of 5 μg / kg, we noted inflammatory necrotic changes and smoothed epithelial folds with a thin mucosa in the colonic wall (Fig. 2, *a*). The number of goblet cells increased by 22.4% ($p = 0.0134$) against the background of small crypt depth. This demonstrated active mucus production. We noted interstitial edema and moderate plethora of capillaries and small veins. There were plenty of enlarged lymphoid follicles in the field of view throughout the entire thickness of the colonic wall. In some parts of the colon, we detected pronounced focal granulocyte infiltration in the mucosa and submucosa (the number of granulocytes decreased by 29.4% compared to the CRS group, $p = 0.00003$), among which eosinophils predominated.

We established that when $ACTH_{6-9}$-PGP was administered at a dose of 50 μg / kg, the severity of morphological changes in the colon decreased (Fig.2, *b*). Pronounced diffuse polymorphic cellular infiltrate with predominance of granulocytes in the superficial parts of the mucosa was still found. The mucosa and submucosa were swollen. The crypts were smoothed, their height did not differ from that in the CRS group ($p = 0.5337$). We revealed a significant increase in the number of goblet cells by 14.3% ($p = 0.0459$). We also detected prominent dyscirculatory abnormalities, such as a large number of dilated, plethoric vessels in the mucosa and submucosa.

After administration of $ACTH_{6-9}$-PGP at a dose of 500 μg / kg, the degree of severity of changes in the colonic mucosa decreased (Fig.2, *c*). We noted epithelial cell proliferation, a significant increase in the crypt depth (by 30.7%, $p = 0.0036$), and a rise in the number of goblet cells (by 24.8%, $p = 0.0427$). Moreover, the total number of cells in the inflammatory infiltrate decreased compared to the control group: lymphocytes – by 38.9% ($p = 0.00006$), granulocytes – by 35.3%

($p = 0.00008$), plasma cells – by 82.4% ($p = 0.00004$), macrophages – by 23.1% ($p = 0.00005$), and mast cells – by 47.3% ($p = 0.00008$). Mild local fibrosis was found in the lamina propria. No signs of edema or inflammatory cell infiltration were observed in the muscular and serous layers.

Table

Morphometric parameters of the rat colon under CRS and administration of $ACTH_{6-9}$–PGP, *Me* [Q_1; Q_3]

Parameter	Controls, $n = 11$	CRS, $n = 11$	CRS + 5, $n = 11$	CRS + 50, $n = 11$	CRS + 500, $n = 11$
Crypt depth, μm	159.4 [136.9; 182.34]	114.5 [86.2; 122.1]*	114.9 [97.9; 123.4]	116.6 [86.6; 130.5]	149.6 [102.5; 166.4]#
Goblet cells, units per field of view	63.20 [42.3; 68.0]	48.3 [34.4; 54.2]*	59.1 [46.1; 67.3]#	55.2 [45.8; 64.6]#	60.3 [42.6; 66.1]#
Granulocytes, %	11 [10; 12]	17 [15; 23]*	12 [11; 13]#	12 [11; 14]#	11 [11; 13]#
Plasma cells, %	2.5 [2; 3]	17 [15; 18]*	5 [5; 7]#	7 [6; 9]#	3 [3; 4]#
Macrophages, %	3 [3; 5]	13 [13; 15]*	13 [11; 15]	14 [13; 16]	10 [10; 11]#
Лимфоциты, %	15 [13; 17]	36 [34; 39]*	22 [19; 24]#	25 [24; 26]#	22 [19; 24]#
Mast cells, units per field of view	5 [5; 5.5]	19 [17.5; 20]*	15 [14; 15]	12 [11.5; 13]#	10 [10; 11]#
Corticosterone, ng / ml	282.4 [168.9; 299.7]	325.4 [251.9; 375.4]*	263.8 [164.6; 302.6]#	294.4 [261.8; 312.8]#	269.8 [145.8; 314.0]#

* $p < 0.05$ compared to the control group (the Mann – Whitney *U*-test); # $p < 0.05$ compared to the CRS group (the Kruskal – Wallis test with the post-hoc Dunn's test).

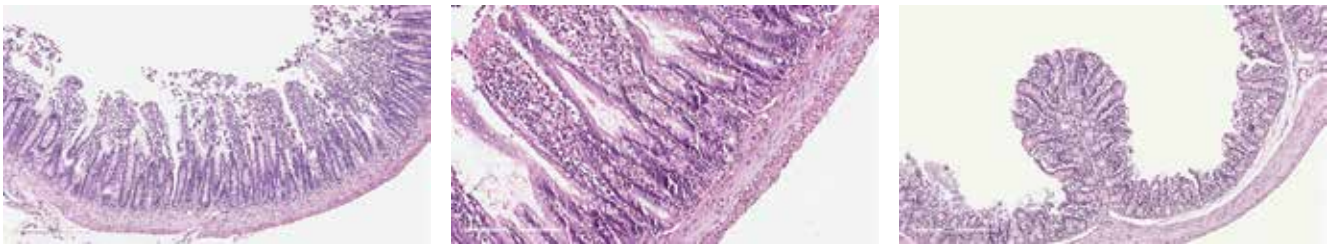

a *b* *c*

Fig. 2. Fragment of the colon from the CRS + 5 group ×100 (*a*); from the CRS + 50 group ×100 (*b*); from the CRS + 500 group, ×40 (*c*)

DISCUSSION

The changes in the structure of the colonic wall established in the current study could be due to increased mucosal permeability and translocation of gut microflora to the underlying membranes. Corticotropin releasing factor (CRF), the production of which is increased under stress, has been previously shown to play a key role in increasing colonic mucosal permeability [14]. This increase under CRF may develop through mast cell-dependent release of tumor necrosis factor alpha and proteases.

Triptases released upon activation of mast cells have been shown to induce tight junction disruption via activation of receptors by epithelial cell protease 2 [14]. In addition, pharmacological inhibition of mast cell activation has been shown to reverse stress-induced increased permeability of the colonic mucosa in various animal models [15, 16]. Furthermore, CRF caused mast cell hyperplasia and increased bacterial adhesion and / or penetration into the gut mucosa of rats, whereas no such changes were observed in mast cell deficient rats [15]. Moreover, under stress, changes in the hemostasis could be observed: both activation and inhibition of its components. In particular, decreases in anticoagulant and fibrinolytic blood activity as well as activation of platelet hemostasis under prolonged stress were established [17]. This could lead to the atrophic changes in the colonic wall.

The anti-inflammatory effects of $ACTH_{6-9}$-PGP in the colonic wall established in the present research could be explained by both central stress-limiting effects of the peptide [8, 9] and its local effect due to the biological polyfunctionality of regulatory peptides [18]. The following mechanisms could underlie the central effects of the peptide. For instance, $ACTH_{6-9}$-PGP can reduce the activity of the hypothalamic – pituitary – adrenal axis by interacting with central MCRs due to its ability to cross the blood – brain barrier [19]. This could be responsible for the decrease in secretion of CRF in the hypothalamus and hence ACTH and glucocorticoids. The decrease in the serum

corticosterone concentration found in this study may be a confirmation of the involvement of the above-described mechanisms in the realization of the anti-inflammatory effect of $ACTH_{6-9}$-PGP. Furthermore, the gut microbiota could affect CRF production in the hypothalamus via mediator production and / or via the vagus nerve [20]. Data on the preventing effect of $ACTH_{6-9}$-PGP on the development of gut dysbiosis [12] suggest another possible pathway for its effects – through its effect on the gut microbiota.

With account of MC1R expression on mast cells [21], it is reasonable to suggest that $ACTH_{6-9}$-PGP may also reduce intestinal permeability due to its local effect via a decrease in mast cell activity. Moreover, $ACTH_{6-9}$-PGP and Pro-Gly-Pro have anticoagulant, fibrinolytic, and anti-platelet activity [22, 23], which may contribute to improved circulation and prevent dystrophic changes in the colonic wall.

CONCLUSION

The study revealed that CRS leads to the development of inflammatory processes in the rat colon. Intraperitoneal administration of $ACTH_{6-9}$-PGP at doses of 50 and 500 μg / kg daily during stress exposure reduced the severity of stress-induced morphological changes in the colon and the serum corticosterone level in the rats. The results of this work and data from other studies on the effects of N-terminal analogs of ACTH indicate the need for studying the mechanisms of their effect on inflammation and searching for targets of $ACTH_{6-9}$-PGP.

REFERENCES

1. Catania A. Neuroprotective actions of melanocortins: a therapeutic opportunity. *Trends Neurosci*. 2008;31(7):353–360. DOI: 10.1016/j.tins.2008.04.002.
2. Yang Y., Hruby V.J., Chen M., Crasto C., Cai M., Harmon C.M. Novel binding motif of ACTH analogues at the melanocortin receptors. *Biochemistry*. 2009;48(41):9775–9784. DOI: 10.1021/bi900634e.
3. Volodina M.A., Sebentsova E.A., Glazova N.Y., Manchenko D.M., Inozemtseva L.S., Dolotov O.V. et al. Correction of long-lasting negative effects of neonatal isolation in white rats using semax. *Acta Naturae*. 2012;4(1):86–92.
4. Svishcheva M.V., Mukhina A.Y., Medvedeva O.A., Shevchenko A.V., Bobyntsev I.I., Kalutskii P.V. et al. Composition of colon microbiota in rats treated with ACTH(4-7)-PGP peptide (semax) under conditions of restraint stress. *Bull. Exp. Biol. Med*. 2020;169(3):357–360. DOI: 10.1007/s10517-020-04886-7.
5. Svishcheva M.V., Mishina Y.S., Medvedeva O.A., Bobyntsev I.I., Mukhina A.Y., Kalutskii P.V. et al. Morphofunctional state of the large intestine in rats under conditions of restraint stress and administration of peptide ACTH(4-7)-PGP (semax). *Bull. Exp. Biol. Med*. 2021;170(3):384–388. DOI: 10.1007/s10517-021-05072-z.
6. Cryan J.F., O'Riordan K.J., Cowan C.S.M., Sandhu K.V., Bastiaanssen T.F.S., Boehme M. et al. The microbiota-gut-brain axis. *Physiol. Rev*. 2019;99(4):1877–2013. DOI: 10.1152/physrev.00018.2018.
7. Levitskaya N.G., Kamenskiy A.A. Melanocortin system. *Advances in Physiology Sciences*. 2009;40(1):44–65 (in Russ.).
8. Dodonova S.A., Bobyntsev I.I., Belykh A.E., Anfilova M.G., Andreeva L.A., Myasoedov N.F. Comparative study of antidepressant activity of N-terminal analogs of adrenocorticotropic hormone in rats. *Kursk Scientific and Practical Bulletin "Human and their health"*. 2019;(4):83–89 (in Russ.). DOI: 10.21626/vestnik/2019-4/10.
9. Levitskaya N.G., Glazova N.Yu., Sebentsova E.A., Manchenko D.M., Andreyeva L.A., Kamenskiy A.A. et al. Nootropic and anxiolytic effects of heptapeptide ACTH6-9Pro-Gly-Pro. *I.M.Sechenov Russian Journal of Physiology*. 2019;105(6):761–770 (in Russ.). DOI: 10.1134/S0869813919060049.
10. Dodonova S.A., Bobyntsev I.I., Belykh A.E., Vorvul' A.O. $ACTH_{6-9}$-PGP improves memory consolidation processes in rats. *Res. Results Pharmacol*. 2021;7(1):27–32. DOI: 10.3897/rrpharmacology.7.62479.
11. Dodonova S.A., Bobyntsev I.I., Belykh A.E., Andreeva L.A., Myasoedov N.F. Changes in the nociceptive response to thermal stimulation in rats following administration of N-terminal analogs of the adrenocorticotropic hormone. *Bulletin of RSMU*. 2021;(6):33–36. DOI: 10.24075/brsmu.2019.085.
12. Vorvul A.O., Bobyntsev I.I., Medvedeva O.A., Mukhina A.Y., Svishcheva M.V., Azarova I.E. et al. ACTH(6-9)-Pro-Gly-Pro ameliorates anxiety-like and depressive-like behaviour and gut mucosal microbiota composition in rats under conditions of chronic restraint stress. *Neuropeptides*. 2022;93:102247. DOI: 10.1016/j.npep.2022.102247.
13. Avtandilov G.G. Problems of pathogenesis and pathoanatomic diagnosis of diseases in terms of morphometry. M.: Meditsina, 1984:285 (in Russ.).
14. Overman E.L., Rivier J.E., Moeser A.J. CRF induces intestinal epithelial barrier injury via the release of mast cell proteases and TNF-α. *PLoS One*. 2012;7(6):e39935. DOI: 10.1371/journal.pone.0039935.
15. Santos J., Yang P.C., Söderholm J.D., Benjamin M., Perdue M.H. Role of mast cells in chronic stress induced colonic epithelial barrier dysfunction in the rat. *Gut*. 2001;48(5):630–636.
16. Santos J., Yates D., Guilarte M., Vicario M., Alonso C., Perdue M.H. Stress neuropeptides evoke epithelial responses via mast cell activation in the rat colon. *Psychoneuroendocrinology*. 2008;33(9):1248–1256. DOI: 10.1016/j.psyneuen.2008.07.002.
17. Spiezia L., Tormene D., Pesavento R., Salmaso L., Simioni P., Prandoni P. Thrombophilia as a predictor of persistent residual vein thrombosis. *Haematologica*. 2008;93(3):479–480. DOI: 10.3324/haematol.12205.
18. Khavinson V.K. Peptide medicines: past, present, future. *Clinical Medicine*. 2020;98(3):165–167 (in Russ.). DOI: 10.30629/0023-2149-2020-98-3-165-177.
19. Shevchenko K.V., Nagaev I.Y., Babakov V.N., Andreeva L.A.,

Shevchenko V.P., Radilov A.S. et al. Proteolysis of His-Phe-Arg-Trp-Pro-Gly-Pro in the blood and brain of rats *in vivo*. *Dokl. Biochem. Biophys*. 2015;464:301–304. DOI: 10.1134/S1607672915050087.
20. Hosoi T., Okuma Y., Nomura Y. Electrical stimulation of afferent vagus nerve induces IL-1beta expression in the brain and activates HPA axis. *Am. J. Physiol. Regul. Integr. Comp. Physiol*. 2000;279(1):R141–R147. DOI: 10.1152/ajpregu.2000.279.1.R141.
21. Adachi S., Nakano T., Vliagoftis H., Metcalfe D.D. Receptor-mediated modulation of murine mast cell function by alpha-melanocyte stimulating hormone. *J. Immunol*. 1999;163(6):3363–3368.
22. Rogozinskaya E.Y., Grigorjeva M.E., Lyapina L.A. Arginine-containing peptides and their effects on normal hemostatic parameters in rats. *Thrombosis, Hemostasis, and Rheology*. 2019;(2):31–36 (in Russ.). DOI: 10.25555/THR.2019.2.0877.
23. Lyapina L.A., Grigor'eva M.E., Andreeva L.A., Myasoedov N.F. Protective antithrombotic effects of proline-containing peptides under the influence of stress on the animal organism. *Biol. Bull. Russ. Acad. Sci.* 2010;37:392–396. DOI: 10.1134/S1062359010040096.

Authors' contribution

Vorvul A.O. – analysis and interpretation of the data. Bobyntsev I.I. – conception and design of the study, critical revision of the manuscript for important intellectual content, final approval of the manuscript for publication. Mishina E.S. – analysis and interpretation of the data, critical revision of the manuscript for important intellectual content. Medvedeva O.A. – conception and design of the study, critical revision of the manuscript for important intellectual content. Andreeva L.A., Myasoedov N.F. – conception and design of the study.

Authors' information

Vorvul Anton O. – Post-Graduate Student, Teaching Assistant, Department of Pathophysiology, Junior Researcher, Research Institute of General Pathology, KSMU, Kursk, vorvul1996@mail.ru, http://orcid.org/0000-0002-1529-6014

Bobyntsev Igor I. – Dr. Sci. (Med.), Professor, Head of the Department of Pathophysiology, Head of the Research Institute of General Pathology, KSMU, Kursk, bobig@mail.ru, http://orcid.org/0000-0001-7745-2599

Mishina Ekaterina S. – Cand. Sci. (Med.), Associate Professor, Department of Histology, Embryology, and Cytology, KSMU, Kursk, katusha100390@list.ru, http://orcid.org/0000-0003-3835-0594

Medvedeva Olga A. – Dr. Sci. (Biology), Professor, Head of the Department of Microbiology, Virology, and Immunology, KSMU, Kursk, olgafrida@rambler.ru, http://orcid.org/0000-0002-2889-155X

Andreeva Lyudmila A. – Cand. Sci. (Chemistry), Head of the Sector for Regulatory Peptides, Department of Chemistry of Physiologically Active Substances, IMG, Moscow, landr@img.ras.ru, http://orcid.org/0000-0002-3927-8590

Myasoedov Nikolai F. – Dr. Sci. (Chemistry), Professor, Academician of the Russian Academy of Sciences, Head of the Department of Chemistry of Physiologically Active Substances, IMG, Moscow, nfm@img.ras.ru, http://orcid.org/0000-0003-1294-102X

(✉) **Vorvul Anton O.,** vorvul1996@mail.ru

Received 11.11.2022;
approved after peer review 05.12.2022;
accepted 08.12.2022

УДК 611.833.4.019
https://doi.org/10.20538/1682-0363-2023-2-21-27

Anatomical variations and coding of the intra-trunk pathways in the thoracodorsal nerve

Gorbunov N.S.[1, 2], Kober K.V.[3], Kasparov E.V.[2], Rostovtsev S.I.[1], Protasyuk E.N.[1]

[1] V.F. Voino-Yasenetsky Krasnoyarsk State Medical University
1, Partizana Zheleznyaka Str., Krasnoyarsk, 660022, Russian Federation

[2] Research Institute of Medical Problems of the North
3i, Partizana Zheleznyaka Str., Krasnoyarsk, 660022, Russian Federation

[3] A.I. Kryzhanovsky Krasnoyarsk Regional Clinical Oncology Center
16, 1st Smolenskaya Str., Krasnoyarsk, 660133, Russian Federation

ABSTRACT

Aim. To study anatomical variations of the intra–trunk pathways in the thoracodorsal nerve bundles and to develop a system for their coding.

Materials and methods. After fixation in a 2% solution of acetic acid using the MBS-10 stereomicroscope, we performed macro- and microscopic intra-trunk dissection of thoracodorsal nerve bundles in 121 specimens obtained from 105 corpses of males and females who died at the age of 40–97 years. Using the obtained findings, we compiled a database in the MS Excel 12.0 software and determined the number of anatomical variations in absolute and relative (% from 121 specimens) units.

Results. The study revealed that the thoracodorsal nerve is a mixed nerve, which consists of 1 motor and 1–3 sensory bundles that variously pass through the spinal nerves, trunks, and the axillary nerve with the formation of 20 intra-trunk pathways. In 77% of cases, sensory bundles arising from the thoracodorsal nerve pass through the posterior bundle, the posterior division, the middle trunk, and the C7 spinal nerve or the inferior trunk and the C8 spinal nerve. In 22% of cases, the thoracodorsal nerve has one or, rarely, two duplicate sensory pathways besides the main one. In 93% of cases, the motor bundle to the thoracodorsal nerve passes through the C7 spinal nerve and the middle trunk, the posterior division, and the posterior bundle. Coding the anatomical variations of the intra-trunk pathways in the direction of sensory bundle «posterior bundle → posterior division → trunk → spinal nerve; motor bundle ← posterior bundle ← posterior division ← trunk ← spinal nerve allows to briefly yet clearly and fully display the morphological diversity of the nerve anatomy.

Conclusion. The identified anatomical variations of the intra-trunk pathways can be useful in the diagnosis of injuries and diseases. They expand indications for the use of spinal nerves, trunks of the brachial plexus, and the thoracodorsal nerve in reconstructive surgery.

Keywords: thoracodorsal nerve, intra-trunk pathways, sensory bundles, motor bundle, mixed bundle, anatomical variations, codes

Conflict of interest. The authors declare the absence of obvious and potential conflicts of interest related to the publication of this article.

Source of financing. The study was supported by the Krasnoyarsk Regional Science Foundation.

Conformity with the principles of ethics. The study was approved by the local Ethics Committee at V.F. Voino-Yasenetsky Krasnoyarsk State Medical University (Protocol No. 91 of 11.09.2018).

For citation: Gorbunov N.S., Kober K.V., Kasparov E.V., Rostovtsev S.I., Protasyuk E.N. Anatomical variations and coding of the intra-trunk pathways in the thoracodorsal nerve. *Bulletin of Siberian Medicine.* 2023;22(2):21–27. https://doi.org/10.20538/1682-0363-2023-2-21-27.

✉ *Gorbunov Nikolay S.,* gorbunov_ns@mail.ru

Вариантная анатомия и коды внутриствольных путей грудоспинного нерва

Горбунов Н.С.[1, 2], Кобер К.В.[3], Каспаров Э.В.[2], Ростовцев С.И.[1], Протасюк Е.Н.[1]

[1] Красноярский государственный медицинский университет (КрасГМУ) им. проф. В.Ф. Войно-Ясенецкого Россия, 660022, г. Красноярск, ул. Партизана Железняка, 1

[2] Научно-исследовательский институт (НИИ) медицинских проблем Севера Россия, 660022, г. Красноярск, ул. Партизана Железняка, 3и

[3] Красноярский краевой клинический онкологический диспансер (КККОД) им. А.И. Крыжановского Россия, 660133, г. Красноярск, ул. 1-я Смоленская, 16

РЕЗЮМЕ

Цель – изучить варианты внутриствольных путей пучков грудоспинного нерва и разработать систему их кодирования.

Материалы и методы. После фиксации в 2%-м растворе уксусной кислоты с помощью стереоскопической лупы МБС-10 выполнено макромикроскопическое внутриствольное препарирование пучков грудоспинного нерва на 121 препарате плечевого сплетения от 105 трупов мужчин и женщин в возрасте 40–97 лет. Из полученных показателей в программе MS Excel 12 сформирована база данных и проведено определение количества встречающихся вариантов строения в абсолютных и относительных (% от 121 препарата) единицах.

Результаты. Проведенное исследование позволило выявить, что грудоспинной нерв является смешанным нервом, состоит из 1–3 чувствительных и одного двигательного пучков, которые неодинаково проходят через спинномозговые нервы, стволы, подмышечный нерв с образованием 20 внутриствольных путей. В 77% случаев чувствительные пучки от грудоспинного нерва проходят через задний пучок, заднее разделение, средний ствол и спинномозговой нерв С7 или нижний ствол и С8. В 22% у грудоспинного нерва кроме основного имеется еще один, редко – два дублирующих чувствительных пути. Двигательный пучок до грудоспинного нерва в 93% проходит через спинномозговой нерв С7 и средний ствол, заднее разделение и задний пучок. Кодирование вариантов внутриствольных путей в направлении чувствительный пучок → задний пучок → заднее разделение → ствол → спинномозговой нерв; двигательный пучок ← задний пучок ← заднее разделение ← ствол ← спинномозговой нерв позволяет кратко, наглядно и полно отобразить все морфологические разнообразия строения.

Заключение. Выявленные варианты внутриствольных путей могут быть полезны при диагностике травм и заболеваний, расширяют показания использования спинномозговых нервов и стволов плечевого сплетения, грудоспинного нерва в реконструктивных операциях.

Ключевые слова: грудоспинной нерв, внутриствольные пути, чувствительные пучки, двигательный пучок, смешанный пучок, варианты, коды

Конфликт интересов. Авторы декларируют отсутствие явных и потенциальных конфликтов интересов, связанных с публикацией настоящей статьи.

Источник финансирования. Исследование поддержано Красноярским краевым фондом науки.

Соответствие принципам этики. Исследование одобрено локальным этическим комитетом КрасГМУ им. проф. В.Ф. Войно-Ясенецкого (протокол № 91 от 11.09.2018).

Для цитирования: Горбунов Н.С., Кобер К.В., Каспаров Э.В., Ростовцев С.И., Протасюк Е.Н. Вариантная анатомия и коды внутриствольных путей грудоспинного нерва. *Бюллетень сибирской медицины.* 2023;22(2):21–27. https://doi.org/10.20538/1682-0363-2023-2-21-27.

INTRODUCTION

The brachial plexus has been studied in detail and is characterized by significant anatomical variations [1, 2]. However, in clinical practice, anatomical variations of the brachial plexus are more common than reported and account for 50% of all features of the nervous system [3]. Despite great uncertainty of the somatotopic arrangement, sensory and motor nerve fibers tend to group into bundles [4], which are studied in sections by histologic, histochemical, and immunohistochemical methods [5, 6]. In clinical practice, the knowledge of anatomical variations of the intra-trunk pathways in the nerve bundles from organs to the central parts of the nervous system is in demand [7, 8]. This is especially relevant due to advances in microsurgical technologies used in peripheral nerve bundles [9, 10]. A detailed comparison and ligation of unifunctional bundles in accordance with their intra-trunk topography are the key to successful restoration of nerve mobility and sensitivity in full [11, 12].

Despite the active use of the thoracodorsal nerve in the clinical practice [13, 14], few studies have been devoted to its fascicular anatomy [15–17]. However, existing works do not describe the features of the path of each thoracodorsal nerve bundle along its entire length with account of functional affiliation.

The aim of this study was to investigate anatomical variations of the intra–trunk pathways in the thoracodorsal nerve bundles and to develop a system for their coding.

MATERIALS AND METHODS

The study was conducted at the Department of Postmortem Examination of the Krasnoyarsk Regional Bureau of Forensic Medical Examination using 121 brachial plexus specimens obtained from 105 corpses of males and females who died at the age of 40–97 years. Most of the examined corpses were male (76–69%); 29–31% were female. The cause of death in all cases was somatic symptom disorder without head, neck, upper limb, and chest injuries.

The brachial plexus was studied on the right side in all corpses, and bilaterally in 16 corpses. The predominant choice of the side was associated with a large number of right-sided injuries and surgical interventions.

Anatomical variations in the thoracodorsal nerve were studied using macro- and microscopic intra-trunk dissection. At the first stage, layer-by-layer anatomical dissection was carried out with isolation of a fragment of the cervical and thoracic spine, radicular filaments, anterior (motor) and posterior (sensory) roots, anterior branches of the spinal nerves, trunks, posterior divisions, posterior bundles, and axillary and thoracodorsal nerves.

The isolated brachial plexus specimen was placed for 1–3 days in a 10% neutral buffered formalin solution and then fixed in a 2% acetic acid solution. The choice of acetic acid is associated with its ability to counteract the shrinkage effect and dissolution of collagen in the epi- and perineurium [18].

At the second stage, macro- and microscopic intra-trunk dissection of the thoracodorsal nerve bundles along the entire length of the brachial plexus (from the latissimus dorsi muscle to the spinal cord) was performed using the MBS-10 stereomicroscope. Special attention was paid to identifying spinal nerve roots through which the thoracodorsal nerve bundles passed, which made it possible to identify their functional affiliation: motor bundles passed through the anterior roots, and sensory bundles passed through the posterior roots.

The article presents the study results after investigating 121 brachial plexus specimens obtained from 105 corpses without gender distinction and bilateral affiliation. This is due to the fact that we did not identify statistically significant gender and bilateral differences in the incidence of anatomical variations of intra-trunk pathways in the thoracodorsal nerve.

All identified features of the intra-trunk pathways in the thoracodorsal nerve were input into the MS Excel 12.0 program (Microsoft Corporation, USA), and the number of anatomical variations in absolute and relative (% from 121 specimens) units was determined.

RESULTS

The macro- and microscopic dissection revealed that the thoracodorsal nerve has clear fascicular anatomy and consists of a different number (1–4) of bundles. Further proximal dissection of these bundles made it possible to determine their functional affiliation and anatomical variations of the intra-trunk pathways. The functional affiliation of the bundles in the thoracodorsal nerve was determined on the basis of their passage through the roots of the spinal nerve: through the posterior roots – sensory bundles, through the anterior roots – motor bundles (Figure).

The precisely established functional affiliation of each thoracodorsal nerve bundle made it possible to determine their number. In 98% of cases (119 / 121), 1–3 sensory bundles and only one motor bundle were

observed in the thoracodorsal nerve. In two plexuses out of 121, sensory and motor bundles in the thoracodorsal nerve were tightly intertwined, and it was not possible to determine their number via intra-trunk dissection. In 119 plexuses where the isolated fascicular anatomy of the thoracodorsal nerve was determined, most often (77% – 92 / 121) one bundle was sensory, and the other one was motor, less often (22% – 26 / 121) two bundles were sensory and one bundle was motor. In one plexus out of 121, there were three sensory and one motor bundles.

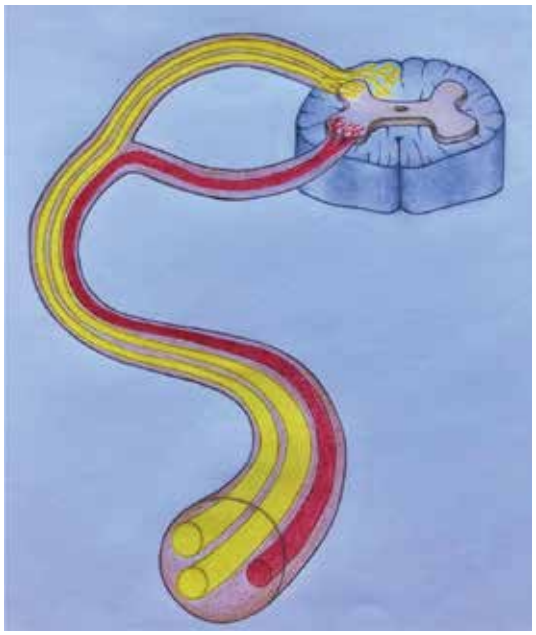

Figure. Schematic representation of the sensory (indicated in yellow) and motor (red) bundles of the thoracodorsal nerve: 1 – spinal cord, 2 – posterior (sensory) root, 3 – anterior (motor) root, 4 – spinal nerve.

In 94% of cases (114 / 121), sensory and motor bundles from the thoracodorsal nerve passed into the posterior bundle of the brachial plexus, and in seven plexuses out of 121, they passed first into the axillary nerve and then also into the posterior bundle. It was further established that the thoracodorsal nerve bundles variously passed in the anterior branches of three spinal nerves: C6, C7, and C8.

Studying the path of each bundle throughout the entire latissimus dorsi muscle to the spinal cord identified 20 anatomical variations of the intra-trunk pathways in the thoracodorsal nerve. To clearly demonstrate the identified pathways, we developed a system for coding the anatomical variations in the direction: sensory bundle → posterior bundle → posterior division → trunk → spinal nerve; motor bundle ← posterior bundle ← posterior division ← trunk ← spinal nerve (Table). As seen from the Table, the first three variations are more common (72% –87 / 121), variations 4–8 are less common (18% – 22 / 121), and the remaining twelve variations are rare and occur in a single case each (10% – 12 / 121).

Table

Codes for anatomical variations of the intra-trunk pathways in the thoracodorsal nerve, *n* = 121

Variation number	Code	Number
1	SB→PB→PD→MT→C7; MB←PB←PD←MT←C7	43
2	SB→PB→PD→IT→C8; MB←PB←PD←MT←C7	30
3	SB→PB→PD→MT→C7; SB→PB→PD→IT→C8; MB←PB←PD←MT←C7	14
4	SB→PB→PD→IT→C8; MB←PB←PD←IT←C8	7
5	SB→PB→PD→MT→C7; SB→PB→PD→MT→C7; MB←PB←PD←MT←C7	5
6	SB→PB→PD→ST→C6; MB←PB←PD←MT←C7	4
7	SB→PB→PD→ST→C6; SB→PB→PD→IT→C8; MB←PB←PD←MT←C7	4
8	SB→Ax→PB→PD→IT→C8; MB←Ax←PB←PD←IT←C8	2
9	SB→PB→PD→ST→C7; MB←PB←PD←ST←C7	1
10	SB→PB→PD→IT→C8; MB←PB←PD←ST←C7	1
11	SB→Ax→PB→PD→IT→C8; MB←Ax←PB←PD←MT←C7	1
12	SB→Ax→PB→PD→IT→C8; MB←Ax←PB←PD←IT←C7	1
13	SB→Ax→PB→PD→MT→C7; SB→Ax→PB→PD→MT→C7; MB←Ax←PB←PD←MT←C7	1
14	SB→Ax→PB→PD→ST→C6; MB←Ax←PB←PD←MT←C7	1
15	SB→PB→PD→ST→C6; MB←PB←PD←IT←C7	1
16	SB→PB→PD→MT→C6; SB→PB→PD→IT→C8; MB←PB←PD←MT←C7	1
17	SB→PB→PD→BC→C6; SB→PB→PD→MT→C7; MB←PB←PD←MT←C7	1
18	MB1DPBDPDDMTDC7	1
19	MB1DAxDPBDPDDMTDC7	1
20	SB→PB→PD→BC→C6; SB→PB→PD→MT→C7; SB→PB→PD→IT→C8; MB←PB←PD←MT←C7	1

Note: SB – sensory bundle; MB – motor bundle; MB - mixed bundle; Ax – axillary nerve; PB – posterior bundle of the brachial plexus; PD – posterior division; ST – superior trunk; MT – middle trunk; IT – inferior trunk; C6, C7, C8 – ventral branches of spinal nerves; → , ←, D – direction of nerve impulse conduction

The coding system allows to briefly yet clearly and fully display all the anatomical variations of the intra-trunk pathways in the thoracodorsal nerve. So, the first anatomical variation is deciphered as follows: the thoracodorsal nerve has a two-bundle structure, where the sensory and motor bundles pass along the C7 spinal nerve, then through the middle trunk, its posterior division, and the posterior bundle.

The study showed that the sensory bundles of the thoracodorsal nerve passed through most components of the brachial plexus. The sensory bundles primarily passed through the C7 spinal nerve and the middle trunk (42% – 51 / 121), as well as through the C8 spinal nerve and the inferior trunk (35% – 42 / 121). It is possible that they are the main sensory pathways in the thoracodorsal nerve. In 22% of cases (26 / 121), the thoracodorsal nerve had one more duplicate sensory pathway besides the main one, and one plexus out of 121 had two duplicate sensory pathways.

Unlike sensory bundles, the motor pathway was not duplicated and passed through the C7 spinal nerve (93% – 112 / 121) and the middle trunk (89% – 108 / 121), less often – through the C8 spinal nerve (nine plexuses out of 121) and the inferior trunk (11 plexuses out of 121), rarely – through the C7 spinal nerve and the superior trunk (two plexuses out of 121).

Thus, using macro- and microscopic dissection of the thoracodorsal nerve, 20 anatomical variations of intra-trunk pathways were identified. Duplicate pathways of sensory bundles were revealed. To illustrate the entire structural diversity and simplify the use of anatomical variations in clinical practice, a coding system for the identified intra-trunk pathway variations was proposed. The obtained data on intra-trunk pathway variations in the thoracodorsal nerve can be used in reconstructive surgery and in clinical practice to diagnose injuries and diseases.

DISCUSSION

The macro- and microscopic intra-trunk dissection revealed that the thoracodorsal nerve is a mixed nerve with clear fascicular anatomy which contains mostly sensory bundles (1–3) and only one motor bundle. These results confirm the findings obtained by B. Gesslbauer et al. (2017), who, using the immunofluorescence method, counted 6,904 (± 3,070) axons in the thoracodorsal nerve, of which 5,977 (± 3,066) were sensory and 927 (± 79) were motor [17]. This predominance of sensory fibers and bundles over motor ones in the nerve allows to get complete information about the state of the latissimus dorsi muscle and to constantly coordinate and correct its contractions.

The determination of the functional affiliation of the thoracodorsal nerve bundles was achieved due to their thorough dissection along the entire length of the brachial plexus after fixation in a 2% acetic acid solution. W. Lu et al. (2008) used a similar technique but managed to dissect the thoracodorsal nerve bundles only to the level of the brachial plexus trunks [15]. We managed to trace the path of the thoracodorsal nerve bundles further – in the spinal nerves and their anterior (motor) and posterior (sensory) roots. We did not find similar works in the available literature.

Such an anatomical approach has two advantages over histochemical, electrophysiological, and instrumental methods and allows not only to accurately determine the functional affiliation of each bundle, but also to trace their path along the entire length of the brachial plexus (from the latissimus dorsi muscle to the spinal cord). As a result, 20 anatomical variations of the intra-trunk pathways in the thoracodorsal nerve were identified. Moreover, variable and stable regions were established. The posterior divisions, the posterior bundle, and the roots of the spinal nerves are stable regions (sensory bundles pass through the posterior roots, motor bundles pass through the anterior roots), while the spinal nerves and trunks are variable ones.

The main number of variations are associated with the unequal passage of sensory and motor bundles through the superior, middle, and inferior trunks, and C6, C7, and C8 spinal nerves. The isolation of the remaining six variations is associated with the passage of the thoracodorsal nerve bundles through the axillary nerve. According to R. Rastogi et al. (2013), the thoracodorsal nerve departed from the axillary nerve in 23% of cases [19], and according to our data, it occurred in seven out of 121 plexuses.

The predominant path for the sensory bundles is the middle trunk and C7 (42%) or the inferior trunk and C8 (35%), and for the motor bundles – C7 (93%) and the middle trunk (89%). This is somewhat different from the findings obtained by W. Lu et al. (2008), who found that more than 52% of motor fibers in the thoracodorsal nerve originate in C7 [15]. According to K. S. Lee (2007), most often (in 60%) the thoracodorsal nerve originates in two spinal nerves C7 and C8, less often – in C6, C7, and C8 (25%), C6 and C7 (10%), and C7 (5%) [20]. We identified one more variation where only the C8 spinal nerve is involved in the formation of the thoracodorsal nerve, which occurred in nine out of 121 plexuses and has not been

described in the literature. Our data differ from the results obtained by W. Lu et al. (2008), which identified only three variations of the path of the thoracodorsal nerve bundles through the trunks: superior and middle (5%), all three trunks (85%), middle and inferior (10%) [15]. According to our data, the passage of bundles through all three trunks was detected only in five plexuses out of 121. Apparently, all observed differences are associated with regional and ethnic features or different amount of studied material.

The study revealed that the thoracodorsal nerve has a single motor pathway and duplicate sensory pathways, which occur in 22% of cases. There is no information in the literature about duplicate sensory pathways in the thoracodorsal nerve.

To illustrate the entire structural diversity, as well as to simplify the use of anatomical variations in clinical practice, we developed a coding system for the identified variations of intra-trunk pathways in the direction: sensory bundle» posterior bundle « posterior division « trunk « spinal nerve; motor bundle ! posterior bundle ! posterior division ! trunk ! spinal nerve.

On the basis of the obtained data, we determined the regularity of the intra-trunk pathway formation in the thoracodorsal nerve. It is characterized by a larger number of variations of sensory bundles in the proximal parts of the brachial plexus. Possibly, embryonic growth of neuronal processes in the rudiment of the arm early along the path is very susceptible to obstacles, which leads to intra-trunk diversity of sensory bundles [21]. A more stable intra-trunk path of the motor bundle is due to the fact that dendrites grow faster and axons orient themselves according to them [22]. Young motor fibers move along existing tracts and encounter fewer obstacles [23].

The identified anatomical variations of the intra-trunk pathways can be useful in the diagnosis of injuries and diseases. They expand indications for the use of spinal nerves, trunks of the brachial plexus, and the thoracodorsal nerve in reconstructive surgery.

CONCLUSION

1. The thoracic nerve is a mixed nerve, which consists of one motor and 1–3 sensory bundles that variously pass through the spinal nerves, trunks, and the axillary nerve with the formation of 20 intra-trunk pathways.

2. In most cases, sensory bundles from the thoracodorsal nerve pass through the posterior bundle, the posterior division, and the middle trunk to the C7 spinal nerve (42%) or the inferior trunk and the C8 spinal nerve (35%). In 22% of cases, the thoracodorsal nerve has one or, rarely, two duplicate sensory pathways besides the main one.

3. The path of the motor bundle to the thoracodorsal nerve is not duplicated and in most cases passes through the C7 spinal nerve (93%) and the middle trunk (89%) and then through the posterior division and the posterior bundle.

4. Coding anatomical variations of the intra-trunk pathways in the thoracodorsal nerve makes it possible to briefly yet clearly and fully display the entire morphological diversity of the nerve anatomy.

REFERENCES

1. Emamhadi M., Chabok S.Y., Samini F., Alijani B., Behzadnia H., Firozabad F.A. et al. Anatomical Variations of Brachial Plexus in Adult Cadavers; A Descriptive Study. *Archives of Bone and Joint Surgery.* 2016;4(3):253–258.
2. Golarz S.R., White J.M. Anatomic variation of the phrenic nerve and brachial plexus encountered during 100 supraclavicular decompressions for neurogenic thoracic outlet syndrome with associated postoperative neurologic complication. *Annals of Vascular Surgery.* 2020;62:70–75. DOI: 10.1016/j.avsg.2019.04.010.
3. Hassan A., Jan N. Anatomical variations in brachial plexus formation and branching pattern in adult cadavers. *Annals of R.S.C.B.* 2021;25(4):4869–4876.
4. Mioton L., Dumanian G.A., De la Garza M., Ko J.H. Histologic analysis of sensory and motor axons in branches of the human brachial plexus. *Plastic and Reconstructive Surgery.* 2019;144(6):1359–1368. DOI: 10.1097/PRS.0000000000006278.
5. Agarwal P., Bajaj J., Sharma D. Techniques for Differentiating Motor and Sensory Fascicles of a Peripheral Nerve – A Review. *Indian Journal of Neurotrauma*. 2020;17(1). DOI: 10.1055/s-0040-1713458.
6. Zhou X., Du J., Qing L., Mee T., Xu X., Wang Zh. et al. Identification of sensory and motor nerve fascicles by immunofluorescence staining after peripheral nerve injury. *J. Transl. Med.* 2021;19(1):207. DOI: 10.1186/s12967-021-02871-w.
7. Osborne N.R., Anastakis D.J., Davis K.D. Peripheral nerve injuries, pain, and neuroplasticity. *Journal of Hand Therapy.* 2018;31(2):184–194. DOI: 10.1016/j.jht.2018.01.011.
8. Llusá M., Morro M.R., Casañas J., Moore A.M. Surgical anatomy of the brachial plexus. In: Shin A.Y., Pulos N. (eds). Operative Brachial Plexus Surgery. Springer, Cham. 2021;19–31. DOI: 10.1007/978-3-030-69517-0_2.
9. Beris A., Gkiatas I., Gelalis I., Papadopoulos D., Kostas-Agnantis I. Current concepts in peripheral nerve surgery. *European Journal of Orthopaedic Surgery and Traumatology*. 2019;29:263–269. DOI: 10.1007/s00590-018-2344-2.
10. Park S.O., Kim J., Kim Il-K., Chung J.H., Jin U.S., Chang H. Minimizing donor site morbidity using the interfascicular nerve splitting technique in single-stage latissimus neuromuscular transfer for facial reanimation. *Correspondence and Communications*. 2021;74(5):1101–1160. DOI: 1016/j.bjps.2020.10.030.

11. Manoukian O.S., Baker J.T., Rudraiah S., Arul M.R., Vella A.T., Domb A.J. et al. Functional polymeric nerve guidance conduits and drug delivery strategies for peripheral nerve repair and regeneration. *Journal of Controlled Release.* 2020Jan.10(317):78–95. DOI: 10.1016/j.jconrel.2019.11.021.
12. Gordon T. Peripheral nerve regeneration and muscle reinnervation. *International Journal of Molecular Sciences.* 2020;21(22):8652. DOI: 10.3390/ijms21228652.
13. Bedarida V., Qassemyar Q., Temam S., Janot F., Kolb F. Facial functional outcomes analysis after reconstruction by vascularized thoracodorsal nerve free flap following radical parotidectomy with facial nerve sacrifice. *Head & Neck*. 2020May;42(5):994–1003. DOI: 10.1002/hed.26076.
14. Guyonvarch P., Benmoussa N., Moya-Plana A., Leymarie N., Mangialardi M.L., Honart J. et al. Thoracodorsal artery perforator free flap with vascularized thoracodorsal nerve for head and neck reconstruction following radical parotidectomy with facial nerve sacrifice: Step-by-step surgical technique video. *Head & Neck.* 2021;43(7):2255–2258. DOI: 10.1002/hed.26701.
15. Lu W., Xu J.G., Wang D.P., Gu Y.D. Microanatomical study on the functional origin and direction of the thoracodorsal nerve from the trunks of brachial plexus. *Wiley InterScience.* 2008;21(6):509–513. DOI: 10.1002/ca.20656.
16. Raksakulkiat R., Leechavengvongs S., Malungpaishrope K., Uerpairojkit C., Witoonchart K., Chongthammakun S. Restoration of winged scapula in upper arm type brachial plexus injury: anatomic feasibility. *J. Med. Assoc. Thai.* 2009;92(6):S244–250.
17. Gesslbauer B., Hruby L.A., Roche A.D., Farina D., Blumer R., Oskar C. et al. Axonal components of nerves innervating the human arm. *Ann. Neurol.* 2017;82(3):396–408. DOI: 10.1002/ana.25018.
18. Oh S.Y., Jung K., Kim E.H. Production of collagen nanofiber using electrospinning dope of acid-soluble collagen isolated from fish skin. *Textile Science and Engineering.* 2020;57(3):186–191. DOI: 10.12772/TSE.2020.57.186.
19. Rastogi R., Budhiraja V., Bansal K. Posterior cord of brachial plexus and its branches: anatomical variations and clinical implication. *ISRN Anat.* 2013;2013:501813. DOI: 10.5402/2013/501813.
20. Lee K.S. Variation of the spinal nerve compositions of thoracodorsal nerve. *Clin. Anat.* 2007;20(6):660–662. DOI: 10.1002/ca.20484.
21. Leijnse J.N., Bakker B.S., D'Herde K. The brachial plexus – explaining its morphology and variability by a generic developmental model. *J. Anat.* 2020;236(5):862–882. DOI: 10.1111/joa.13123.
22. Brushart T., Kebaisch F., Wolinsky R., Skolasky R., Li Z., Barker N. Sensory axons inhibit motor axon regeneration *in vitro. Experimental Neurology.* 2019;323:113073. DOI: 10.1016/j.expneurol.2019.113073.
23. Spead O., Poulain F.E. Trans-axonal signaling in neural circuit wiring. *International Journal of Molecular Sciences.* 2020;21(14):5170. DOI: 10.3390/ijms21145170.

Authors' contribution

Gorbunov N.S. – scientific supervisor of the study, final approval of the manuscript for publication. Kober K.V., Kasparov E.V., Rostovtsev S.I., Protasyuk E.N. – carrying out of the research, collection and analysis of the data.

Authors' information

Gorbunov Nikolay S. – Dr. Sci. (Med.), Professor, Department of Operative Surgery and Topographic Anatomy, V.F. Voino-Yasenetsky Krasnoyarsk State Medical University; Leading Researcher, Research Institute of Medical Problems of the North, Krasnoyarsk, gorbunov_ns@mail.ru, http://orcid.org/0000-0003-4809-4491

Kober Kristina V. – Surgical Oncologist, A.I. Kryzhanovsky Krasnoyarsk Regional Clinical Oncology Center, Krasnoyarsk, k-kober@mail.ru, http://orcid.org/0000-0001-5209-182X

Kasparov Eduard W. – Dr. Sci. (Med.), Professor, Director of the Research Institute of Medical Problems of the North, Krasnoyarsk, rsimpn@scn.ru, http://orcid.org/0000000259881688

Rostovtsev Sergey I. – Dr. Sci. (Med.), Associate Professor, Department of Anesthesiology and Resuscitation, V.F. Voino-Yasenetsky Krasnoyarsk State Medical University, Krasnoyarsk, rostovcev.1960@mail.ru, http://orcid.org/0000-0002-1462-7379

Protasyuk Ekaterina N. – Resident, V.F. Voino-Yasenetsky Krasnoyarsk State Medical University, Krasnoyarsk, demonshire@mail.ru, http://orcid.org/0000-0002-1204-7821

(✉) **Gorbunov Nikolay S.,** gorbunov_ns@mail.ru

Received 29.06.2022;
approved after peer review 03.11.2022;
accepted 08.12.2022

УДК 616.12-008.46:616.13-004.6:616.12-008.3-073.96
https://doi.org/10.20538/1682-0363-2023-2-28-38

Heart failure with preserved left ventricular ejection fraction in non-obstructive coronary artery disease: clinical utility of heart rate variability

Grakova E.V.[1], Kopeva K.V.[1], Gusakova A.M.[1], Smorgon A.V.[1], Akhmedov Sh.D.[1], Kalyuzhin V.V.[2], Teplyakov A.T.[1]

[1]Cardiology Research Institute, Tomsk National Research Medical Center (NRMC), Russian Academy of Sciences
111a, Kievskaya Str., Tomsk, 634012, Russian Federation

[2] Siberian State Medical University
2, Moscow Trakt, Tomsk, 634050, Russian Federation

ABSTRACT

Aim. To evaluate the role of heart rate variability in the pathogenesis of chronic heart failure with preserved ejection fraction (HFpEF) in patients with non-obstructive coronary artery disease (CAD).

Materials and methods. The cross-sectional study included 65 patients (55.4% were males) with non-obstructive CAD. Non-obstructive CAD (stenosis < 50%) was confirmed by coronary computed tomography angiography. Heart rate variability (HRV) was evaluated by 24-hour Holter monitoring; parameters of time series and spectral analysis were analyzed.

Results. Depending on the presence of HFpEF, the patients were divided into 2 groups: group 1 (n = 48) included patients with HFpEF, and group 2 (n = 17) encompassed patients without it. In patients with HFpEF, a statistically significant decrease in the total HRV and parasympathetic effects on the heart rate, mainly at night, as well as increased activity of cerebral ergotropic systems were revealed. In group 1, the values of the time series analysis of HRV and QT dispersion based on the study of RR interval duration (SDANN and SDNNidx) had a significant direct relationship with the level of myocardial stress in diastole, the value of vascular resistance, and the E / e' ratio. The cut-off values of SDNNidx and pNN50 were identified, that may be used as markers for early diagnosis of HFpEF.

Conclusion. In patients with non-obstructive CAD and HFpEF, it is advisable to perform 24-hour Holter monitoring and assess HRV parameters by the time series analysis, which, compared with the spectral analysis, has a closer relationship with the characteristics of left ventricular diastolic function and afterload.

Keywords: heart failure, preserved ejection fraction, non-obstructive coronary artery disease, heart rate variability, biomarkers

Conflict of interest. The authors declare the absence of obvious and potential conflicts of interest related to the publication of this article.

Source of financing. The study was supported by the Russian Science Foundation grant No. 22-25-20019 "Studying the role of humoral markers and autonomic regulation of the cardiac system in the pathogenesis of heart failure with preserved left ventricular ejection fraction" (https://rscf.ru/project/22-25-20019/) and the Administration of the Tomsk Region.

Conformity with the principles of ethics. All patients signed an informed consent to participate in the study. The study was approved by the local Ethics Committee at Cardiology Research Institute of Tomsk NRMC (Protocol No. 177 of 30.10.2018).

✉ *Kopeva Kristina V.,* kristin-kop@inbox.ru

For citation: Grakova E.V., Kopeva K.V., Gusakova A.M., Smorgon A.V., Akhmedov Sh.D., Kalyuzhin V.V., Teplyakov A.T. Heart failure with preserved left ventricular ejection fraction in non-obstructive coronary artery disease: clinical utility of heart rate variability. *Bulletin of Siberian Medicine.* 2023;22(2):28–38. https://doi.org/10.20538/1682-0363-2023-2-28-38.

Сердечная недостаточность с сохраненной фракцией выброса левого желудочка при неокклюзирующем коронарном атеросклерозе: клиническая полезность оценки вариабельности сердечного ритма

Гракова Е.В.[1], Копьева К.В.[1], Гусакова А.М.[1], Сморгон А.В.[1], Ахмедов Ш.Д.[1], Калюжин В.В.[2], Тепляков А.Т.[1]

[1] Научно-исследовательский институт (НИИ) кардиологии,
Томский национальный исследовательский медицинский центр (НИМЦ) Российской академии наук
Россия, 634012, г. Томск, ул. Киевская, 111а

[2] Сибирский государственный медицинский университет (СибГМУ)
Россия, 634050, г. Томск, Московский тракт, 2

РЕЗЮМЕ

Цель – оценить роль вегетативной дисрегуляции ритма сердца в патогенезе хронической сердечной недостаточности (ХСН) с сохраненной фракцией выброса (СНсФВ) у больных с необструктивным поражением коронарных артерий (КА).

Материалы и методы. В одномоментное исследование включено 65 пациентов (55,4% мужского пола) с впервые диагностированным необструктивным поражением КА. Необструктивное поражение КА (стеноз менее 50%) подтверждено данными компьютерной коронарной ангиографии. Вариабельность сердечного ритма исследовали посредством суточного мониторирования электрокардиограммы (ЭКГ), рассматривая показатели временного и спектрального анализа.

Результаты. В зависимости от наличия СНсФВ пациенты были разделены на две группы: в первую ($n = 48$) вошли больные с СНсФВ, во вторую ($n = 17$) – пациенты без ХСН. У пациентов с СНсФВ на фоне неокклюзирующего атеросклероза коронарного русла обнаружено статистически значимое снижение общей вариабельности сердечного ритма и парасимпатических влияний на сердце преимущественно в ночное время, а также повышенная активность церебральных эрготропных систем. Установлено, что у пациентов первой группы значения показателей временного анализа дисперсии ритма сердца, основанных на исследовании продолжительности интервалов R-R ЭКГ (SDANN и SDNNidx), имели прямую статистически значимую связь с уровнем миокардиального стресса в диастолу, величиной сердечно-сосудистого сопротивления, а также соотношением скорости трансмитрального кровотока в раннюю фазу диастолы и скорости раннего диастолического смещения боковой части фиброзного кольца митрального клапана. Определены пороговые значения SDNNidx и pNN50, которые у таких пациентов могут использоваться в качестве маркера для ранней диагностики СНсФВ.

Заключение. У пациентов с необструктивным поражением КА и СНсФВ при выполнении суточного мониторирования ЭКГ целесообразна оценка параметров дисперсии ритма сердца, анализируемых временными методами, которые по сравнению с показателями спектрального анализа имеют более тесную связь с характеристиками диастолической функции и постнагрузки левого желудочка.

Ключевые слова: сердечная недостаточность, сохраненная фракция выброса, неокклюзирующий коронарный атеросклероз, вариабельность ритма сердца, биомаркеры

Конфликт интересов. Авторы декларируют отсутствие явных и потенциальных конфликтов интересов, связанных с публикацией настоящей статьи.

Источник финансирования. Исследование выполнено за счет гранта Российского научного фонда № 22-25-20019 «Изучение роли гуморальных маркеров и вегетативной регуляции сердечной деятельности в патогенезе сердечной недостаточности с сохраненной фракцией выброса левого желудочка» (https://rscf.ru/project/22-25-20019/) и средств Администрации Томской области.

Соответствие принципам этики. Все пациенты подписали информированное согласие на участие в исследовании. Исследование одобрено локальным этическим комитетом НИИ кардиологии Томского НИМЦ (протокол № 177 от 30.10.2018).

Для цитирования: Гракова Е.В., Копьева К.В., Гусакова А.М., Сморгон А.В., Ахмедов Ш.Д., Калюжин В.В., Тепляков А.Т. Сердечная недостаточность с сохраненной фракцией выброса левого желудочка при неокклюзирующем коронарном атеросклерозе: клиническая полезность оценки вариабельности сердечного ритма. *Бюллетень сибирской медицины.* 2023;22(2):28–38. https://doi.org/10.20538/1682-0363-2023-2-28-38.

INTRODUCTION

In the last decade, a lot of data have been obtained pointing to a wide variety of etiological factors and describing the features of their effect on the pathogenesis of heart failure with preserved ejection fraction (HFpEF). In the same patient, several mechanisms often coexist, initiating symptomatic chronic heart failure (CHF), but the degree of activation of each of them in patients with HFpEF can vary greatly [1, 2].

It is known that an imbalance of the autonomic nervous system is one of the possible mechanisms for the development of CHF and its decompensation [3–5]. In particular, the results of the Women's Health Initiative cohort study that included 28,603 postmenopausal women (mean age 62.6 years) without coronary artery disease (CAD) and CHF demonstrated that low total heart rate variability (HRV) was associated with an increased risk of hospitalization for HFpEF (odds ratio (OR) 1.22; 95% confidence interval (CI) 1.02–1.47) [5].

A number of researchers have found a relationship between HRV and expression of inflammation and coagulation markers in patients with a high risk of developing cardiovascular complications, including patients with CHF and acute coronary syndrome [6–9]. In particular, it was found that activation of the cholinergic anti-inflammatory pathway, in which efferent inhibition of proinflammatory cytokines by the vagus nerve occurs, leads to a decrease in the content of systemic inflammation-associated proteins [10], and non-invasive stimulation of the vagus nerve through activation of the α7 nicotinic acetylcholine receptor can provide anti-inflammatory, antioxidant, and anti-apoptotic effects [11].

There are a few studies that reveal the relationship between changes in HRV and the development of CAD and CHF, as well as an increase in all-cause mortality [3, 9, 12]. The analysis of HRV in patients with CAD has shown that autonomic dysregulation is associated with multivessel coronary artery disease and the presence of coronary artery occlusions and lesions of the left coronary artery and plays an important role as a screening tool for high-risk groups [13]. It has been established that reduced HRV in CAD patients is associated with age, late postinfarction heart remodeling, development of left ventricular systolic and diastolic dysfunction, and the clinical severity of heart failure [14] and is involved in the development of electrical instability of the heart [15]. At the same time, we have not been able to find works on the assessment of HRV in patients with HFpEF and non-obstructive CAD in the available scientific literature.

The aim of the study was to evaluate the role of HRV in the pathogenesis of HFpEF in patients with non-obstructive CAD.

MATERIALS AND METHODS

The study was conducted in accordance with the provisions of the Declaration of Helsinki and approved by the local Ethics Committee at Cardiology Research Institute, Tomsk National Research Medical Center of the Russian Academy of Sciences (Protocol No. 177 of 30.10.2018). All patients signed an informed consent to participate in the study.

The study included 48 patients (60.4% were men) aged 61.5 (55; 60) years with new-onset HFpEF and non-obstructive CAD (group 1). The control group consisted of patients without symptoms and signs of CHF of comparable age (group 2). *Inclusion criteria:* non-obstructive (< 50%) CAD; left ventricular diastolic dysfunction / increased left ventricular (LV) filling pressure and preserved LV ejection fraction (EF); N-terminal pro-brain natriuretic peptide (NT-proBNP) ≥ 125 pg / ml; a signed informed consent to participate in the study. *Exclusion criteria:* prior myocardial infarction; elective coronary revascularization or prior revascularization; elevated systolic or diastolic blood pressure (> 180 or > 110 mm Hg, respectively); systolic hypotension < 80 mm Hg; second / third-de-

gree atrioventricular block, sick sinus syndrome; high ectopic activity of the atria and / or ventricles (> 10 extrasystoles per hour); hypertrophic and dilated cardiomyopathy; valvular defect (mitral, tricuspid or aortic valve insufficiency or stenosis ≥ 2 degree); prior pulmonary embolism with pulmonary hypertension (systolic pressure in the pulmonary artery ≥ 45 mm Hg); chronic atrial fibrillation; severe course of bronchial asthma and chronic obstructive pulmonary disease; pathology of the thyroid gland, severe renal (glomerular filtration rate according to the CKD-EPI equation < 30 ml / min / m²) and liver failure; inflammatory diseases of the myocardium and pericardium; hemoglobin level < 100 g / l.

At the time of enrollment, the patients were not receiving optimal drug therapy, given the fact that CHF was newly diagnosed. The frequency of prescribing β-blockers ranged from 17.6 to 19.4%, angiotensin-converting enzyme (ACE) inhibitors – 11.8–19.4%, angiotensin II AT_1 receptor blockers – 17.6–29.4%, statins – 35.3–41.2%, and diuretics – 5.9–29.4%. The patients who received β-blockers discontinued to take them the day before 24-hour Holter monitoring.

The content of the soluble form of ST2 protein (sST2) and NT-proBNP in the blood serum *in vitro* was determined by enzyme-linked immunosorbent assay (ELISA). Photometric detection of immunochemical reaction passage was performed on the Infinite F50 microplate reader (Tecan, Australia). Fasting blood was sampled from the ulnar vein in the morning after 16-hour fasting into vacutainers. We used kits from Critical Diagnostics Presage® ST2 Assay (USA) and Biomedica (Canada).

Echocardiography (EchoCG) was performed for all patients according to a standard protocol using the EPIQ system (Philips Ultrasound Inc., USA). The structures of the heart were visualized using B- and M-scans according to the standard technique. An obligatory criterion for diagnosing HFpEF was the value of LVEF ≥ 50%. All studies were conducted by one highly qualified specialist. The assessment of LV diastolic function was based on four parameters: early diastolic velocity at the lateral mitral annulus (lateral e'), the ratio of peak early diastolic velocity of the transmitral flow to the mean early diastolic velocity at the mitral annulus (E/e'), left atrial volume index, and peak tricuspid regurgitation velocity. LV diastolic dysfunction was diagnosed if at least three of the four parameters discussed were outside the reference range. LV global longitudinal strain (GLS) was assessed using 2D speckle tracking. Some of the parameters were calculated using the formulas:

– left ventricular end-systolic elastance (Es) = ESP / ESV; where ESP is LV end-systolic pressure, ESV is LV end-systolic volume.

– arterial elastance (Ea) = ESP / SV; where SV is stroke volume.

– LV myocardial stress (MS) in systole = SBP × ESP / LV PWT in systole × (1 + (LV PWT / ESD)); where SBP is systolic blood pressure, ESD is LV end-systolic dimension, and PWT is posterior wall thickness.

– LV myocardial stress (MS) in diastole = DBP × EDP / LV PWT in diastole × (1 + (LV PWT / EDD)); where DBP is diastolic blood pressure, EDD is LV end-diastolic dimension, and PWT is posterior wall thickness.

LV MS is a parameter that characterizes the force of myocardial fibers per unit cross-section of the LV wall and quantitatively reflects the values of LV pre- and afterload. At the end of diastole, it expresses preload, and at the end of systole, it expresses afterload (dynes / cm²).

HRV was assessed by 24-hour Holter monitoring. At least 12 hours before and during 24-hour ECG monitoring, the patients were forbidden to drink coffee, tea, and cola and to smoke. During the ECG recording, routine daily activities were allowed. The parameters of HRV quantification were analyzed: SDNN – standard deviation of all normal RR (NN) intervals of the sinus rhythm; SDANN – standard deviation of the average NN-intervals for each of the 5-minute segments during a 24-hour recording; SDNNidx – mean of the standard deviations of NN intervals in all 5-minute segments of a 24-hour recording; RMSSD – square root of the mean of the squares of differences between adjacent NN intervals; NN50 (100, 200) is the number of pairs of adjacent NN intervals that differ by more than 50 (100, 200) ms; pNN50 (100, 200)% is the value of NN50 (100, 200) divided by the total number of NN intervals in the analyzed recording period.

At the same time, the parameters of the HRV time series analysis were interpreted as follows: the parameters obtained by processing direct measurements of RR intervals (in particular, SDNN, SDANN, SDNNidx) generally reflect the degree of efferent sympathetic influences on the heart (with an increase in sympathetic efferentation, the values of the parameters decrease), whereas the parameters calculated on the basis of the difference between the RR intervals (RMSSD, NN50, pNN50) reflect tension in the

parasympathetic nervous system (with an increase in the efferent activity of the vagus nerve, the values of the parameters rise). Using the spectral analysis, the power of the spectrum was estimated in the range of very low (< 0.04 Hz) frequencies (VLF is a parameter which is associated with the activity of cerebral ergotropic systems and the renin – angiotensin system), low (0.04–0.15 Hz) frequencies (LF is a marker of sympathetic modulation), and high (0.15–0.4 Hz) frequencies (HF is a marker of the parasympathetic nervous system activity), and the LF / HF ratio (the so-called sympatho-vagal balance) was determined.

All patients underwent coronary computed tomography angiography. For contrast-enhanced scanning, 70–90 ml of a nonionic contrast agent (370 mg Iopamidol, Bracco Diagnostics, Italy) was injected intravenously through an 18G catheter at a flow rate of 5–5.5 ml / s.

Statistical processing was performed using the STATISTICA 10.0 software (StatSoft Inc., USA). The normality of distribution of the variables was assessed using the Shapiro – Wilk test. The homogeneity of variance was assessed using the Levene's test. Quantitative data were presented as the median and the interquartile range *Me* (Q_{25} ; Q_{75}). The Mann – Whitney *U*-test was used to test statistical hypotheses when comparing two independent samples. To search for relationships between variables, a correlation analysis was used with the calculation of the Spearman's rank correlation coefficient. For qualitative features, contingency tables were analyzed using the Pearson's χ^2 test or Fisher's exact test, when the expected value in any of the cells in the table with given boundaries was below 10. To assess the sensitivity and specificity of the models and select the cut-off values, the ROC analysis was used with the construction of curves and the calculation of the area under the curve (AUC). AUC value > 0.70 was considered significant. The marginal significance level of *p* for all statistical analysis procedures used was 0.05.

RESULTS

At the time of inclusion in the study, the groups were comparable in most clinical and demographic characteristics (Table 1). Patients of group 1 smoked more often and had impaired carbohydrate metabolism, while there were no statistically significant differences in the level of glycated hemoglobin.

Table 1

Baseline clinical and demographic characteristics

Parameter	Group 1, *n* = 48, (+) HFpEF	Group 2, *n* = 17, (–) HFpEF	*p*
Age, years, *Me* (Q_{25} ; Q_{75})	61.5 (55; 66)	62 (58; 63)	0.124
Men, *n* (%)	29 (60.4)	7 (41.2)	0.059
BMI, kg / m^2, *Me* (Q_{25} ; Q_{75})	29.7 (27.6; 32.0)	30.8 (28.35; 33.95)	0.254
Hypertension, *n* (%)	39 (81.2)	13 (76.5)	0.161
Type 2 DM, *n* (%)	11 (22.9)	2 (11.8)	0.013
HbA1c, %, *Me* (Q_{25} ; Q_{75})	6.3 (5.8; 7.5)	6.1 (6.0; 7.6)	0.068
COPD, *n* (%)	5 (10.4)	1 (5.9)	0.718
Smoking, *n* (%)	15 (31.25)	3 (17.6)	0.011
GFR, ml / min / 1.73 m^2	82.8 (67.3; 82.7)	85 (71; 89)	0.476
Total cholesterol, mmol / l, *Me* (Q_{25} ; Q_{75})	4.98 (3.67; 5.25)	5.09 (3.76; 6.5)	0.532
LDL-C, mmol / l, *Me* (Q_{25} ; Q_{75})	3.13 (2.15; 3.51)	2.33 (1.24; 3.37)	0.856
HDL-C, mmol / l, *Me* (Q_{25} ; Q_{75})	1.07 (0.85; 1.31)	1.52 (1.25; 1.79)	0.889
Triacylglycerols, mmol / l, *Me* (Q_{25} ; Q_{75})	1.78 (1.23; 1.97)	1.26 (1.17; 1.36)	0.870
Hemoglobin, g / l, *Me* (Q_{25} ; Q_{75})	134 (121; 143)	145 (140; 157)	0.464
Potassium, mmol / l, *Me* (Q_{25} ; Q_{75})	4.67 (4.12; 5.01)	4.47 (4.43; 5.01)	0.517
Fibrinogen, g / l, *Me* (Q_{25} ; Q_{75})	3.27 (3.14; 3.14)	3.16 (2.86; 3.36)	0.767
NT-proBNP, pg / ml, *Me* (Q_{25} ; Q_{75})	404.2 (249.5; 1,533.4)	58 (43.65; 74.35)	0.004
sST2, ng / ml, *Me* (Q_{25} ; Q_{75})	29.18 (23.17; 31.09)	19.42 (18.24; 22.29)	0.012

Note: BMI – body mass index; DM – diabetes mellitus; GFR – glomerular filtration rate; COPD – chronic obstructive pulmonary disease; LDL-C – low-density lipoprotein cholesterol; HDL-C – high-density lipoprotein cholesterol; HbA1c – glycated hemoglobin; NT-proBNP – N-terminal pro-brain natriuretic peptide; sST2 – soluble form of the ST2 protein.

In patients with non-obstructive CAD and HFpEF, compared to patients of the control group, we noted early signs of depressed LV contractility associated with changes in the characteristics of pre- and afterload (Table 2), in particular, impaired mechanics of the LV (decrease in LV global longitudinal strain: –14.4% [–13.1; –17.6] vs –18.9% [–14.4; –21.4], $p = 0.003$), increased myocardial stress in diastole, reflecting true hemodynamic load on the heart muscle (157.48 [142.06; 164.70] dynes / cm^2 vs 142.15 [133.31; 149.97] dynes / cm^2, $p = 0.028$) and arterial elastance (0.60 [0.55; 0.92] mm Hg / ml vs 0.56 [0.53; 0.61] mm Hg / ml, $p = 0.021$) against the background of a decrease in end-systolic elastance (2.30 [1.64; 3.0] mm Hg / ml vs 0.56 [2.75; 3.16] mm Hg / ml, $p = 0.018$).

The results of the HRV assessment revealed that patients with HFpEF, compared to persons without CHF, had chronotropic incompetence throughout the entire monitoring period, manifested by a decrease ($p < 0.01$) in the values of time series parameters: SDNNidx (night) by 29.9% (47 [44; 65] ms and 67 [52; 208] ms, respectively) and SDNNidx (day) by 14.3% (56 [52; 71] ms and 64 [55; 183] ms, respectively), as well as a decrease in the values of most parameters characterizing the parasympathetic nervous system activity ($p < 0.01$) mainly at night – RMSSD by 73.9% (23 [12; 31] ms and 40 [32; 328] ms, respectively), NN50, NN100, NN200 – by 5–8 times, pNN50(100, 200)% – by 2.5–6 times.

In patients with HFpEF, compared to patients without CHF, a significant change in the HRV frequency characteristics was revealed, indicating an increase in the influence of cerebral ergotropic structures with simultaneous inhibition of the parasympathetic nervous system activity: an increase in VLF ($p = 0.004$) and a decrease in CHF ($p = 0.016$). Table 3 shows the parameters of HRV, for which statistically significant differences were found. Other parameters did not differ between the groups.

Table 2

Echocardiography findings in patients of groups 1 and 2, *Me* (Q_{25}; Q_{75})

Parameter	Group 1, $n = 48$, (+) HFpEF	Group 2, $n = 17$, (–) HFpEF	p
LVEF, %	62 (58.5; 65)	65 (64; 66)	0.392
LA, mm	42 (39; 46)	40 (38; 43)	0.734
LV EDV, ml	111 (100; 125)	108 (97.5; 116)	0.306
LV ESV, ml	37.5 (32; 43)	34.5 (33.5; 39.5)	0.205
IVS, mm	10.5 (10.5; 11.1)	9.75 (9.0; 10)	0.065
LVPW, mm	10 (9; 10)	9.5 (9.0; 10.0)	0.329
Peak E, cm / sec	77 (69; 94)	63 (56; 72)	0.032
Peak A, cm / sec	65 (63; 88)	69 (66; 76.5)	0.053
E/A	1.29 (1; 1.36)	0.9 (0.74; 1.0)	0.024
E/e’	13.5 (13; 13.6)	12 (11; 13)	0.019
LAVI, ml / m^2	2.8 (2.78; 2.87)	2.6 (2.3; 2.76)	0.021
LV MMind, g / m^2	87 (80; 97)	82 (75.5; 86.5)	0.283
MS in diastole, dyne / cm^2	157.48 (142.06; 164.70)	142.15 (133.31; 149.97)	0.028
Ea, mm Hg / ml	0.60 (0.55; 0.92)	0.56 (0.53; 0.61)	0.021
Es, mm Hg / ml	2.30 (1.64; 3.0)	2.75 (2.55; 3.16)	0.018

Note: LAVI – left atrial volume index; LV – left ventricle; PW – posterior wall, MMind – myocardial mass index; EDV – end-diastolic volume; ESV – end-systolic volume; LA – left atrium; IVS – interventricular septum; Peak E – the peak velocity of early diastolic flow; Peak A – the peak flow velocity due to atrial systole; E/A - ratio of the peak early diastolic flow velocity (E) to the flow at atrial systole (A); E/e’ - the ratio of peak early diastolic velocity of the transmitral flow to the mean early diastolic velocity at the mitral annulus; Ea – atrial elastance; Es – end-systolic elastance of the left ventricle.

Table 3

HRV parameters in patients of groups 1 and 2, *Me* (Q_{25}; Q_{75})

Parameter	Group 1, $n = 48$, (+) HFpEF	Group 2, $n = 17$, (–) HFpEF	p
Mean NN during the day, ms	978 (897; 993)	835 (732; 959)	0.003
SDNNidx at night, ms	47 (44; 65)	67 (52; 208)	0.003
SDNNidx all day, ms	56 (52; 71)	64 (55; 183)	0.039
RMSSD at night, ms	23 (12; 31)	40 (32; 328)	0.001

Table 3 (continued)

Parameter	Group 1, *n* = 48, (+) HFpEF	Group 2, *n* = 17, (–) HFpEF	*p*
NN50 at night, *n* (%)	494 (352; 1,671)	2,681 (627; 18,518)	0.002
pNN50 at night, %	2.8 (1.2; 9.50)	13.9 (5.1; 61.5)	0.002
NN100 at night, *n* (%)	47 (24; 164)	368 (135; 8,485)	0.001
pNN100 at night, %	0.2 (0; 0.9)	1.4 (0.5; 33.5)	0.001
NN200 at night, *n* (%)	28 (9; 34)	191 (31; 2,037)	0.003
NN200 all day, *n* (%)	289 (43; 534)	400 (141; 12,571)	0.029
pNN200 during the day , %	0.4 (0; 0.9)	1 (0.2; 16.1)	0.010
pNN200 at night, %	0.1 (0; 0.1)	0,6 (0.2; 31.4)	0.001
pNN200 all day, %	0.3 (0.1; 0.9)	0.9 (0.2;21.3)	0.016
VLF, ms^2	2,570 (1,992; 3,016)	2,341 (1,634; 2,731)	0.004
HF, ms^2	347 (214; 509)	514 (371; 627)	0.016

Note: Mean NN – the average value of the duration of all RR (NN) intervals of sinus rhythm; SDNNidx – mean of the standard deviations of NN intervals in all 5-minute segments of a 24-hour recording; RMSSD – square root of the mean of the squares of differences between adjacent NN intervals; NN50(100, 200) – the number of pairs of adjacent NN intervals that differ by more than 50 (100, 200) ms; pNN50(100, 200)% – the value of NN50 (100, 200) divided by the total number of NN intervals in the analyzed recording period; VLF – spectrum power in the range of very low (< 0.04 Hz) frequencies; HF – spectrum power in the range of high (0.15–0.4 Hz) frequencies.

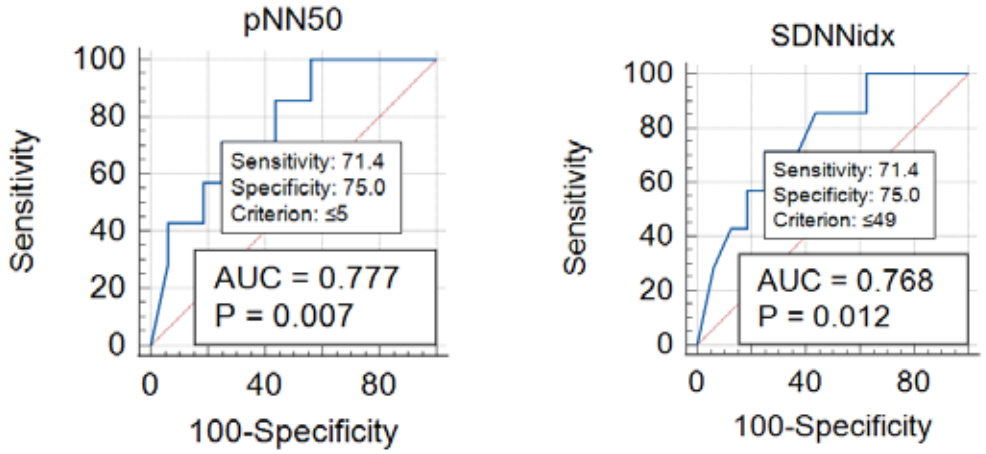

Figure. Cut-off values for SDNNidx (day) and pNN50 (night) for the optimal binary classification of patients with non-obstructive CAD depending on the presence or absence of HFpEF (ROC analysis): y-axis – sensitivity (%), x-axis – 100 minus specificity (%). The boxes represent the sensitivity and specificity scores for the respective decision rule threshold (criterion), as well as the AUC values and the significance level *p*.

Based on the ROC analysis, the values of SDNNidx ≤ 49 ms (AUC = 0.768; $p = 0.012$) and pNN50 ≤ 5 ms (AUC = 0.777; $p = 0.007$) were determined as cut-off values, which are associated with the presence of HFpEF in patients with non-obstructive CAD (Figure).

The results of the correlation analysis demonstrated the relationship between HRV studied by the time series parameters (in particular, SDANN) and the level of sST2 in the blood serum ($r = 0.354$; $p = 0.018$), but not the "classical" CHF biomarker – NT-proBNP. It was also established for the first time that the SDANN value was correlated with MS in diastole ($r = 0.35$; $p = 0.006$), and SDNNidx was correlated with arterial elastance ($r = 0.301$; $r = 0.045$).

DISCUSSION

It is known that autonomic dysregulation is one of the mechanisms for the development of CHF with reduced LVEF and is characterized by a steady increase in sympathetic excitation and a decrease in parasympathetic activity [4, 16]. The results of the analysis of turbulence and QT dispersion (in particular, SDNN) of the heart rate make it possible to identify individuals at the highest risk of adverse outcomes among patients with HFpEF [17]. HRV is also impaired in

symptomatic CAD, especially after myocardial infarction, and is inversely associated with the progression of CAD [12, 18, 19]. In particular, in patients with cardiovascular diseases without signs of myocardial ischemia, an inverse correlation ($p < 0.05$) was established between the presence of non-obstructive (< 50%) stenosis of one or more coronary arteries, on the one hand, and the value of pNN50 (for the anterior interventricular branch and right coronary artery – $r = –0.387$ and $r = –0.365$, respectively, and for the anterior interventricular branch with RMSSD – $r = –0.404$), as well as the power of the spectrum in the HF range ($r = –0.393$, $p < 0.05$), on the other.

This allowed the authors to conclude that the severity and degree of CAD are associated with a shift in the autonomic regulation of the heart toward sympathetic predominance [18]. Other data have been published showing that HRV parameters are associated with the severity of occlusion, multivessel CAD, and lesions of the left coronary artery [19]. At the same time, according to other authors [20], after adjusting for age, sex, body mass index, and heart rate, statistically significant differences between patients with CAD and those with unchanged coronary arteries in a number of logarithmic HRV parameters (pNN10%, pNN20%, LF, and HF) disappeared.

In our study, it was found that in patients with HFpEF and non-obstructive CAD, the activity of most parasympathetic nervous system parameters was suppressed ($p < 0.01$) mainly at night. We also noted a significant change in the frequency characteristics of HRV during 24-hour Holter monitoring, indicating the primacy of sympathetic influences on the heart over parasympathetic ones, which is confirmed by the data of other researchers [12, 16, 17]. Primary suppression of parasympathetic activity in the mechanism of HRV reduction in cardiovascular diseases and the subsequent predominance of the sympathetic nervous system are confirmed by the results of a meta-analysis by S.C. Fang et al. [12].

The pathophysiology of the sympatho-vagal imbalance in cardiovascular diseases may be associated with the influence of risk factors, including obesity, diabetes mellitus and CAD [4, 12, 21, 22]. In our study, patients in group 1 were more often diagnosed with diabetes mellitus, which, according to a number of researchers [4, 12, 22], could also make a certain contribution to the development and progression of autonomic dysfunction. However, given a short duration of the disease, the absence of significant differences in the level of glycemic control according to the HbA1c assessment, and a small sample size, the contribution of this risk factor to the development mechanism and prognosis of HFpEF will be the subject of further research.

The principal mechanism of CAD leading to autonomic dysregulation is still unknown. Most researchers tend to believe that the balance between short-term and long-term HRV components, even in asymptomatic individuals without signs of myocardial ischemia with progression of CAD shifts toward parasympathetic withdrawal with the primacy of sympathetic regulation [4, 9, 12, 17, 18, 23]. This confirms the hypothesis that CAD is one of the determinants of HRV [20]. It is hypothesized that the cause of these changes in patients with typical cardialgia and the absence of atherosclerotic lesions in the coronary bed may also be coronary microvascular dysfunction [20, 22], which, in turn, has a trigger potential for changes in myocardial metabolism, activation of the neurohumoral system, and development of HFpEF [24]. At the same time, regulation of the microvasculature function varies significantly in different tissues depending on their function and nutritional needs. In particular, it has been proven that, for example, retinal microvessels do not have sympathetic innervation, and variability in the filling of the myocardial microvasculature is functionally directly related to HRV [25].

In non-obstructive CAD, HFpEF is triggered actually due to progressive impairment of the endothelial function, which affects a decrease in coronary and myocardial reserves, initiation of diastolic dysfunction, and overproduction of humoral factors leading to perivascular fibrosis and apoptosis of cardiomyocytes [26]. On the other hand, according to D. Aronson et al. [6], neurohormonal activation, manifested by overexpression of proinflammatory cytokines (interleukin (IL)-6, tumor necrosis factor (TNF)-α, and C-reactive protein (CRP)) [1, 8, 27], dysregulation of vascular tone in the context of a decrease in nitric oxide production, and excessive activity of biomarkers (renin, aldosterone, norepinephrine) leads to HRV depression. The authors showed that some HRV parameters in the time domain were inversely correlated with the level of endothelin 1 (SDNN, $r = –0.38$, $p = 0.002$; SDANN5, $r = –0.48$, $p < 0.0001$), while overexpression of endothelin 1 was also associated with some frequency parameters of HRV – with full power ($r = –0.32$, $p = 0.01$) and ultra-low frequency power ($r = –0.43$, $p = 0.0004$), but not with indices of parasympathetic (HF) or sympatho-vagal (LF) modulation. According to the correlation analysis of the data

obtained in our study, associations were found not only between the parameters of total HRV and the level of sST2 (r = 0.354; p = 0.018), but also with the traditional CHF biomarker NT-proBNP. In the CATSTAT-HF study, regardless of the NT-proBNP level, sST2 was an accurate predictor of in-hospital death and heart failure decompensation in 90 patients with ischemic and non-ischemic CHF (LVEF 43.4 ± 16.4%) [9].

Previously, we showed that in patients with HFpEF corresponding to NYHA functional classes I–II and III, the level of sST2 was 28.8 and 46.3%, respectively, which was higher than in the control group [26]. Given the fact that no clear differences in the angiography characteristics were obtained, it is logical to assume that expression of one of the biomarkers studied at this stage, approaching the upper limit of the normal range, is pathogenetically associated with initiation of endothelial dysfunction and, possibly, development of perivascular fibrosis, which was confirmed in single studies of other scientists.

According to B. Arshi et al. [4], the role of the sympathetic nervous system in the development or progression of LV diastolic dysfunction and new-onset heart failure has not been widely studied, which emphasizes the need for new knowledge about the pathophysiology of autonomic regulation in patients with cardiovascular diseases leading to the development of HFpEF. In patients with HFpEF against the background of non-obstructive CAD, we found an increase in the early transmitral flow velocity (E) and a significant increase in the E/e' ratio, which was related to an increase in the activity of the sympathetic nervous system. At the same time, in patients of group 1, the values of the time series parameters of QT dispersion based on the study of the duration of RR intervals (SDANN and SDNNidx) had a direct significant relationship with MS in diastole, the value of arterial elastance, and the E/e' ratio.

Comparison of these results with the data of other authors turned out to be difficult, since they are presented in the scientific literature in single studies. In particular, A.-M. Vintilaˇ et al. [28] refer to the results of a retrospective study by A. Jian et al. (2019), who found that of all the analyzed HRV parameters, only SDANNidx was associated with left atrial dilatation. A. Tanindi et al. (2012) showed that in patients with HFpEF, compared to healthy volunteers, lower HRV values were detected, and HRV depression was directly associated with the progression of LV diastolic dysfunction. Finally, the results of the examination of patients retrospectively included in the population-based Rotterdam study revealed significant associations of HRV parameters (RMSSD and SDNN adjusted for heart rate) with parameters of transmitral flow and tissue Doppler in diastole, as well as the left atrial size [4].

The presence of such associations between parameters of autonomic regulation of the heart rate, diastolic dysfunction, and the level of the humoral biomarker that is not directly related to hemodynamic overload but affects the development and progression of cardiac hypertrophy, myocardial fibrosis, and myocardial dysfunction, in our opinion, reflects the compensatory negative activation of neurohormonal pathways that trigger the development and progression of HFpEF. These data suggest that a comprehensive assessment of HRV parameters, sST2 level, diastolic myocardial stress, and arterial elastance may be useful for early diagnosis of HFpEF.

There is no doubt that interpretation and correct comparison of the results of the HRV study in certain groups of patients can be difficult due to the often different duration of ECG recording, gender, and phenotypic (LVEF value) differences, which makes it necessary to continue research in this area.

CONCLUSION

When performing 24-hour Holter monitoring in patients with non-obstructive CAD and HFpEF, it is advisable to assess the parameters of QT dispersion using the time series analysis, which, compared to spectral analysis parameters, has a closer relationship with the characteristics of diastolic function and LV afterload. The cut-off values of SDNNidx (≤ 49 ms; AUC = 0.768; p = 0.012) and pNN50 (≤ 5 ms; AUC = 0.777; p = 0.007) were determined as a marker for early diagnosis of HFpEF.

Limitations of the study included**:** 1) a small sample size of patients; in this regard, at this stage of the study, we did not analyze HRV in subgroups of patients formed depending on the severity of HFpEF and the presence / absence of diabetes mellitus; 2) in this study, we did not evaluate the prognostic value of HRV depression (clinical outcomes and the prognostic value of QT dispersion parameters will be assessed in the currently ongoing 12-month cohort study).

REFERENCES

1. Adamczak D.M., Oduah M.T., Kiebalo T., Nartowicz S., Bęben M., Pochylski M. et al. Heart Failure with Preserved Ejection Fraction-a Concise Review. *Curr. Cardiol. Rep.* 2020July9;22(9):82. DOI: 10.1007/s11886-020-01349-3.

2. Bosanac J., Straus L., Novaković M., Košuta D., Božič Mijovski M., Tasič J. et al. HFpEF and atrial fibrillation: the enigmatic interplay of dysmetabolism, biomarkers, and vascular endothelial dysfunction. *Dis. Markers.* 2022Oct.25;2022:9539676. DOI: 10.1155/2022/9539676.
3. Patel V.N., Pierce B.R., Bodapati R.K., Brown D.L., Ives D.G., Stein P.K. Association of Holter-Derived Heart Rate Variability Parameters With the Development of Congestive Heart Failure in the Cardiovascular Health Study. *JACC Heart Fail.* 2017;5(6):423−431. DOI: 10.1016/j.jchf.2016.12.015.
4. Arshi B., Geurts S., Tilly M.J., van den Berg M., Kors J.A., Rizopoulos D. et al. Heart rate variability is associated with left ventricular systolic, diastolic function and incident heart failure in the general population. *BMC Med.* 2022Feb.21;20(1):91. DOI: 10.1186/s12916-022-02273-9.
5. Baig M., Moafi-Madani M., Qureshi R., Roberts M.B., Allison M., Manson J.E. et al. Heart rate variability and the risk of heart failure and its subtypes in post-menopausal women: The Women's Health Initiative study. *PLoS One.* 2022Oct.25;17(10):e0276585. DOI: 10.1371/journal.pone.0276585.
6. Aronson D., Mittleman M.A., Burger A.J. Role of endothelin in modulation of heart rate variability in patients with decompensated heart failure. *Pacing Clin. Electrophysiol.* 2001Nov.;24(11):1607−1615. DOI: 10.1046/j.1460-9592.2001.01607.x.
7. Lanza G.A., Sgueglia G.A., Cianflone D., Rebuzzi A.G., Angeloni G., Sestito A. et al. SPAI (Stratificazione Prognostica dell'Angina Instabile) Investigators. Relation of heart rate variability to serum levels of C-reactive protein in patients with unstable angina pectoris. *Am. J. Cardiol.* 2006;97(12):1702–1706. DOI: 10.1016/j.amjcard.2006.01.029.
8. Carney R.M., Freedland K.E. Depression and heart rate variability in patients with coronary heart disease. *Cleve. Clin. J. Med.* 2009;76Suppl.2(Suppl.2):S13–17. DOI: 10.3949/ccjm.76.s2.03.
9. Borovac J.A., Glavas D., Susilovic Grabovac Z., Supe Domic D., Stanisic L., D'Amario D. et al. Circulating sST2 and catestatin levels in patients with acute worsening of heart failure: a report from the CATSTAT-HF study. *ESC Heart Fail.* 2020;7(5):2818–2828. DOI: 10.1002/ehf2.12882.
10. Pavlov V.A., Tracey K.J. The cholinergic anti-inflammatory pathway. *Brain Behav. Immun.* 2005;19(6):493–499. DOI: 10.1016/j.bbi.2005.03.015.
11. Carandina A., Lazzeri G., Villa D., Di Fonzo A., Bonato S., Montano N. et al. Targeting the autonomic nervous system for risk stratification, outcome prediction and neuromodulation in ischemic stroke. *Int. J. Mol. Sci.* 2021Feb.26;22(5):2357. DOI: 10.3390/ijms22052357.
12. Fang S.C., Wu Y.L., Tsai P.S. Heart Rate Variability and Risk of All-Cause Death and Cardiovascular Events in Patients With Cardiovascular Disease: A Meta-Analysis of Cohort Studies. *Biol. Res. Nurs.* 2020;22(1):45–56. DOI: 10.1177/1099800419877442.
13. Goessl V.C., Curtiss J.E., Hofmann S.G. The effect of heart rate variability biofeedback training on stress and anxiety: a meta-analysis. *Psychol. Med.* 2017;47(15):2578–2586. DOI: 10.1017/S0033291717001003.
14. Kalyuzhin V.V., Bardak A.L., Teplyakov A.T., Kamaev D.Yu. Complex of factors affecting QT dispersion in survivors of myocardial infarction. *Cardiology.* 2002;42(8):8−10 (in Russ.).
15. Lysenkova N.O., Rumyantsev M.I., Kratnov A.E. The role of the autonomic nervous system in the development of fatal cardiac arrhythmias in patients with coronary heart disease. *Doktor.Ru.* 2016;11(128):33–35 (in Russ.).
16. Shaffer F., Ginsberg J.P. An overview of heart rate variability metrics and norms. *Front. Public Health.* 2017Sept.28;5:258. DOI: 10.3389/fpubh.2017.00258.
17. Ksela J., Rupert L., Djordjevic A., Antonic M., Avbelj V., Jug B. Altered heart rate turbulence and variability parameters predict 1-year mortality in heart failure with preserved ejection fraction. *J. Cardiovasc. Dev. Dis.* 2022July2;9(7):213. DOI: 10.3390/jcdd9070213.
18. Simula S., Vanninen E., Lehto S., Hedman A., Pajunen P., Syvänne M. et al. Heart rate variability associates with asymptomatic coronary atherosclerosis. *Clin. Auton. Res.* 2014;24(1):31−37. DOI: 10.1007/s10286-013-0220-z.
19. Feng J., Wang A., Gao C., Zhang J., Chen Z., Hou L. et al. Altered heart rate variability depend on the characteristics of coronary lesions in stable angina pectoris. *Anatol. J. Cardiol.* 2015;15(6):496−501. DOI: 10.5152/akd.2014.5642.
20. Elhakeem R.F., Lutfi M.F., Ali A.B.M., Sukkar M.Y. Can short-term heart rate variability predict coronary artery disease in patients undergoing elective coronary angiography due to typical chest pain? *J. Clin. Transl. Res.* 2020;6(2):66−70.
21. Muslimova E.F., Rebrova T.Yu., Archakov E.A., Akhmedov S.D., Budnikova O.V., Batalov R.E. et al. Polymorphic variants of genes encoding Ca(2+)-transporting sarcoplasmic reticulum proteins in the progression of chronic heart failure. *Russian Journal of Cardiology*. 2019;(10):48−52 (in Russ.). DOI: 10.15829/1560-4071-2019-10-48-52.
22. Shah S.J., Lam C.S.P., Svedlund S., Saraste A., Hage C., Tan R.S. et al. Prevalence and correlates of coronary microvascular dysfunction in heart failure with preserved ejection fraction: PROMIS-HFpEF. *Eur. Heart J.* 2018;39(37):3439−3450. DOI: 10.1093/eurheartj/ehy531.
23. Mizobuchi A., Osawa K., Tanaka M., Yumoto A., Saito H., Fuke S. Detrended fluctuation analysis can detect the impairment of heart rate regulation in patients with heart failure with preserved ejection fraction. *J. Cardiol.* 2021;77(1):72−78. DOI: 10.1016/j.jjcc.2020.07.027.
24. Kopeva K.V., Maltseva A.N., Machula A.V., Grakova E.V., Zavadovsky K.V. The role of microvascular dysfunction in the pathogenesis of heart failure with preserved ejection fraction. *Kazan Medical Journal.* 2022;103(6):918−927 (in Russ.). DOI: 10.17816/KMJ109034.
25. Kiselev A.R., Gridnev V.I. Oscillatory processes in vegetative regulation of cardiovascular system (review). *Saratov Journal of Medical Scientific Research.* 2011;7(1):34−39 (in Russ.).
26. Grakova E.V., Kopeva K.V., Gusakova A.M., Smorgon A.V., Maltseva A.N., Mochula A.V. et al. The role of humoral markers in the pathogenesis of heart failure with preserved ejection fraction in patients with non-obstructive coronary artery disease. *Russian Journal of Cardiology*. 2022;27(10):51−62 (in Russ.). DOI: 10.15829/1560-4071-2022-5162.
27. Straburzyńska-Migaj E., Ochotny R., Wachowiak-Baszyńska A., Straburzyńska-Lupa A., Leśniewska K., Wiktorowicz K.

et al. Cytokines and heart rate variability in patients with chronic heart failure. *Kardiol. Pol.* 2005;63(5):478–485.
28. Vintilaˇ A.-M., Horumbaˇ M., Vintilaˇ V.D. Arterial hypertension and heart failure with preserved ejection fraction – associations between echocardiography and heart rate variability. *J. Hypertens. Res.* 2019;5(3):119–125.

Authors' contribution

Grakova E.V. – conception and design of the study, coordination of the study, drafting of the article, final approval of the manuscript for publication. Kopeva K.V. – acquisition and interpretation of clinical data and HRV parameters, compilation of a database, statistical processing of the data, critical revision of the manuscript for important intellectual content, final approval of the manuscript for publication. Gusakova A.M. – determination of the levels of biomarkers in the blood serum, acquisition and interpretation of the data, compilation of a database, final approval of the manuscript for publication. Smorgon A.V. – carrying out of the echocardiography study, acquisition and interpretation of the data, compilation of a database, final approval of the manuscript for publication. Akhmedov Sh.D., Kalyuzhin V.V. – review of the literature, interpretation of the data, drafting of the article, final approval of the manuscript for publication. Teplyakov A.T. – coordination of the study, drafting of the article, final approval of the manuscript for publication.

Authors' information

Grakova Elena V. – Dr. Sci. (Med.), Leading Researcher, Department of Myocardial Pathology, Cardiology Research Institute, Tomsk NRMC of RAS, Tomsk, gev@cardio-tomsk.ru, http://orcid.org/0000-0003-4019-3735

Kopeva Kristina V. – Cand. Sci. (Med.), Researcher, Department of Myocardial Pathology, Cardiology Research Institute, Tomsk NRMC of RAS, Tomsk, kristin-kop@inbox.ru, http://orcid.org/0000-0002-2285-6438

Gusakova Anna M. – Cand. Sci. (Med.), Researcher, Department of Clinical Laboratory Diagnostics, Cardiology Research Institute, Tomsk NRMC of RAS, Tomsk, anna@cardio-tomsk.ru, http://orcid.org/0000-0002-3147-3025

Smorgon Andrey V. – Junior Researcher, Department of Ultrasound and Functional Diagnostics, Cardiology Research Institute, Tomsk NRMC of RAS, Tomsk, sav@cardio-tomsk.ru, http://orcid.org/0000-0002-6531-7223

Akhmedov Shamil D. – Dr. Sci. (Med.), Professor, Leading Researcher, Department of Cardiovascular Surgery, Cardiology Research Institute, Tomsk NRMC of RAS, Tomsk, shamil@cardio-tomsk.ru, https://orcid.org/0000-0003-2758-7107

Kalyuzhin Vadim V. – Dr. Sci. (Med.), Professor, Head of the Division of Advanced-Level Therapy, Siberian State Medical University, Tomsk, kalyuzhinvv@mail.ru, http://orcid.org/0000-0001-9640-2028

Teplyakov Alexander T. – Dr. Sci. (Med.), Professor, Principal Researcher, Cardiology Research Institute, Tomsk NRMC of RAS, Tomsk, Vgelen1970@gmail.com, http://orcid.org/0000-0003-0721-0038

(✉) **Kopeva Kristina V.,** kristin-kop@inbox.ru

Received 11.02.2023;
approved after peer review 17.02.2023;
accepted 27.02.2022

УДК 616.36-008.52-056.7:577.213
https://doi.org/10.20538/1682-0363-2023-2-39-45

Study of molecular genetic markers of Gilbert's syndrome

Ivanova A.A.[1], Gurazheva A.A.[1], Mel'nikova E.S.[1], Nemcova E.G.[3], Maksimov V.N.[1, 2]

[1] Research Institute of Internal and Preventive Medicine – Branch of the Institute of Cytology and Genetics, Siberian Branch of the Russian Academy of Sciences
175/1, B. Bogatkova Str., Novosibirsk, 630089, Russian Federation

[2] Novosibirsk State Medical University (NSMU)
52, Krasnyj Prospekt Str., Novosibirsk, 630091, Russian Federation

[3] North-Western State Medical University named after I.I. Mechnikov
41, Kirochnaya Str., Saint-Petersburg, 191015, Russian Federation

ABSTRACT

Aim. To study new molecular genetic markers of Gilbert's syndrome (GS).

Materials and methods. It was a case – control study. The GS group included 125 people (mean age 38.5 ± 11.9 years, 58.9% were men) with unconjugated hyperbilirubinemia; known causes of unconjugated hyperbilirubinemia were excluded. The control group (n = 323, mean age 48.9 ± 11.9 years, 53.2% were men) was a random sample of individuals from the DNA bank of participants of the HAPIEE and MONICA projects. DNA was isolated by phenol – chloroform extraction from venous blood. Genotyping of groups by rs3064744, rs34993780, rs56059937, rs4148323, and rs4124874 single nucleotide polymorphisms (SNPs) in the *UGT1A1* gene was performed by polymerase chain reaction followed by the polyacrylamide gel analysis according to the author's protocols.

Results. For rs34993780 and rs56059937, no carriers of a rare allele were found in the GS group and the control group. In the GS group, two carriers of a heterozygous mutation rs4148323 were found. Statistically significant differences between the groups were found in the frequencies of rs4124874: homozygous GG was statistically significantly more common in the GS group than in the control group (odds ratio (OR) = 11.8, 95% confidence interval (CI) 6.9–20.3, $p < 0.001$).

Conclusion. The GG genotype of rs4124874 in the *UGT1A1* gene is associated with an increased risk of GS. Carriers of the rare heterozygous mutation rs4148323 were found in the GS group.

Keywords: Gilbert's syndrome, rs3064744, rs34993780, rs56059937, rs4148323, rs4124874, *UGT1A1* gene, unconjugated hyperbilirubinemia

Conflict of interest. The authors declare the absence of obvious and potential conflicts of interest related to the publication of this article.

Source of financing. The authors state that they received no funding for the study.

Conformity with the principles of ethics. All patients signed an informed consent to participate in the study. The study was approved by the Ethics Committee Research Institute of Internal and Preventive Medicine – Branch of the Institute of Cytology and Genetics, Siberian Branch of the Russian Academy of Sciences.

For citation: Ivanova A.A., Gurazheva A.A., Mel'nikova E.S., Nemcova E.G., Maksimov V.N. Study of molecular genetic markers of Gilbert's syndrome. *Bulletin of Siberian Medicine.* 2023;22(2):39–45. https://doi.org/10.20538/1682-0363-2023-2-39-45.

✉ *Ivanova Anastasiya A.,* ivanova_a_a@mail.ru

Исследование молекулярно-генетических маркеров синдрома Жильбера

Иванова А.А.[1], Гуражева А.А.[1], Мельникова Е.С.[1], Максимов В.Н.[1, 2], Немцова Е.Г.[3]

[1] Научно-исследовательский институт терапии и профилактической медицины (НИИТПМ) – филиал «Федеральный исследовательский центр Институт цитологии и генетики Сибирского отделения Российской академии наук» (ИЦиГ СО РАН)
Россия, 630089, г. Новосибирск, ул. Б. Богаткова, 175/1

[2] Новосибирский государственный медицинский университет (НГМУ)
Россия, 630091, г. Новосибирск, Красный проспект, 52

[3] Северо-Западный государственный медицинский университет (СЗГМУ) им. И.И. Мечникова
Россия, 191015, г. Санкт-Петербург, ул. Кирочная, 41

РЕЗЮМЕ

Цель исследования – поиск новых молекулярно-генетических маркеров синдрома Жильбера (СЖ).

Материалы и методы. Дизайн исследования – «случай – контроль». Группа СЖ включает 125 человек (средний возраст 38,5 ± 11,9 лет, 58,9% мужчин) с неконъюгированной гипербилирубинемией, у которых исключены известные ее причины. Группа контроля (n = 323, средний возраст 48,9 ± 11,9 лет, 53,2% мужчины) – случайная выборка лиц из банка ДНК участников проектов HAPIEE, MONICA. ДНК выделена методом фенолхлороформной экстракции из венозной крови. Генотипирование групп по вариантам нуклеотидной последовательности rs3064744, rs34993780, rs56059937, rs4148323, rs4124874 гена *UGT1A1* выполнено методом полимеразной цепной реакции с последующим анализом на полиакриламидном геле по авторским протоколам.

Результаты. По однонуклеотидным вариантам rs34993780, rs56059937 не найдено носителей редкого аллеля в группе СЖ и контрольной группе. В группе лиц с СЖ найдены два носителя мутации rs4148323 в гетерозиготной форме. По частотам однонуклеотидного варианта rs4124874 найдены статистически значимые различия между группами: гомозиготный генотип GG статистически значимо чаще встречается в группе СЖ по сравнению с контрольной группой (отношение шансов 11,8; 95%-й доверительный интервал 6,9– 20,3; $p < 0{,}001$).

Заключение. Генотип GG однонуклеотидного варианта rs4124874 гена *UGT1A1* ассоциирован с повышенным риском СЖ. В группе лиц с СЖ найдены носители редкой мутации rs4148323 в гетерозиготной форме.

Ключевые слова: синдром Жильбера, rs3064744, rs34993780, rs56059937, rs4148323, rs4124874, ген *UGT1A1,* неконъюгированная гипербилирубинемия

Конфликт интересов. Авторы декларируют отсутствие явных и потенциальных конфликтов интересов, связанных с публикацией настоящей статьи.

Источник финансирования. Исследование выполнено при финансовой поддержке Правительства Новосибирской области в рамках ГЗ № 122031700094-5.

Соответствие принципам этики. Все пациенты подписали информированное согласие на участие в исследовании. Исследование одобрено локальным этическим комитетом НИИ ТПМ – филиал ИЦиГ СО РАН, протокол № 24 от 26.04.2022.

Для цитирования: Иванова А.А., Гуражева А.А., Мельникова Е.С., Максимов В.Н., Немцова Е.Г. Исследование молекулярно-генетических маркеров синдрома Жильбера. *Бюллетень сибирской медицины.* 2023;22(2):39–45. https://doi.org/10.20538/1682-0363-2023-2-39-45.

INTRODUCTION

Gilbert's syndrome (GS) (jaundice, dyspeptic symptoms, asthenic vegetative syndrome, psychoemotional disorders) is a genetically determined form of unconjugated hyperbilirubinemia, which occurs in 2–10% of Europeans [1]. Currently, the available confirmatory testing for the diagnosis of GS is a molecular genetic study of the rs3064744 mutation (the number of TA repeats in the promoter) in the *UGT1A1* gene. It is known that carriage of a homozygous 7TA/ 7 TA mutation does not always lead to the development of clinical signs of GS, which is associated with low expressivity and penetrance of the genetic

variant [1]. In some cases, unconjugated hyperbilirubinemia can develop in the 6TA / 7TA and 6TA/ 6 TA genotypes of the rs3064744 mutation [2, 3].

It is assumed that there are other mutations that lead to the development of GS and affect the intensity of its clinical manifestations. The search for these mutations will help to confirm the diagnosis in individuals with clinical signs of GS, but without carriage of the homozygous 7TA/7TA genotype of the rs3064744 mutation.

The aim of the study was to search for new molecular genetic markers of GS.

MATERIALS AND METHODS

It was a case – control study.

The GS group (n = 125, mean age 38.5 ± 11.9 years, 58.9% were men) was formed by gastroenterologists. It included persons with unconjugated hyperbilirubinemia who underwent a standard clinical examination. Individuals with known causes of unconjugated hyperbilirubinemia were excluded from the group. DNA was isolated from venous blood by phenol – chloroform extraction.

The control group (n = 323, mean age 48.9 ± 11.9 years, 53.2% were men) was a random sample of individuals from the DNA bank of participants of the HAPIEE and MONICA projects. DNA was isolated from the venous blood by phenol – chloroform extraction.

For 104 people from the GS group, molecular genetic diagnosis was previously performed to determine the number of TA repeats in the promoter of the *UGT1A1* gene (rs3064744) [3]. The number of TA repeats in the promoter of the *UGT1A1* gene was determined in the control group and 21 remaining persons from the GS group by polymerase chain reaction followed by the polyacrylamide gel analysis (Fig. 1).

For rs3064744 genotyping, the following primers were used: 5'-AACATTAACTTGGTGTATCGATTGG-3'(F) and 5'-CTTTGCTCCTGCCAGAGGTTC-3'(R). The 25 µl PCR mixture included: 75 mM Tris-HCI (pH 9.0), 20 mM $(NH_4)_2SO_4$, 0.01% Tween 20 solution, 3.0 mM $MgCl_2$, 0.8 mM of each primer, 0.2 mM dNTP mixture, 2 µg DNA, and 1 unit of DNA polymerase. Amplification was carried out under the following temperature conditions: 33 cycles, including denaturation at 95 °C for 30 seconds, primer annealing at 57 °C for 30 seconds, and elongation at 72 °C for 30 seconds. The size of the amplification product was 82 bp for the 6TA / 6TA genotype, 82 bp and 84 bp for the 6TA / 7TA genotype, and 84 bp for the 7TA / 7TA genotype.

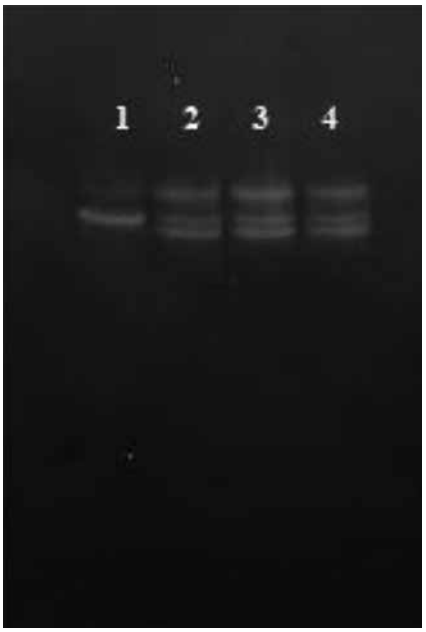

Fig. 1. The electropherogram of rs3064744 mutation amplification products on polyacrylamide gel: 1 – 7TA / 7TA genotype, 2, 3 –6TA / 7TA genotype, 4 – control sample with the 6TA / 7TA genotype

According to the literature, four single nucleotide polymorphisms (SNPs) of the *UGT1A1* gene were selected for the study as new molecular genetic markers of GS: rs34993780 (*UGT1A1*7*), rs56059937 (*UGT1A*62*), rs4148323 (*UGT1A1*6*), and rs4124874 (*UGT1A1*60*). Genotyping was carried out by the polymerase chain reaction followed by the polyacrylamide gel analysis of restriction fragment length polymorphism according to the author's protocols.

For rs34993780 genotyping, the following primers were used: 5'-AGTTTGTGATGAGGCACA-3'(F) and 5'-TTCTTAACTCGCCCTTTT -3'(R). The 25 µl PCR mixture included: 10 µl of a RT-PCR mixture No. M-428 (2.5 ×) (Syntol, Russian Federation), 1.2 mM $MgCl_2$, 0.6 mM of each primer, 2 µg of DNA. Amplification was carried out under the following temperature conditions: 33 cycles, including denaturation at 95 °C for 30 seconds, primer annealing at 56 °C for 30 seconds, and elongation at 72 °C for 20 seconds. Restriction was performed with 10 units of the RsaI restriction enzyme (SibEnzyme, Novosibirsk). The size of the amplification product was 190 bp. After restriction, products of 121 bp, 63 bp, and 6 bp were detected for the TT genotype, products of 127 bp and 63 bp were detected for the GG genotype, and all listed products were detected for the heterozygous TG genotype (127 bp, 121 bp, 63 bp, 6 bp).

For rs56059937 genotyping, the following primers were used: 5'-ACCTTGAAGACGTACCCTGTGGTA-3'(F) and 5'-TGATCACACGCTGCAGGA-3'(R). The 25 µl PCR mixture included: 12.5 µl of the BioMaster LR HS-PCR-Color (2×) reaction mixture (BIOLABMIX, Novosibirsk), 1.0 mM of each primer, 2 µg of DNA. Amplification was carried out under the following temperature conditions: 35 cycles, including denaturation at 95 °C for 30 seconds, primer annealing at 60 °C for 30 seconds, and elongation at 72 °C for 30 seconds. Restriction was performed with 10 units of the RsaI restriction enzyme (SibEnzyme, Novosibirsk). The size of the amplification product was 109 bp. After restriction, 96 bp and 13 bp products were detected for the TT genotype, 85 bp, 13bp, and 11 bp products were detected for the CC genotype, and all listed products were detected for the heterozygous TC genotype (96 bp, 85 bp, 13 bp, 11 bp).

For rs4148323 genotyping, the following primers were used: 5'-GTCCCATGCTGGGAAGATACTGTT-3'(F) and 5'-ACGTCTTCAAGGTGTAAAATGGGC-3'(R). The 25 µl PCR mixture included: 12.5 µl of the BioMaster LR HS-PCR-Color reaction mixture (2×) (BIOLABMIX, Novosibirsk), 1.2 mM of each primer, 2 µg of DNA. Amplification was carried out under the following temperature conditions: 35 cycles, including denaturation at 95 °C for 30 seconds, primer annealing at 60 °C for 30 seconds, and elongation at 72 °C for 30 seconds. Restriction was performed with 10 units of the HaeIII restriction enzyme (SibEnzyme, Novosibirsk). The size of the amplification product was 164 bp. After restriction, 99 bp and 65 bp products were detected for the AA genotype, 75 bp, 65 bp, and 24 bp products were detected for the GG genotype, and all listed products were detected for the heterozygous GA genotype (99 bp, 75 bp, 65 bp, 24 bp).

For rs4124874 genotyping, the following primers were used: 5'-GATTAACCAAAGAACATTCTAACGG-3'(F) and 5'-TGATGTTCTCAAATTGCTTTGTTCG -3'(R). The 25 µl PCR mix included: 75 mM Tris-HCI (pH 9.0), 20 mM $(NH_4)_2SO_4$, 0.01% Tween 20, 3.5 mM $MgCl_2$, 1.2 mM of each primer, 0.2 mM dNTP mixture, 2 µg DNA, 1 unit of DNA polymerase. Amplification was carried out under the following temperature conditions: 35 cycles, including denaturation at 95 °C for 30 seconds, primer annealing at 60 °C for 30 seconds, and elongation at 72 °C for 30 seconds. Restriction was carried out with 10 units of the TaqI restriction enzyme (SibEnzim, Novosibirsk). The size of the amplification product was 209 bp. After restriction, a 209 bp product was detected for the GG genotype, 186 bp and 23 bp products were detected for the TT genotype, and all listed products were detected for the heterozygous TG genotype (209 bp, 186 bp, 23 bp).

The results of the genotyping were statistically processed, using the chi-square test. The correspondence of genotype frequencies to the Hardy – Weinberg equilibrium in the control group was assessed. Comparison of the groups by genotype and allele frequencies and a relative risk for a particular allele or genotype were calculated by contingency tables using the Pearson's chi-square test and the Fisher's exact test with the Yates' continuity correction. The differences were statistically significant at $p < 0.05$.

RESULTS

The search for molecular genetic markers of GS was started in 2012–2016, when the rs3064744 mutation (the number of TA repeats in the promoter) in the *UGT1A1* gene was determined in a group of individuals with unconjugated hyperbilirubinemia (n = 104) [3]. Currently, the group has been extended to 125 people. Genotype frequencies of the rs3064744 mutation in the extended group are shown in Fig. 2. In the control group, formed from the DNA bank of the participants in the HAPIEE and MONICA projects, the rs3064744 mutation of the *UGT1A1* gene was also searched for. 12% of persons from the control group were carriers of the homozygous 7TA / 7TA variant (Fig. 2). Statistically significant differences between the groups were found by the genotype frequencies in the rs3064744 mutation ($p < 0.001$). The 7TA / 7TA genotype of the rs3064744 mutation was more common in the GS group than in the control group (odds ratio (OR) 12.9, 95% confidence interval (CI) 7.9–21.3, $p < 0.001$).

No carriers of the rare allele in rs34993780 (*UGT1A1*7*) and rs56059937 (*UGT1A*62*) were found in the GS group and the control group. Two carriers of a heterozygous rs4148323 mutation (*UGT1A1*6*) were found in the GS group. Both patients were also heterozygous carriers of the rs3064744 mutation in the *UGT1A1* gene (6TA / 7TA).

The genotype frequencies of the rs4124874 variant (*UGT1A1*60*) comply with the Hardy – Weinberg equilibrium in the control group (χ^2= 3.81). Significant differences between the groups were found by frequencies of rs4124874 (*UGT1A1*60*) ($p < 0.001$) (Fig. 3). The homozygous genotype GG was significantly more common in the GS group than in the con-

trol group (OR 11.8, 95% CI 6.9–20.3, $p < 0.001$). The G allele of the rs4124874 variant was a risk allele for GS (OR 7.4, 95% CI 4.9–11.1, $p < 0.001$).

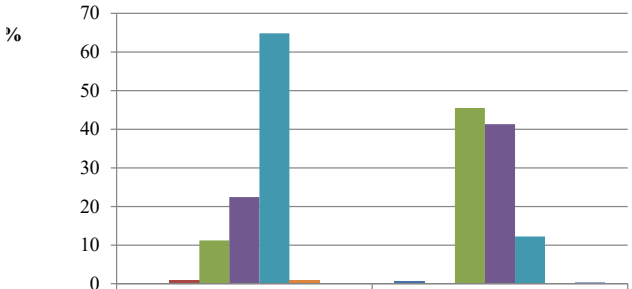

	GS group	Control group
5TA/6TA	0	0.7
5TA/7TA	0.8	0
6TA/6TA	11.2	45.5
6TA/7TA	22.4	41.3
7TA/7TA	64.8	12.2
6TA/8TA	0.8	0
6TA/9TA	0	0.3

Fig. 2. Genotype frequencies of rs3064744 in the GS and control groups

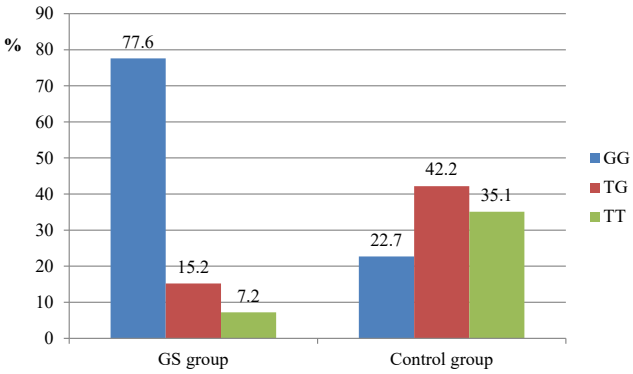

Fig. 3. Genotype frequencies of rs4124874 in the GS and control groups

There are literature data that indicate that the rs4124874 variant is linked to the rs3064744 promoter variant [4]. Combinations of rs4124874 and rs3064744 genotypes in the GS group are presented in Table.

Table

Combinations of rs4124874 and rs3064744 genotypes in the GS group

		rs4124874		
		GG	TG	TT
rs3064744	5TA/7TA	1	0	0
	6TA/6TA	3	2	9
	6TA/7TA	14	14	0
	6TA/8TA	1	0	0
	7TA/7TA	76	3	0

The combination of 7TA / 7TA genotype of rs3064744 and GG genotype of rs4124874 was significantly more common (OR 14.9, 95% CI 8.1–27.4, $p < 0.001$) in the GS group than in the control group. The combinations of the 6TA / 7TA genotype of rs3064744 and TG genotype of rs4124874 (OR 0.22, 95% CI 0.05–0.98, $p = 0.032$), 6TA / 6TA genotype of rs3064744 and TT genotype of rs4124874 (OR 0.16, 95% CI 0.07–0.33, $p < 0.001$), as well as 6TA / 7TA genotype of rs3064744 and TG genotype of rs4124874 (OR 0.25, 95% CI 0.13–0.47, $p < 0.001$) were less common in the GS group than in the control group.

DISCUSSION

According to the results of the study, in 64.8% of persons from the GS group, the number of TA repeats (rs3064744) in the promoter of the *UGT1A1* gene was increased to seven in two copies of the gene, which, according to the literature, is associated with a decrease in the activity of the UDP-glucuronosyltransferase 1A1 enzyme and can lead to development of clinical symptoms of GS [5, 6]. 22.4% of individuals with unconjugated hyperbilirubinemia were carriers of the 6TA / 7TA genotype of rs3064744, and 11.2% had the normal 6TA / 6TA genotype. Moreover, there were carriers of rare genotypes (5TA / 7TA and 6TA / 8TA) in the group. The predominant number of persons from the control group were carriers of the 6TA / 6TA and 6TA / 7TA genotypes, in which the development of clinical symptoms of GS most often did not occur (86.8%). However, the control group contained carriers of the 7TA / 7TA genotype (12.2%), as well as carriers of rare 5TA / 6TA and 6TA / 9TA genotypes. The control group was a random sample from the DNA bank of participants of the HAPIEE and MONICA projects. For the control group, there were no data on previous episodes of unconjugated hyperbilirubinemia or diagnosed GS. There might be a small number of individuals with diagnosed or undiagnosed GS in the control group. However, the area of research interest was individuals from the GS group with the 6TA / 6TA, 6TA / 7TA genotypes, and unconjugated hyperbilirubinemia, in which other causes, except for genetic ones, were excluded.

The rs34993780 (*UGT1A1*7*), rs56059937 (*UGT1A1*62*), and rs4148323 (*UGT1A1*6*) mutations are associated with the development of GS [5–9]. At the same time, these variants are common for GS in Asians; we did not find any studies on variants in relation to GS in Europeans. According to the study,

there were no carriers of rare alleles of the rs34993780 (*UGT1A1*7*) and rs56059937 (*UGT1A*62*) mutations in the GS group and the control group, which may indicate a really small contribution of these variants to the development of GS in Caucasians. However, to confirm this conclusion, it is necessary to conduct a study on a larger sample of individuals with GS.

In the SG group, two heterozygous carriers of the rs4148323 (*UGT1A1*6*) variant were identified, who were also carriers of the heterozygous 6TA / 7TA genotype of the rs3064744 mutation. It is known that the rs4148323 (*UGT1A1*6*) variant in the homozygous form is associated with the development of GS and a decrease in the activity of the UDP-glucuronosyltransferase 1A1 enzyme by 70% compared to the wild type [5]. Two people from the GS group with unconjugated hyperbilirubinemia were highly likely to be compound heterozygotes for variants that are associated with the development of GS in the homozygous form.

It can be assumed that individuals with clinical symptoms of GS, but with the 6TA / 6TA and 6TA / 7TA genotypes of the rs3064744 mutation are carriers of other *UGT1A1* gene mutations, which causes a change in the activity of the enzyme and clinical manifestations of the syndrome. Therefore, for individuals with the 6TA / 6TA and 6TA / 7TA genotypes of the rs3064744 mutation, unconjugated hyperbilirubinemia, and suspected GS, Sanger sequencing of the *UGT1A1* gene may be more effective to search for other pathogenic variants of the nucleotide sequence of the gene that cause the development of clinical manifestations of GS.

The rs4124874 variant (*UGT1A1*6*, g.172270T>G) is a common variant in the population; the rare allele frequency is about 0.43 for Europeans (gnomAD). The G allele frequency in the control group according to our results is 0.44. The variant is associated with the transcriptional activity of the *UGT1A1* gene and is involved in the development of clinical symptoms of GS in the presence of other variants of the *UGT1A1* gene [10]. According to ClinVar, rs4124874 is a variant with conflicting interpretations of pathogenicity (likely pathogenic, pathogenic, benign, GS risk factor). According to our study, the GG genotype and the G allele of the rs4124874 variant are a risk genotype and a risk allele for GS.

Combinations of the 6TA / 6TA genotype of rs3064744, the TG or TT genotype of rs4124874, the 6TA / 7TA genotype of rs3064744, and the TG genotype of rs4124874 are significantly more common in the control group, which indicates that most likely these combinations of genotypes do not lead to the development of GS.

CONCLUSION

The rs4124874 SNP of the *UGT1A1* gene is associated with GS: the GG genotype and the G allele of the variant are the risk genotype and the risk allele for GS. In the GS group, carriers of the rare heterozygous rs4148323 mutation (UGT1A1*6) were found, who were also carriers of the 6TA / 7TA genotype of the rs3064744 mutation. According to the results of the study, we can conclude that the rs3064744 mutation is not the only important factor in the development of clinical symptoms of GS.

The molecular genetic study of the number of TA repeats in the promoter of the *UGT1A1* gene (rs3064744) is a necessary and first step in the molecular genetic diagnosis of GS, because in almost 65% of cases it is sufficient and allows to identify the 7TA / 7TA genotype, which is associated with GS.

For individuals with the 6TA / 6TA or 6TA / 7TA genotypes of the rs3064744 mutation, unconjugated hyperbilirubinemia, and suspected GS, the next effective step in the molecular genetic diagnosis should be Sanger sequencing of the *UGT1A1* gene to search for other mutations and variants that may cause the development of clinical manifestations of GS.

REFERENCES

1. King D., Armstrong M.J. Overview of Gilbert's syndrome. *Drug Ther. Bull*. 2019;57(2):27–31. DOI: 10.1136/dtb.2018.000028. PMID: 30709860.
2. Kringen M.K., Piehler A.P., Grimholt R.M., Opdal M.S., Haug K.B., Urdal P. Serum bilirubin concentration in healthy adult North-Europeans is strictly controlled by the UGT1A1 TA-repeat variants. *PLoS One*. 2014;9(2):e90248. DOI: 10.1371/journal.pone.0090248.
3. Maruo Y., D'Addario C., Mori A., Iwai M., Takahashi H., Sato H. et al. Two linked polymorphic mutations (A(TA)7TAA and T-3279G) of UGT1A1 as the principal cause of Gilbert syndrome. *Hum. Genet.* 2004;115(6):525–526. DOI: 10.1007/s00439-004-1183-x.
4. Steventon G. Uridine diphosphate glucuronosyltransferase 1A1. *Xenobiotica*. 2020;50(1):64–76. DOI: 10.1080/00498254.2019.1617910.
5. Gazzin S., Masutti F., Vitek L., Tiribelli C. The molecular basis of jaundice: An old symptom revisited. *Liver Int*. 2017;37(8):1094–1102. DOI: 10.1111/liv.13351.
6. Udomuksorn W., Elliot D.J., Lewis B.C., Mackenzie P.I., Yoovathaworn K., Miners J.O. Influence of mutations associated with Gilbert and Crigler-Najjar type II syndromes on the glucuronidation kinetics of bilirubin and other UDP-glucuronosyltransferase 1A substrates. *Pharmacogenet Genomics*. 2007;17(12):1017–1029. DOI: 10.1097/

FPC.0b013e328256b1b6.
7. Zhou J., Yang C., Zhu W., Chen S., Zeng Y., Wang J. et al. Identification of Genetic Risk Factors for Neonatal Hyperbilirubinemia in Fujian Province, Southeastern China: A Case-Control Study. *Biomed. Res. Int.* 2018;2018:7803175. DOI: 10.1155/2018/7803175.
8. Bale G., Avanthi U.S., Padaki N.R., Sharma M., Duvvur N.R., Vishnubhotla V.R.K. Incidence and risk of gallstone disease in Gilbert's syndrome patients in indian population. *J. Clin. Exp. Hepatol*. 2018;8(4):362–366. DOI: 10.1016/j.jceh.2017.12.006.
9. Sugatani J., Yamakawa K., Yoshinari K., Machida T., Takagi H., Mori M. et al. Identification of a defect in the UGT1A1 gene promoter and its association with hyperbilirubinemia. *Biochem. Biophys. Res. Commun.* 2002;292(2):492–497. DOI: 10.1006/bbrc.2002.6683.

Authors' contribution

Ivanova A.A. – formation of groups, conception and design, statistical processing of the data, analysis and interpretation of the data. Gurazheva A.A., Mel'nikova E.S. – carrying out of the molecular genetic study. Nemcova E.G. – formation of the GS group. Maksimov V.N. – critical revision of the manuscript for important intellectual content, final approval of the manuscript for publication.

Authors' information

Ivanova Anastasiya A. – Cand. Sci. (Med.), Senior Researcher, Laboratory for Molecular and Genetic Studies of Internal Diseases, Research Institute of Internal and Preventive Medicine – Branch of the Institute of Cytology and Genetics, Siberian Branch of the Russian Academy of Sciences, Novosibirsk, ivanova_a_a@mail.ru, http://orcid.org/0000-0002-9460-6294

Gurazheva Anna A. – Junior Researcher, Laboratory for Molecular and Genetic Studies of Internal Diseases, Research Institute of Internal and Preventive Medicine – Branch of the Institute of Cytology and Genetics, Siberian Branch of the Russian Academy of Sciences, Novosibirsk, annapalna1@mail.ru, http://orcid.org/0000-0003-1547-624X

Mel'nikova Elizaveta S. – Junior Researcher, Laboratory for Molecular and Genetic Studies of Internal Diseases, Research Institute of Internal and Preventive Medicine – Branch of the Institute of Cytology and Genetics, Siberian Branch of the Russian Academy of Sciences, Novosibirsk, jarinaleksi@list.ru, http://orcid.org/0000-0002-9033-1588

Nemcova Elena G. – Cand. Sci. (Med.), Associate Professor, Department of Propaedeutics of Internal Diseases, Gastroenterology and Dietology named after S. M. Ryss, Faculty of Medicine, North-Western State Medical University named after I.I. Mechnikov, St. Petersburg, neg-85@yandex.ru, http://orcid.org/0000-0003-1501-6796

Maksimov Vladimir N. – Dr. Sci. (Med.), Professor, Head of the Laboratory for Molecular and Genetic Studies of Internal Diseases, Research Institute of Internal and Preventive Medicine – Branch of the Institute of Cytology and Genetics, Siberian Branch of the Russian Academy of Sciences; Professor, Department of Medical Genetics and Biology, Faculty of Preventive Medicine, Novosibirsk State Medical University, Novosibirsk, medik11@mail.ru, http://orcid.org/0000-0002-7165-4496

(✉) **Ivanova Anastasiya A.,** ivanova_a_a@mail.ru

Received 02.11.2022;
approved after peer review 16.11.2022;
accepted 08.12.2022

УДК 576.3.08:57.086.1
https://doi.org/10.20538/1682-0363-2023-2-46-52

Viability of mononuclear cells in leukocyte concentrates at the stages of their preparation, freezing, and thawing

Isaeva N.V., Minaeva N.V., Utemov S.V., Sherstnev Ph.S., Zorina N.A., Zmeeva Yu.S., Butolina M.A.

Kirov Research Institute of Hematology and Blood Transfusion
72, Krasnoarmeyskaya Str., Kirov, 610027, Russian Federation

ABSTRACT

Aim. To evaluate the viability of mononuclear cells (MNCs) in leukocyte concentrates (LCs) at the stages of their preparation, freezing, and thawing.

Materials and methods. The study material included 44 LCs from donors of allogeneic hematopoietic stem cells (HSCs) and 189 autologous LCs from patients with oncohematological disorders. LCs were obtained from donors and patients by leukocytapheresis after mobilization of HSCs. LCs from patients were frozen with dimethyl sulfoxide (DMSO) used as a cryoprotectant at a final concentration of 5% and stored in liquid nitrogen. LCs were thawed before transplantation. A total of 161 LCs were immediately transfused to the recipient after thawing, and 28 LCs were washed from DMSO before transfusion. Flow cytofluorometry was used to determine the percentage of MNC populations that excluded 7-aminoactinomycin D (7-AAD).

Results. The viability of peripheral blood MNCs in donors and patients was close to 100%. It was found that leukocytapheresis and cryopreservation with DMSO did not affect the viability of MNCs. The freezing of LCs with DMSO, storage in liquid nitrogen, and thawing resulted in a significant decrease in the content of viable MNCs (p = 0.0025), while no effect of LC storage duration on the viability of MNCs was revealed. Following DMSO removal from LCs, significantly more HSCs remained in a viable state than without washing (94.4 [94.5; 95.2] % vs. 86.7 [67.6; 92.9] %, (p = 0.0051); for other MNC populations, except monocytes, the differences in the viability index were also statistically significant.

Conclusion. The viability of MNCs in LCs is recommended to be used as an independent characteristic of the transplant quality. In obtaining LCs and mixing them with the cryoprotectant DMSO, the viability of MNCs does not decrease, while in thawed LCs, it decreases significantly. Thawing of LCs with removal of DMSO allows to achieve the best viability of HSCs and most MNC populations.

Keywords: leukocyte concentrate, viability, 7-aminoactinomycin D, mononuclear cells, hematopoietic stem cells, dimethyl sulfoxide

Conflict of interest. The authors declare the absence of obvious and potential conflicts of interest related to the publication of this article.

Source of financing. The authors state that they received no funding for the study.

Conformity with the principles of ethics. The protocol of the study was approved by the local Ethics Committee at Kirov Research Institute of Hematology and Blood Transfusion (Protocol No. 27 of 23.09.2021).

For citation: Isaeva N.V., Minaeva N.V., Utemov S.V., Sherstnev Ph.S., Zorina N.A., Zmeeva Yu.S., Butolina M.A. Viability of mononuclear cells in leukocyte concentrates at the stages of their preparation, freezing, and thawing. *Bulletin of Siberian Medicine.* 2023;22(2):46–52. https://doi.org/10.20538/1682-0363-2023-2-46-52.

✉ *Isaeva Natalia V.,* isaevanatalia@yandex.ru

Жизнеспособность ядросодержащих клеток в лейкоконцентратах на этапах их получения, замораживания и декриоконсервирования

Исаева Н.В., Минаева Н.В., Утемов С.В., Шерстнев Ф.С., Зорина Н.А., Змеева Ю.С., Бутолина М.А.

Кировский научно-исследовательский институт гематологии и переливания крови (КНИИГиПК)
Россия, 610027, г. Киров, ул. Красноармейская, 72

РЕЗЮМЕ

Цель – оценить жизнеспособность ядросодержащих клеток (ЯСК) в лейкоконцентратах (ЛК) на этапах их получения, замораживания и декриоконсервирования.

Материалы и методы. Материал исследования – 44 ЛК доноров аллогенных гемопоэтических стволовых клеток (ГСК) и 189 аутологичных ЛК онкогематологических больных. Лейкоконцентраты доноров и больных получали методом автоматического лейкоцитафереза после мобилизации ГСК. Лейкоконцентраты больных замораживали под защитой диметилсульфоксида (ДМСО) с конечной концентрацией 5% и хранили в жидком азоте. Лейкоконцентраты декриоконсервировали перед трансплантацией, 161 ЛК после декриоконсервирования сразу переливали реципиенту, 28 ЛК перед переливанием отмывали от ДМСО. Процент не пропускающих 7-аминоактиномицин D (aminoactinomycin D, 7-AAD) популяций ЯСК определяли методом проточной цитофлуориметрии.

Результаты. Жизнеспособность ЯСК периферической крови доноров и больных приближалась к 100%. Показано отсутствие влияния аппаратного лейкоцитафереза и процедуры смешивания с ДМСО на жизнеспособность ЯСК. Замораживание ЛК под защитой ДМСО, хранение в жидком азоте и их декриоконсервирование приводили к значимому снижению содержания жизнеспособных ЯСК (p = 0,0025), при этом влияние длительности хранения ЛК на жизнеспособность ЯСК не выявлено. В результате отмывания от ДМСО в жизнеспособном состоянии сохраняется существенно больше ГСК, чем без отмывания (94,4 [94,5; 95,2]% против 86,7 [67,6; 92,9]%; p = 0,0051); для других популяций ЯСК, кроме моноцитов, различия показателя жизнеспособности также статистически значимы.

Заключение. Жизнеспособность ЯСК в ЛК рекомендуется использовать как самостоятельную характеристику качества трансплантата. В процессе получения ЛК и их смешивания с криоконсервантом ДМСО жизнеспособность ЯСК не снижается, а в декриоконсервированных ЛК значительно падает. Декриоконсервирование ЛК с отмыванием от ДМСО позволяет достигать лучшей жизнеспособности ГСК и большинства популяций ЯСК.

Ключевые слова: лейкоконцентрат, жизнеспособность, 7-аминоактиномицин D, ядросодержащие клетки, гемопоэтические стволовые клетки, диметилсульфоксид.

Конфликт интересов. Авторы декларируют отсутствие явных и потенциальных конфликтов интересов, связанных с публикацией настоящей статьи.

Источники финансирования. Авторы заявляют об отсутствии финансирования при проведении исследования.

Соответствие принципам этики. Исследование одобрено локальным этическим комитетом КНИИГиПК (протокол № 27 от 23.09.2021).

Для цитирования: Исаева Н.В., Минаева Н.В., Утемов С.В., Шерстнев Ф.С., Зорина Н.А., Змеева Ю.С., Бутолина М.А.Жизнеспособность ядросодержащих клеток в лейкоконцентратах на этапах их получения, замораживания и декриоконсервирования. *Бюллетень сибирской медицины.* 2023;22(2):46–52. https://doi.org/10.20538/1682-0363-2023-2-46-52.

INTRODUCTION

Hematopoietic stem cell transplantation (HSCT) is an effective method of therapy for hemoblastosis and hematopoietic depressions [1, 2]. In modern conditions, the transplant material, leukocyte concentrates (LCs) with a sufficient content of hematopoietic stem cells (HSCs), can be obtained by leukocytapheresis. If it is necessary to preserve the transplant material for a long time (more than 72 hours), the technologies of its freezing with cryoprotectants are used. [3]. Kirov Re-

search Institute of Hematology and Blood Transfusion of the Federal Medical and Biological Agency has accumulated many years of experience in carrying out transplantations of autologous and allogeneic HSCs and harvesting allogeneic HSCs for other transplant centers [4].

Obtaining transplant material involves several technological procedures that ensure stable transplant function and guarantee the success of HSCT. The ability to restore hematopoiesis in the recipient is directly related to the transfused dose of HSCs. In accordance with the requirements of the European Society on Blood and Bone Marrow Transplantation, quality control of the cellular product is mandatory, the calculation of HSC is required, and it is necessary to assess cellular elements that are potentially capable of harming the patient. In cases where the product is subject to any manipulations affecting its composition, confirmation of the viability of cells in the product becomes particularly relevant (URL:https://www.ebmt.org/8th-edition-fact-jacie-standards, accessed: 13.10.21).

Currently, HSCs are evaluated in accordance with the recommendations of the International Society of Hematotherapy and Graft Engineering (ISHAGE) [5]. A HSC-containing LC is a sufficiently heterogeneous cellular product [6]. The ISHAGE protocol regulating the calculation of HSCs is widely used for the certification of a cell product, but such an assessment does not provide any information about the viability of cells. Viable MNCs are cells whose membrane remains non-permeable to nuclear staining dyes. Viability testing can be based on supravital staining of cell samples with various dyes. Currently, it has become possible to use fluorescent DNA dyes, such as propidium iodide, 7-aminoactinomycin D, and SYTO dyes [7].

A decrease in the number of viable leukocytes during LC storage can negatively affect the calculated value of the target transplantation dose of HSCs and the parameters of engraftment [8], while an increase in the proportion of non-viable cells in LC can lead to the emergence of various cell degradation products in it [9].

The aim of the study was to evaluate the viability of MNCs in LCs at the stages of their preparation, freezing, and thawing.

MATERIALS AND METHODS

The material for the study was blood and LC samples from donors of allogeneic HSCs, as well as patients with oncohematological disorders. The blood samples were taken for examination immediately before the start of leukocytapheresis. The LCs of the donors and patients were harvested using an anticoagulant for automatic leukocytapheresis. The LCs of the patients were cryopreserved by mixing with a solution of DMSO at a final concentration of 5% and dextran. LCs were frozen in liquid nitrogen vapors at 30–35 cm above the surface of liquid nitrogen (–145…–160 °C), followed by transfer to the liquid nitrogen medium.

Immediately before transplantation, 161 LCs were thawed in an aqueous medium at a temperature of 39–41 °C, then the LCs were transfused to the patient. Another part of HSC-containing LCs (n = 28) was washed from DMSO after thawing by adding a mixture of albumin and polyglukin to the cell suspension (in a ratio of 1:4). After centrifugation at 2,000g for 5 min, the supernatant was removed, and the cell precipitate was resuspended in a mixture of albumin and polyglukin. The stages of preparation of the transplant material are shown in Fig. 1.

Stages of studying the viability of MNCs	Transplantation material	
	Allogenic HSCs (n = 44)	Allogenic HSCs (n = 44)
1. Mobilization of HSCs	peripheral blood	peripheral blood
2. Obtaining LCs by leukocytapheresis	native LCs	native LCs
3. Mixing LCs with DMSO		LCs mixed with DMSO
4. Freezing LCs, storage of LCs in liquid nitrogen vapor, thawing of LCs	LCs without washing from DMSO (n = 161)	LCs washed from DMSO (n = 28)

Fig. 1. Assessment of MNC viability (stages, material)

Blood and LC samples were diluted with a phosphate-buffered saline (PBS) containing 0.5% bovine serum albumin to achieve a leukocyte concentration of 5×10^9 / l. The samples were incubated in the dark for 15 min at a temperature of 20–24 °C with conjugates of monoclonal antibodies to CD45 and CD34 with fluorochromes, fluorescein isothiocyanate, and phycoerythrin, respectively, and with a 7-AAD solution. The samples were tested on the BD FACSCanto™ II flow cytometer (BD Biosciences, USA). We took into account the proportion of 7-AAD-negative events in each MNC population.

STADIA (Russian Federation) and Microsoft Excel were used for statistical analysis of the obtained results. The data were presented as the median and the interquartile range *Me* (Q_{25}; Q_{75}). We used the Van der Waerden test to perform a comparative analysis of unrelated aggregates and the Wilcoxon test for related ones. In multiple comparisons, the values of the criteria were determined using the Bonferroni correction. The correlation was established by calculating the Spearman's rank correlation coefficient. The differences were considered statistically significant at $p < 0.05$.

RESULTS

The number of 7-AAD-negative MNCs in the blood taken before the start of leukocytapheresis from the donors and patients turned out to be comparable (99.8 (97.5; 99.9)% and 99.7(98.1; 99.9)%, respectively, $p = 0.1109$). The content of viable MNCs in native LC in the donors was 99.6 (98.5; 99.8)%, in the patients – 98.4 (97.5; 99.8)%. The obtained values did not differ from those in the blood samples from which LCs were prepared ($p = 0.1241$ for the donor group; $p = 0.0893$ for the patient group).

The difference in the proportion of 7-AAD-negative MNCs in native LCs of the patients and in LCs mixed with DMSO was not statistically significant (Table 1). There was a significant decrease in the viability of MNCs in LCs after thawing. An increase in the permeability of the MNC membranes for the vital 7-AAD dye was recorded in the LC samples that were thawed both without additional manipulation – washing from DMSO, and with it. The relative number of 7-AAD-negative MNCs in the LCs that were not washed from DMSO turned out to be significantly lower than in the LCs after washing from DMSO.

The relationship between the proportion of viable cells and the storage time of patients' LCs in the frozen state before thawing and transplantation was studied, a correlation between these two parameters was not revealed ($r = 0.11$).

Table 1

Content of viable mononuclear cells in leukocyte concentrates, *Me* (Q_{25}; Q_{75})

Stages of viability control of MNCs in LCs		Content of 7-AAD-negative cells, %
Native LC, $n = 189$	I	98.4 (97.5; 99.8)
LC mixed with DMSO, $n = 189$	II	96.1 (94.0; 98.8)
LC without washing from DMSO, $n = 161$	III	80.6 (76.0; 89.4)
LC after washing from DMSO, $n = 28$	IV	92.2 (85.2; 96.4)
p		I–II = 0.1124; II–III = 0.0025; II–IV = 0.0087; III–IV = 0.0054

Fig. 2 shows the distribution of thawed LCs of the patients according to the content of viable MNCs in them. Three ranges of viability were taken into account: 80% or less, 90–80.1%, and 95.5–90.1%. In the LCs washed from DMSO, critical levels (from 80% to 62.2%) of MNC viability were recorded in 7.1% (2 out of 28) of cases, in the unwashed LCs – in 44.1% (71 out of 161) of cases.

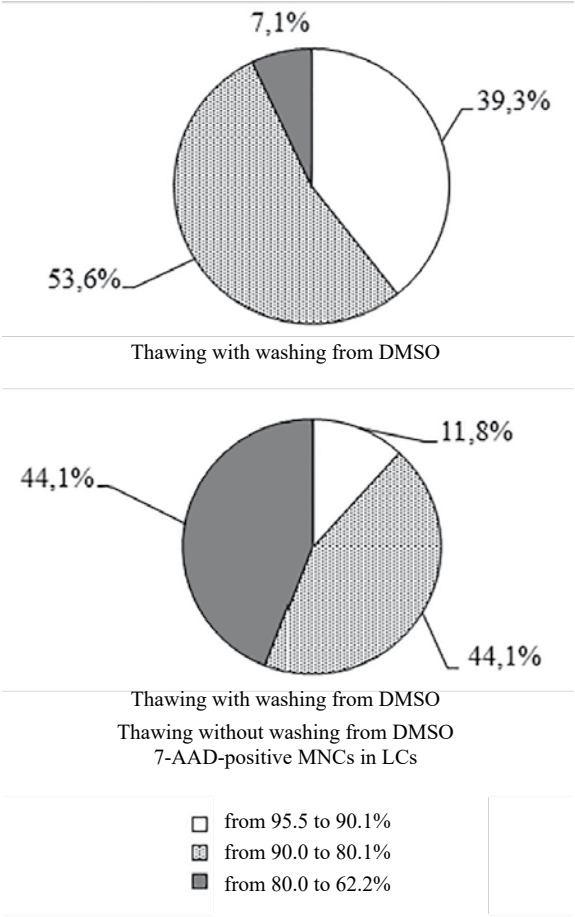

Fig. 2. Distribution of thawed leukocyte concentrates according to the content of viable mononuclear cells

Among all MNCs, the HSC content was 0.6%; lymphocytes – 44.6%, monocytes – 31.5%, granulocytes – 21.9%, erythrokaryocytes – 1.4%. The population of granulocytes that were thawed and were not washed from DMSO turned out to be the least viable (Table 2). In the LCs thawed with subsequent washing from DMSO, higher viability values of most cell populations were revealed compared to those in the LCs which were not washed. The only exception was the population of monocytes.

Table 2

Content of viable mononuclear cells in thawed leukocyte concentrates, *Me* (Q_{25}; Q_{75})

Types of MNCs	The content of 7-AAD-negative cells		*p*
	in LCs without washing from DMSO, %	in LCs washed from DMSO, %	
Leucocytes	81.8 (75.1; 90.4)	89.3 (86.3; 93.7)	0.0338
HSC	86.7 (67.6; 92.9)	94.4 (94.5; 95.2)	0.0051
– lymphocytes	93.4 (87.9; 96.9)	95.5 (93.5; 97.7)	0.0455
– monocytes	94.9 (93.5; 96.0)	97.4 (98.1; 92.6)	0.0718
– granulocytes	36.7 (22.8; 53.5)	58.8 (52.1; 65.6)	0.0006
Erythrokaryocytes	69.0 (56.6; 82.9)	90.8 (84.9; 95.5)	0.0008

DISCUSSION

Supravital cell staining with an automatic analysis of the results in laser flow cytofluorometry was used to assess the viability of MNCs in LCs. The 7-AAD dye is easily embedded between cytosine and guanine bases and is detected in the red region of the visible spectrum (635–675 nm). If simultaneous staining of cells with fluorochrome-conjugated monoclonal antibodies to cellular determinants is necessary, 7-AAD is considered preferable among fluorescent DNA dyes [10]. The percentage of 7-AAD-negative MNCs should be recommended as an informative parameter of LC control at technological stages of production and storage.

As a result of the conducted research, it is shown that the viability of blood and native LCs is approaching 100%, the variation of the parameter is extremely insignificant. The information obtained is consistent with the results of the study on stem cell viability, in which several DNA dyes were used [7]. The number of 7-AAD-negative MNCs in HSC-containing LCs and the blood from which they were obtained coincided. Consequently, leukocytapheresis and anticoagulant addition do not have a negative effect on the permeability of MNC membranes.

Since 2003, highly purified DMSO at a concentration of 10% has been used for cryopreservation of transplant material. The molecular basis of the DMSO effect on cell membranes is still being investigated [11]. It is known that various concentrations of DMSO have fundamentally different mechanisms of action on HSCs [12]. The information given in the literature on the viability of cryopreserved HSCs, their repopulating ability, and the timing of hematopoiesis recovery [13, 14, 3] do not allow to draw final conclusions about the optimal DMSO concentration.

A possible effect of concentrated DMSO at the stage of its introduction into the LCs was studied. The number of 7-AAD-negative MNCs in LCs mixed with DMSO at a final concentration of 5% and in native LCs did not differ significantly. The conclusion was made about the reasonability of the method used for introducing a concentrated DMSO solution into the cell product. A significant decrease in the MNC viability in thawed LCs was revealed both with and without washing from DMSO, compared with that in native LCs mixed with a cryoprotectant. The results obtained are consistent with the literature data [15]. The relationship between the storage time (from 7 to 120 days) and the number of 7-AAD-negative MNCs released from cold suspended animation was not confirmed, freezing and thawing are probably the most critical for the permeability of MNC plasma membranes.

It is known that DMSO can have a toxic effect on the human body when used as a cryoprotectant [16]. To reduce the toxic effect of DMSO on the recipient's body, such approaches as lowering the hematocrit of the cell product [17], washing HSC-containing cell products [18], and using ice recrystallization inhibitors [8] are studied. Non-viable MNCs may have a fragmented membrane or represent naked nuclei [9]. It was found, that in the LCs washed from DMSO, there are more viable MNCs than in the LCs that were not washed. As a result of washing, the DMSO-containing resuspension solution in LCs is partially replaced with a mixture of albumin and polyglukin, the contact time of MNCs with extracellular DMSO is reduced [18].

LC is a product that is only slightly enriched with stem cells compared to peripheral blood [7]. The per-

centage of HSCs in LCs averaged 0.6%, the largest proportion among all MNCs was represented by cellular elements that do not have repopulating properties. At the same time, the number of CD45-positive cells directly affects the estimated transplantation dose of HSCs [19]. When LCs are thawed without washing, granulocytes undergo the greatest destruction, which is consistent with the reports of researchers [20]. Given high sensitivity of membranes of granulocytic components and their significant proportion in LCs, the granulocyte population makes the greatest contribution to reducing the viability of all MNCs after thawing. When washing from DMSO, greater viability of most of the isolated MNC populations was observed, except for monocytes. Presumably, washing hinders the increase in the permeability of MNC plasma membranes. In addition, it cannot be ruled out that non-viable MNCs are selectively removed during LC washing.

The possibility of loading the transplant material with cell degradation products is another aspect of the negative impact that the destruction of MNC membranes has on the recipient's body. The danger of enriching blood components with such substances during storage was discussed [9].

CONCLUSION

The viability of MNCs in LCs is recommended to be used as an independent characteristic of the transplant quality. In the process of obtaining LCs and mixing them with DMSO, the viability of MNCs does not decrease, while in thawed LCs, it decreases significantly. Thawing of LCs with the removal of DMSO allows to achieve the best viability of HSCs and most MNC populations.

REFERENCES

1. Donnenberg V.S., Ulrich H., Tárnok A. Cytometry in Stem Cell Research and Therapy. *Cytometry A.* 2013; 83(1): 1–4. DOI: 10.1002/cyto.a.22243.
2. Passweg J.R., Baldomero H., Bader P., Bonini C., Cesaro S., Dreger P., Duarte R.F., Dufour C., Kuball J., Farge-Bancel D., Gennery A., Kröger N., Lanza F., Nagler A., Sureda A. and Mohty M. Hematopoietic stem cell transplantation in Europe 2014: more than 40000 transplants annually. *Bone Marrow Transplantation*. 2016; 51: 786–792. DOI:10.1038/bmt.2016.2.
3. Galmes A., Gutierrez A., Sampol A., Canaro M., Morey M., Iglesias J., Matamoros N., Duran M. A., Novo A., Bea M. D., Galan P., Balansat J., Martínez J., Bargay J., Besalduch J. Long-term hematological reconstitution and clinical evaluation of autologous peripheral blood stem cell transplantation after cryopreservation of cells with 5% and 10% dimethyl sulfoxide at – 80 degrees C in a mechanical freezer. *Haematologica*. 2007; 92: 986 – 989. DOI: 10.3324/haematol.11060.
4. Loginova M.A., Malysheva N.A., Minaeva N.V., Paramonov I.V. Evaluation of the effectiveness of the register of potential donors of hematopoietic stem cell. *Russian Journal of Hematology and Transfusiology.* 2020;365(3):91–298 (in Russ.). DOI: 10.35754/0234-5730-2020-65-3-291-298.
5. Barnett D., Granger V., Kraan J., Whitby L., Reilly J.T., Papa S., Gratama J.W. Reduction of intra- and interlaboratory variation in CD34- stem cell enumeration using stable test material, standard protocols and targeted training. *Br J Haematol.* 2000; 108 (3):784 – 792. DOI: 10.1046/j.1365-214.
6. Saraceni F., Shem-Tov N., Olivieri A., Nagler A. Mobilized peripheral blood grafts include more than hematopoietic stem cells: the immunological perspective. *Bone Marrow Transplantation.* 2015; 50(7): 886–891. DOI: 10.1038/bmt.2014.330.
7. López M.C., Lawrence D. A. Proficiency testing experience for viable CD34+ stem cell analysis. *Transfusion*. 2008; 48(6): 1115-1121. DOI: 10.1111/j.1537-2995.2008.01652.x.
8. Briard J.G., Jahan S., Chandran P., Allan D., Pineault N., Ben R.N. Small-Molecule Ice Recrystallization Inhibitors Improve the Post-Thaw Function of Hematopoietic Stem and Progenitor Cells. *ACS Omega.* 2016; 1(5): 1010-1018. DOI: 10.1021/acsomega.6b00178.
9. Wagner T., Guber S.E., Stubenrauch M.-L., Lanzer G. Low propidium iodide intensity in flow cytometric white blood cell counting as a marker of cell destruction? *Transfusion*. 2005; 45 (2): 228-233. DOI: 10.1111/j.1537-2995.
10. Trusov G.A., Chaplenko A.A., Semenova I.S., Melnikova E.V., Olefir Yu.V. Use of Flow Cytometry for Quality Evaluation of Biomedical Cell Products. *BlOpreparations. Prevention, Diagnosis, Treatment.* 2018;18(1):16–24 (in Russ.). DOI: 10.30895/2221-996X-2018-18-1-16-24.
11. Fernández M. L., Reigada R. Effects of Dimethyl Sulfoxide on Lipid Membrane Electroporation. *The Journal of Physical Chemistry B* 2014, 118 (31), 9306-9312. DOI: 10.1021/jp503502s.
12. Smagur A., Mitrus I, Giebel S, Sadus-Wojciechowska M., Najda J., Kruzel T., Czerw T., Gliwinska J., Prokop M., Glowala-Kosinska M, Chwieduk A., Holowiecki J. Smugar, I. Impact of different dimethyl sulphoxide concentrations on cell recovery, viability and clonogenic potential of cryopreserved peripheral blood hematopoietic stem and progenitor cells. *Vox Sang.* 2013; 104 (3): 240-247. DOI: 10.1111/j.1423-0410.2012.01657.x.
13. Curcoy A.I., Alcorta I., Estella J., Rives S., Toll T., Tuset E. Cryopreservation of HPCs with high cell concentration in 5-percent DMSO for transplantation to children. *Transfusion.* 2002; 42: 962. DOI: 10.1046/j.1525-1438.2002.00198.x.
14. Abrahamsen J.F., Rusten L., Bakken A. M., Bruserud O. Better preservation of early hematopoietic progenitor cells when human peripheral blood progenitor cells are cryopreserved with 5 percent dimethylsulfoxide instead of 10 percent dimethylsulfoxide. *Transfusion.* 2004; 44: 785 – 789. DOI: 10.1111/j.1537-2995.2004.03336.x.
15. Akkok CA, Liseth K, Hervig T, Ryningen A, Bruserud O., Ersvaer E. Use of different DMSO concentrations for cryopreservation of autologous peripheral blood stem cell grafts does not have any major impact on levels of leukocyte- and

platelet-derived soluble mediators. *Cytotherapy*. 2009; 11: 749 – 760. DOI: 10.1080/14653240902980443.
16. Kollerup M.B, Hilscher M., Zetner D., Rosenberg J. Adverse reactions of dimethyl sulfoxide in humans: a systematic review. *F1000Research.*2018; 7: 1-18.DOI: 10.12688/f1000research.16642.2.
17. Tonev I., Simeonov S., Mitkov I., Ilieva M., Petrov Y., Ganeva P., Arnaudov G., Spassov B., Mincheff M. Viability of hematopoetic stem cells following storage at – 80 °C with 5 % dimethylsulfoxide and hematologic recovery in transplanted myeloma patients. *HemaSphere.* 2019; 3: 343-344. DOI: 10.1097/01.hs9.0000561400.99877.49.4.
18. Shu Z, Heimfeld S, Gao D. Hematopoietic SCT with cryopreserved grafts: adverse reactions after transplantation and cryoprotectant removal before infusion. *Bone Marrow Transplant*. 2014; 49(4): 469–476. DOI: 10.1038/bmt.2013.152.
19. Gutensohn K1, Jessen M, Ketels A, Gramatzki M, Humpe A. Flow cytometric analyses of CD34+ cells with inclusion of internal positive controls. *Transfusion.* 2012; 2 (52): 284-290. DOI: 10.1111/j.1537-2995.2011.03259.x.
20. Bai L, Xia W, Wong K, Reid C, Ward C, Greenwood M. Infused neutrophil dose and haematopoietic recovery in patients undergoing autologous transplantation. *Bone Marrow Transplant.* 2014; 49(5): 725. DOI: 10.1038/bmt.2014.14.

Authors' contribution

Isaeva N.V. – conception and design, analysis and interpretation of data, drafting of the manuscript. Minaeva N.V. – critical revision of the manuscript for important intellectual content. Sherstnev Ph.S., Utemov S.V., Zmeeva Yu. S., Butolina M.A. – collection, analysis and interpretation of data. Zorina Natalia A. – selection and management of donors and patients.

Authors' information

Isaeva Natalia V. – Cand. Sci. (Biology), Senior Researcher, Laboratory of Cellular and Molecular Immunology, Kirov Research Institute of Hematology and Blood Transfusion, Kirov, isaevanatalia@yandex.ru, http://orcid.org/0000-0001-9766-5137

Minaeva Natalia V. – Cand. Sci. (Med.), Deputy Clinical Director, Kirov Research Institute of Hematology and Blood Transfusion, Kirov,mnvgem@gmail.com, http://orcid.org/0000-0002-8479-3217

Utemov Sergey V. – Cand. Sci. (Med.), Leading Researcher, Laboratory of Cellular Technologies, Kirov Research Institute of Hematology and Blood Transfusion, Kirov, utemov@niigpk.ru, http://orcid.org/0000-0002-2045-2034

Sherstnev Philip S. – Cand. Sci. (Med.), Head of the Department of Transfusiology and Hematopoietic Stem Cell Processing, Kirov Research Institute of Hematology and Blood Transfusion, Kirov, sherstnyov_phil@mail.ru, http://orcid.org/0000-0002-1751-8522

Zorina Natalia A. – Cand. Sci. (Med.), Head of the Department of Chemotherapy and Bone Marrow Transplantation, Kirov Research Institute of Hematology and Blood Transfusion, Kirov, zorina@niigpk.ru, http://orcid.org/0000-0003-1948-209X

Zmeeva Yuliya S. – Junior Researcher, Laboratory of Cellular and Molecular Immunology, Kirov Research Institute of Hematology and Blood Transfusion, Kirov, zmeevajs@mail.ru, http://orcid.org/0000-0003-2034-425X

Butolina Maria A. – Laboratory Assistant, Laboratory of Cellular Technologies, Kirov Research Institute of Hematology and Blood Transfusion, Kirov, butolina.maria@yandex.ru, http://orcid.org/0000-0002-5408-6028

(✉) **Isaeva Natalia V.,** isaevanatalia@yandex.ru

Received 22.10.2021;
approved after peer review 16.05.2022;
accepted 08.12.2022

УДК 616.12-008.46-036.12-037:616.146.2-073.432
https://doi.org/10.20538/1682-0363-2023-2-53-60

Renal venous Doppler ultrasound – a new parameter for predicting outcomes in patients with decompensated heart failure

Kobalava Zh.D.[1], Safarova A.F.[1, 2], Aslanova R.Sh.[1, 2], Vatsik-Gorodetskaya M.V.[2]

[1] Peoples' Friendship University of Russia (RUDN University)
8, Miklukho-Maklaya Str., Moscow, 117198, Russian Federation

[2] Vinogradov City Clinical Hospital
61, Vavilova Str., 117292, Moscow, Russian Federation

ABSTRACT

Aim. To assess the frequency, dynamics, and prognostic value of renal venous congestion using Doppler ultrasound in patients with decompensated heart failure (DHF).

Materials and methods. A prospective, single-center study included 124 patients with DHF (mean age 70 ± 12 years, 51.6% were males), left ventricular ejection fraction (LVEF) 44 [34; 55] %, N-terminal pro B-type natriuretic peptide (NT-proBNP) 1,609 [591; 2,700] pg / ml. All patients underwent a standard physical examination and laboratory and instrumental tests, including the assessment of the NT-proBNP level. Renal venous blood flow was assessed using pulsed-wave Doppler ultrasound. The presence of continuous renal blood flow was considered as the absence of venous congestion, while intermittent blood flow (two-phase and single-phase flow) indicated venous congestion. Rehospitalization for DHF and reaching a composite endpoint (rehospitalization for DHF and cardiovascular mortality) within 12 months after discharge were selected as endpoints.

Results. At admission, continuous renal venous blood flow was observed in 34 (27.4%) patients, intermittent renal venous blood flow was found in 90 (72.6%) patients: two-phase flow in 62 (50%) and single-phase flow in 28 (22.6%) patients with DHF. At discharge, 66 (53.2%) patients had intermittent renal venous blood flow: two-phase flow in 50 (40.3%) and single-phase flow in 16 (12.9%) patients. Correlations of renal venous congestion with the levels of NT-proBNP, serum iron, uric acid, creatinine, LVEF, systolic pressure in the pulmonary artery (SPPA), and the development of acute kidney injury (AKI) were revealed. Persistent renal venous congestion at discharge was significantly associated with a higher probability of rehospitalization for DHF (hazard ratio (HR) 1.93 95% confidence interval (CI) (1.017–3.67); $p = 0.044$) and a composite endpoint (HR 2.66, 95% CI (1.43–4.96); $p = 0.002$).

Conclusion. In patients with DHF, it is necessary to evaluate renal venous blood flow using pulsed-wave Doppler ultrasound to stratify patients with development of cardiovascular complications within 12 months.

Keywords: DHF, renal venous blood flow, renal venous congestion, NT-proBNP

Conflict of interest. The authors declare the absence of obvious or potential conflicts of interest related to the publication of this article.

Source of financing. The authors state that they received no funding for the study.

Conformity with the principles of ethics. All patients signed an informed consent to participate in the study. The study was approved by the local Ethics Committee at RUDN University (Protocol No. of 16.11.2021).

For citation: Kobalava Zh.D., Safarova A.F., Aslanova R.Sh., Vatsik-Gorodetskaya M.V. Renal venous Doppler ultrasound – a new parameter for predicting outcomes in patients with decompensated heart failure. *Bulletin of Siberian Medicine.* 2023;22(2):53–6. https://doi.org/10.20538/1682-0363-2023-2-53-60.

✉ *Aslanova Rena Sh.,* rena.aslan@yandex.ru

Почечная венозная допплерография – новый параметр для прогнозирования исходов у пациентов с декомпенсацией хронической сердечной недостаточности

Кобалава Ж.Д.[1], Сафарова А.Ф.[1, 2], Асланова Р.Ш.[1, 2], Вацик-Городецкая М.В.[2]

[1] Российский университет дружбы народов (РУДН)
Россия, 117198, г. Москва, ул. Миклухо-Маклая, 8

[2] Городская клиническая больница им. В.В. Виноградова ДЗМ
117292, Россия, г. Москва, ул. Вавилова, 61

РЕЗЮМЕ

Цель: оценить частоту, динамику и прогностическое значение почечного венозного застоя, оцененного с помощью допплерографии, у пациентов с декомпенсацией хронической сердечной недостаточности (ДХСН).

Материалы и методы. В проспективное одноцентровое исследование были включены 124 пациента с ДХСН, в том числе 51,6% мужчин, средний возраст 70 ± 12 лет. Пациенты имели следующие показатели: фракция выброса левого желудочка (ФВ ЛЖ) 44 [34;55]%, N-терминальный мозговой натрийуретический пептид (NT-proBNP1609) [591;2 700] пг/мл. Всем пациентам проводили стандартное физическое, лабораторно-инструментальные исследования, включая уровень NT-proBNP. Оценку почечного венозного кровотока проводили с помощью импульсно-волновой допплерографии. Наличие непрерывного почечного кровотока расценивали как отсутствие венозного застоя, в то время как прерывистый (двухфазный и однофазный кровоток) указывал на венозный застой. В качестве конечных точек были выбраны повторная госпитализация по поводу ДХСН и достижение комбинированной точки (регоспитализация по поводу ДХСН и сердечно-сосудистая смертность) в течение 12 мес после выписки.

Результаты. При поступлении непрерывный почечный венозный кровоток отмечался у 34 (27,4%), прерывистый почечный венозный кровоток – у 90 (72,6%): двухфазный – у 62 (50%) и однофазный – у 28 (22,6%) пациентов с ДХСН. При выписке у 66 (53,2%) пациентов сохранялся прерывистый почечный венозный кровоток: двухфазный – у 50 (40,3%) и однофазный – у 16 (12,9%). Выявлены корреляции почечного венозного застоя с уровнем NT-proBNP, сывороточного железа, мочевой кислоты, креатинина, ФВ ЛЖ, систолического давления в легочной артерии и развитием острого почечного повреждения. Сохраняющийся почечный венозный застой при выписке достоверно ассоциировался с более высокой вероятностью повторной госпитализации по поводу ДХСН (отношение рисков (ОР) 1,93 95%-й доверительный интервал (ДИ) (1,017–3,67); $p = 0,044$) и комбинированной конечной точки (ОР 2,66 95%-й ДИ (1,43–4,96); $p = 0,002$).

Заключение. У пациентов с ДХСН целесообразно оценивать почечный венозный кровоток с помощью импульсно-волновой допплерографии для стратификации пациентов с развитием сердечно-сосудистых осложнений в течение 12 мес.

Ключевые слова: ДХСН, почечный венозный кровоток, почечный венозный застой, NT-proBNP

Конфликт интересов. Авторы декларируют отсутствие явных и потенциальных конфликтов интересов, связанных с публикацией настоящей статьи.

Источник финансирования. Авторы заявляют об отсутствии финансирования при проведении исследования.

Соответствие принципам этики. Все пациенты подписали информированное согласие на участие в исследовании. Исследования одобрено локальным этическим комитетом РУДН (протокол № б/н от 16.11.2021).

Для цитирования: Кобалава Ж.Д., Сафарова А.Ф., Асланова Р.Ш., Вацик-Городецкая М.В. Почечная венозная допплерография – новый параметр для прогнозирования исходов у пациентов с декомпенсацией хронической сердечной недостаточности. *Бюллетень сибирской медицины.* 2023;22(2):53–60. https://doi.org/10.20538/1682-0363-2023-2-53-60.

INTRODUCTION

In recent years, cardiorenal interactions in patients with decompensated heart failure (DHF) have attracted increasing attention due to a significant increase in the prevalence of combined cardiac and renal dysfunction. The frequency of deterioration in the functional state of the kidneys in patients with DHF is 45–63.6%, and it is an unfavorable prognostic factor leading to repeated hospitalizations and an increase in the cardiovascular mortality [1].

Currently, the role of venous congestion and an increase in central venous pressure in the deterioration of kidney function in DHF is being discussed [2]. Until recently, the diagnosis of renal venous congestion presented certain difficulties due to the invasiveness and laboriousness of the study.

N. Iida. et al. were the first to propose a method for assessing renal venous blood flow using Doppler ultrasound. P. Nijst et al. revealed the relationship between changes in the nature of renal venous blood flow using this technique and deterioration in kidney function in patients with DHF and recommended it to control diuretic therapy in patients with DHF [3, 4].

Currently, there are no universal criteria for detecting renal venous congestion, which emphasizes the relevance of studies to compare the clinical and prognostic value of the proposed method in patients with DHF.

The aim of the study was to assess the frequency, dynamics, and prognostic value of renal venous congestion in patients with DHF using Doppler ultrasound.

MATERIALS AND METHODS

A prospective, single-center study included 124 patients hospitalized at the Heart Failure Center of at Vinogradov City Clinical Hospital from December 2020 to December 2021 (Table 1). Exclusion criteria were malignant neoplasms in the active phase, severe valvular defects, and somatic symptom disorders.

All patients underwent standard clinical and laboratory tests, including determination of N-terminal probrain natriuretic peptide (NT–proBNP) (Vector-Best, Russia). The Stagnation Scale was used to assess clinical stagnation [5]. An ultrasound examination of the heart and renal blood flow was performed using the VIVID E90 premium system (GE, Healthcare).

The nature of the renal blood flow was assessed using pulsed-wave Doppler ultrasound with the patient lying on the left side using a convex or sector sensor with simultaneous ECG recording on the monitor of the device. Normally, the Doppler renal blood flow curve is continuous. A discontinuous renal blood flow pattern with systolic and diastolic phases (as a minor deviation) and a discontinuous flow pattern with a diastolic phase (as a pronounced deviation) were considered as venous congestion (Fig. 1) [6].

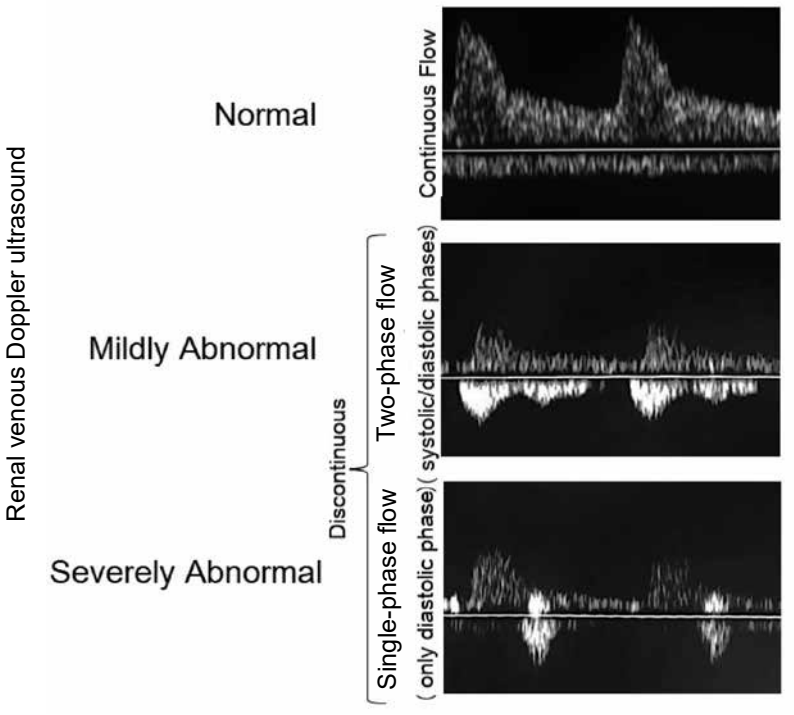

Fig. 1. Algorithm for the ultrasound assessment of renal venous blood flow

Table 1

Characteristics of patients with DHF, *n* = 124

Parameter	Value
Gender, men, *n* (%)	64 (52)
Age, years, *M* ± *SD*	70 ± 12
BMI, kg / m², *Me [IQR]*	32.4 [27.7; 38.35]
Smoking, *n* (%)	23 (19)
Arterial hypertension, *n* (%)	110 (89)
Ischemic heart disease, *n* (%)	65 (52)
Atrial fibrillation, *n* (%)	73 (59)
Type 2 diabetes mellitus, *n* (%)	43 (35)
CKD, *n* (%)	91 (73.4)
AKI, *n* (%)	29 (23.4)
NYHA, FC, *n* (%)	
II	28 (22)
III	54 (44)
IV	42 (34)
Stagnation Scale, score, *Me [IQR]*	9 [6; 12.5]
LVEF, %, *Me [IQR]*	44 [34; 55]
LVEF:	
< 40%, *n* (%)	48 (38.7)
41–49%, *n* (%)	23 (18.5)
≥ 50%, *n* (%)	53 (42.8)
SPPA, mm Hg, *Me [IQR]*	48 [34; 60]
Renal venous blood flow pattern:	
continuous, *n* (%)	34 (27.4)
discontinuous, *n* (%)	90 (72.6)
two-phase, *n* (%)	62 (50)
single-phase, *n* (%)	28 (22.6)
NT-proBNP, pg / ml, *Me [IQR]*	1,609 [591; 2,700]
Creatinine, μmol / l, *Me [IQR]*	103.5 [84; 125]
GFR, ml / min / 1.73 m², *Me [IQR]*	54.3 [43; 67.4]
Blood potassium, mmol / l, *Me [IQR]*	4.35 [3.9; 4.6]
Urea, mmol / l, *Me [IQR]*	7.4 [5.3; 9.7]
Uric acid, mmol / l, *Me [IQR]*	438 [327; 570]
Iron, mmol / l, *Me [IQR]*	6.9 [4.4; 12.1]

Note: BMI – body mass index, AKI – acute kidney injury, SPPA – systolic pressure of the pulmonary artery, GFR – glomerular filtration rate, LVEF – left ventricular ejection fraction, FC HF – functional class of heart failure, CKD – chronic kidney disease, NT -proBNP – N-terminal brain natriuretic peptide (here and in Table 2–4).

All patients received standard HF therapy during and after hospitalization. The duration of follow-up after discharge was 12 months. The assessment of short-term and long-term outcomes was performed using the EMIAS database. Rehospitalization for DHF and death from cardiovascular complications during the follow-up period were selected as endpoints.

Statistical analysis was performed using Statistica (version 10.0; Statsoft), MedCalc Software's VAT Version 19.0, and SPSS (version 26.0). Quantitative data were presented as the arithmetic mean and the standard deviation of the mean *M* ± *SD* (for normal distribution) or as the median and the interquartile range *Me [IQR]* (for non-normal distribution). The significance of differences between the two groups of quantitative variables was assessed using the Mann – Whitney *U*-test and the Kruskal – Wallis test. Qualitative variables were represented by absolute and relative values *n* (%). To compare the groups by the frequency of qualitative variables, the Pearson's chi-square test ($\chi 2$) was used. The survival probability was estimated by constructing Kaplan – Meier survival curves; comparison was made using the log rank test. Univariate and multivariate Cox regression analysis models were used to assess the predictive value of different methods for the risk of death from or rehospitalization for DHF. The differences were considered statistically significant at $p < 0.05$.

RESULTS

On admission, the incidence of renal venous congestion in patients with DHF was 72.6%; at discharge, renal venous congestion persisted in 53.2% of patients. The dynamics of renal venous blood flow during hospitalization is shown in Fig. 2.

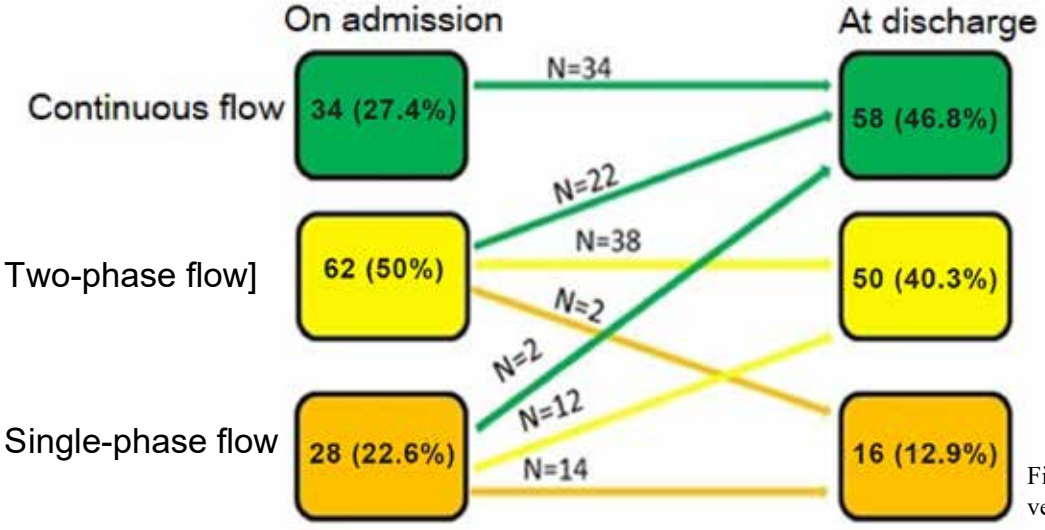

Fig. 2. Dynamics of renal venous blood flow

At admission, patients with renal venous congestion had significantly higher incidence of CKD in history, development of AKI during hospitalization, higher levels of SPPA, NT-proBNP, and uric acid, and lower serum iron levels compared to patients without renal venous congestion (Table 2). Table 3 shows comparative characteristics of patients with changes in renal venous blood flow at discharge. Associations of renal venous congestion on admission and discharge with the studied parameters are presented in Table 4. The Cox regression analysis demonstrated an independent predictive value of renal venous congestion in relation to rehospitalization for DHF and achievement of the composite endpoint (Table 5).

Table 2

Comparative characteristics of patients with DHF with the absence and presence of renal venous congestion at admission

Parameter	Patients without renal venous congestion, *n* = 34	Patients with renal venous congestion, *n* = 90	*p*
LVEF < 40%, *n* (%) 41–49%, *n* (%) ≥ 50%, *n* (%)	 11 (32.4) 3 (8.8) 20 (58.8)	 37 (42.2) 20 (22.2) 32 (35.6)	0.045
Stagnation Scale, score, *Me [IQR]*	6 [4; 8]	11 [7; 13]	0.000
SPPA, mm Hg, *Me [IQR]*	34 [27; 40]	56 [40; 62]	<0.000
CKD in the medical history, *n* (%)	18 (52.9)	73 (81.1)	0.001
AKI, *n* (%)	2 (5.9)	27 (30)	0.004
Nt-proBNP, pg / ml, *Me [IQR]*	482.5 [339; 2,109]	1,699 [1,065; 3,131]	0.000
Creatinine, μmol / l, *Me [IQR]*	88 [74.7; 105]	109 [89; 134.6]	0.000
GFR, ml / min / 1.73m²	57.35 [50.8; 75]	53 [38; 61.9]	0.018
Urea, mmol / l, *Me [IQR]*	6.35 [4.72; 8.6]	7.66 [6.32; 10.5]	0.020
Uric acid, mmol / l, *Me [IQR]*	382.3 [285.1; 514.2]	501.63 [365.8; 587]	0.040
Potassium, mmol / l, *Me [IQR]*	4.2 [3.75; 4.55]	4.4 [4.05; 4.76]	0.027
Iron, mmol / l, *Me [IQR]*	10.86 [7.25; 15.17]	6.99 [5.32; 11.1]	0.023

Table 3

Characteristics of patients with DHF with changes in renal venous blood flow at discharge

Parameter	Persistence of continuous blood flow, *n* = 34	From discontinuous to continuous flow, *n* = 24	Persistence of discontinuous flow, *n* = 66	*p*
Gender, men, *n* (%)	14 (41.2)	15 (62.5)	35 (53)	0.26
Age, years, *Me [IQR]*	75.5 [68; 81]	67 [62.5; 72.5]	71.5 [64; 81]	0.125
Arterial hypertension, *n* (%)	31 (91.2)	23 (95.8)	56 (84.8)	0.300
Ischemic heart disease, *n* (%)	19 (55.9)	14 (58.3)	32 (48.5)	0.634
CKD, *n* (%)	18 (53)	21 (87.5)	52 (78.8)	0.004
AKI, *n* (%)	3 (8.8)	5 (20.8)	17 (25.8)	0.018
Atrial fibrillation, *n* (%)	18 (53)	13 (54.2)	42 (63.6)	0.513
Type 2 diabetes mellitus, *n* (%)	9 (26.5)	10 (41.7)	24 (36.6)	0.447
NYHA, FC, *n* (%) II III IV	 9 (26.5) 18 (52.9) 7 (20.6)	 7 (29.2) 11 (45.8) 6 (25)	 12 (18.2) 25 (37.8) 29 (44)	0.148
LVEF, %, *Me [IQR]*	52 [38; 58]	42 [33; 49]	44 [34; 55]	0.613
LVEF, *n* (%) < 40% 41–49% ≥ 50%	 11 (32.4) 3 (8.8) 20 (58.8)	 9 (37.5) 9 (37.5) 6 (25)	 28 (42.4) 11 (16.7) 27 (40.9)	0.017
NT-proBNP, pg / ml, *Me [IQR]*	482.5 [339; 2,109]	1,670.5 [905; 2,429]	1,700.5 [1,140; 3,412]	0.002
Creatinine, μmol / l, *Me [IQR]*	88 [74.7; 105]	108.5 [95.27; 130]	109 [87; 137]	0.001
GFR, ml / min / 1.73 m², *Me [IQR]*	57.35 [5-78; 75]	53.7 [45.57; 59.7]	53 [35.9; 66.7]	0.061
Blood potassium, mmol / l, *Me [IQR]*	4.2 [3.72; 4.55]	4.35 [4.05; 4.6]	4.41 [4.08; 4.77]	0.075
Urea, mmol / l, *Me [IQR]*	6.35 [4.72; 8.6]	7.45 [6.06; 9.9]	8.32 [6.56; 11.2]	0.053
Uric acid, mmol / l, *Me [IQR]*	382.3 [285.1; 514.2]	438.8 [399.3; 560]	505.4[357.15; 623.34]	0.107
Iron, mmol / l, *Me [IQR]*	10.86 [7.25; 11.78]	7.62 [5.8; 11]	6.77 [5.12; 11.2]	0.067

Table 4

Correlations of renal venous blood flow with laboratory and instrumental data in patients with DHF at admission and discharge

Parameter	On admission	At discharge
History of atrial fibrillation, *n* (%)	$p = 0.007$, $R = 0.24$	–
History of CKD	$p = 0.000$, $R = 0.32$	–
AKI, *n* (%)	$p = 0.041$, $R = 0.25$	–
Stagnation Scale, score	$p = 0.000$, $R = 0.48$	–
LVEF, *n* (%)	$p = 0.021$, $R = –0.20$	–
LVEF < 40% 41–49% > 50%	$p = 0.017$, $R = –0.21$	–
SPPA, mm Hg	$p = 0.000$, $R = 0.50$	–
Nt-proBNP, pg / ml	$p = 0.000$, $R = 0.25$	$p = 0000$, $R = 0.30$
Creatinine, μmol / l	$p = 0.000$, $R = 0.34$	$p = 0.003$, $R = 0.25$
GFR, ml / min / 1.73 m²	$p = 0.020$, $R = –0.21$	$p = 0.018$, $R = –0.21$
Iron, mmol / l	$p = 0.012$, $R = –0.26$	–
Uric acid, μmol / l	$p = 0.024$, $R = 0.25$	–
Potassium, mmol / l	$p = 0.014$, $R = 0.22$	–

Table 5

Cox regression analysis for renal venous congestion in terms of a risk of endpoint development

	Univariate regression analysis		Multivariate regression analysis	
	OR, 95% CI	*p*	OR, 95% CI	*p*
Rehospitalization for DHF	1.97 (1.03–3.75)	0.038	1.93 (1.017–3.67)	0.044
Composite endpoint	2.72 (1.46–5.06);	0.002	2.66 (1.43–4.96);	0.002

Note: OR – odds ratio, 95% CI – 95% confidence interval. The multivariate regression analysis included age, gender, LVEF < 40%, history of coronary artery disease, arterial hypertension, type 2 diabetes, CKD, and an increase in BMI a week prior to hospitalization.

Fig. 3 and Fig. 4 show the Kaplan – Meier curves for the cumulative survival probability (rehospitalizations and composite endpoints) depending on the presence of renal venous congestion.

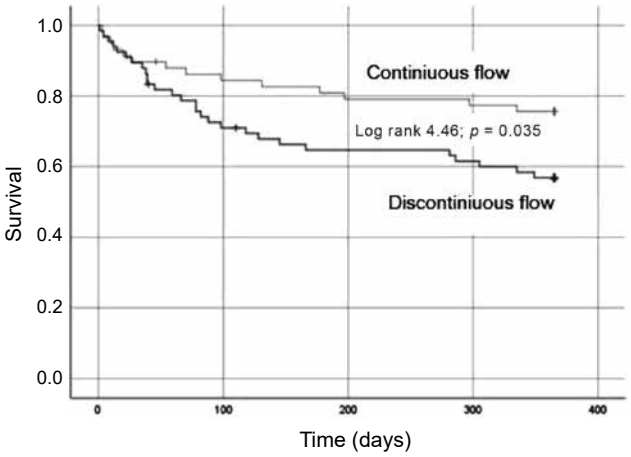

Fig. 3. Kaplan – Meier curves for cumulative survival probability (rehospitalizations) depending on the presence of renal venous congestion

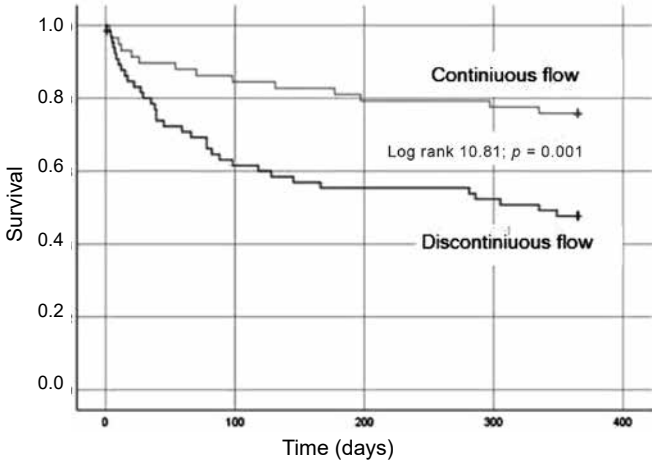

Fig. 4. Kaplan – Meier curves for cumulative survival probability (composite endpoints) depending on the presence of renal venous congestion

DISCUSSION

In our study, patients with DHF on admission were characterized by high incidence of venous renal congestion (in 72.6% of cases), assessed by Doppler ultrasound of the kidneys. Persistent renal venous congestion at discharge (in 53.2% of cases) was associated with the risk of one-year adverse outcomes. Our data are consistent with those of a recent study by A. Puzzovivo et al., who also found an association of venous renal congestion on ultrasound with the development of DHF and death during 36- month follow-up [7].

For many years, renal venous Doppler ultrasound has been used to assess non-cardiac conditions associated with elevated renal interstitial pressure, such as obstructive uropathy or diabetic nephropathy [8, 9]. However, recent data support the use of this imaging modality to assess intrarenal hemodynamics in HF [3, 4, 10].

A study by N. Iida et al., which examined the relationship of renal Doppler curves with the development of adverse outcomes among 224 patients with DHF, showed that discontinuous renal blood flow, including single-phase flow, had the most unfavorable prognosis (one-year survival < 40%) [3].

According to our results, renal venous congestion was associated with creatinine, GFR, uric acid, and potassium levels, development of AKI during hospitalization, and history of CKD. F. Husain-Syed et al. also found an association between renal venous congestion and worsening renal function in patients with HF [11].

The relationships revealed can be explained by the development mechanism of cardiac and renal dysfunction in HF, in which there is a decrease in cardiac output, an increase in intra-abdominal pressure, as well as an increase in venous pressure in the kidneys, leading to the occurrence of venous congestion, including renal one [12]. It is known that even minor renal damage in patients with HF is associated with high all-cause and cardiovascular mortality [13, 14].

CONCLUSION

In patients with DHF, the assessment of renal venous blood flow revealed high incidence of renal venous congestion and its prognostic value in the development of adverse outcomes, which makes it reasonable to use this technique in this group of patients.

Limitations and prospects of the study. The limitations of the study are associated with a small sample size and a relatively short follow-up period of 12 months.

There is an obvious need for a multicenter clinical study to investigate the nature of renal venous blood flow and its impact on the development of cardiovascular complications in patients with DHF.

REFERENCES

1. Kobalava Z.D., Villevalde S.V., Efremovtseva M.A. Cardiorenal interaction in decompensated chronic heart failure. *Rational Pharmacotherapy in Cardiology.* 2016;12(2):138–146 (in Russ.). DOI: 10.20996/1819ю6446-2016-12-2-138-146.
2. Damman K., Valente M.A., Voors A.A., O'Connor C.M., van Veldhuisen D.J., Hillege H.L. Renal impairment, worsening renal function, and outcome in patients with heart failure: an updated meta-analysis. *Eur. Heart J.* 2014;35(7):455469. DOI: 10.1093/eurheartj/eht386.
3. Iida N., Seo Y., Sai S., Machino-Ohtsuka T., Yamamoto M., Ishizu T. et al. Clinical implications of intrarenal hemodynamic evaluation by Doppler ultrasonography in heart failure. *JACC Heart Fail*. 2016;4(8):674–882. DOI: 10.1016/j.jchf.2016.03.016.
4. Nijst P., Martens P., Dupont M., Tang W.H.W., Mullens W. Intrarenal flow alterations during transition from euvolemia to intravascular volume expansion in heart failure patients. *JACC Heart Fail. 2*017;5(9):672–681. DOI: 10.1016/j.jchf.2017.05.006.
5. Belenkov Yu.N., Mareev V.Yu. Principles of rational treatment for heart failure. M. Media Medica, 2000:266 (in Russ.).
6. Yamamoto M., Seo Y., Iida N., Ishizu T., Yamada Y., Nakatsukasa T. et al. Prognostic impact of changes in intrarenal venous flow pattern in patients with heart failure. *J. Card. Fail*. 2021;27(1):20–28. DOI: 10.1016/j.cardfail.2020.06.016.
7. Puzzovivo A., Monitillo F., Guida P., Leone M., Rizzo C., Grande D. et al. Renal venous pattern: a new parameter for predicting prognosis in heart failure outpatients. *J. Cardiovasc. Dev. Dis.* 2018;5(4):52. DOI: 10.3390/jcdd5040052.
8. Vadana B.M., Pasumarthy A., Penumalli N., Bellapa N.C. Renal venous Doppler study in obstructive uropathy. *J. Clin. Diagn. Res.* 2015;9(11):TC13–15. DOI: 10.7860/JCDR/2015/15546.6794.
9. Jeong S.H., Jung D.C., Kim S.H. Renal venous Doppler ultrasonography in normal subjects and patients with diabetic nephropathy: value of venous impedance index measurements. *J. Clin. Ultrasound.* 2011;39(9):512–518. DOI: 10.1002/jcu.20835.
10. Caraba A., Iurciuc S., Munteanu A., Iurciuc M. Hyponatremia and renal venous congestion in heart failure patients. *Dis. Markers*. 2021;2021:6499346. DOI: 10.1155/2021/6499346.
11. Husain-Syed F., Birk H.W., Ronco C., Schörmann T. et al. Doppler-derived renal venous stasis index in the prognosis of right heart failure. *J. Am. Heart Assoc.* 2019;8(21):e013584. DOI: 10.1161/JAHA.119.013584.
12. Ronco C., Haapio M., House A.A., Anavekar N., Bellomo R. Cardiorenal syndrome. *J. Am. Coll. Cardiol.* 2008;52(19):1527–1539. DOI: 10.1016/j.jacc.2008.07.051.
13. McCullough P.A., Li S., Jurkovitz C.T., Stevens L.A., Wang C., Collins A.J. et al. CKD and cardiovascular disease in screened

high-risk volunteer and general populations: the Kidney Early Evaluation Program (KEEP) and National Health and Nutrition Examination Survey (NHANES) 1999–2004. *Am. J. Kidney Dis*. 2008;51(4–2):S38–45. DOI: 10.1053/j.ajkd.2007.12.017.

14. Foley R.N., Murray A.M., Li S., Herzog C.A., McBean A.M., Eggers P.W. et al. Chronic kidney disease and the risk for cardiovascular disease, renal replacement, and death in the United States Medicare population, 1998 to 1999. *J. Am. Soc. Nephrol*. 2005;16(2):489–495. DOI: 10.1681/ASN.2004030203.

Authors' information

Kobalava Zhanna D. – Dr. Sci. (Med.), Professor, Head of the Department of Internal Medicine with the Subspecialty of Cardiology and Functional Diagnostics named after V.S. Moiseev, RUDN University, Moscow, zkobalava@mail.ru, https://orcid.org/0000-0003-1126-4282

Safarova Ayten F.– Dr. Sci. (Med.), Professor, Department of Internal Medicine with the Subspecialty of Cardiology and Functional Diagnostics named after V.S. Moiseev, RUDN University, Moscow; Physician, Functional Diagnostics Unit, Vinogradov City Clinical Hospital, Moscow, aytensaf@mail.ru, https://orcid.org/0000-0003-2412-5986

Aslanova Rena Sh. – Post-Graduate Student, Department of Internal Medicine with the Subspecialty of Cardiology and Functional Diagnostics named after V.S. Moiseev, RUDN University, Moscow; Cardiologist, Cardiology Unit, Vinogradov City Clinical Hospital, Moscow, rena.aslan@yandex.ru, https://orcid.org/0000-0003-0244-2112

(✉) **Aslanova Rena Sh.,** rena.aslan@yandex.ru

Received 03.10.2022;
approved after peer review 20.10.2022;
accepted 08.12.2022

УДК 616-056.257:577.121]-072.5:579.22:579.61
https://doi.org/10.20538/1682-0363-2023-2-61-67

Features of bacterial DNA taxonomy in blood of patients with various metabolic phenotypes of obesity

Kolesnikova I.M.[1], Karbyshev M.S.[1], Gaponov A.M.[2, 3], Khusnutdinova D.R.[4], Grigoryeva T.V.[4], Kamaldinova D.R.[4], Borisenko O.V.[1], Makarov V.V.[5], Yudin S.M.[5], Roumiantsev S.A.[1, 2], Shestopalov A.V.[1, 2, 6]

[1] *Pirogov Russian National Research Medical University*
1, Ostrovityanova Str., Moscow, 117997, Russian Federation

[2] *Center for Molecular Health*
32, Nakhimovsky Av., Moscow, 117218, Russian Federation

[3] *V.A. Negovsky Federal Research and Clinical Center of Intensive Care Medicine and Rehabilitology*
25/2, Petrovka Str., Moscow, 107031, Russian Federation

[4] *Kazan (Volga Region) Federal University*
18, Kremlyovskaya Str., Kazan, 420008, Russian Federation

[5] *Center for Strategic Planning and Management of Medical and Biological Health Risks*
10/1, Pogodinskaya Str., Moscow, 119121, Russian Federation

[7] *Dmitry Rogachev National Medical Research Center of Pediatric Hematology, Oncology, and Immunology*
1, Samory Mashela Str., Moscow, 117997, Russian Federation

ABSTRACT

Aim. To study the blood microbiome taxonomy in patients with metabolically healthy obesity (MHO) and metabolically unhealthy obesity (MUHO).

Materials and methods. The study included healthy donors without obesity (n = 116) and obese patients who were divided into subgroups with MHO (n = 36) and MUHO (n = 53). Bacterial DNA isolated from blood samples was subject to metagenomic sequencing of the v3–v4 variable region in the 16S rRNA gene. We compared the frequency of isolating certain taxa from the samples and the proportion of these taxa in the total pool of bacterial DNA in the blood.

Results. MUHO patients showed an increase in Lachnospiraceae, Ruminococcaceae, and Prevotellaceae, which are the main taxa in gut microbiota. This may indicate greater intestinal permeability in such patients. Obese patients, regardless of the metabolic phenotype of obesity, more often had Rhodobacteraceae, Streptomycetaceae, Leuconostocaceae, and Burkholderiaceae DNA in their blood. Nocardioidaceae, Flavobacteriaceae, Hyphomicrobiaceae, and Gaiellaceae DNA were more frequently present in the blood microbiome of patients with MHO, whereas MUHO patients more often had S24-7, Nocardiaceae, and Helicobacteraceae DNA in their blood. Many members of these families inhabit soil and water, which may indicate increased skin barrier permeability in obese patients. Additionally, a higher number of Helicobacteraceae-positive blood samples in the MUHO patient group may indicate increased translocation from the stomach.

Conclusion. Obesity is accompanied by changes in the taxonomic composition of the blood microbiome. Moreover, the nature of the changes depends on the metabolic phenotype of obesity and the permeability of external barriers.

Keywords: blood microbiome, bacterial DNA in blood, obesity, metabolically healthy obesity, metabolically unhealthy obesity

✉ *Kolesnikova Irina M.,* ir.max.kolesnikova@gmail.com

Conflict of interest. The authors declare the absence of obvious or potential conflicts of interest related to the publication of this article.

Source of financing. The study was carried out under the contract No. 0373100122119000041 within the project "Creating a biobank of blood serum and stool samples obtained from healthy donors and patients with obesity, metabolic syndrome, type 2 diabetes, and intestinal mucosal barrier dysfunction to reveal candidate species-non-specific mediators of quarum sensing systems in human gut microbiota, modulating endocrine and metabolic function of the adipose tissue".

Conformity with the principles of ethics. All patients signed an informed consent to participate in the study. The study was approved by the local Ethics Committee at Pirogov Russian National Research Medical University (Protocol No.186 of 26.06.2019) and Rostov State Medical University (Protocol No. 20/19 of 12.12.2019).

For citation: Kolesnikova I.M., Karbyshev M.S., Gaponov A.M., Khusnutdinova D.R., Grigoryeva T.V., Kamaldinova D.R., Borisenko O.V., Makarov V.V., Yudin S.M., Roumiantsev S.A., Shestopalov A.V. Features of bacterial DNA taxonomy in blood of patients with various metabolic phenotypes of obesity. *Bulletin of Siberian Medicine.* 2023;22(2):61–67. https://doi.org/10.20538/1682-0363-2023-2-61-67.

Особенности таксономической принадлежности бактериальной ДНК крови у пациентов с различными метаболическими фенотипами ожирения

Колесникова И.М.[1], Карбышев М.С.[1], Гапонов А.М.[2, 3], Хуснутдинова Д.Р.[4], Григорьева Т.В.[4], Камальдинова Д.Р.[4], Борисенко О.В.[1], Макаров В.В.[5], Юдин С.М.[5], Румянцев С.А.[1, 2], Шестопалов А.В.[1, 2, 6]

[1] Российский национальный исследовательский медицинский университет (РНИМУ) им. Н.И. Пирогова Россия,117997, г. Москва, ул. Островитянова, 1

[2] Общество с ограниченной ответственностью «Центр молекулярного здоровья» (ООО «ЦМЗ») Россия, 117218, г. Москва, пр. Нахимовский, 32

[3] Федеральный научно-клинический центр реаниматологии и реабилитологии (ФНКЦ РР) им. В.А. Неговкого Россия, 107031, г. Москва, ул. Петровка, 25/2

[4] Казанский (Приволжский) федеральный университет (КФУ) Россия, 420008, г. Казань, ул. Кремлевская, 18

[5] Центр стратегического планирования и управления медико-биологическими рисками здоровью Россия, 119121, г. Москва, Погодинская, 10/1

[6] Национальный медицинский исследовательский центр детской гематологии, онкологии и иммунологии (НМИЦ ДГОИ) им. Дмитрия Рогачева Россия, 117997, г. Москва, ул. Саморы Машела, 1, ГСП-7

РЕЗЮМЕ

Цель. Изучить таксономический состав микробиома крови у пациентов со следующими фенотипами: метаболически здоровым ожирением (МЗО) и метаболически нездоровым ожирением (МНЗО).

Материалы и методы. В исследование включены здоровые доноры без ожирения (n = 116) и пациенты с ожирением, которые были разделены на подгруппы с МЗО (n = 36) и МНЗО (n = 53). Из образцов венозной крови выделяли бактериальную ДНК и проводили метагеномное секвенирование вариабельного участка v3–v4 гена 16S рРНК. Сравнивалась как частота выделения отдельных таксонов из образцов, так и доля, приходящаяся на эти таксоны в общем пуле бактериальной ДНК крови.

Результаты. Для пациентов с МНЗО было характерно увеличение доли Lachnospiraceae, Ruminococcaceae

и Prevotellaceae, которые являются основными представителями кишечной микробиоты, что может являться следствием большей кишечной проницаемости, характерной для таких пациентов. Вне зависимости от метаболического фенотипа у пациентов с ожирением из образцов крови чаще выделялась ДНК Rhodobacteraceae, Streptomycetaceae, Leuconostocaceae и Burkholderiaceae. При МЗО также чаще обнаруживалась в крови ДНК Nocardioidaceae, Flavobacteriaceae, Hyphomicrobiaceae и Gaiellaceae, а у пациентов с МНЗО – S24-7, Nocardiaceae и Helicobacteraceae. Многие представители этих семейств являются обитателями почв и вод, что может свидетельствовать об усилении проницаемости кожного барьера у пациентов с ожирением. Также большая представленность Helicobacteraceae у пациентов с МНЗО может указывать на усиление транслокации из желудка.

Заключение. Ожирение приводит к выраженным изменениям в таксономическом составе микробиома крови, при этом характер изменений зависит от метаболического фенотипа ожирения и проницаемости внешних барьеров.

Ключевые слова: микробиом крови, бактериальная ДНК крови, ожирение, метаболически здоровое ожирение, метаболически нездоровое ожирение

Конфликт интересов. Авторы декларируют отсутствие явных и потенциальных конфликтов интересов, связанных с публикацией настоящей статьи.

Источник финансирования. Работа выполнена в рамках договора № 0373100122119000041 по проекту «Создание банка биообразцов сыворотки крови и фекалий от здоровых доноров и пациентов с ожирением, метаболическим синдромом, сахарным диабетом II типа, нарушением мукозального барьера желудочно-кишечного тракта с целью выявления кандидатных видонеспецифических медиаторов систем quorum sensing микробиоты человека, модулирующих эндокринную и метаболическую функцию жировой ткани».

Соответствие принципам этики. Все пациенты подписали информированное согласие на участие в исследовании. Исследование одобрено локальным этическим комитетом РНИМУ им. Н.И. Пирогова (протокол № 186 от 26.06.2019) и РостГМУ (протокол № 20/19 от 12.12.2019).

Для цитирования: Колесникова И.М., Карбышев М.С., Гапонов А.М., Хуснутдинова Д.Р., Григорьева Т.В., Камальдинова Д.Р., Борисенко О.В., Макаров В.В., Юдин С.М., Румянцев С.А., Шестопалов А.В. Особенности таксономической принадлежности бактериальной ДНК крови у пациентов с различными метаболическими фенотипами ожирения *Бюллетень сибирской медицины.* 2023;22(2):61–67. https://doi.org/10.20538/1682-0363-2023-2-61-67.

INTRODUCTION

Since the beginning of the XX century and the development of DNA sequencing technologies, works have appeared demonstrating the presence of bacterial DNA encoding 16S rRNA in blood samples obtained from both healthy individuals and patients with various pathologies [1–3]. To date, evidence of the presence of human blood microbiome is undoubtful, but its role in pathology remains unclear. The main source of microbial DNA in the blood is bacterial translocation from the gut and, to a lesser extent, from extraintestinal microbiomes [3].

There is a decrease in the diversity of gut microbiota in obesity compared to healthy donors, and body mass index (BMI) is negatively correlated with the total amount of microbial DNA in the gut [4, 5]. At the same time, an increase in blood microbiome diversity is observed in obese individuals [6]. Metabolic disorders are associated with increased intestinal permeability due to both internal (e.g., hyperglycemia) and external (changes in the gut microbiome, presence of excessive carbohydrates and / or fats in the diet) causes [7]. Obesity, however, does not always lead to the development of metabolic disorders, so there are metabolically healthy obesity (MHO) and metabolically unhealthy obesity (MUHO) phenotypes, respectively [8]. To date, there are no works demonstrating differences in the taxonomic composition of the blood microbiome depending on the metabolic phenotype of obesity, which became the aim of our study.

MATERIALS AND METHODS

A one-stage cohort study was carried out from 2018 to 2020 at the Center for Digital and Translational Biomedicine LLC, Center for Molecular Health, Department of Internal Medicine No. 3, RostSMU, Ministry of Health of Russia and Kazan (Volga Region) Federal University. Two groups were included in the study: a control group and obese patients. The con-

trol group included 116 healthy donors (BMI 18.5–24.9 kg / m^2) without metabolic disorders and arterial hypertension. The selection criteria for the obese patient group were BMI ≥ 30 kg / m^2 and waist circumference greater than 102 cm in men or 88 cm in women. According to the NCEP-ATP III criteria, obese patients were divided by the metabolic phenotype into a group with MHO (n = 36) and with MUHO (n = 53). Obesity was considered metabolically unhealthy if the patient was characterized by three or more criteria: 1) waist circumference (> 102 cm in men; > 88 cm in women); 2) serum triglycerides (≥ 1. 7 mmol / l); 3) high-density lipoprotein (HDL) cholesterol (< 1.03 mmol / l in men; < 1.29 mmol / l in women); 4) blood pressure (systolic ≥ 130 mm Hg; diastolic ≥ 85 mm Hg); 5) fasting glucose (≥ 5.6 mmol / l) [9].

Venous blood sampling followed by microbial DNA isolation was performed in all individuals according to the manufacturer's protocol (QIAamp BiOstic Bacterimia DNA Kit, Qiagen, Germany). Sequencing of the v3–v4 variable region of the 16S rRNA gene was performed on the Illumina MiSeq platform (USA) according to the manufacturer's recommendations. The obtained 16S rRNA gene sequences (reads) were analyzed using QIIME software (version 1.9.1) and Greengenes reference database (v. 13.8) with 97% similarity threshold between sequences. Data on taxon representation in the total pool of reads are given in fractions (0–1), which were calculated based on the number of mapped reads for each taxon. In addition, the frequency of DNA detection from the blood samples in each of the studied groups (%) was analyzed.

A statistical analysis was performed using the MedCalc® Statistical Software platform (MedCalc Software Ltd, Belgium). Given the absence of normal distribution in the fractions of individual taxa in the total pool of bacterial DNA in the blood, the data are presented as the median and the interquartile range Me [Q_{25}–Q_{75}]. A comparative analysis of the data sets was performed using the Kruskal – Wallis test. To establish the differences in the frequency of taxa in patients of different groups, the Pearson's chi-square test was used. The differences were considered statistically significant at $p \leq 0.05$.

RESULTS

We analyzed the taxonomic composition of the blood microbiome at the level of families that were identified in more than 25% of patients in at least one of the studied groups. On the one hand, the choice of families as a studied taxonomic level was explained by the fact that it provided a sufficiently detailed description of the blood microbiome and, on the other hand, included a relatively small number of unidentified taxa. The data obtained were compared by the frequency of detection of families from the blood samples (%) and by the proportion of each taxon in the total pool of bacterial DNA in the blood.

Lachnospiraceae, Ruminococcaceae, Prevotellaceae, Bacteroidaceae, Sphingomonadaceae, Staphylococcaceae, Corynebacteriaceae, Moraxellaceae, Micrococcaceae, Propionibacteriaceae were the main families in the blood microbiome. DNA from each of these families was detected in more than 75% of patients and accounted for more than 0.02% of the total bacterial DNA pool in the blood. In total, these families accounted for 0.548 [0.417–0.619] of the microbial DNA in the blood.

Both MHO and MUHO patients were characterized by specific changes in the blood microbiome, which was manifested both by changes in the proportion of individual families in the total bacterial DNA pool and in the frequency of detection of individual taxa (Table 1).

Table 1

Identified differences in the DNA content of individual families in the blood in MHO and MUHO patients, %, Me [Q_{25}–Q_{75}]

Family	Control group	Patients with MHO	Patients with MUHO
Lachnospiraceae	97.41% 0.103 [0.044–0.160]	97.22% 0.092 [0.033–0.211]	98.11% 0.152 [0.092–0.207]*
Ruminococcaceae	96.55% 0.083 [0.033–0.152]	100.00% 0.070 [0.038–0.114]	98.11% 0.117 [0.059–0.139]†
Prevotellaceae	86.21% 0.029 [0.012 – 0.065]	94.44% 0.036 [0.011–0.103]	94.34% 0.049 [0.025–0.115]*
Staphylococcaceae	93.97% 0.023 [0.009–0.053]	97.22% 0.018 [0.007–0.047]	88.68% 0.009 [0.004–0.027]*†
Caulobacteraceae	70.69% 0.010 [0.000–0.029]	58.33% 0.004 [0.000–0.024]	62.26% 0.003 [0.000–0.012]*
Rhodobacteraceae	39.66% 0.000 [0.000–0.008]	55.56%* 0.002 [0.000–0.012]	64.15%* 0.005 [0.000–0.011]*
Sphingomonadaceae	75.86% 0.022 [0.002–0.052]	75.00% 0.009 [0.000–0.060]	75.47% 0.005 [0.001–0.015]*†
S24-7	31.90% 0.000 [0.000–0.002]	47.22% 0.000 [0.000–0.007]*	69.81%* 0.005 [0.000–0.018]*†
Nocardiaceae	35.34% 0.000 [0.000–0.006]	50.00% 0.001 [0.000–0.010]	52.83%* 0.001 [0.000–0.010]
Nocardioidaceae	31.03% 0.000 [0.000–0.003]	50.00%* 0.000 [0.000–0.007]	41.55% 0.000 [0.000–0.007]
Streptomycetaceae	15.52% 0.000 [0.000–0.000]	33.33%* 0.000 [0.000–0.005]*	33.96%* 0.000 [0.000–0.003]*

Table (continued)

Family	Control group	Patients with MHO	Patients with MUHO
Flavobacteriaceae	25.00% 0.000 [0.000–0.000]	52.78%* 0.001 [0.000–0.014]*	26.42%† 0.000 [0.000–0.001]†
Helicobacteraceae	12.93% 0.000 [0.000–0.000]	16.67% 0.000 [0.000–0.000]	26.42%* 0.000 [0.000–0.001]
Burkholderiaceae	35.34% 0.000 [0.000–0.004]	55.56%* 0.001 [0.000–0.006]	54.72%* 0.001 [0.000–0.007]
Hyphomicrobiaceae	16.38% 0.000 [0.000–0.000]	41.67%* 0.000 [0.000–0.005]*	24.53% 0.000 [0.000–0.000]†
Bradyrhizobiaceae	44.83% 0.000 [0.000–0.008]	33.33% 0.000 [0.000–0.005]	22.64%* 0.000 [0.000–0.000]*
[*Barnesiellaceae*]	38.79% 0.000 [0.000–0.011]	11.11%* 0.000 [0.000–0.000]*	35.81%† 0.000 [0.000–0.009]†
Leuconostocaceae	9.48% 0.000 [0.000–0.000]	27.78%* 0.000 [0.000–0.001]*	32.08%* 0.000 [0.000–0.002]*
Gaiellaceae	15.52% 0.000 [0.000–0.000]	30.56%* 0.000 [0.000–0.002]	20.75% 0.000 [0.000–0.000]
Verrucomicrobiaceae	33.62% 0.000 [0.000–0.005]	16.67%* 0.000 [0.000–0.000]*	47.17%† 0.000 [0.000–0.012]†

* differences are significant compared to the control group ($p \leq 0.05$), † differences are significant compared to patients with MHO ($p \leq 0.05$).

Most of the changes in the blood microbiome in patients with MHO and MUHO were characterized by increasing frequency of DNA detection of individual families in the blood samples, which in some cases entailed an increase in the proportion of these taxa in the total pool of bacterial DNA in the blood. Regardless of the metabolic phenotype, DNA from the *Rhodobacteraceae, Streptomycetaceae, Leuconostocaceae,* and *Burkholderiaceae* families was more frequently detected in obese patients. *Nocardioidaceae, Flavobacteriaceae, Hyphomicrobiaceae*, and *Gaiellaceae* DNA was also detected in the blood of individuals with MHO, and *S24-7*, *Nocardiaceae*, and *Helicobacteraceae* DNA was detected in patients with MUHO. At the same time, in MUHO patients, *Lachnospiraceae* and *Prevotellaceae* were more abundant compared to Group 1 and *Ruminococcaceae* were more abundant compared to MHO patients, despite similar frequency of isolation of these families from the blood samples of each study group. These taxa accounted for about ⅕ of the total pool of bacterial DNA in the blood in healthy donors and patients with MHO, whereas in MHO patients, these families accounted for almost ⅓.

In addition, in both MHO and MUHO patients, there was a decrease in the proportion of several families in the blood microbiome. DNA [*Barnesiellaceae*] and *Verrucomicrobiaceae* were less frequently isolated from the blood in patients with MHO. In MUHO patients, the content of *Staphylococcaceae*, *Caulobacteraceae*, and *Sphingomonadaceae* was lower compared to Group 1, despite similar frequency of detecting DNA of these taxa from the blood samples. Moreover, *Bradyrhizobiaceae* DNA was detected less frequently in these patients.

DISCUSSION

The obtained data indicate that obesity leads to significant changes in the blood microbiome at the family level, and the features of the blood microbiome depend on the metabolic phenotype of obesity. At the phylum level, the taxonomic composition of the blood microbiome is similar in healthy donors and obese patients [6].

Both the patients with MHO and patients with MUHO were characterized by the spectrum of taxa whose DNA was detected from the blood samples of these patients more frequently than in the control group. Interestingly, representatives of *Rhodobacteraceae, Streptomycetaceae, Burkholderiaceae, Nocardioidaceae, Flavobacteriaceae, Hyphomicrobiaceae, Gaiellaceae*, and *Nocardiaceae*, which were detected in the blood samples of MHO and MUHO patients with increased frequency, are mostly soil and water inhabitants. Such habitats suggest that translocation of DNA from these taxa into the blood may occur from the surface of the skin or respiratory tract. Obese patients are characterized by a large body surface area, which may cause increased percutaneous translocation of microbial DNA. In addition, obesity causes changes in skin physiology and leads to increased permeability of the skin barrier [10]. It seems that obesity, regardless of its metabolic phenotype, is accompanied by increased translocation of bacterial DNA from the skin surface.

An increase in the proportion of the *Lachnospiraceae, Ruminococcaceae,* and *Prevotellaceae* families in the total pool of bacterial DNA in the blood was noted in patients with MUHO. Representatives of these families are anaerobes and the main representatives of the gut microbial flora. MUHO is associated with the presence of smoldering systemic inflammation and greater permeability of the intestinal wall [7, 8]. Thus, it can be assumed that the increased proportion of *Lachnospiraceae, Ruminococcaceae,* and *Prevotellaceae* in MUHO is a consequence of greater translocation of microbial DNA from the intestine, common in such patients.

An increased frequency of *Helicobacteraceae* DNA detection was also prevailing in MUHO pa-

tients. Since the main representative of this family is *Helicobacter pylori*, it can be assumed that MUHO is also associated with increased permeability of the gastric wall to bacterial DNA. Thus, MUHO seems to be characterized by increased microbial translocation from both intestinal and extraintestinal microbiomes, which can be caused by damaged barrier in the presence of chronic inflammation.

CONCLUSION

Obesity, regardless of its metabolic phenotype, is accompanied by changes in the taxonomic composition of bacterial DNA in the blood. Both MHO and MUHO are characterized by an increase in the frequency of isolating DNA of soil and water resident families, which may indicate large translocation of microbial DNA from the skin surface. At the same time, patients with MUHO also have an increased content of DNA of gastric and intestinal flora representatives in the blood, which may indicate greater permeability of these barriers to bacterial DNA. Thus, changes in the taxonomic composition of the blood microbiome may indicate permeability of external barriers of the body.

REFERENCES

1. Nikkari S., McLaughlin I.J., Bi W., Dodge D.E., Relman D.A. Does blood of healthy subjects contain bacterial ribosomal DNA? *J. Clin. Microbiol*. 2001;39(5):1956–1959. DOI: 10.1128/JCM.39.5.1956-1959.2001.
2. Fedorov N.A., Yolov A.A., Zhiburt E.B., Sukhanov Y.S., Kruglov A.N., Stonogin A.V. et al. Frequency of detection of bacterial DNA in whole blood of donors. *Reports of the Russian Academy of Sciences.* 2005;402(6):841–843 (in Russ.). DOI: 10.1007/s10630-005-0085-y.
3. Castillo D.J., Rifkin R.F., Cowan D.A., Potgieter M. The healthy human blood microbiome: Fact or fiction? *Front. Cell. Infect. Microbiol*. 2019;9:1–12. DOI: 10.3389/fcimb.2019.00148.
4. Gaponov A.M., Volkova N.I., Ganenko L.A., Naboka Yu.L., Markelova M.I., Siniagina M.N. et al. Characteristics of the colonic microbiome in patients with different obesity phenotypes (the original article). *Journal of Microbiology, Epidemiology and Immunobiology.* 2021;98(2):144–155. DOI: 10.36233/0372-9311-66.
5. Kotrova A.D., Shishkin A.N., Voropaeva L.S., Lavrenova N.S., Slepyh L.A., Lukashenko M.V. et al. Gender assessment of the gut microbiome in obese patients. *Clinical Gastroenterology*. 2021;(10):91–99 (in Russ.). DOI: 10.31146/1682-8658-ecg-194-10-91-99.
6. Shestopalov A.V., Kolesnikova I.M., Gaponov A.M., Grigoryeva T.V., Khusnutdinova D.R., Kamaldinova D.R. et al. Effect of metabolic type of obesity on blood microbiome. *Problems of Biological, Medical, and Pharmaceutical Chemistry*. 2022;25(2):35–41 (in Russ.). DOI: 10.29296/25877313-2022-02-06.
7. Massier L., Blüher M., Kovacs P., Chakaroun R.M. Impaired intestinal barrier and tissue bacteria: pathomechanisms for metabolic diseases. *Front. Endocrinol. (Lausanne)*. 2021;12(March):1–18. DOI: 10.3389/fendo.2021.616506.
8. Iacobini C., Pugliese G., Blasetti Fantauzzi C., Federici M., Menini S. Metabolically healthy versus metabolically unhealthy obesity. *Metabolism. Elsevier Inc.* 2019;92:51–60. DOI: 10.1016/j.metabol.2018.11.009.
9. Phillips C.M. Metabolically healthy obesity: Definitions, determinants and clinical implications. *Rev. Endocr. Metab. Disord.* 2013;14(3):219–227. DOI: 10.1007/s11154-013-9252-x.
10. Hirt P.A., Castillo D.E., Yosipovitch G., Keri J.E. Skin changes in the obese patient. *J. Am. Acad. Dermatol.* 2019;81(5): 1037–1057. DOI: 10.1016/j.jaad.2018.12.070.

Authors' contribution

Kolesnikova I.M., Karbyshev M.S., Khusnutdinova D.R., Kamaldinova D.R., Borisenko O.V. – analysis and interpretation of the data. Gaponov A.M., Grigoryeva T.V., Makarov V.V. – conception and design, justification of the manuscript or critical revision of the manuscript for important intellectual content. Yudin S.M. – conception and design, final approval of the manuscript for publication. Roumiantsev S.A., Shestopalov A.V. – conception and design, justification of the manuscript or critical revision of the manuscript for important intellectual content, final approval of the manuscript for publication.

Authors' information

Kolesnikova Irina M. – Senior Lecturer, Department of Biochemistry and Molecular Biology, Medical Faculty, Pirogov Russian National Research Medical University, Moscow, ir.max.kolesnikova@gmail.com, https://orcid.org/0000-0003-0269-0343

Karbyshev Mikhail S. – Cand. Sci. (Biology), Associate Professor, Department of Biochemistry and Molecular Biology, Medical Faculty, Pirogov Russian National Research Medical University, Moscow, karbyshevms@biocad.ru, https://orcid.org/0000-0001-5969-3874

Gaponov Andrey M. – Cand. Sci. (Med.), Head of the Department of Infectious Immunology, Center of Digital and Translational Biomedicine, Center for Molecular Health, Moscow; Leading Researcher, Laboratory for Molecular Mechanisms of Critical States, V.A. Negovsky Federal Research and Clinical Center of Intensive Care Medicine and Rehabilitology, Moscow, zorba@yandex.ru, https://orcid.org/0000-0002-3429-1294

Khusnutdinova Dilyara R. – Junior Researcher, Kazan (Volga Region) Federal University, Kazan, tatabio@inbox.ru, https://orcid.org/0000- 0002-9982-9059

Grigoryeva Tatiana V. – Cand. Sci. (Biology), Senior Researcher, Kazan (Volga Region) Federal University, Kazan, tatabio@inbox.ru, https://orcid.org/0000-0001-5314-7012

Kamaldinova Dilyara R. – Researcher, Kazan (Volga Region) Federal University, Kazan, tatabio@inbox.ru, https://orcid.org/0000-0002-9663-4408

Borisenko Olga V. – Cand. Sci. (Med.), Associate Professor, Department of Biochemistry and Molecular Biology, Medical Faculty, Pirogov Russian National Research Medical University, Moscow, borisenko_olga07@mail.ru, https://orcid.org/0000-0001-8007-6045

Makarov Valentin V. – Cand. Sci. (Biology), Head of the Department, Center for Strategic Planning and Management of Medical and Biological Health Risks, Moscow, makarov@cspmz.ru, https://orcid.org/0000-0001-9495-0266

Yudin Sergey M. – Dr. Sci. (Med.), Professor, Director General, Center for Strategic Planning and Management of Medical and Biological Health Risks, Moscow, yudin2005@mail.ru, https://orcid.org/0000-0002-7942-8004

Roumiantsev Sergey A. – Dr. Sci. (Med.), Professor, Corresponding Member of the Russian Academy of Sciences, Director, Center for Molecular Health, Moscow; Head of the Department of Oncology, Hematology and Radiotherapy, Pediatric Faculty, Pirogov Russian National Research Medical University, Moscow, s_roumiantsev@mail.ru, https://orcid.org/0000-0002-7418-0222

Shestopalov Alexander V. – Dr. Sci. (Med.), Professor, Deputy Director, Center for Molecular Health, Moscow; Director, Department of Postgraduate Education, Residency, and Postgraduate Studies, Dmitry Rogachev National Medical Research Center of Pediatric Hematology, Oncology and Immunology, Moscow; Head of the Department of Biochemistry and Molecular Biology, Medical Faculty, Pirogov Russian National Research Medical University, Moscow, al-shest@yandex.ru, https://orcid.org/0000-0001-5969-3874

(✉) **Kolesnikova Irina M.,** ir.max.kolesnikova@gmail.com

Received 27.07.2022;
approved after peer review 29.10.2022;
accepted 08.12.2022

УДК 616.71-006-074:615.38
https://doi.org/10.20538/1682-0363-2023-2-68-77

Galectin-3 in the blood serum of patients with bone tumors

Kushlinskii N.E.[1, 4], Kovaleva O.V.[1], Prishchep P.L.[1], Zybina N.N.[2], Jurisic V.[3], Alferov A.A.[1, 4], Kuzmin Yu.B.[1, 4], Goryacheva I.O.[1], Kuznetsov I.N.[1, 4], Bulytcheva I.V.[1], Varfolomeeva S.R.[1], Sushentsov E.A.[1], Gershtein E.S.[1, 4], Rogozhin D.V.[1], Yanushevich O.O.[4], Stilidi I.S.[1]

[1] N.N. Blokhin National Medical Research Center of Oncology
24, Kashirskoe Shosse Str., Moscow, 115522, Russian Federation

[2] A.M. Nikiforov All-Russian Center for Emergency and Radiation Medicine EMERCOM of Russia
4 / 2, Lebedeva Str., St. Petersburg, 194044, Russian Federation

[3] University of Kragujevac
69, Svetozara Markovicha Str., Kragujevac, 34000, Serbia

[4] A.I. Evdokimov Moscow State University of Medicine and Dentistry
20/1, Delegatskaya Str., Moscow, 127473, Russian Federation

ABSTRACT

Background. Due to diversity of cancer, the functional role of galectin-3 is rather controversial; however, for many types of neoplasms, the marker acts as a tumor growth promoter.

Aim. To perform a comparative analysis of galectin-3 levels in the blood serum of healthy individuals and patients with benign, borderline, and malignant bone tumors divided into two age groups (under and over 18 years of age) based on the main clinical and morphological characteristics of the disease and prognosis.

Materials and methods. The study included 201 patients with benign, borderline (giant cell tumors, locally aggressive tumors), and malignant bone tumors and 31 healthy donors. The galectin-3 level was determined in the blood serum before treatment with Human Galectin-3 ELISA kit (R&D, USA).

Results. The level of galectin-3 in the blood serum of patients with benign and malignant bone tumors was statistically significantly higher than that in the control group of patients both under and over 18 years. In patients with borderline bone tumors, a trend toward an increase in the galectin-3 concentration compared with the controls was revealed. The ROC analysis for galectin-3 in patients with bone sarcomas showed that the area under the curve (AUC) comprised 0.795 ($p < 0.0001$) in the group of patients over 18 years and 0.868 ($p = 0.0008$) in the individuals under 18 years. For malignant bone tumors in patients over 18 years, the sensitivity of this method was 71.3%, and specificity was 71.43% (optimal cut-off level was 8.09 ng / ml; $p < 0.0001$), while in patients under 18 years, the sensitivity of the method was 80%, and specificity was 90% (optimal cut-off level was 5.49 ng / ml; $p < 0.001$). No significant associations between the serum galectin-3 level and the clinical and morphological characteristics of bone neoplasms were found both in patients under and over 18 years of age. However, it could be noted that the highest concentration of the marker was found in chordomas and at earlier stages of the disease. In patients over 18 years with chondrosarcoma and osteosarcoma, no correlation between the marker and the disease prognosis was found.

Conclusion. An increase in the galectin-3 level in the blood serum was observed in all age groups of patients with both benign and malignant bone tumors. However, the sensitivity and specificity of the method assessed by the ROC analysis do not allow to apply this marker for the diagnosis of bone tumors.

Keywords: bone tumors, galectin-3, blood serum, prognosis

Conflict of interest. The authors declare the absence of obvious or potential conflict of interest related to the publication of this article.

Source of financing. The authors state that they received no funding for the study.

✉ *Kushlinskii Nikolay E.,* biochimia@yandex.ru

Conformity with the principles of ethics. All patients signed an informed consent to participate in the study. The study was approved by the local Ethics Committee at N.N. Blokhin National Medical Research Center of Oncology.

For citation: Kushlinskii N.E., Kovaleva O.V., Prishchep P.L., Zybina N.N., Jurisic V., Alferov A.A., Kuzmin Yu.B., Goryacheva I.O., Kuznetsov I.N., Bulytcheva I.V., Varfolomeeva S.R., Sushentsov E.A., Gershtein E.S., Rogozhin D.V., Yanushevich O.O., Stilidi I.S. Galectin-3 in the blood serum of patients with bone tumors. *Bulletin of Siberian Medicine.* 2023;22(2):68–77. https://doi.org/10.20538/1682-0363-2023-2-68-77.

Галектин-3 в сыворотке крови больных опухолями костей

Кушлинский Н.Е.[1, 4], Ковалева О.В.[1], Прищеп П.Л.[1], Зыбина Н.Н.[2], Юришич В.[3], Алферов А.А.[1, 4], Кузьмин Ю.Б.[1, 4], Горячева И.О.[1], Кузнецов И.Н.[1, 4], Булычева И.В.[1], Варфоломеева С.Р.[1], Сушенцов Е.А.[1], Герштейн Е.С.[1, 4], Рогожин Д.В.[1], Янушевич О.О.[4], Стилиди И.С.[1]

[1] Национальный медицинский исследовательский центр (НМИЦ) онкологии им. Н.Н. Блохина
Россия, 115522, г. Москва, Каширское шоссе, 24

[2] Всероссийский центр экстренной и радиационной медицины (ВЦЭРМ) им. А.М. Никифорова МЧС России
Россия, 194044, г. Санкт-Петербург, ул. Лебедева, 4/2

[3] Университет Краугеваца
Сербия, 34000, г. Краугевац, ул. Светозара Марковича, 69

[4] Московский государственный медико-стоматологический университет (МГМСУ) им. А.И. Евдокимова
Россия, 127473, г. Москва, ул. Делегатская, 20/1

РЕЗЮМЕ

Введение. Ввиду многогранности онкологических заболеваний функциональная роль галектина-3 достаточно противоречива, однако для многих типов новообразований маркер играет роль промотора опухолевого роста.

Цель исследования – сравнительный анализ уровней галектина-3 в сыворотке крови здоровых доноров, больных доброкачественными, пограничными и злокачественными новообразованиями костей в двух возрастных группах до и старше 18 лет с учетом основных клинико-морфологических характеристик заболевания и прогноза.

Материалы и методы. В исследование включен 201 пациент с доброкачественными, пограничными (гигантоклеточные опухоли, «локально агрессивные» опухоли), злокачественными новообразованиями костей и 31 здоровый донор. Концентрацию галектина-3 определяли в сыворотке крови до лечения наборами реактивов для прямого иммуноферментного анализа Human Galectin-3 (R&D, США).

Результаты. Показано, что содержание галектина-3 в сыворотке крови больных доброкачественными и злокачественными опухолями костей статистически значимо выше, чем в контрольной группе, как в возрасте до, так и старше 18 лет. У пациентов с пограничными опухолями костей отмечена тенденция к увеличению концентрации галектина-3 по сравнению с контролем. ROC-анализ для галектина-3 у больных саркомами костей показал, что площадь под ROC-кривой составила 0,795 ($p < 0,0001$) в группе пациентов в возрасте старше 18 лет и 0,868 ($p = 0,0008$) в группе пациентов в возрасте до 18 лет. Для злокачественных новообразований костей у больных в возрасте старше 18 лет чувствительность данного метода составила 71,3%, специфичность 71,43% (пороговый уровень 8,09 нг/мл; $p < 0,0001$), а у пациентов в возрасте младше 18 лет чувствительность этого метода составила 80%, специфичность 90% при пороговом уровне 5,49 нг/мл ($p < 0,001$). В обеих возрастных группах не найдено значимых ассоциаций содержания сывороточного галектина-3 с клинико-морфологическими характеристиками новообразований костей, однако следует отметить, что наибольшая концентрация маркера обнаружена при хордомах и на более ранних стадиях заболевания. У больных хондросаркомой и остеосаркомой старше 18 лет не выявлено связи маркера с прогнозом заболевания.

Заключение. Повышение содержания галектина-3 в сыворотке крови наблюдалось во всех возрастных группах пациентов как с доброкачественными, так и злокачественными новообразованиями костей, однако чувствительность и специфичность теста по данным ROC-анализа недостаточны для использования данного маркера для диагностики опухолей костей.

Ключевые слова: опухоли костей, галектин-3, сыворотка крови, прогноз

Конфликт интересов. Авторы декларируют отсутствие явных и потенциальных конфликтов интересов, связанных с публикацией настоящей статьи.

Источник финансирования. Авторы заявляют об отсутствии финансирования при проведении исследования.

Соответствие принципам этики. Все пациенты подписали информированное согласие на участие в исследовании. Исследование одобрено локальным этическим комитетом НМИЦ онкологии им. Н.Н. Блохина, протокол № 5 от 02.10.2022 г.

Для цитирования: Кушлинский Н.Е., Ковалева О.В., Прищеп П.Л., Зыбина Н.Н., Юришич В., Алферов А.А., Кузьмин Ю.Б., Горячева И.О., Кузнецов И.Н., Булычева И.В., Варфоломеева С.Р., Сушенцов Е.А., Герштейн Е.С., Рогожин Д.В., Янушевич О.О., Стилиди И.С. Галектин-3 в сыворотке крови больных опухолями костей. *Бюллетень сибирской медицины.* 2023;22(2):68–77. https://doi.org/10.20538/1682-0363-2023-2-68-77.

INTRODUCTION

Galectins are a group of galactoside-binding lectins that play specific roles both intra- and extracellularly. They trigger cytokine secretion and cellular migration, proliferation, and apoptosis. Extracellularly, galectins facilitate cell – cell interactions and interaction of cells with the extracellular matrix. Galectins bind with glycans (oligosaccharides) on the intracellular membrane surface, participating in ligation of macromolecules and formation of signaling pathways. Diverse functions of galectins have sparked the interest of researchers in unveiling their role in the pathogenesis of various diseases and pathologies.

Out of 15 galectins currently known, galectin-3 attracts special interest of researchers due to its involvement in tissue fibrosis and its potential application as a marker for cardiac failure. Galectin-3 has been found to be involved in various pathological processes, including inflammation [2], fibrosis, as well as cardiac [3, 4] and kidney [5] diseases, diabetes mellitus [6], viral infections [7], autoimmune [8] and neurodegenerative [9] diseases, and cancer [10].

The functional role of galectin-3 in the context of cancers is rather controversial, owing to their diversity. On the one hand, galectin-3 plays a role as a tumor growth promoter for many types of neoplasms. An increase in the expression of this protein is associated with proliferation and invasion of pancreatic cancer cells [11]. Galectin-3 expression, both at the mRNA and protein level, is increased in malignant liver tumors compared to normal tissues [12]. Overexpression of galectin-3 is also observed in diffuse large B-cell lymphoma and is associated with an advanced stage and a worse prognosis of this disease [13]. Increased galectin-3 expression correlates with an unfavorable prognosis in patients with nasopharyngeal carcinoma [14] and colorectal cancer [15]. Increased galectin-3 expression was also found in gastric tumors [16], and its overexpression and nuclear localization were associated with peritoneal dissemination of such tumors [17]. Galectin-3 overexpression led to the intensification of motility and invasion of lung cancer cells [18].

On the other hand, in some tumor types, galectin-3 may function as a tumor suppressor. Thus, a decrease in its expression is associated with a more malignant phenotype of breast and endometrial cancer [19]. For prostate cancer, a gradient decrease in galectin-3 expression from normal and conventionally normal tissue to tumor one was observed [20]. Suppression of the expression of this protein by siRNA reduced the migratory, invasive, and colony-forming ability of prostate cancer cells [21].

Although galectin-3 expression has been studied in the majority of solid tumors, its functional role in bone neoplasms is still unknown. An increased level of galectin-3 in the blood serum of osteosarcoma patients was reported, and its expression in the tumor was higher than in adjacent healthy tissues and correlated with disease stage and metastasis. The authors suggest that in the future, galectin-3 might become a prognostic marker for osteosarcoma [22]. It was shown that suppression of galectin-3 expression in osteosarcoma cells *in vitro* led to a decline in their metastatic potential [23]. Some authors suggest that galectin-3 may serve as a marker for the differential diagnosis of chordomas and myxoid chondrosarcomas. No data are available on the association between the levels of tissue and soluble forms of galectin-3 for other types of bone tumors.

The aim of this study was to perform a comparative analysis of galectin-3 levels in the blood serum of healthy individuals and patients with benign, borderline, and malignant bone tumors, taking into consideration the clinical and pathological characteristics of the disease and its prognosis.

MATERIALS AND METHODS

The study involved 201 patients with benign, borderline, and malignant bone tumors, 36 of whom were under 18 years old. The control group comprised 31 healthy individuals, 10 of whom were under 18 years old. All procedures involving patients and healthy individuals performed in the study complied with the standards of the Ethics Committee at N.N. Blokhin National Medical Research Center of Oncology and the Declaration of Helsinki adopted in 1964 and its further amendments or comparable ethical norms. Each study participant signed an informed consent to participate in the study. All patients underwent an examination and treatment at N.N. Blokhin National Medical Research Center of Oncology. The clinical and radiological diagnosis of the neoplasm was confirmed by the morphological examination according to the WHO histologic classification of bone tumors (2020). The main characteristics of the control and bone tumor groups are presented in Table 1–3.

Table 1

Number of patients in the study groups

Study groups	Age under 18 years	Age over 18 years
Control	10 (32.3%)	21 (67.7%)
Benign bone tumors (BBT)	11 (26.2%)	31 (73.8%)
Borderline bone tumors (BlBT)	–	19 (100%)
Malignant bone tumors (MBT)	25 (17.9%)	115 (82.1%)

Table 2

Characteristics of the bone tumor patients aged over 18 years old, *n* (%)

Parameter	Value
Age, years, *Me* (Q_{25}–Q_{75})	48 (34-57)
Sex:	
male;	61 (53.1%)
female	54 (46.9%)
Histologic tumor type:	
osteosarcoma;	35 (30.5%)
chondrosarcoma;	69 (60.0%)
chordoma;	6 (5.3%)
Ewing sarcoma	5 (4.2%)
Stage:	
I;	37 (32.2%)
II;	66 (57.4%)
III–IV	12 (10.4%)
Grade:	
G1–G2;	64 (61.6%)
G3	40 (38.4%)
Tumor size (T):	
T1;	24 (20.9%)
T2;	84 (73.1%)
T3–T4	7 (6.0%)
Nodal status:	
N0;	111 (96.6%)
N1	4 (3.4)
Distant metastasis (M):	
M0	110 (95.7%)
M1	5 (4.3%)
Type of the bone:	
spongy / flat	54 (47.0%)
tubular	61 (53.0%)
Localization:	
upper limb;	21 (18.3%)
thoracic cage / vertebral column;	9 (7.7%)
pelvis;	42 (36.6%)
lower limb	43 (37.4%)

Table 3

Characteristics of the bone tumor patients aged under 18 years old, *n* (%)

Parameter	Value
Age, years, *Me* (Q_{25}–Q_{75})	12 (9–15)
Sex:	
male;	12 (48%)
female	13 (52%)
Histologic tumor type:	
osteosarcoma;	17 (68%)
chondrosarcoma;	1 (28%)
Ewing sarcoma	7 (4%)
Stage:	
I;	–
II;	21 (84%)
III–IV	4 (16%)
Grade:	
G1–G2;	1 (32%)
G3	17 (68%)
Tumor size (T):	
T1;	–
T2;	24 (96%)
T3–T4	1 (4%)
Nodal status:	
N0;	25 (100%)
N1	–
Distant metastasis (M):	
M0	21 (84%)
M1	4 (16%)
Type of the bone:	
spongy / flat	2 (8%)
tubular	23 (92%)
Localization:	
upper limb;	–
thoracic cage / vertebral column;	2 (8%)
pelvis;	1 (4%)
lower limb	22 (88%)

The galectin-3 concentration was measured in pretreatment blood serum using the Human Galectin-3 ELISA kit (R&D, USA) in accordance with the manufacturer's guidelines and expressed in nanograms (ng) per 1 ml of serum.

The data were analyzed using GraphPad Prism 9.4. The nonparametric Mann – Whitney and Kruskal – Wallis tests were used to compare independent groups. Overall survival was assessed using the Kaplan – Meier method, and the statistical significance of differences between the curves was evaluated using the log rank test. The differences were considered statistically significant at $p < 0.05$.

RESULTS

We analyzed the levels of galectin-3 in both the control group and patients with different types of bone tumors. The median serum content of galectin-3 in healthy donors who were over 18 years of age was 6.48 ng / ml, which was significantly lower than in patients with malignant bone tumors within the corresponding age group (10.18 ng / ml; $p < 0.0001$) (Table 4).

Table 4

Galectin-3 level in patients with bone tumors based on age, ng / ml, *Me* (Q_{25}–Q_{75})

Parameter	Age ≥ 18 years	*p*	Age < 18 years	*p*
Control [1]	6.48 (3.32–8.49)	–	4.15 (3.93–5.23)	–
Benign bone tumors [2]	8.72 (6.53–11.45)	0.035 (1vs2)	7.85 (6.69–12.75)	0.001 (1vs2)
Borderline bone tumors[3]	8.88 (6.19–10.88)	0.077 (1vs3)	–	–
Malignant bone tumors[4]	10.18 (7.52–12.55)	< 0.0001 (1vs4)	7.22 (5.92–11.35)	0.002 (1vs4)

The content of galectin-3 in the blood serum of patients with benign and malignant tumors was statistically significantly higher than that in the control group both in adult patients (over 18 years old) and in patients of the younger age group (under 18 years old) (Table 4). For borderline tumors diagnosed only in adult patients, a trend toward an increase in the galectin-3 level was also noted, compared to the control group.

The information value of a galectin-3 level as a diagnostic method was analyzed by evaluating its sensitivity and specificity by the ROC analysis. The results are shown in Fig. 1.

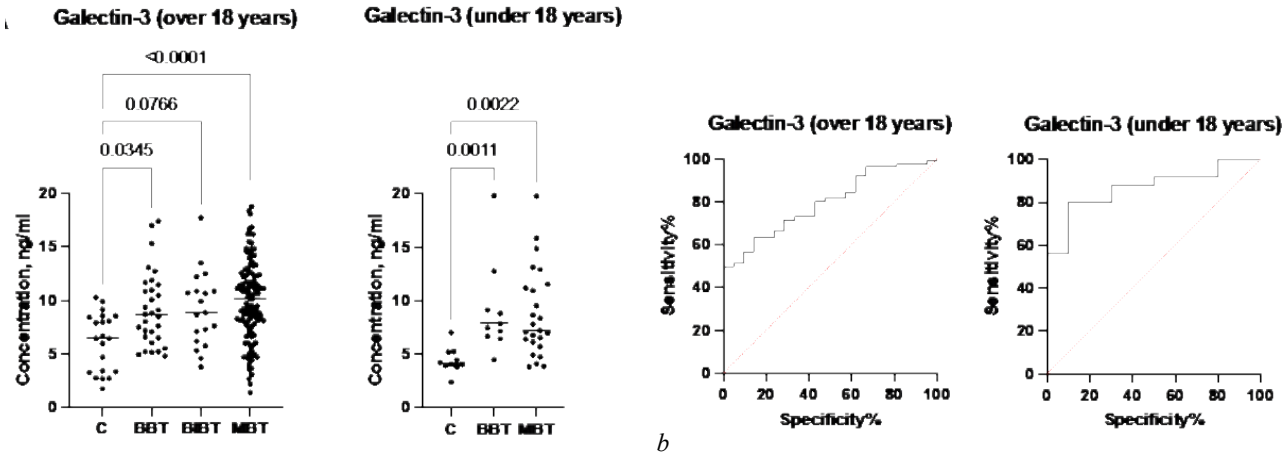

Fig. 1. Serum galectin-3 level in patients with benign, borderline, and malignant bone tumors as well as in healthy donors with regard to age: *a* – comparative analysis, *b* – ROC analysis of the diagnostic value (AUC 0.795 ($p < 0.0001$) in the group of patients over 18 years old and AUC 0.868 ($p = 0.0008$) in the group of patients under 18 years old)

For malignant bone tumors in patients over 18 years of age, the sensitivity was 71.3%, and specificity was 71.4% (the optimal cut-off level was 8.09 ng / ml; $p < 0.0001$), while in patients under 18 years old, the sensitivity of the method was 80%, and specificity was 90% (optimal cut-off level was 5.49 ng / ml; $p < 0.001$).

Next, we analyzed serum galectin-3 levels according to the main clinical and morphological characteristics of the disease for patients over 18 years of age (Table 5).

No significant associations between serum galectin-3 levels and clinical or morphological characteristics of bone neoplasms were found in the age

group of individuals over 18 years old. However, it should be noted that the highest levels of galectin-3 were detected in chordomas and at earlier stages of the disease.

At the next stage of the study, we analyzed galectin-3 levels in the blood serum of patients under 18 years of age, depending on the main clinical and morphological characteristics of the disease (Table 6). No significant associations were found between the main clinical and morphological characteristics of the disease and galectin-3 levels in the group of patients under 18 years old, as well as in the group of patients over 18 years old (Table 5, 6).

Table 5

Serum level of galectin-3 in patients with malignant bone tumors aged over 18 years depending on the clinical and morphological characteristics of the disease

Parameter	Galectin-3, ng / ml		
	Me	Q_{25}–Q_{75}	*p*
Age: – <48; – >=48	 9.15 10.66	 6.66–11.6 8.2–13.65	0.084
Sex: – male; – female	 9.21 10.93	 7.12–11.68 7.95–13.73	0.106
Histologic tumor type: – osteosarcoma (1); – chondrosarcoma (2); – chordoma (3); Ewing sarcoma (4)	 10.18 9.5 14.7 9.09	 7.00–11.81 7.49–12.34 11.64–14.62 5.88–14.32	0.06 (2vs3)
Stage: I; II; III–IV	 10.76 9.84 8.99	 7.99–13.34 6.99–11.75 6.51–12.36	>0.99
Grade: G1–G2; G3	 10.25 9.43	 8.13–12.52 6.04–11.57	0.43
Tumor size (T): T1; T2; T3–T4	 10.16 10.25 8.05	 6.67–14.34 8.03–12.19 4.74–12.41	>0.99
Nodal status: N0; N1	 10.31 7.64	 7.74–12.55 4.52–14.5	0.51
Distant metastasis (M): M0 M1	 10.25 9.28	 7.51–12.55 7.36–13.69	0.96
Type of the bone: spongy / flat tubular	 10.67 9.46	 8.18–12.75 6.69–12.31	0.28
Localization: upper limb; thoracic cage / vertebral column; pelvis; lower limb	 8.69 10.17 10.68 10.31	 4.87–12.57 8.85–15.12 7.35–12.59 8.05–12.36	>0.99

Table 6

Serum content of galectin-3 in patients with malignant bone tumors under the age of 18 years depending on the clinical and morphological characteristics of the disease

Characteristic	Galectin-3, ng / ml		
	Me	Q_{25}–Q_{75}	*p*
Age: < 12 >12	 7.07 9.67	 6.13–9.53 4.89–15.1	0.42
Sex: male; female	 9.81 6.54	 6.85–12.57 4.85–8.67	0.12
Histologic tumor type: osteosarcoma (1) chondrosarcoma (2) Ewing sarcoma (3)	 8.38 8.66 6.99	 6.06–12.32 – 4.76–7.81	 >0.99 (1vs2) 0.65 (1vs3) >0.99 (2vs3)
Stage: I (1) II (2) III–IV (3)	 – 6.99 9.92	 – 5.32–11.24 8.02–13.94	 >0.15 (2vs3)
Grade: –G1–G2 –G3	 4.11 7.52	 – 6.2–11.44	 –
Tumor size (T): T1; T2; T3–T4	 7.15 7.81	 8.81–11.44 –	 –
Nodal status: N0; N1	 7.22 –	 5.92–11.35 –	 –
Distant metastasis (M): M0 M1	 6.99 9.92	 5.32–11.24 8.02–13.94	 0.15
Type of the bone: spongy / flat tubular	 6.76 7.22	 5.7–7.81 6.13–11.52	 0.60
Localization upper limb (1) thoracic cage / vertebral column (2) pelvis (3) lower limb (4)	 – 5.92 7.81 7.80	 – 5.7–6.13 – 6.04–11.87	 >0.99 (2vs3) >0.58 (2vs4) > 0.99 (3vs4)

At the final stage of the study, we assessed the prognostic value of the galectin-3 level in the groups of patients aged over 18 years old with the most common malignant bone neoplasms, which were osteosarcoma and chondrosarcoma (Fig. 2).

The presented data show that the serum levels of galectin-3 are not a significant prognostic factor in bone sarcomas for the general group of patients with malignant bone neoplasms, as well as for two experimental groups with bone-forming (osteosarcoma) and cartilage-forming (chondrosarcoma) tumors, respectively.

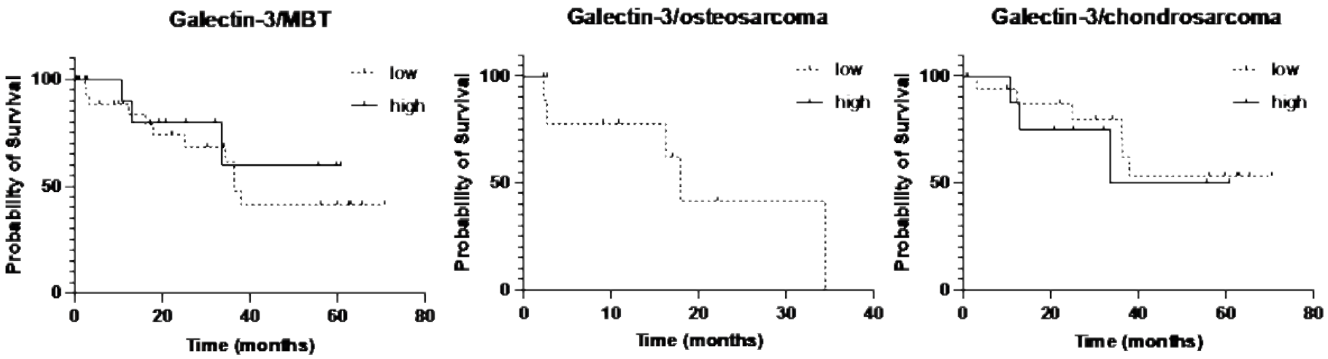

Fig. 2. Prognostic value of the galectin-3 level in three groups: in the general group of patients with malignant bone tumors, in osteosarcoma patients, and in chondrosarcoma patients over 18 years old.

DISCUSSION

A comparative study was conducted to analyze the levels of galectin-3 in the blood serum of patients with benign, borderline, and malignant bone tumors of various histologic types and healthy donors in the control group. The analysis of the data obtained revealed a statistically significant increase in the serum levels of galectin-3 in the majority of patients with bone tumors. It is worth noting that this increase was noted in both age groups (under 18 and over 18 years old) for both benign and malignant bone tumors.

However, the ROC analysis indicated that the sensitivity and specificity of the method were insufficient to use this marker for the diagnosis of bone tumors. Similar findings have been reported in the literature for other types of solid tumors [24], which suggest high sensitivity but low specificity of this biochemical diagnostic method.

In our study, we observed a trend toward an increase in the galectin-3 levels in patients over 18 years old with chordoma, while no significant differences in the galectin-3 levels were observed in other histologic types of bone tumors. In the group of patients under 18 years old, the lowest content of galectin-3 was detected in Ewing sarcoma, that contradicts the data on tissue expression of this protein, which suggests significantly higher expression of galectin-3 in Ewing sarcomas than in osteosarcomas in children [25].

Regarding the association between the galectin-3 level and other clinical and morphological characteristics of the disease, no significant regularities were found in the age group over 18 years old. In the group of patients under 18 years old, we observed a trend toward a rise in the galectin-3 levels in cases with unfavorable clinical characteristics such as advanced stage, presence of metastases, and low grade of tumor differentiation.

However, we did not find any significant prognostic value of serum galectin-3 levels both in the general group of malignant bone tumors and in primary histologic types of bone sarcomas (osteosarcoma and chondrosarcoma). It is worth noting that the prognostic value of galectin-3 is ambiguous in many tumor types, including colorectal cancer, where high levels of this protein are associated with an unfavorable prognosis [26], whereas the opposite results were reported for breast and stomach cancers [27]. Therefore, the significance of galectin-3 in bone tumors requires further investigation.

CONCLUSION

Currently, among the 15 known galectins, galectin-3 attracts the greatest interest of researchers due to its involvement in many pathological processes, including cancer. However, its functional role in malignant tumors is diverse and rather contradictory. On the one hand, it acts as a promoter of tumor growth, and on the other hand, it can function as a tumor suppressor. Our data demonstrated a significant increase in the serum galectin-3 level in patients with benign and malignant bone tumors in comparison to the control group, both in adult patients (over 18 years old) and in younger patients (under 18 years old). Although the diagnostic value of the marker in these two groups was significantly different from the controls according to the ROC analysis, the sensitivity and specificity of galectin-3 alone in patients with bone sarcomas aged < 18 years old was 80% and 90%, respectively (the optimal cut-off level in the controls was 5.49 ng / ml; $p = 0.001$). It may potentially be used as a marker in

the diagnosis of bone sarcomas in a bigger sample in the future.

However, the serum levels of galectin-3 did not differ between patients with benign, borderline, and malignant bone tumors. In addition, the highest levels of galectin-3 were detected in the serum of chordoma patients and at earlier stages of the disease. We did not observe any significant associations of galectin-3 with the main clinical and morphological characteristics of malignant tumors both in the group of patients under 18 years old and in the group of patients over 18 years old.

According to the literature, the prognostic value of galectin-3 in many tumor types is also ambiguous. In this study, the serum galectin-3 level was not a significant prognostic factor in the general group of patients with malignant bone tumors, as well as in the two most commonly revealed bone-forming (osteosarcoma) and cartilage-forming (chondrosarcoma) bone tumors, respectively. It should be noted that at this stage of research, the use of serum galectin-3 as a diagnostic marker of bone tumors has not been fully determined and requires further research.

REFERENCES

1. Dumic J., Dabelic S., Flögel M. Galectin-3: an open-ended story. *Biochim. Biophys. Acta.* 2006;1760(4):616–635. DOI: 10.1016/j.bbagen.2005.12.020.
2. Liu F.T., Hsu D.K. The role of galectin-3 in promotion of the inflammatory response. *Drug News Perspect*. 2007;20(7):455–460. DOI: 10.1358/dnp.2007.20.7.1149628.
3. Clementy N., Garcia B., André C., Bisson A., Benhenda N., Pierre B. et al. Galectin-3 level predicts response to ablation and outcomes in patients with persistent atrial fibrillation and systolic heart failure. *PLoS One.* 2018;13(8):e0201517. DOI: 10.1371/journal.pone.0201517.
4. Asleh R., Enriquez-Sarano M., Jaffe A.S., Manemann S.M., Weston S.A., Jiang R. et al Galectin-3 Levels and Outcomes After Myocardial Infarction: A Population-Based Study. *J. Am. Coll. Cardiol.* 2019;73(18):2286–2295. DOI: 10.1016/j.jacc.2019.02.046.
5. Chen S.C., Kuo P.L. The role of galectin-3 in the kidneys. *Int. J. Mol. Sci.* 2016;17(4):565. DOI: 10.3390/ijms17040565.
6. Li Y., Li T., Zhou Z., Xiao Y. Emerging roles of galectin-3 in diabetes and diabetes complications: A snapshot. *Rev. Endocr. Metab. Disord.* 2022;23(3):569–577. DOI: 10.1007/s11154-021-09704-7.
7. Wang W.H., Lin C.Y., Chang M.R., Urbina A.N., Assavalapsakul W., Thitithanyanont A. et al. The role of galectins in virus infection - A systemic literature review. *J. Microbiol. Immunol. Infect.* 2020;53(6):925–935. DOI: 10.1016/j.jmii.2019.09.005.
8. De Oliveira F.L., Gatto M., Bassi N., Luisetto R., Ghirardello A., Punzi L. et al. Galectin-3 in autoimmunity and autoimmune diseases. *Exp. Biol. Med. (Maywood).* 2015;240(8):1019–1028. DOI: 10.1177/1535370215593826.
9. Ashraf G.M., Baeesa S.S. Investigation of gal-3 expression pattern in serum and cerebrospinal fluid of patients suffering from neurodegenerative disorders. *Front. Neurosci.* 2018;12:430. DOI: 10.3389/fnins.2018.00430.
10. Song L., Tang J.W., Owusu L., Sun M.Z., Wu J., Zhang J. Galectin-3 in cancer. *Clin. Chim. Acta.* 2014;431:185–191. DOI: 10.1016/j.cca.2014.01.019.
11. Xie L., Ni W.K., Chen X.D., Xiao M.B., Chen B.Y., He S. et al. The expressions and clinical significances of tissue and serum galectin-3 in pancreatic carcinoma. *J. Cancer Res. Clin. Oncol.* 2012;138(6):1035–1043. DOI: 10.1007/s00432-012-1178-2.
12. Matsuda Y., Yamagiwa Y., Fukushima K., Ueno Y., Shimosegawa T. Expression of galectin-3 involved in prognosis of patients with hepatocellular carcinoma. *Hepatol. Res.* 2008;38(11):1098–1111. DOI: 10.1111/j.1872-034X.2008.00387.x.
13. Kim S.J., Lee S.J., Sung H.J., Choi I.K., Choi C.W., Kim B.S. et al. Increased serum 90K and Galectin-3 expression are associated with advanced stage and a worse prognosis in diffuse large B-cell lymphomas. *Acta Haematol.* 2008;120(4):211–216. DOI: 10.1159/000193223.
14. Acikalin M.F., Etiz D., Gurbuz M.K., Ozudogru E., Canaz F., Colak E. Prognostic significance of galectin-3 and cyclin D1 expression in undifferentiated nasopharyngeal carcinoma. *Med. Oncol.* 2012;29(2):742–749. DOI: 10.1007/s12032-011-9971-3.
15. Endo K., Kohnoe S., Tsujita E., Watanabe A., Nakashima H., Baba H. et al. Galectin-3 expression is a potent prognostic marker in colorectal cancer. *Anticancer Res.* 2005;25(4):3117–3121.
16. Zhang X.M., Yao G.Y., Zhang B.Y., Wang L.L., Zhao M. [Study on the expression and significance of Galectin-3 and CDC25B mRNA in human gastric carcinoma]. *Zhonghua Yi Xue Yi Chuan Xue Za Zhi.* 2009;26(3):288–292. (In Chinese). DOI: 10.3760/cma.j.issn.1003-9406.2009.03.011.
17. Yang Z.M., Wu X.T., He T., Da M.X., Luo T., Qian K. [Expression of galectin-3 mRNA in gastric cancer with peritoneal metastasis]. *Sichuan Da Xue Xue Bao Yi Xue Ban.* 2006;37(1):105–108. (In Chinese).
18. O'Driscoll L., Linehan R., Liang Y.H., Joyce H., Oglesby I., Clynes M. Galectin-3 expression alters adhesion, motility and invasion in a lung cell line (DLKP), *in vitro*. *Anticancer Res.* 2002;22(6A):3117–3125.
19. Castronovo V., Van Den Brûle F.A., Jackers P., Clausse N., Liu F.T., Gillet C. et al. Decreased expression of galectin-3 is associated with progression of human breast cancer. *J. Pathol.* 1996;179(1):43–48. DOI: 10.1002/(SICI)1096-9896(199605)179:1<43::AID-PATH541>3.0.CO;2-N.
20. Knapp J.S., Lokeshwar S.D., Vogel U., Hennenlotter J., Schwentner C., Kramer M.W. et al. Galectin-3 expression in prostate cancer and benign prostate tissues: correlation with biochemical recurrence. *World J. Urol.* 2013;31(2):351–358. DOI: 10.1007/s00345-012-0925-y.
21. Wang Y., Nangia-Makker P., Tait L., Balan V., Hogan V., Pienta K.J. et al. Regulation of prostate cancer progression

by galectin-3. *Am. J. Pathol.* 2009;174(4):1515–1523. DOI: 10.2353/ajpath.2009.080816.
22. Zhou X., Jing J., Peng J., Mao W., Zheng Y., Wang D. et al. Expression and clinical significance of galectin-3 in osteosarcoma. *Gene.* 2014;546(2):403–407. DOI: 10.1016/j.gene.2014.04.066.
23. Park G.B., Kim D.J., Kim Y.S., Lee H.K., Kim C.W., Hur D.Y. Silencing of galectin-3 represses osteosarcoma cell migration and invasion through inhibition of FAK/Src/Lyn activation and β-catenin expression and increases susceptibility to chemotherapeutic agents. *Int. J. Oncol.* 2015;46(1):185–194. DOI: 10.3892/ijo.2014.2721.
24. Dong R., Zhang M., Hu Q., Zheng S., Soh A., Zheng Y. et al. Galectin-3 as a novel biomarker for disease diagnosis and a target for therapy. *Int. J. Mol. Med.* 2018;41(2):599–614. DOI: 10.3892/ijmm.2017.3311.
25. Crompton B.D., Stewart C., Taylor-Weiner A., Alexe G., Kurek K.C., Calicchio M.L. et al. The genomic landscape of pediatric Ewing sarcoma. *Cancer Discov.* 2014;4(11):1326–1341. DOI: 10.1158/2159-8290.CD-13-1037.
26. Huang Z., Ai Z., Li N., Xi H., Gao X., Wang F. et al. Over expression of galectin-3 associates with short-term poor prognosis in stage II colon cancer. *Cancer Biomark.* 2016;17(4):445–455. DOI: 10.3233/CBM-160661.
27. Okada K., Shimura T., Suehiro T., Mochiki E., Kuwano H. Reduced galectin-3 expression is an indicator of unfavorable prognosis in gastric cancer. *Anticancer Res.* 2006;26(2B):1369–1376.

Authors' contribution

Kushlinskii N.E., Gershtein E.S., Yanushevich O.O., Stilidi I.S. – research topic for the study, conception and design, coordination of the study, editing of the article. Kovaleva O.V., Zybina N.N., Jurisic V. – statistical processing of the results, review of literature, drafting of the article. Prishchep P.L., Varfolomeeva S.R, Sushentsov E.A. – work with patients, treatment. Alferov A.A., Kuzmin Yu.B., Kuznetsov I.N. – acquisition of experimental data. Rogozhin D.V., Bulytcheva I.V. – morphological examination of the tumors.

Authors' information

Kushlinskii Nikolay E. – Dr. Sci. (Med.), Professor, Academician of RAS, Head of the Laboratory for Clinical Biochemistry, N.N. Blokhin National Medical Research Center of Oncology, Moscow, biochimia@yandex.ru, https://orcid.org/0000-0002-3898-4127

Kovaleva Olga V. – Cand. Sci. (Biology), Senior Researcher, Laboratory for Regulation of Cellular and Viral Oncogenes, N.N. Blokhin National Medical Research Center of Oncology, Moscow, ovkovleva@gmail.com, https://orcid.org/0000-0001-6132-9924

Prishchep Polina L. – Pediatric Surgeon Oncologist, Institute of Pediatric Oncology and Hematology, N.N. Blokhin National Medical Research Center of Oncology, Moscow, Paulig92@mail.ru, https://orcid.org/0000-0003-0810-8238

Zybina Natalia N. – Dr. Sci. (Biology), Professor, Head of the Laboratory Diagnostics Department, A.M. Nikiforov All-Russian Center for Emergency and Radiation Medicine EMERCOM of Russia, St. Petersburg, zybinan@inbox.ru, https://orcid.org/0000-0002-5422-2878

Jurisic Vladimir – MD, PhD, Professor, University of Kragujevac, Faculty of Medical Sciences, Kragujevac, Serbia, jurisicvladimir@gmail.com, https://orcid.org/0000-0001-6525-128X

Alferov Alexander A. – Clinical Laboratory Diagnostics Doctor, Laboratory for Clinical Biochemistry, N.N. Blokhin National Medical Research Center of Oncology, Moscow, aleksandr.alferov@yahoo.com, https://orcid.org/0000-0003-3585-5693

Kuzmin Yury B. – Research Technician, Laboratory for Clinical Biochemistry, N.N. Blokhin National Medical Research Center of Oncology, Moscow, yriikuzmin@yandex.com, https://orcid.org/0000-0001-9684-2509

Goryacheva Irina O. – Clinical Laboratory Diagnostics Doctor, Laboratory for Clinical Biochemistry, N.N. Blokhin National Medical Research Center of Oncology, Moscow, irina.goriacheva@gmail.com, https://orcid.org/0000-0001-5522-291X

Kuznetsov Igor N. – Cand. Sci. (Biology), Senior Laboratory Technician, Department for Clinical Biochemistry and Laboratory Diagnostics, A.I. Evdokimov Moscow State University of Medicine and Dentistry, Moscow, npkredo@yandex.ru, https://orcid.org/0000-0003-0866-5561

Bulytcheva Irina V. – Dr. Sci. (Med.), Pathologist, N.N. Blokhin National Medical Research Center of Oncology, Moscow, irena@boulytcheva.com, https://orcid.org/0000-0001-7592-4249

Varfolomeeva Svetlana R. – Dr. Sci. (Med.), Professor, Director, Institute of Pediatric Oncology and Hematology, N.N. Blokhin National Medical Research Center of Oncology, Moscow, s.varfolomeeva@ronc.ru, https://orcid.org/0000-0001-6131-1783

Sushentsov Eugeny A. – Cand. Sci. (Med.), Head of the Department for Surgical Methods of Treatment (Oncoorthopedics), N.N. Blokhin National Medical Research Center of Oncology, Moscow, crcspine@rambler.ru, https://orcid.org/0000-0003-3672-1742

Gershtein Elena S. – Dr. Sci. (Biology), Professor, Leading Researcher, Laboratory for Clinical Biochemistry, N.N. Blokhin National Medical Research Center of Oncology, Moscow, esgershtein@gmail.com, https://orcid.org/0000-0002-3321-801X

Rogozhin Dmitry V. – Dr. Sci. (Med.), Head of the Pathology Department, N.N. Blokhin National Medical Research Center of Oncology, Moscow, pathol.777@mail.ru, https://orcid.org/0000-0003-0777-9152

Yanushevich Oleg O. – Dr. Sci. (Med.), Professor, Academician of RAS, Rector of A.I. Evdokimov Moscow State University of Medicine and Dentistry, Moscow, mail@msmsu.ru, https://orcid.org/0000-0003-0059-4980

Stilidi Ivan S. – Dr. Sci. (Med.), Professor, Academician of RAS, Director of N.N. Blokhin National Medical Research Center of Oncology, Moscow, ronc@list.ru, https://orcid.org/0000-0002-0493-1166

(✉) **Kushlinskii Nikolay E.,** biochimia@yandex.ru

Received 28.12.2022;
approved after peer review 16.01.2023;
accepted 27.02.2023

УДК 616.12-008.46-036.12-037:616.146.2-073.432
https://doi.org/10.20538/1682-0363-2023-2-78-87

mRNA level of antioxidant genes and activity of NADPH-generating enzymes in rotenone-induced parkinsonism in rats

Kryl'skii E.D., Razuvaev G.A., Popova T.N., Nikhaev L.E., Akinina A.I.

Voronezh State University
1, Universitetskaya Sq., Voronezh, 394018, Russian Federation

ABSTRACT

Aim. To analyze the mRNA level of genes encoding antioxidant enzymes and the transcription factors Nrf2 and Foxo1 regulating their expression and the activity of glucose-6-phosphate dehydrogenase (G6PDH) and NADP-dependent isocitrate dehydrogenase (NADP-IDH) and assess the correlation between these parameters, oxidative status, and motor coordination parameters in rats with rotenone-induced parkinsonism.

Materials and methods. The study was performed on male Wistar rats aged 4–6 months and weighing 200–250 g.Parkinsonism was modeled by subcutaneous administration of rotenone for 10 days at a dose of 2.5 mg / kg. To confirm the development of the pathology, motor coordination tests and histological staining of the cerebral cortex and striatum with hematoxylin and eosin were used. The oxidative status was analyzed based on the levels of conjugated dienes, carbonyl amino acid residues in proteins, and α-tocopherol. The enzyme activity was studied spectrophotometrically by the formation of NADPH. Real-time PCR was used to analyze the level of gene mRNA.

Results. During the study, an increase in serum and brain concentrations of conjugated dienes, carbonyl amino acid residues, and α-tocopherol was observed in the experimental group of rats compared to the controls. It could be associated with the redistribution of this compound between tissues during pathology development. The animals with experimental parkinsonism, in addition, were characterized by a decrease in the mRNA level of the *Sod1*, *Gpx1*, *Gsr*, *Gsta2*, *Nfe2l2*, and *Foxo1* genes, as well as the activity of G6PDH and NADP-IDH. In the rats with experimental parkinsonism, a negative correlation of NADPH-IDH activity in the brain with serum α-tocopherol level and a positive correlation with *Gpx1* and *Foxo1* mRNA levels in the striatum were found. The level of oxidatively modified proteins in the brain of the animals with PD was negatively correlated with the concentration of *Gsta2* mRNA in the striatum, while the specific activity of G6PDH in the serum was characterized by the positive relationship with grip strength.

Conclusion. The data obtained indicate that the inhibition of transcription of the genes encoding antioxidant enzymes and regulatory factors Nrf2 and Foxo1 contributed significantly to the development of oxidative stress in PD. A decrease in the activity of G6PDH and NADP-IDH led to a decrease in the availability of NADPH, which is a limiting factor in the functioning of the glutathione antioxidant system. Obviously, the inhibition of G6PDH and NADP-IDH was also an important pathogenic factor in the progression of the pathology. Along with a decrease in the content of antioxidant gene mRNA in the brain tissues, the level of α-tocopherol increased in the rats with parkinsonism, which could be the result of an imbalance in the functioning of antioxidant system.

Keywords: Parkinson's disease, oxidative stress, antioxidant system, glucose-6-phosphate dehydrogenase, NADP-dependent isocitrate dehydrogenase

Conflict of interest. The authors declare the absence of obvious or potential conflicts of interest related to the publication of this article.

Source of financing. The authors state that they received no funding for the study.

Conformity with the principles of ethics. The study was approved by the Biomedical Ethics Committee at Voronezh State University (Protocol No. 42-02 of 04.10.2021).

✉ *Kryl'skii Evgenii D.,* evgenij.krylsky@yandex.ru

For citation: Kryl'skii E.D., Razuvaev G.A., Popova T.N., Nikhaev L.E., Akinina A.I. mRNA level of antioxidant genes and activity of NADPH-generating enzymes in rotenone-induced parkinsonism in rats. *Bulletin of Siberian Medicine.* 2023;22(2):78–87. https://doi.org/10.20538/1682-0363-2023-2-78-87.

Уровень мРНК генов антиоксидантной системы и активность НАДФН-генерирующих ферментов при ротенон-индуцированном паркинсонизме у крыс

Крыльский Е.Д., Разуваев Г.А., Попова Т.Н., Нихаев Л.Е., Акинина А.И.

Воронежский государственный университет (ВГУ)
Россия, 394018, г. Воронеж, Университетская пл., 1

РЕЗЮМЕ

Цель. Исследование уровня мРНК генов антиоксидантных ферментов и регулирующих их экспрессию транскрипционных факторов Nrf2 и Foxo1, активности глюкозо-6-фосфатдегидрогеназы (Г6ФДГ) и никотинамидадениндинуклеотидфосфат-изоцитратдегидрогеназы (НАДФ-ИДГ), а также анализ корреляционных связей между данными параметрами, состоянием оксидативного статуса и моторно-координационными показателями у крыс с ротенон-индуцированным паркинсонизмом.

Материалы и методы. Исследование было выполнено на крысах самцах Вистар в возрасте 4–6 мес и массой 200–250 г. Паркинсонизм моделировали путем подкожного введения в течение 10 сут ротенона в дозе 2,5 мг/кг. Для подтверждения развития патологии использовали моторно-координационные тесты и гистологические методы с окрашиванием коры полушарий и полосатого тела головного мозга гематоксилином и эозином. Состояние оксидативного статуса оценивали на основании концентрации диеновых конъюгатов, карбонильных остатков аминокислот в белках и α-токоферола. Активность ферментов исследовали спектрофотометрически по образованию НАДФН. Для анализа уровня мРНК генов использовали метод полимеразной цепной реакции в реальном времени.

Результаты. В ходе исследования у крыс опытной группы по сравнению с контролем наблюдалось возрастание в сыворотке крови и мозге концентрации диеновых конъюгатов, карбонильных остатков аминокислот, а также α-токоферола, что могло быть связано с перераспределением данного соединения между тканями при развитии патологии. Для животных с экспериментальным паркинсонизмом, кроме этого, было характерно снижение уровня мРНК генов *Sod1*, *Gpx1*, *Gsr*, *Gsta2*, *Nfe2l2* и *Foxo1*, а также активности Г6ФДГ и НАДФ-ИДГ. У крыс с экспериментальным паркинсонизмом была найдена отрицательная корреляция активности НАДФ-ИДГ в мозге с концентрацией α-токоферола в сыворотке и положительная – с уровнем мРНК *Gpx1* и *Foxo1* в полосатом теле головного мозга. Уровень окислительно-модифицированных белков в мозге животных с патологией отрицательно коррелировал с концентрацией мРНК *Gsta2* в полосатом теле, а удельная активность Г6ФДГ в сыворотке характеризовалась наличием положительной взаимосвязи с силой хвата.

Заключение. Полученные данные свидетельствуют, что угнетение транскрипции генов антиоксидантных ферментов и регуляторных факторов Nrf2 и Foxo1 вносило существенный вклад в развитие окислительного стресса при БП. Наблюдаемое снижение активности Г6ФДГ и НАДФ-ИДГ уменьшало доступность НАДФН – лимитирующего фактора для функционирования глутатионовой антиоксидантной системы, что также, очевидно, являлось важным патогенетическим фактором прогрессирования патологии. Наряду со снижением в тканях мозга содержания мРНК генов антиоксидантных ферментов, у крыс с паркинсонизмом возрастала концентрация α-токоферола, что могло быть результатом развития дисбаланса в функционировании антиоксидантной системы.

Ключевые слова: болезнь Паркинсона, окислительный стресс, антиоксидантная система, глюкозо-6-фосфатдегидрогеназа, НАДФ-изоцитратдегидрогеназа

Конфликт интересов. Авторы декларируют отсутствие явных и потенциальных конфликтов интересов, связанных с публикацией настоящей статьи.

Источник финансирования. Авторы заявляют об отсутствии финансирования при проведении исследования.

Соответствие принципам этики. Исследование одобрено этическим комитетом по экспертизе биомедицинских исследований Воронежского государственного университета (протокол № 42-02 от 04.10.2021).

Для цитирования: Крыльский Е.Д., Разуваев Г.А., Попова Т.Н., Нихаев Л.Е., Акинина А.И. Уровень мРНК генов антиоксидантной системы и активность НАДФН-генерирующих ферментов при ротенон-индуцированном паркинсонизме у крыс. *Бюллетень сибирской медицины.* 2023;22(2):78–87. https://doi.org/10.20538/1682-0363-2023-2-78-87.

INTRODUCTION

Parkinson's disease (PD) is the second most common neurodegenerative disease after Alzheimer's and the most common movement disorder in the world. The pathogenesis of PD is characterized by a loss of dopaminergic neurons in the substantia nigra and the presence of Lewy bodies in the midbrain, which are aggregates of proteins with impaired folding, including α-synuclein [1]. Neurodegeneration in PD also occurs in the noradrenergic, serotonergic, and cholinergic systems, the cerebral cortex, the optic bulb, and parts of the autonomic nervous system [2].

Oxidative stress has been demonstrated to occur early in the development of PD. Thus, uncontrolled generation of reactive oxygen species (ROS) is a causal factor in the death of dopaminergic neurons rather than an effect of other pathogenetic factors of neurodegeneration [3]. The antioxidant system protects neurons from oxidative stress and includes such enzymes as superoxide dismutase, catalase, glutathione enzymes, and non-enzymatic antioxidants. The nuclear factor-erythroid-2-related factor 2 (Nrf2) is a key regulatory factor responsible for the implementation of the antioxidant response. Under steady state conditions, the Nrf2 protein binds to the Kelch-like ECH-associated protein (KEAP1) in the cytoplasm, whereby it is ubiquitinated and undergoes proteasomal degradation.

Oxidative stress causes disruption of the Nrf2 – KEAP1 complex, leading to the release of Nrf2 and its nuclear translocation. Nrf2 in the nucleus activates the expression of antioxidant responsive elements (ARE)-containing genes encoding, among others, antioxidant enzymes [4]. Foxo1 is another regulatory factor involved in cell survival under oxidative stress. This protein modulates the activity of numerous genes, including genes related to antioxidant enzymes, autophagy, and apoptosis, in particular tumor necrosis factor-α, FAS-ligand (tumor necrosis factor ligand superfamily member 6), caspase-3, caspase-8 and caspase-9 [5]. Nicotinamide adenine dinucleotide phosphate (NADPH), which is necessary for the reduction of oxidized glutathione, is another important defense component that limits the functioning of glutathione-related enzymes of the antioxidant system. The main source of NADPH is the pentose phosphate pathway, with glucose-6-phosphate dehydrogenase (G6PDH) as the key enzyme [6]. NADP-dependent isocitrate dehydrogenase (NADP-IDH) can act as an alternative source of NADPH. This enzyme is localized predominantly in the cytoplasm, but a small amount of enzyme activity is also found in the mitochondria. NADP-IDH ensures the coordination of carbon and nitrogen metabolism and is also involved in the generation of NADPH [7].

Studies have shown that about 70% of neurons die before the onset of clinical symptoms of PD. In this regard, research revealing strategies to maintain redox homeostasis, as well as possibilities of early diagnosis of parkinsonism seems relevant [8]. Currently, experimental PD induced by rotenone administration remains the preferred model of pathology and consistently mimics the neuropathological features of PD due to the ability of rotenone to reproduce the progressive nature of the disease with characteristic slow cell death, motor disturbances, and signs of α-synucleinopathy [9]. We have previously shown that the activity of glutathione-related enzymes and catalase is inhibited in rats with rotenone-induced parkinsonism [10]. At the same time, studies demonstrating the relationship between AREs at the transcriptional level, NADPH-supplying enzymes, and oxidative status parameters in experimental PD remain very limited in the literature.

The aim of this work was to investigate the mRNA level of genes encoding antioxidant enzymes and the transcription factors Nrf2 and Foxo1 regulating their expression, to evaluate the activity of G6PDH and NADP-IDH, and to assess the correlation between these parameters, oxidative status, and motor coordination indices in rats with rotenone-induced parkinsonism.

MATERIALS AND METHODS

The study was performed on male Wistar rats aged 4–6 months and weighing 200–250 g. The animals were kept in 12 hour light : 12 hour dark cycle with *ad libitum* access to food and feed. The composition of the animal feed is given in Appendix 1. The work was performed in compliance with the principles of humanity set out in the European Community directives (86/609/EEC) and the Declaration of Helsinki. PD in the rats was modeled by subcutaneous administration of rotenone at a dose of 2.5 mg / kg as a solution in 98% purified olive oil and 2% dimethyl sulfoxide for 10 days [11]. The animals were randomly divided into two experimental groups of 12 animals each. Group 1 consisted of animals that received subcutaneous injections of the vehicle. Group 2 consisted of rats with PD. Twenty-four hours after the last injection, the rats were analyzed for motor indices, then they were sacrificed, and biological material was taken.

The following tests were used to assess the animals' motor skills and coordination: 1) the animal was placed in a transparent cage, after switching on the video recording, the researcher left the room. The video recorded the number of upright postures in 3 minutes [11]; 2) the rat was held and allowed to catch the electronic scale bracket with its forelegs. The scales were pulled back and the maximum value of the index was recorded [12]; 3) the animal was placed in a transparent cage and a piece of sticky paper was glued to its head. The time for the rat to perceive a stimulus and remove the paper from the head was recorded [13]. All tests were performed three times, and the average value of the parameters was calculated.

Brain tissue from three rats from each group was used to prepare histologic specimens stained with hematoxylin and eosin. The rats were anesthetized, the brains were quickly extracted and immersed in 10% neutral buffered formalin for 2 hours, then washed in running water for 24 hours. After tissue dehydration with ethanol and paraffin embedding, 5-μm-thick sections were prepared using the HM-325 rotary microtome (Thermo Fisher Scientific, USA), followed by staining with hematoxylin and eosin. Images were acquired using the AxioLab A1 light microscope (Zeiss, Germany) and the AxioCam 105 color camera. At least five fields of view for each slide were evaluated.

To analyze the concentration of conjugated dienes (CD), heptane and isopropanol were added to the test sample, the mixture was stirred and precipitated by centrifugation at 3,000g. The heptane supernatant phase was diluted with ethanol and analyzed spectrophotometrically at 233 nm [14]. To assess the degree of oxidative modification of proteins (OMP), a method based on the ability of carbonyl amino acid residues to interact with 2,4-dinitrophenylhydrazine (2,4-DNPH) to form 2,4-dinitrophenylhydrazones with absorbance at 370 nm was used [15]. The sample was diluted with 100 mM phosphate buffer (pH 7.4), 10 mM 2,4-DNPH in 2.5 M HCl was added, the mixture was incubated for 1 hour, and then 20% TCA was added. After cooling, the samples were centrifuged at 3,000g, washed with 10% TCA and ethanol – ethyl acetate mixture (1:1), then dissolved in 2 ml of 8 M urea. The concentration of α-tocopherol was determined by a method based on photometry of a chromogenic Fe^{2+} – orthophenatroline complex [16]. Ethanol and hexane were added to the test sample, centrifuged at 3,000 g, then the hexane layer was removed, and hexane was evaporated in a water bath. Benzene and ferric chloride were added to the dry residue. After 5 min, 0.05% orthophenatroline was added, then the optical density at 510 nm was measured after 2 min. Total RNA was isolated using Extract RNA reagent (Eurogen, Russia). The quality of RNA was controlled by agarose gel electrophoresis. Reverse transcription for each sample was performed using the MMLV RT kit (Eurogen, Russia). The Ct of each gene was normalized to the geometric mean Ct of *Gapdh* and *Actβ* used as housekeeping genes (Appendix 2). The following primers were used in the study: Sod1 F: 5'-CCAGCGGATGAAGAGAGG-3',
Sod1 R: 5'-GGACACATTGGCCACACC-3',
Cat F: 5'-CAGCGACCAGATGAAGCA-3',
Cat R: 5'-GGTCAGGACATCGGGTTTC-3',
Nfe2l2 F: 5'-GCCTTGTACTTTGAAGACTGTATGC-3',
Nfe2l2 R: 5'-GCAAGCGACTGAAATGTAGGT-3',
Foxo1 F: 5'-AGATCTACGAGTGGATGGTGAAGAG-3',
Foxo1 R: 5'-GGACAGATTGTGGCGAATTGAAT-3',
Gsta2 F: 5'-CGGGAATTTGATGTTTGACC-3',
Gsta2 R: 5'-AGAATGGCTCTGGTCTGTGC-3',
Gpx1 F: 5'-TTTCCCGTGCAATCAGTTC-3',
Gpx1 R: 5'-GGACATACTTGAGGGAATTCAGA-3',
Gapdh F: 5'-CCCTCAAGATTGTCAGCAATG-3',
Gapdh R: 5'-AGTTGTCATGGATGACCTTGG-3',
Actb F: 5'-CCCGCGAGTACAACCTTCT-3',
Actb R: 5'-CGTCATCCATGGCGAACT-3',
Gsr F: 5'-TTCCTCATGAGAACCAGATCC-3'
Gsr R: 5'-CTGAAAGAACCCATCACTGGT-3'.

Real-time polymerase chain reaction (PCR) was performed using qPCRmix-HS SYBR (Eurogen, Rus-

sia) on the ANK-32 device (Syntol, Russia). The results were analyzed using the $2^{-\Delta\Delta Ct}$ method. The reaction specificity was evaluated using melting curves.

NADP-IDH activity was measured in the medium consisting of 50 mM Tris-HCl buffer (pH 7.8), 1.5 mM isocitrate, 2 mM $MnCl_2$, and 0.4 mM NADP. The spectrophotometric medium for the assessment of G6PDH activity was 50 mM Tris-HCl buffer (pH 7.8) containing 3.2 mM glucose-6-phosphate, 0.25 mM NADP, and 1.0 mM $MgCl_2$. The enzymatic activity was evaluated by the change in the optical density at 340 nm using the Hitachi U1900 spectrophotometer (Japan). The biuret test was used to determine protein content.

The results were analyzed by SPSS Statistics 23.0. The one-sample Kolmogorov – Smirnov test was used to analyze the normality of distribution of the variables. Variable values in groups were compared using Student's *t*-test or Mann – Whitney test. To identify correlations between the studied variables, the Pearson's correlation coefficient was used for variables with normal distribution, and the Spearman's rank correlation coefficient was applied for variables with non-normal distribution. This study presented moderate (0.30–0.69) and strong (> 0.70) correlations. The differences were considered statistically significant at $p < 0.05$.

RESULTS

Our study showed that the development of rotenone-induced parkinsonism in the rats was accompanied by a significant ($p < 0.05$) change in motor coordination parameters (Table 1). Thus, rotenone administration led to a decrease in the number of upright postures and grip strength, as well as an increase in the time taken to remove the paper from the head. In addition, the induction of pathology was confirmed by morphological changes in the brain tissues (Fig. 1). In particular, a decrease in the number of neurons, the development of their atrophy and pycnosis, condensation of nuclei, and infiltration of the tissue with glial cells were observed in the cortex and striatum of the rats with experimental PD.

Table 1

Motor coordination parameters in the rats with rotenone-induced parkinsonism, *Me* (Q_1–Q_3)

Parameter	Group		*p*
	Controls (*n* = 12)	Rats with PD (*n* = 12)	
Number of upright postures	11.0 (9.5–12.0)	4.0 (2.0–7.0)	0.002
Grip strength, kg	0.300 (0.269–0.300)	0.157(0.135–0.200)	0.001
Paper removal, sec	21.5 (15.3–40.8)	127.0 (91.8–152.5)	0.003

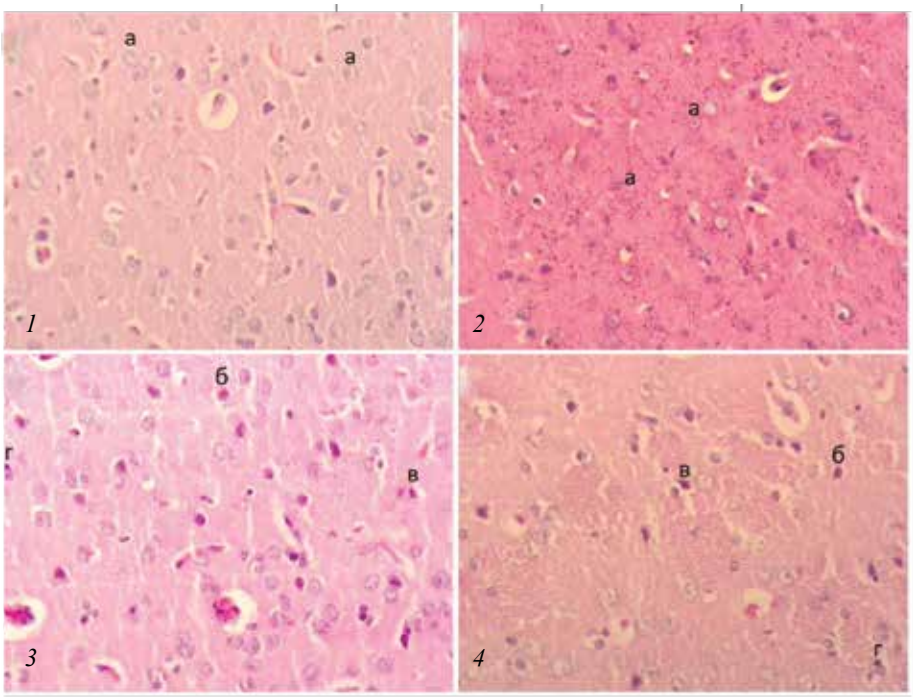

Fig. 1. Hematoxylin and eosin staining of brain tissues in the rats: the cortex (*1*), the striatum (*2*) in normal conditions and in rotenone-induced parkinsonism (*3, 4*), x 400. Large, scattered multipolar neurons with vesicular nuclei were visualized on tissue sections of the control rats (*a*). The development of the pathology was characterized by the presence of cells with a darker nucleus (*b*), wrinkled cells with signs of karyolysis (*c*), as well as glial cell infiltration (*d*)

The development of rotenone-induced parkinsonism in the rats was accompanied by activation of free radical-induced oxidation, as evidenced by an increase ($p < 0.05$) in CD concentration and OMP in the blood serum and brain of the animals (Fig. 2). At the same time, for the rats with experimental PD, an increase ($p < 0.05$) in α-tocopherol level in the tissues was also observed.

Our data indicated that a decrease in mRNA levels of genes encoding antioxidant enzymes and transcription factors Nrf2 and Foxo1 was observed in PD animals, which is in agreement with our earlier data on enzyme activity in experimental PD [10]. Thus, the results of this work demonstrated a decrease ($p < 0.01$) in the level of Nrf2 mRNA (*Nfe2l2* gene) in the cortex and striatum of the animals with pathology (Fig. 3). A similar trend was also observed for Foxo1 mRNA ($p < 0.05$). These changes in the PD rats were associated with decreased ($p < 0.05$) mRNA levels of superoxide dismutase, glutathione peroxidase, glutathione reductase, and glutathione transferase genes in the striatum (*Sod1*, *Gpx1*, *Gsr*, *Gsta2* genes, respectively). The expression of the catalase gene (*Cat*) did not change significantly.

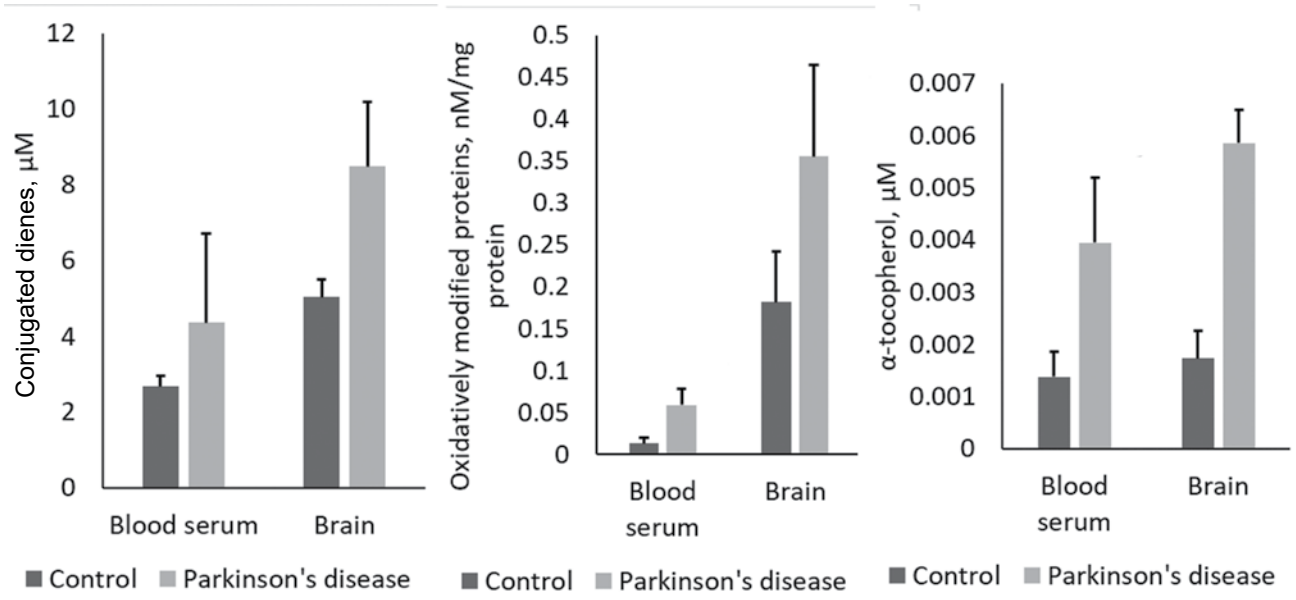

a *b* *c*

Fig. 2. The concentration of conjugated dienes (*a*), oxidized amino acid residues in proteins (b), and α-tocopherol (c) in the brain and blood serum of the control rats and animals with rotenone-induced parkinsonism, *Me* (Q_1–Q_3)

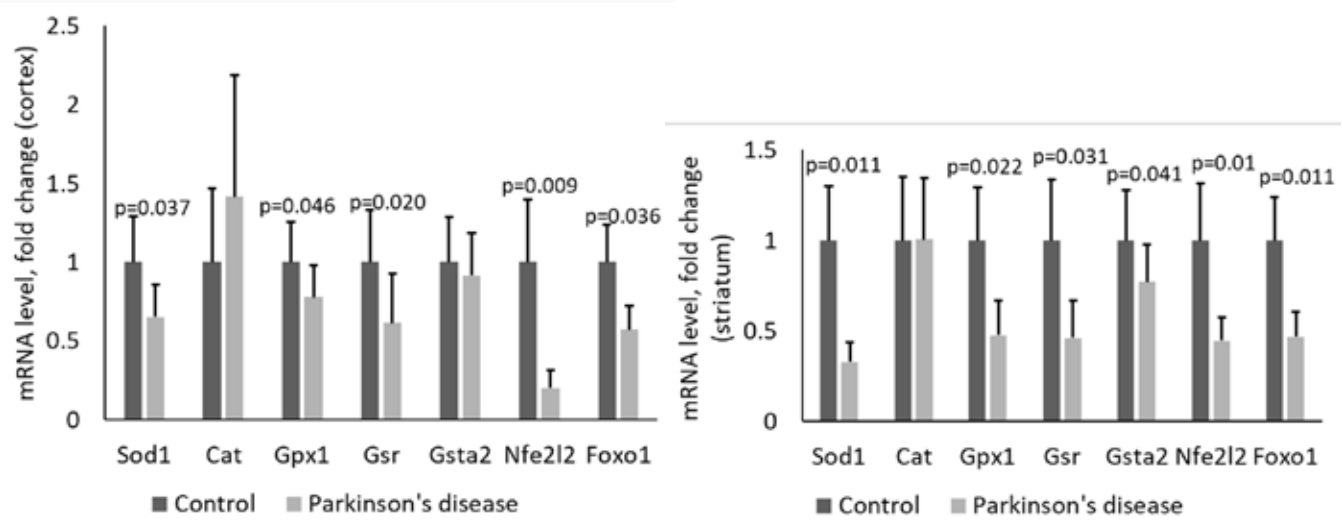

Fig. 3. The mRNA level of genes encoding antioxidant enzymes and regulatory factors in the cortex and striatum of the brain in the control rats and animals with rotenone-induced parkinsonism, $M \pm SD$

The study found that the activity of NADPH-generating enzymes G6PDH and NADP-IDH decreased ($p < 0.05$) in the serum and brain of the rats with experimental PD (Table 2). Similar changes were observed for the activity of these enzymes expressed in unit / mg protein. At the same time, the specific activity of G6PDH in the brains of the animals with pathology did not change significantly, which could be associated with a decrease in the total protein content ($p = 0.032$).

The correlation analysis confirmed the correlation between motor coordination parameters, oxidative status parameters, mRNA levels of the studied genes, and the activity of NADPH-generating enzymes in the rats with rotenone-induced parkinsonism (Table 3).

Table 2

Activity of NADPH-generating enzymes in the blood serum and brain of the rats with rotenone-induced parkinsonism, *Me* (Q_1–Q_3)

Parameter	Tissue	Group		*p*
		Controls ($n = 12$)	Rats with PD ($n = 12$)	
NADP-IDH, unit / ml, unit / g of wet weight	Blood serum	0.024 (0.017–0.071)	0.011 (0.010–0.023)	0.009
	Brain	1.005 (0.352–1.378)	0.451 (0.268–0.550)	0.037
NADP-IDH, unit /mg of protein	Blood serum	0.000270 (0.000194–0.000673)	0.000126 (0.000096–0.000253)	0.01
	Brain	0.010078 (0.008777–0.014880)	0.005692 (0.004279–0.007018)	0.041
G6PDH, unit / ml, unit / g of wet weight	Blood serum	0.034 (0.021–0.046)	0.013 (0.012–0.019)	0.004
	Brain	0.450 (0.239–0.518)	0.390 (0.273–0.398)	0.036
G6PDH, unit / mg of protein	Blood serum	0.000414 (0.000309–0.000575)	0.000281 (0.000249–0.000349)	0.031
	Brain	0.011762 (0.006048–0.012862)	0.007308 (0.002237–0.018642)	0.594
Total protein, g / l	Blood serum	76.5 (53.8–107.6)	58.0 (39.1–61.6)	0.043
	Brain	18.2 (13.2–25.1)	13.4 (8.8–16.9)	0.032

Table 3

Correlations between the studied parameters in the animals with rotenone-induced parkinsonism

Parameters	*r*	*p*
Grip strength – specific serum G6PDH activity	0.673	0.023
Level of oxidative modification of proteins in the brain – *Gsta2* mRNA level in the striatum	–0.848	0.049
NADP-IDH activity in the brain – *Gpx1* mRNA level in the striatum	0.877	0.022
NADP-IDH activity in the brain – *Foxo1* mRNA level in the striatum	0.825	0.043
Concentration of α-tocopherol in the serum – time of paper removal	0.916	0.029
Serum α-tocopherol concentration – NADP-IDH activity in the brain	–0.709	0.049

DISCUSSION

PD is a common neurodegenerative disease whose pathogenesis is closely related to oxidative stress and characterized by a late onset of clinical symptoms. Therefore, it is of interest to investigate the regulatory aspects of redox homeostasis in experimental PD. In this study, we evaluated the transcriptional regulation of the antioxidant system and the activity of NADPH-supplying enzymes for the glutathione-related antioxidant system in the rats with rotenone-induced parkinsonism.

The results of the study showed that the animals with experimental PD were characterized by increased levels of free radical-induced oxidation products, in particular lipid peroxidation (LPO) products – CDs and oxidized amino acid residues in proteins. ROS-induced protein oxidation plays a special role in the pathogenesis of PD. Oxidative stress induces glycol oxidation reactions and modification of free amino groups in proteins, which leads to formation of advanced glycation end products. These products provide cross-linking of protein molecules, which contributes to transformation of neurofilament proteins into insoluble aggregates, the presence of which in neurons is a key feature in the PD pathogenesis [17].

The antioxidant system provides protection against oxidative stress and includes enzymes, such as superoxide dismutase, catalase, glutathione peroxidase, glutathione reductase, and glutathione transferase. *Sod1* encodes a Cu, Zn-superoxide dismutase isoenzyme, predominantly localized in the cytoplasm, which is known to maintain resistance to 1-methyl-4-phenyl-1,2,3,6-tetrahydropyridine, the toxin that causes experimental PD [18]. *Gpx1* is the gene for the glutathione peroxidase-1 isoenzyme, the most abundant glutathione peroxidase in mammalian tissues [19].

Gsta2 encodes an enzyme from the glutathione transferase superfamily that provides detoxification of electrophiles, carcinogens, and drugs. Alpha-class of glutathione transferases are the most versatile enzymes, among which Gsta2 is one of the key ARE-controlled proteins protecting against oxidative stress [20]. Our studies demonstrated decreased mRNA levels of these enzyme-related genes in the striatum and cerebral cortex of the pathological animals. The findings are consistent with previous results indicating impaired functioning of antioxidant system enzymes in experimental PD [10].

The negative correlation between the level of *Gsta2* mRNA in the striatum and the content of oxidatively modified proteins in the brain confirms the significant role of reduced expression of antioxidant system genes in the development of oxidative stress in parkinsonism. Apparently, the observed changes were due to decreased mRNA levels of Nrf2 and Foxo1 factors, which are key regulators of genes contributing to cellular resistance to oxidative stress. Thus, Nrf2 is known to be a crucial activator of expression of genes encoding antioxidant enzymes and NADPH-supplying enzymes. Nrf2 also modulates mitochondrial function and reduces the intensity of inflammation in neurodegeneration [21, 22]. Foxo transcription factors, including Foxo1, play an important role in a number of physiological processes, such as the regulation of metabolism, cell cycle, and responses to stressors, including excessive generation of ROS. There is evidence that inhibition of the PI3K-AKT-Foxo signaling pathway in rats with PD exacerbates oxidative stress in nigral dopaminergic neurons [23]. At the same time, we did not show a significant decrease in mRNA levels for the *Cat* gene as well as *Gsta2* in the cerebral cortex of the rats with the pathology. Apparently, at the endpoint of the experiment, the mRNA levels of these genes were still fairly stable and did not progress to the stage of decompensation.

We also showed that the rats with rotenone-induced parkinsonism are characterized by decreased activity of the brain and serum NADPH-generating enzymes G6PDH and NADP-IDH. The decreased efficiency of NADPH generation also seems to contribute significantly to the dysfunction of antioxidant enzymes and the development of oxidative stress in PD. Thus, there are data showing a significant role of these enzymes in cellular resistance to overproduced ROS [24, 25]. Moreover, it was shown that increased G6PDH activity in transgenic mice caused their lower susceptibility to 1-methyl-4-phenyl-1,2,3,6-tetrahydropyridine and inhibited the development of PD signs [26]. The positive correlation that we showed between the grip strength of the PD animals and the specific activity of G6PDH in the blood serum confirms the role of reduced activity of NADPH-generating enzymes in the development of coordination disorders in parkinsonism. In addition, the positive correlation between NADP-IDH activity in the brain and mRNA levels of *Gpx1* and *Foxo1* indicates a significant mutual influence of NADPH-generating enzymes and the transcriptional activity of antioxidant genes.

Alpha-tocopherol belongs to the non-enzymatic antioxidants capable of effectively normalizing the oxidative status in cells by preventing LPO and stabilizing the membrane structure. The α-tocopherol transporter protein (αTTP) is the main regulator of α-tocopherol distribution in the body [27]. In the brain, αTTP regulates apolipoprotein E-mediated transport of the vitamin from astrocytes to the adjacent neurons. The expression of αTTP increases in astrocytes under oxidative stress, which facilitates the distribution of α-tocopherol to neurons, thereby protecting them from oxidative damage [28]. Our results showed that the rats with parkinsonism were characterized by an increase in the concentration of α-tocopherol in the blood serum and brain along with intensification of free radical-induced oxidation.

This trend was observed along with depressed activity of antioxidant enzymes [10] and their gene transcription, indicating the development of an imbalance in the functioning of the antioxidant system in PD. This is supported by the presence of a positive correlation between the serum α-tocopherol concentration and the time for the rats to remove the paper, as well as the activity of NADP-IDH in the brain of the animals with experimental PD.

CONCLUSION

Our study demonstrated that the development of rotenone-induced parkinsonism was associated with a decrease in mRNA levels of most of the studied antioxidant enzyme genes, which seems to be correlated with a decrease in the activity of Nrf2 and Foxo1 genes. These changes appeared to underlie a decrease in the activity of antioxidant enzymes, an increase in the intensity of free radical-induced oxidation and, as a consequence, the development of oxidative stress in PD. A decrease in the activity of NADPH-generating enzymes G6PDH and NADP-IDH, which are essential for the functioning of the antioxidant system, appeared to be another pathogenetic mechanism

of the impaired oxidative status in the tissues of the pathological animals. At the same time, in the rats with rotenone-induced parkinsonism, an increase in the serum and brain α-tocopherol concentration was observed, which could be the result of an imbalance in the functioning of the antioxidant system under oxidative stress.

REFERENCES

1. Blauwendraat C., Nalls M.A., Singleton A.B. The genetic architecture of Parkinson's disease. *Lancet Neurol*. 2020;19(2):170–178. DOI: 10.1016/S1474- 4422(19)30287-X.
2. Raza C., Anjum R., Shakee N.U.A. Parkinson's disease: Mechanisms, translational models and management strategies. *Life Sci*. 2019;226:77–90. DOI: 10.1016/j.lfs.2019.03.057.
3. Trist B.G., Hare D.J., Double K.L. Oxidative stress in the aging substantia nigra and the etiology of Parkinson's disease. *Aging Cell*. 2019;18(6):e13031. DOI: 10.1111/acel.13031.
4. Hannan Md.A., Dash R., Sohag A.A.M., Haque Md.N., Moon I.S. Neuroprotection against oxidative stress: phytochemicals targeting TrkB signaling and the Nrf2-ARE antioxidant system. *Front. Mol. Neurosci*. 2020;13:116. DOI: 10.3389/fnmol.2020.00116.
5. Xing Y., Li A., Yang Y., Li X., Zhang L., Guo H. The regulation of FOXO1 and its role in disease progression. *Life Sciences*. 2018;193:124–131. DOI: 10.1016/j.lfs.2017.11.030.
6. Nóbrega-Pereira S., Fernandez-Marcos P.J., Brioche T., Gomez-Cabrera M.C., Salvador-Pascual A., Flores J.M. et al. G6PD protects from oxidative damage and improves health span in mice. *Na.t Commun*. 2016;7:10894. DOI: 10.1038/ncomms10894.
7. Popova T., Pinheiro de Carvalho M.A.A., Matasova L., Medvedeva L. Regulation of mitochondrial NADP-isocitrate dehydrogenase in rat heart during ischemia. *Mol. Cell Biochem*. 2007;294(1–2):97–105. DOI: 10.1007/s11010-006-9249-9.
8. Ball N., Teo W.P., Chandra S., Chapman J. Parkinson's disease and the environment. *Front. Neurol*. 2019;10:218. DOI: 10.3389/fneur.2019.00218.
9. Farombi E.O., Awogbindin I.O., Farombi T.H., Oladele J.O., Izomoh E.R., Aladelokun O.B. et al. Neuroprotective role of kolaviron in striatal redo-inflammation associated with rotenone model of Parkinson's disease. *Neurotoxicology*. 2019;73:132–141. DOI: 10.1016/j.neuro.2019.03.005.
10. Kryl'skii E.D., Razuvaev G.A., Popova T.N., Akinina A.I., Nihaev L.E. Functioning of the antioxidant defense system in rotenone-induced Parkinson's disease. *Bulletin of Experimental Biology and Medicine*. 2021;171(6):701–707 (in Russ.). DOI: 10.47056/0365-9615-2021-171-6-701-707.
11. Ablat N., Lv D., Ren R., Xiaokaiti Y., Ma X., Zhao X. et al. Neuroprotective effects of a standardized flavonoid extract from safflower against a rotenone-induced rat model of Parkinson's disease. *Molecules*. 2016;21(9):1107. DOI: 10.3390/molecules21091107.
12. Sharma S., Kumar P., Deshmukh R. Neuroprotective potential of spermidine against rotenone induced Parkinson's disease in rats. *Neurochemistry International*. 2018;116:104–111. DOI: 10.1016/j.neuint.2018.02.010.
13. Park H.J., Lee P.H., Bang O.Y., Lee G., Ahn Y.H. Mesenchymal stem cells therapy exerts neuroprotection in a progressive animal model of Parkinson's disease. *Journal of Neurochemistry*. 2008;107(1):141–151. DOI: 10.1111/j.1471-4159.2008.05589.x.
14. Recknagel R.O., Ghoshal A.K. Lipoperoxidation of rat liver microsomal lipids induced by carbon tetrachloride. *Nature*. 1966;210(5041):1162–1163. DOI: 10.1038/2101162a0.
15. Reznick A.Z., Packer L. Oxidative damage to proteins: spectrophotometric method for carbonyl assay. *Methods Enzymol*. 1994;233:357–363. DOI: 10.1016/S0076-6879(94)33041-7.
16. Desai I.D., Martinez F.E. Bilirubin interference in the colorimetric assay of plasma vitamin E. *Clin. Chim. Acta*. 1986;154(3):247–250. DOI: 10.1016/0009-8981(86)90040-9.
17. Sharma A., Weber D., Raupbach J., Dakal T.C., Fließbach K., Ramirez A. et al. Advanced glycation end products and protein carbonyl levels in plasma reveal sex-specific differences in Parkinson's and Alzheimer's disease. *Redox. Biol*. 2020;34:101546. DOI: 10.1016/j.redox.2020.101546.
18. Tripanichkul W., Jaroensuppaperch E.-O. Ameliorating effects of curcumin on 6-OHDA-induced dopaminergic denervation, glial response, and SOD1 reduction in the striatum of hemiparkinsonian mice. *Eur. Rev. Med. Pharmacol. Sci.* 2013;17(10):1360–1368.
19. Toppo S., Vanin S., Bosello V., Tosatto S.C.E. Evolutionary and structural insights into the multifaceted glutathione peroxidase (Gpx) superfamily. *Antioxid. Redox. Signal.* 2008;10(9):1501–1514. DOI: 10.1089/ars.2008.2057.
20. Liu J., Liu H., Zhao Z., Wang J., Guo D., Liu Y. Regulation of Actg1 and Gsta2 is possible mechanism by which capsaicin alleviates apoptosis in cell model of 6-OHDA-induced Parkinson's disease. *Biosci. Rep.* 2020;40(6):BSR20191796. DOI: 10.1042/BSR20191796.
21. Jayaram S., Krishnamurthy P.T. Role of microgliosis, oxidative stress and associated neuroinflammation in the pathogenesis of Parkinson's disease: The therapeutic role of Nrf2 activators. *Neurochem. Int*. 2021;145:105014. DOI: 10.1016/j.neuint.2021.105014.
22. Tejo F.V., Quintanilla R.A. Contribution of the Nrf2 pathway on oxidative damage and mitochondrial failure in Parkinson and Alzheimer's disease. *Antioxidants (Basel)*. 2021;10(7):1069. DOI: 10.3390/antiox10071069.
23. Gong J., Zhang L., Zhang Q., Li X., Xia X.J., Liu Y.Y. et al. Lentiviral vector-mediated SHC3 silencing exacerbates oxidative stress injury in nigral dopamine neurons by regulating the PI3K-AKT-FoxO signaling pathway in rats with Parkinson's disease. *Cell Physiol. Biochem*. 2018;49(3):971–984. DOI: 10.1159/000493228.
24. Itsumi M., Inoue S., Elia A.J., Murakami K., Sasaki M., Lind E.F. et al. Idh1 protects murine hepatocytes from endotoxin-induced oxidative stress by regulating the intracellular NADP(+)/NADPH ratio. *Cell Death Differ*. 2015;22(11):1837–1845. DOI: 10.1038/cdd.2015.38.
25. Wang Y.P., Zhou L.S., Zhao Y.Z., Wang S.W., Chen L.L., Liu L.X. et al. Regulation of G6PD acetylation by SIRT2 and KAT9 modulates NADPH homeostasis and cell surviv-

al during oxidative stress. *EMBO J*. 2014;33(12):1304–1320. DOI: 10.1002/embj.201387224.

26. Mejías R., Villadiego J., Pintado C.O., Vime P.J., Gao L., Toledo-Aral J.J. et al. Neuroprotection by transgenic expression of glucose-6-phosphate dehydrogenase in dopaminergic nigrostriatal neurons of mice. *Journal of Neuroscience*. 2006;26(17):4500–4508. DOI: 10.1523/JNEUROSCI.0122-06.2006.
27. Ulatowski L., Dreussi C., Noy N., Barnholtz-Sloan J., Klein E., Manor D. Expression of the α-tocopherol transfer protein gene is regulated by oxidative stress and common single-nucleotide polymorphisms. *Free Radic. Biol. Med*. 2012;53(12):2318–2326. DOI: 10.1016/j.freeradbiomed.2012.10.528.
28. Ulatowski L., Manor D. Vitamin E trafficking in neurologic health and disease. *Annu. Rev. Nutr*. 2013;33:87–103. DOI: 10.1146/annurev-nutr-071812-161252.

Authors' contribution

Kryl'skii E.D. – conception and design, analysis and interpretation of the data, justification of the manuscript. Razuvaev G.A. – acquisition of the data, analysis and interpretation of the data, justification of the manuscript. Popova T.N. – justification of the manuscript, critical revision of the manuscript for important intellectual content, final approval of the manuscript for publication. Nikhaev L.E., Akinina A.I. – acquisition of the data, analysis and interpretation of the data.

Authors' information

Kryl'skii Evgenii D. – Cand. Sci. (Biology), Associate Professor, Department of Medical Biochemistry and Microbiology, Voronezh State University, Voronezh, evgenij.krylsky@yandex.ru, orcid.org/0000-0002-8855-5515

Razuvaev Grigory A. – Student, Department of Medical Biochemistry and Microbiology, Voronezh State University, Voronezh, storiesofgames@gmail.com

Popova Tatyana N. – Dr. Sci. (Biology), Professor, Dean of the Faculty of Medicine and Biology, Voronezh State University, Voronezh, biomed-popova@yandex.ru, orcid.org/0000-0002-9660-3054

Nikhaev Leonid E. – Student, Department of Medical Biochemistry and Microbiology, Voronezh State University, Voronezh, nikhaev.l@yandex.ru.

Akinina Alina I. – Student, Department of Medical Biochemistry and Microbiology, Voronezh State University, Voronezh, alina_0611@bk.ru.

(✉) **Kryl'skii Evgenii D.,** evgenij.krylsky@yandex.ru

Received 30.03.2022;
approved after peer review 25.08.2022;
accepted 08.12.2022

УДК 616.12-089.8-78:616.132.2-089.86:616.127-007.6
https://doi.org/10.20538/1682-0363-2023-2-88-96

Characteristics of left ventricular and cardiac hemodynamic remodeling after on-pump or off-pump coronary artery bypass grafting

Mayanskaya S.D.[1], Abzalova G.F.[2], Garaeva L.A.[3], Abdulianov I.V.[3], Teplyakov A.T.[4], Berezikova E.N.[5], Grebenkina I.A.[5]

[1] *Kazan State Medical University*
49, Butlerova Str., Kazan, Republic of Tatarstan, 420012, Russian Federation

[2] *Interregional Clinical and Diagnostic Center*
12A, Karbysheva Str., Kazan, Republic of Tatarstan, 420101, Russian Federation

[3] *Kazan State Medical Academy – branch of the Russian Medical Academy of Continuing Education*
11, Mushtari Str., Kazan, Republic of Tatarstan, 420012, Russian Federation

[4] *Cardiology Research Institute, Tomsk National Research Medical Center (NRMC), Russian Academy of Sciences*
111a, Kievskaya Str., Tomsk, 634012, Russian Federation

[5] *Novosibirsk State Medical University (NSMU)*
52, Krasnyi Av., Novosibirsk, 630091, Russian Federation

ABSTRACT

Aim. To study the comparative dynamics of left ventricular (LV) remodeling after on-pump and off-pump coronary artery bypass grafting.

Materials and methods. The study included 129 patients with verified coronary artery disease (CAD) who underwent coronary artery bypass grafting (CABG) with cardiopulmonary bypass (on-pump CABF) or beating heart surgery (off-pump CABG). All patients underwent transthoracic echocardiography (TTE) and volumetric compression oscillometry (VCO) before surgery, as well as one week and four months after it. The results were compared in groups divided according to the surgical technique and the presence of previous myocardial infarction using variation series, the Tukey's post-hoc test, the Pearson correlation coefficient, and the Spearman's rank correlation coefficient.

Results. According to TTE data, no difference in hemodynamic parameters between the groups in the postoperative period was noted. According to VCO data, a significant difference was revealed in the off-pump group without previous MI one week after surgery: an increase in cardiac output (CO) ($p < 0.001$), an increase in stroke volume (SV) and stroke index (SI) ($p = 0.005$), LV power (LVP) ($p = 0.015$), and also a rise in cardiac index and LVP four months after the surgery. In the on-pump group of patients with previous MI a week after CABG, a decrease in the LVP ($p < 0.001$) and dynamic changes of energy expenditure ($p < 0.001$) were observed. The correlation analysis revealed moderate correlations between the inotropic parameters of cardiac hemodynamics SV, SI, CO, LVP and blood pressure (BP) ($r\pi = 0.33–0.47$; $p < 0.001$) and strong correlations between SV, SI, CO, LVP and ejection fraction (EF) ($r\pi = 0.63–0.68$; $p < 0.001$).

Conclusion. Seven days after the off-pump CABG, an improvement in some hemodynamic parameters and all inotropic parameters of the heart was revealed compared with the on-pump group. Four months after the off-pump surgery, positive hemodynamic remodeling was observed compared with the postoperative period after the on-pump CABG.

Keywords: coronary artery bypass grafting, off-pump surgery, remodeling

Conflict of interest. The authors declare the absence of obvious or potential conflicts of interest related to the publication of this article.

✉ *Mayanskaya Svetlana D.,* smayanskaya@mail.ru

Source of financing. The authors state that they received no funding for the study.

For citation: Mayanskaya S.D., Abzalova G.F., Garaeva L.A., Abdulianov I.V., Teplyakov A.T., Berezikova E.N., Grebenkina I.A. Characteristics of left ventricular and cardiac hemodynamic remodeling after on-pump or off-pump coronary artery bypass grafting. *Bulletin of Siberian Medicine.* 2023;22(2):88–96. https://doi.org/10.20538/1682-0363-2023-2-88-96.

Особенности ремоделирования миокарда левого желудочка и сердечной гемодинамики после коронарного шунтирования on-pump или off-pump

Маянская С.Д.[1], Абзалова Г.Ф.[2], Гараева Л.А.[3], Абдульянов И.В.[3], Тепляков А.Т.[4], Березикова Е.Н.[5], Гребенкина И.А.[5]

[1] Казанский государственный медицинский университет (КГМУ)
Россия, Республика Татарстан, 420012, г. Казань, ул. Бутлерова, 49

[2] Межрегиональный клинико-диагностический центр (МКДЦ)
Россия, Республика Татарстан, 420101, г. Казань, ул. Карбышева, 12а

[3] Казанская государственная медицинская академия (КГМА) – образовательный филиал Российской медицинской академии непрерывного профессионального образования (РМАНПО)
Россия, Республика Татарстан, 420012, г. Казань, ул. Муштари, 11

[4] Научно-исследовательский институт (НИИ) кардиологии, Томский национальный исследовательский медицинский центр (НИМЦ) Российской академии наук
Россия, 634012, г. Томск, ул. Киевская, 111а

[5] Новосибирский государственный медицинский университет (НГМУ)
Россия, 630091, г. Новосибирск, Красный пр., 52

РЕЗЮМЕ

Цель исследования. Изучить сравнительную динамику ремоделирования левого желудочка (ЛЖ) после операций коронарного шунтирования (КШ) с использованием методов искусственного кровообращения (ИК) и на бьющемся сердце.

Материалы и методы. В исследование включены 129 пациентов с верифицированной ишемической болезнью сердца (ИБС), которым было выполнено КШ в условиях ИК (on-pump) или на бьющемся сердце (off-pump). Всем пациентам перед операцией, через 1 нед и через 4 мес проводилась эхокардиография (ЭХОКГ) и объемная компрессионная осциллометрия (ОКО), результаты которых сравнивались в группах, разделенных по методике операции и в зависимости от наличия перенесенного инфаркта миокарда с использованием вариационных рядов, апостериорного критерия Тьюки, коэффициента Пирсона и коэффициента Спирмена.

Результаты. По данным ЭХОКГ не выявлено разницы гемодинамических показателей в группах сравнения в постоперационном периоде. По данным ОКО в группе «off-pump без постинфарктного кардиосклероза (ПИКС)» через 1 нед после операции отмечены статистические отличия следующих показателей: увеличение сердечного выброса (СВ) ($p < 0,001$), ударный объем (УО) и ударный индекс (УИ) ($p = 0,005$), мощность ЛЖ (МЛЖ) ($p = 0,015$), а также увеличение сердечного индекса и МЛЖ через 4 мес. В группе пациентов с ПИКС и on-pump через 1 нед после КШ наблюдалось снижение показателей МЛЖ ($p < 0,001$) и динамики расхода энергии ($p < 0,001$). При проведении корреляционного анализа были получены умеренные связи между инотропными параметрами сердечной гемодинамики УО, УИ, СВ, МЛЖ и артериального давления ($r\pi = 0,33–0,47$; $p < 0,001$) и заметные связи между УО, УИ, СВ, МЛЖ и фракцией выброса ($r\pi = 0,63–0,68$; $p < 0,001$).

Заключение. После операции КШ, выполненной off-pump, через 7 сут отмечено улучшение некоторых гемодинамических показателей и всех показателей инотропной функции сердца по сравнению с пациентами

on-pump. К 4-му мес после операции off-pump наблюдалось положительное гемодинамическое ре-ремоделирование по сравнению с послеоперационным периодом после on-pump.

Ключевые слова: коронарное шунтирование, off-pump, ремоделирование

Соответствие принципам этики. Все пациенты подписали информированное согласие на участие в исследовании. Исследование одобрено комитетом по этике КГМУ (протокол № 10 от 03.03.2011).

Конфликт интересов. Авторы декларируют отсутствие явных и потенциальных конфликтов интересов, связанных с публикацией настоящей статьи.

Источник финансирования. Авторы заявляют об отсутствии финансирования при проведении исследования.

Для цитирования: Маянская С.Д., Абзалова Г.Ф., Гараева Л.А., Абдульянов И.В., Тепляков А.Т., Березикова Е.Н., Гребенкина И.А. Особенности ремоделирования миокарда левого желудочка и сердечной гемодинамики после коронарного шунтирования on-pump или off-pump. *Бюллетень сибирской медицины.* 2023;22(2):88–96. https://doi.org/10.20538/1682-0363-2023-2-88-96.

INTRODUCTION

In recent years, mortality from cardiovascular diseases (CVD) has been steadily decreasing thanks to the mass introduction of interventional methods of treatment and diagnosis of coronary heart disease (CHD) into clinical practice. Nevertheless, coronary artery bypass grafting (CABG) is still the surgery of choice in case of widespread multivessel atherosclerotic lesions of the coronary arteries (CA) with significant calcification, proximal stenosis of the left CA, as well as in patients with diabetes mellitus (DM) [1–3]. In such a group of patients, a successfully performed open heart surgery and direct myocardial revascularization lead to an improvement in the clinical condition, an improved functional class of angina pectoris, and an increase in the left ventricular ejection fraction (LVEF) [4, 5].

CABG can be performed both with the aid of cardiopulmonary bypass (CPB) and pharmacological cold crystalloid cardioplegia (PCCC) (on-pump CABG) and on a beating heart (off-pump CABG) [6–8]. During a surgery with the use of extracorporeal circulation, the heart undergoes ischemia and cardioplegia with further reperfusion. In this case, a condition known as stunned myocardium occurs, which causes a delay in the restoration of LV contractile function.

Direct myocardial revascularization on a beating heart (off-pump CABG) was developed to avoid reperfusion complications, increase the effectiveness of surgical treatment, and reduce postoperative mortality. The advantages of this approach include the absence of traumatic damage to blood cells, shorter surgery duration, and the absence of complications associated with CPB [9, 10].

However, there are still insufficient data in the modern literature on differences in remodeling of the heart and blood vessels in patients with CHD who underwent on-pump and off-pump direct revascularization. Such data are extremely important, since they would allow to plan postoperative rehabilitation of patients, taking into account the structural and functional remodeling of the LV of the heart, namely changes in the mass of the myocardium, the heart chambers, heart anatomy, its systolic and diastolic function, EF, etc.

The aim of this study was to conduct a comparative study of the changes in LV remodeling in patients with CHD after on-pump and off-pump surgical myocardial revascularization to optimize postoperative rehabilitation.

MATERIALS AND METHODS

The study included 129 patients with CHD aged 39–76 years (mean age 57.2 ± 8.6 years) with severe stenotic changes in CA, confirmed by coronary angiography (CAG), with different systolic LV function, who were scheduled for CABG.

The exclusion criteria from the study were considered to be acute coronary syndrome (ACS), acute cerebrovascular accident (ACA), cooccurring valvular pathology requiring surgical intervention; aneurysm of the aorta and LV, conditions after pacemaker implantation, as well as cancer, acute inflammatory, broncho-obstructive, rheumatic, endocrine, and infectious diseases. All patients underwent coronary artery or mammary artery bypass grafting with the placement of one, two (36.1%), and more than three shunts (63.9%).

All the examined patients were divided into four groups: group 1 – patients with postinfarction car-

diosclerosis (PICS), who underwent on-pump CABG with the aid of CPB (n = 47); group 2 – patients without PICS, who underwent on-pump CABG (n = 27); group 3 – patients with PICS, who underwent off-pump CABG (n = 28); group 4 – patients without PICS who underwent off-pump CABG (n = 27). CHD was confirmed by CAG. Comparative characteristics of patients by gender, age, presence of risk factors for CVD and concomitant diseases in the groups are presented in Table 1.

Table 1

Comparative characteristics of patients in groups, *n* (%)

Parameter	Group 1, n = 47	Group 2, n = 27	Group 3, n = 28	Group 4, n = 27
Average age, years, $M \pm SD$	60.5 ± 1.0	61.3 ± 1.2	57.6 ± 2.2	64.8 ± 2.8
Men	37 (78.7)	19 (70.3)	10 (35.7)	13 (48.1)
BMI, kg / m^2 $M \pm SD$	29.4 ± 4.7	27.8 ± 4.3	28.9 ± 4.1	29.2 ± 4.7
Smoking	25 (53.2)	14 (51.8)	10 (35.7)	14 (51.8)
EH	25 (53.2)	22 (81.5)	10 (35.7)	13 (48.1)
One damaged CA	12 (25.5)	10 (37.0)	8 (28.6)	10 (37.0)
≥2 damaged CAs	31 (65.9)	17 (62.9)	6 (21.4)	6 (22.2)
Left coronary main trunk stenosis	4 (8.5)	–	–	–
Diabetes mellitus	14 (29.8)	6 (22.2)	2 (7.1)	4 (14.8)
CABG (1–2 shunts)	14 (29.8)	15 (55.5)	10 (35.7)	10 (37.0)
CABG (≤3 shunts)	33 (70.2)	12 (44.4)	4 (14.3)	6 (22.2)

Note: EH – essential hypertension, BMI – body mass index, LCA – left coronary artery.

Transthoracic echocardiography (TTE) and volumetric compression oscillometry (VCO) were performed three times: before CABG, as well as7 days and 4 months after the surgery to assess remodeling and hemodynamics of the heart. The study was conducted with patients receiving standard drug therapy for CHD and chronic heart failure (CHF).

TTE was performed using Vivid 7 Dimension Pro, a high-performance ultrasound system. TTE was carried out immediately before the surgery, as well as 7 days and 4 months after CABG. The following parameters were evaluated during TTE: the LV end-diastolic diameter (EDD), the LV end-diastolic volume (EDV), the LV end-systolic volume (ESV), LVEF (using the Simpson's method), the interventricular septal thickness at end-diastole (IST), the left ventricular posterior diastolic wall thickness (LVPDWT), and the left atrial volume. The geometric remodeling of LV was evaluated by calculating indices for relative wall thickness (RWT), EDV, LV myocardial mass (LVMM), and left atrial volume (LAV).

VCO was performed using the APCO-8-RIC blood circulation parameter analyzer (Setal company, Kazan) [11]. This method is based on estimating changes in the volume of large arteries using an original measuring system. The examination method consists in automatic injection of air into the cuff at a controlled speed and simultaneous observation of oscillations on the monitor until the compression threshold and subsequent automatic decompression are reached. Patients undergoing this examination should be in the sitting position. They should fast prior to examination. The cuff is adjusted for every patient. Then, using the device software, the following hemodynamic parameters were calculated: cardiac output (CO); cardiac index (CI); stroke volume (SV); stroke index (SI); left ventricular power (LVP) (the product of SV and mean hemodynamic pressure); left ventricular ejection time (LVET) – the time interval from aortic valve opening to aortic valve closure and the phase of systole during which the left ventricle ejects blood into the aorta; volumetric flow rate (VFR) – the volume of blood being pumped by a single ventricle of the heart per one minute; energy for the displacement of one liter of blood (EDB). The values of the LV contractility, CO per minute, and the total ejection time per one minute allow to determine the energy spent for displacement of one liter of blood through the LV per one minute.

A statistical analysis was carried out using the IBM SPSS Statistics 20 software, which was used for the parametric and nonparametric analysis. Testing the compared aggregates for normality of distribution was evaluated by the Mann – Whitney – Wilcoxon test. The Fischer's exact test was used to study qualitative characteristics. The differences between the groups were considered statistically significant at

$p < 0.05$. When statistically significant differences were found between the groups, a pairwise comparison of aggregates was performed using the Tukey's post hoc test. Paired correlations were assessed by the Pearson's correlation coefficient (rπ) for interval variables and by the Spearman's rank correlation coefficient for ordinary values. The data were presented as absolute and relative values of *n (%)* and as the mean and the standard deviation $M \pm SD$.

RESULTS

The analysis of myocardial remodeling parameters according to the TTE data, depending on the presence or absence of PICS, is presented in Table 2.

Table 2

Changes in myocardial remodeling parameters according to the TTE data depending on the surgery type and the presence of PICS, *M ± SD*

Parameter	Period	Group 1, *n* = 47	Group 2, *n* = 27	Group 3, *n* = 28	Group 4, *n* = 27
LVMM	Before CABG,	239.5 ± 11.5	178.8 ± 7.0	220.8 ± 20.4	188.6 ± 6.2
	7 days after and	219.0 ± 11.0*	163.1 ± 8.8*	193.5 ± 14.5*	170.3 ± 5.7**
	4 months after the surgery	195.5 ± 9.3###	152.1 ± 5.3###	167.1 ± 10.8##	151.7 ± 5.4###
IST, cm	Before CABG,	1.10 ± 0.04	1.10 ± 0.04	1.15 ± 0.07	1.14 ± 0.05
	7 days after	1.06 ± 0.04*	1.07 ± 0.03*	1.10 ± 0.06	1.09 ± 0.05
	and 4 months after the surgery	1.0 ± 0.03###	1.02 ± 0.02###	1.02 ± 0.05#	1.01 ± 0.03###
LVPW, cm	Before CABG,	0.99 ± 0.04	1.0 ± 0.02	1.06 ± 0.06	1.01 ± 0.04
	7 days after	0.99 ± 0.03	1.0 ± 0.02	0.98 ± 0.05	1.01 ± 0.03
	and 4 months after the surgery	0.93 ± 0.02#	0.98 ± 0.02	0.95 ± 0.03#	0.96 ± 0.02##
LVRWT	Before CABG,	0.37 ± 0.02•	0.41 ± 0.01	0.43 ± 0.02	0.44 ± 0.02
	7 days after	0.36 ± 0.01	0.41 ± 0.02	0.39 ± 0.02*	0.41 ± 0.01
	and 4 months after the surgery	0.34 ± 0.01###	0.40 ± 0.01##	0.36 ± 0.02#	0.39 ± 0.01#
LVEDV, ml	Before CABG,	133.5 ± 8.8	82.4 ± 4.1	102.8 ± 8.2	78.8 ± 3.5
	7 days after	113.2 ± 6.6***	73.9 ± 3.6***	92.1 ± 8.7**	69.5 ± 3.4**
	and 4 months after the surgery	104.2 ± 5.3###	71.3 ± 3.0###	85.3 ± 6.2###	63.9 ± 2.6##
LAV, ml	Before CABG,	72.9 ± 3.8	58.3 ± 2.3	85.0 ± 9.2	60.4 ± 2.8
	7 days after	66.8 ± 3.4***	54.5 ± 2.2***	75.1 ± 6.8*	56.7 ± 2.6***
	and 4 months after the surgery	64.4 ± 2.6###	52.1 ± 1.9###	57.3 ± 4.2#	52.5 ± 2.5###
EF, %	Before CABG,	45.0 ± 1.4•	58.7 ± 0.7	52.5 ± 2.0	60.7 ± 0.9
	7 days after	44.7 ± 1.5	57.0 ± 0.7	50.5 ± 1.7	58.7 ± 1.3
	and 4 months after the surgery	48.5 ± 1.6##	61.9 ± 0.8	54.4 ± 1.8	61.8 ± 1.0

Note: LVPW – left ventricular posterior wall; LVEDV – left ventricular end-diastolic volume; LVMM – LV myocardial mass; ISP – interventricular septum; RWT – relative LV wall thickness; LAV – left atrial volume; EF – ejection fraction.

• statistical differences between the baseline parameters in groups 1 and 3: LVRWT $p = 0.023$; EF $p = 0.009$; statistical differences between the groups in baseline parameters and on day 7 after CABG: * $p < 0.05$; ** $p < 0.005$; $p < 0.001$***; statistical differences between the groups in baseline parameters and 4 months after CABG: # $p < 0.05$; ## $p < 0.005$ ### $p < 0.001$.

When assessing the differences in baseline TTE parameters between the groups of patients, we obtained statistically significant data on only two parameters – RWT and LVEF. Thus, in patients with a history of MI who underwent off-pump CABG (group 3), the thickness of the LV wall was less than in the group of patients who underwent on-pump surgery (group 1), while the EF was slightly higher. However, the differences in these parameters between the groups in the postoperative period were insignificant.

During the follow-up period, in all groups of patients, regardless of the presence of PICS and the type of surgery, a significant decrease in LVMM was observed as early as one week after CABG and especially by the 4th month postoperatively (Table 2). At the same time, the LV mass decreased evenly in all groups, regardless of the type of CABG. Changes in LVRWT compared to the baseline level became statistically significant only 4 months after the surgery. LVED and LAV decreased as early as one week after the surgery, and an even more pronounced decrease was observed after 4 months. The changes in EF in the early postoperative period were insignificant. However, 4 months after CABG, a statistically significant increase in this parameter was observed in the group of patients with PICS operated with the use of CPB and PCCC – from 45.0 ± 1.4 to 48.5 ± 1.6% ($p = 0.004$), which was probably due to the fact that myocardial contractility was initially lower in this group. The parameters of cardiac hemodynamics obtained using VCO are presented in Table 3.

Table 3

Hemodynamic parameters at baseline, 7 days after, and 4 months after the surgery in patients who underwent CABG, *M* ± *SD*

Parameter	Group 1, *n* = 47	Group 2, *n* = 27	Group 3, *n* = 28	Group 4, *n* = 27
CO, l / min				
Before CABG;	5.1 ± 0.1	5.2 ± 0.2	5.6 ± 0.3	4.8 ± 0.2
after 7 days;	4.9 ± 0.2	5.1 ± 0.2	5.5 ± 0.3	5.5 ± 0.2*
after 4 months	5.4 ± 0.2●	6.1 ± 0.3**	6.1 ± 0.3●	6.5 ± 0.2**
SV, ml:				
Before CABG;	83.1 ± 2.7	79.9 ± 3.7	92.9 ± 5.2	78.6 ± 5.5
after 7 days;	63.2 ± 2.7*	66.1 ± 3.8*	84.1 ± 6.9	85.8 ± 4.7*
after 4 months	79.4 ± 2.8	87.6 ± 4.3**	90.3 ± 6.4	97.2 ± 5.5**
SI, l / m^2:				
Before CABG;	42.4 ± 1.5	43.7 ± 1.8	48.2 ± 3.2	43.0 ± 2.7
after 7 days;	34.9 ± 1.5*	36.3 ± 2.2*	43.1 ± 4.5	48.5 ± 2.5*
after 4 months	41.1 ± 1.4	48.1 ± 2.4**	47.2 ± 3.9	54.8 ± 2.8**
LVP, W:				
Before CABG;	3.5 ± 0.2	3.4 ± 0.3	3.6 ± 0.4	2.9 ± 0.2
after 7 days;	2.6 ± 0.1*	3.0 ± 0.2	3.5 ± 0.4	3.5 ± 0.2*
after 4 months	3.3 ± 0.2	3.7 ± 0.2	4.0 ± 0.4	4.1 ± 0.3**
CI, l / min^2:				
Before CABG;	2.7 ± 0.1	2.8 ± 0.1	3.0 ± 0.2	2.7 ± 0.1
after 7 days;	2.6 ± 0.1	2.7 ± 0.1	2.9 ± 0.3	3.0 ± 0.1*
after 4 months	2.9 ± 0.1**	3.3 ± 0.2**	3.3 ± 0.2	3.6 ± 0.2**
LVET, sec:				
Before CABG;	300.3 ± 10.1	309.0 ± 17.3	365.9 ± 40.7	309.8 ± 16.1
after 7 days;	297.4 ± 11.6	268.0 ± 17.6	409.9 ± 55.1	326.9 ± 33.2
after 4 months	322.6 ± 13.0	326.8 ± 17.1	331.2 ± 33.7	378.8 ± 28.2
VFR, ml / sec:				
Before CABG;	285.1 ± 14.1	280.8 ± 19.7	294.9 ± 29.8	235.9 ± 27.3
after 7 days;	235.6 ± 12.2	261.3 ± 16.8	306.0 ± 29.1	252.1 ± 37.2
after 4 months	267.6 ± 11.8	296.9 ± 16.9	294.3 ± 27.0	292.8 ± 36.2
EDB, W·sec:				
Before CABG;	12.2 ± 0.2	11.7 ± 0.3	12.1 ± 0.5	11.5 ± 0.3
after 7 days;	11.1 ± 0.2*	11.2 ± 0.3	11.6 ± 0.4	11.7 ± 0.4
after 4 months	12.4 ± 0.3	12.9 ± 0.4**	12.9 ± 0.5	12.7 ± 0.5**

* statistical differences between baseline values and values on day 7 after the surgery:
CO, SV, SI $p < 0.001$ (group 4 $p < 0.005$); LVP (group 1 $p < 0.001$; group 4 $p = 0.015$); CI (group 4 $p < 0.001$); EDB (group 1 $p < 0.001$).
**statistical differences between baseline values and values 4 months after the surgery: CO $p < 0.05$; $p < 0.01$; SV $p < 0.005$; SI $p < 0.001$; CI < 0.005; EDB $p < 0.05$; ● statistical differences between the groups, $p < 0.05$.

According to the data obtained one week after the surgery, CO practically did not change, with the exception of patients in group 4 (off-pump CABG without PICS), in which this parameter increased from 4.8 ± 0.2 to 5.5 ± 0.2 l / min ($p < 0.001$). However, already 4 months after CABG in all patients, the mean value of LV CO was higher than before the surgery, and in the groups after off-pump CABG, this parameter was higher compared to patients who underwent on-pump surgery ($p < 0.05$). However, statistically significant differences were found only in the groups of patients without PICS.

One week after the surgery, LV SV and SI significantly decreased in patients operated with the aid of CPB and PCCC ($p < 0.001$), whereas in group 3, a decrease in these parameters was not significant ($p = 0.164$), and in group 4, on the contrary, their increase was statistically significant ($p = 0.005$). Four months after CABG, these parameters of LV hemodynamic remodeling in patients with a history of MI increased to values comparable to the baseline level. At the same time, the most pronounced increase in LV SV and SI was observed in group 4 without PICS.

In group 1 (with PICS), one week after CABG with the use of CPB and PCCC, there was a significant decrease in LV power ($p < 0.001$), whereas in groups 2 and 3 this parameter was comparable to the baseline values ($p = 0.093$ and $p = 0.397$, respectively). In

group 4 (without PICS after beating heart CABG), the level of LVP on day 7 after the surgery increased significantly ($p = 0.015$). Four months after the surgery, this parameter in all groups, except for group 4, turned out to be comparable to the baseline level, whereas in the latter, its further increase was observed. In group 4, there was a similar increase in CI.

Finally, changes in the energy spent for the displacement of one liter of blood through the LV one week after the surgery were characterized by a statistically significant decrease from 12.2 ± 0.2 to 11.1 ± 0.2 W • sec in patients of group 1 (with PICS and after on-pump CABG) ($p < 0.001$). In groups 1, 2, and 3, the values of EDB were comparable to the baseline level. Four months after the surgery, the average values increased in all groups, but a statistically significant increase was revealed in patients without MI. During the correlation analysis, moderate associations were obtained between the inotropic parameters of cardiac hemodynamics SV, SI, CO, LVP and blood pressure ($r\pi = 0.33–0.47$; $p < 0.001$), and noticeable associations were found between SV, SI, CO, LVP and EF ($r\pi = 0.63–0.68$; $p < 0.001$).

DISCUSSION

It is known that after direct myocardial revascularization, the heart adapts to new functioning conditions, which causes structural and functional remodeling [12]. The effect of the CABG type (on-pump or off-pump) on the parameters of intracardiac hemodynamics and cardiac remodeling is yet to be studied, since data on the changes in cardiac parameters in the postoperative period can be used both to assess the effectiveness of surgical treatment [13, 14] and to select a rehabilitation program for patients after bypass surgery, depending on the surgery type.

It is still not entirely clear how functional and anatomical remodeling of the LV occurs in the postoperative period and what role the surgery type (on-pump or off-pump) plays in it. However, already one week after CABG, and especially by the end of the 4th month, regardless of the type of surgery and MI in history, a decrease in LVMM, IST, LVPWT, and RWT was noted. Apparently, processes occurring after revascularization, which preserved the viability of the myocardium, contribute to rapid normalization of the structural and anatomical parameters of the myocardium and improvement of LV pumping function, which is confirmed by a significant increase in these parameters by the end of the follow-up.

Similar changes were noted in the volume parameters of the heart – LVED and LAV, which decreased. All this was accompanied by regular changes in the main parameter of myocardial contractility – EF, which first decreased and then reached the baseline level or even slightly increased [15]. However, all these changes were rather general and did not allow to identify differences in cardiac remodeling in both on-pump and off-pump CABG. In the end, surgical revascularization, regardless of the surgery type, led to positive structural and anatomical changes in the heart. In this situation, it seemed important to evaluate not only structural, but also hemodynamic cardiac remodeling in the groups after different types of CABG.

In this regard, a number of cardiac hemodynamic parameters were evaluated using VCO. This method is available, has no technical limitations, and can be easily reproduced in practice, which is especially important for consistent observation of changes. According to the results of this study, a significant difference was revealed in almost all the main hemodynamic parameters, such as CO, CI, SV, and SI of the LV, depending on the type of CABG. Thus, in group 1 (with PICS and after on-pump CABG), a decrease in these parameters was observed for 1 week, while in patients in groups 3 and 4 (off-pump CABG), the parameters decreased slightly. On the contrary, in group 4 (without PICS), a statistically significant increase in the parameters was noted. Four months after the surgery, hemodynamic parameters stabilized in all groups. However, in group 4, these parameters were significantly higher.

We did not reveal a close correlation between the parameters of TTE, VCO, and nonparametric data reflecting risk factors, concomitant diseases, PICS, and the number of shunts in the arteries. Therefore, we can assume that such dependence on the surgery type is associated not only with different severity of CHD in the groups, but also, probably, with the duration of surgery, traumas from surgical intervention, ischemic and reperfusion injuries, the fact that the procedure is not physiological and, of course, the cardiodepressive effect of the on-pump surgery.

According to various researchers, in on-pump CABG, suppression of cardiac hemodynamic parameters is noted almost two hours after surgery and leads to a decrease in EF on average from 50 to 30%. At the same time, cardiac contractility can be restored by the end of day 1 after CABG or even much later [16, 17]. Our data also confirm the cardiodepressive effect of on-pump CABG, which leads to a rapid decrease in LV power and a decrease in its EDB per 1 minute. At

the same time, after off-pump CABG, this decrease was practically not observed, which may be due to relatively rapid recovery of myocardial activity after hibernation, even in severe patients. At the same time, the history of MI significantly slowed down restoration of the inotropic function of the heart, regardless of the CABG type. Nevertheless, the systolic function stabilized much faster in the group of patients who underwent a beating heart CABG.

CONCLUSION

Thus, the surgery type affects not only the structural and anatomical remodeling of the heart, but also, largely, the parameters of cardiac hemodynamics in the postoperative period. In patients with CHD 7 days after off-pump CABG, there was a significant improvement in all parameters of inotropic heart function compared to patients who underwent on-pump surgery. Four months after off-pump CABG, the parameters of positive hemodynamic remodeling became even more noticeable than in patients after on-pump surgery. This indicates faster and better recovery of the myocardium and allows to optimize the rehabilitation program depending on the surgery type.

REFERENCES

1. Polyakov R.S., Abugov S.A., Zhbanov I.V., Sahakyan Y.M., Puretsky M.V., Pirkova A.A., et al. Coronary stenting in patients with coronary heart disease with multivessel damage of the coronary bed and low scores on the SYNTAX SCORE scale. *Kardiologiia*. 2013;53(10):4–9 (in Russ.).
2. Locker C. Off-pump or on-pump coronary artery bypass grafting in diabetes: Is this the important question?. *J. Thorac. Cardiovasc. Surg.* 2019;157(3):970–971. DOI: 10.1016/j.jtcvs.2018.08.069.
3. Zhang X., Wu Z., Peng X. et al. Prognosis of Diabetic Patients Undergoing Coronary Artery Bypass Surgery Compared With Nondiabetics: A Systematic Review and Meta-analysis. *J. Cardiothorac. Vasc. Anesth.* 2011;25(2):288–298. DOI: 10.1053/j.jvca.2010.09.021.
4. Mohr F., Morice M., Kappetein A. et al. Coronary artery bypass graft surgery versus percutaneous coronary intervention in patients with three-vessel disease and left main coronary disease: 5-year follow-up of the randomised, clinical SYNTAX trial. *The Lancet*. 2013;381(9867):629–638. DOI: 10.1016/s0140-6736(13)60141-5.
5. Panza J., Velazquez E., She L. et al. Extent of Coronary and Myocardial Disease and Benefit From Surgical Revascularization in LV Dysfunction. *J. Am. Coll. Cardiol.* 2014;64(6):553–561. DOI: 10.1016/j.jacc.2014.04.064.
6. Simard T., Hibbert B., Pourdjabbar A. et al. Percutaneous coronary intervention with or without on-site coronary artery bypass surgery: A systematic review and meta-analysis. *Int. J. Cardiol.* 2013;167(1):197–204. DOI: 10.1016/j.ijcard.2011.12.035.
7. Ma G., Fan Y., Shao W., Qi L. Meta-Analysis for the Prognosis of On-Pump Versus Off-Pump Coronary Artery Bypass Grafting. *J. Am. Coll. Cardiol.* 2018;72(3):344–345. DOI: 10.1016/j.jacc.2018.03.544.
8. Takagi H., Ando T., Mitta S. Meta-Analysis Comparing ≥10-Year Mortality of Off-Pump Versus On-Pump Coronary Artery Bypass Grafting. *Am. J. Cardiol*. 2017;120(11):1933–1938. DOI: 10.1016/j.amjcard.2017.08.007.
9. Kim K., Choi J., Oh S. et al. Twenty-year experience with off-pump coronary artery bypass grafting and early postoperative angiography. *Ann. Thorac. Surg.* 2020;109(4):1112–1119. DOI: 10.1016/j.athoracsur.2019.07.053.
10. Smart N., Dieberg G., King N. Long-term outcomes of on-versus off-pump coronary artery bypass grafting. *J. Am. Coll. Cardiol.* 2018;71(9):983–991. DOI: 10.1016/j.jacc.2017.12.049.
11. Shidlovskaya S.A., Dedebaeva L.B., Degtyarev V.A., Chomakhidze P.S., Kopylov F.Yu. Use of volumetric compression oscillometry in patients with arterial hypertension. *Kardiologiya i Serdechno-Sosudistaya Khirurgiya.* 2015;8(2):33–37 (in Russ.). DOI: 10.17116/kardio20158233-37.
12. Shi Y., Denault A., Couture P., Butnaru A., Carrier M., Tardif J. Biventricular diastolic filling patterns after coronary artery bypass graft surgery. *J. Thorac. Cardiovasc. Surg.* 2006;131(5):1080–1086.e3. DOI: 10.1016/j.jtcvs.2006.01.015.
13. Mathison M., Edgerton J., Horswell J., Akin J., Mack M. Analysis of hemodynamic changes during beating heart surgical procedures. *Ann. Thorac. Surg.* 2000;70(4):1355–1360. DOI: 10.1016/s0003-4975(00)01590-3.
14. Liu J., Tanaka N., Murata K. et al. Prognostic value of pseudonormal and restrictive filling patterns on left ventricular remodelingand cardiac events after coronary artery bypass grafting. *Am. J. Cardiol.* 2003;91(5):550–554. DOI: 10.1016/s0002-9149(02)03304-0.
15. Martinez E. No Major Differences in 30-Day Outcomes in High-Risk Patients Randomized to Off-Pump Versus On-Pump Coronary Bypass Surgery: The Best Bypass Surgery Trial. *Yearbook of Critical Care Medicine.* 2010;121(4):498–504. DOI: 10.1161/CIRCULATIONAHA.109.880443.
16. Ng K., Popovic Z., Troughton R., Navia J., Thomas J., Garcia M. Comparison of left ventricular diastolic function after on-pump versus off-pump coronary artery bypass grafting. *Am. J. Cardiol*. 2005;95(5):647–650. DOI: 10.1016/j.amjcard.2004.10.043.
17. Zhao D., Edelman J., Seco M., Bannon P., Vallely M. Long-term outcomes following off-pump coronary artery bypass grafting. *J. Am. Coll. Cardiol*. 2018;72(3):345–347. DOI: 10.1016/j.jacc.2018.04.068.

Authors' contribution

Mayanskaya S.D., Abzalova G.F., Berezikova E.N. – conception and design.

Abzalova G.F. – collection and processing of material, statistical processing of the data. Mayanskaya S.D., Garaeva L.A. – drafting of the manuscript. Mayanskaya S.D., Abdulianov I.V., Teplyakov A.T., Grebenkina I.A. – editing of the manuscript.

Authors' information

Mayanskaya Svetlana D. – Dr. Sci. (Med.), Professor of the Department of Hospital Therapy, KSMU, Kazan, smayanskaya@mail.ru, https://orcid.org/0000-0001-6701-5395

Abzalova Guzel F. – Cand. Sci. (Med.), Functional Diagnostics Doctor, Interregional Clinical and Diagnostic Center, Kazan, guselka88@bk.ru

Garaeva Lilia A. – Cand. Sci. (Med.), Assistant, Department of Cardiology, X-ray Endovascular and Cardiovascular Surgery, KSMA, branch of RMACPE, Kazan, garaevalily@gmail.com, https://orcid.org/0000-0002-9427-6037

Abdulianov Ildar V. – Cand. Sci. (Med.), Associate Professor, Head of the Department of Cardiology, X-ray Endovascular and Cardiovascular Surgery, KSMA, branch of RMACPE; Cardiovascular Surgeon, Cardiac Surgery Department No. 2, Interregional Clinical and Diagnostic Center, Kazan, ildaruna@mail.ru, https://orcid.org/0000-0003-2892-2827

Teplyakov Alexander T. – Dr. Sci. (Med.), Professor, Honored Scholar of the Russian Federation, Principal Researcher, Cardiology Research Institute, Tomsk NRMC, Tomsk, Vgelen1970@gmail.com, https://orcid.org/0000-0003-0721-0038

Berezikova Ekaterina N. – Dr. Sci. (Med.), Associate Professor, Department of Polyclinic Therapy and General Medical Practice, NSMU, Novosibirsk, https://orcid.org/0000-0002-9630-0213

Grebenkina Irina A. – Cand. Sci. (Med.), Assistant, Department of Polyclinic Therapy and General Medical Practice, NSMU, Novosibirsk, https://orcid.org/0000-0002-5563-2983

(✉) **Mayanskaya Svetlana D.,** smayanskaya@mail.ru

Received 05.09.2022;
approved after peer review 14.10.2022;
accepted 08.12.2022

УДК 616-056.257-06:616.248]-002-053.2
https://doi.org/10.20538/1682-0363-2023-2-97-103

The cytokine profile in obesity and asthma in children

Tarabrina A.A.[1], Ogorodova L.M.[1], Samoilova Yu.G.[1], Fedosenko S.V.[1], Fedorova O.S.[1], Petrov V.A.[1], Podchinenova D.V.[1], Boyko A.S.[2]

[1] Siberian State Medical University
2, Moscow Trakt, Tomsk, 634050, Russian Federation

[2] Mental Health Research Institute, Tomsk National Research Medical Center (NRMC), Russian Academy of Sciences
4, Aleutskaya Str., Tomsk, 634014, Russian Federation

ABSTRACT

Background. Childhood obesity is one of the pressing problems in modern healthcare, since it is associated with a high risk of non-communicable diseases, such as bronchial asthma (BA).

The aim. To determine the features of cytokine profiles in children with and without BA, depending on body weight and visceral fat area.

Materials and methods. At the first stage, 506 Tomsk schoolchildren underwent anthropometry with the calculation of the body mass index (BMI) and measurement of the visceral fat area (VFA) using the InBody 770 analyzer. Fifty-one (51) children from the first stage were included in the second clinical and diagnostic stage. The children were divided into four clinical groups: "Obesity" (n = 17), "Visceral Obesity" (n = 7), "Asthma" (n = 15), and "Healthy Children" (n = 12). In all study participants, the levels of interleukin (IL)-6, IL-8, IL-4, IL-10, and immunoglobulin (Ig) E in the blood serum were determined by the multiplex assay (MagPix and Luminex 200 c analyzers). Statistical data analysis was carried out using the Statistica 10.0 software package and the 4.2.2 version of R.

Results. The levels of IL-10 in the "Asthma" ($p < 0.006$) and "Obesity" ($p < 0.008$) groups were significantly higher than in the "Visceral Obesity" group. Significantly higher levels of IL-8 were found in patients with asthma ($p < 0.003$) and obesity ($p < 0.003$) compared to the "Visceral Obesity" group. Higher concentrations of IL-6 were found in the "Asthma" ($p < 0.001$) and "Obesity" ($p < 0.028$) groups compared to the "Visceral Obesity" group.

Conclusion. Similar upward changes in IL-6, IL-8, and IL-10 in children with asthma and obesity without a history of asthma may explain the contribution of obesity to a risk of asthma in children, possibly through excessive production of these proinflammatory cytokines that contribute to the implementation of Th2-mediated allergic inflammation.

Keywords: asthma, obesity, visceral obesity, inflammation, cytokines

Conflict of interest. The authors declare the absence of obvious and potential conflicts of interest related to the publication of this article.

Source of financing. The authors state that they received no funding for the study.

Conformity with the principles of ethics. A legally authorized representative of every child signed an informed consent to carrying out of the procedures. The study was approved by the local Ethics Committee at Siberian State Medical University (Protocol No. 8459/2 of 28.10.2020).

For citation: Tarabrina A.A., Ogorodova L.M., Samoilova Yu.G., Fedosenko S.V., Fedorova O.S., Petrov V.A., Podchinenova D.V., Boyko A.S. The cytokine profile in obesity and asthma in children. *Bulletin of Siberian Medicine.* 2023;22(2):97–103. https://doi.org/10.20538/1682-0363-2023-2-97-103.

✉ *Tarabrina Anna A.,* Aa.tarabrina@mail.ru

Цитокиновый профиль при ожирении и бронхиальной астме у детей

Тарабрина А.А.[1], Огородова Л.М.[1], Самойлова Ю.Г.[1], Федосенко С.В.[1], Федорова О.С.[1], Петров В.А.[1], Подчиненова Д.В.[1], Бойко А.С.[2]

[1] *Сибирский государственный медицинский университет (СибГМУ)*
Россия, 634050, г. Томск, Московский тракт, 2

[2] *Научно-исследовательский институт (НИИ) психического здоровья, Томский национальный исследовательский медицинский центр (НИМЦ) Российской академии наук*
Россия, 634014, г. Томск, ул. Алеутская, 4

РЕЗЮМЕ

Введение. Детское ожирение является одной из актуальных проблем современного здравоохранения, поскольку связано с высоким риском возникновения хронических неинфекционных заболеваний, таких как бронхиальная астма (БА).

Цель исследования – определение особенности цитокиновых профилей у детей с диагностированной БА и без нее в зависимости от массы тела и площади висцерального жира.

Материалы и методы. На первом этапе 506 школьникам г. Томска выполнена антропометрия с расчетом индекса массы тела, измерение площади висцеральной жировой ткани на аппарате Inbody 770. Во второй клинико-диагностический этап включен 51 ребенок из первого этапа. Сформированы четыре клинические группы: «ожирение» (n = 17), «висцеральное ожирение» (n = 7), «бронхиальная астма» (n = 15) и здоровые дети (n = 12). Всем участникам определен уровень интерлейкина (IL) 6, 8, 4, 10 и иммуноглобулина (Ig) E в сыворотке крови путем мультиплексного анализа (анализаторы MagPix и Luminex 200 с). Статистический анализ данных проведен с помощью пакета программы Statistica for Windows 10.0, а также с использованием языка R (версия 4.2.2).

Результаты. Уровень IL-10 в группах «бронхиальная астма» (p < 0,006) и «ожирение» (p <0,008) был достоверно более высоким по сравнению с группой «висцеральное ожирение». При оценке IL-8 установлен достоверно более высокий уровень у больных БА (p < 0,003) и ожирением (p < 0,003) чем при висцеральном ожирении. Более высокие концентрации IL-6 выявлены в группах «бронхиальная астма» (p < 0,001) и «ожирение» (p < 0,028) по сравнению с группой «висцеральное ожирение».

Заключение. Схожие изменения IL-6, IL-8, IL-10 в сторону их повышения у детей, страдающих бронхиальной астмой и ожирением без анамнеза астмы, могут объяснять вклад ожирения как фактора риска при астме у детей, возможно, через избыточную продукцию указанных провоспалительных цитокинов, способствующих реализации аллергического Th2-опосредованного воспаления.

Ключевые слова: бронхиальная астма, ожирение, висцеральное ожирение, воспаление, цитокины

Конфликт интересов. Авторы декларируют отсутствие явных и потенциальных конфликтов интересов, связанных с публикацией настоящей статьи.

Источник финансирования. Авторы заявляют об отсутствии финансирования при проведении исследования.

Соответствие принципам этики. До проведения предусмотренных процедур законным представителем ребенка подписано информированное согласие. Исследование одобрено локальным этическим комитетом СибГМУ (протокол № 8459/2 от 28.10.2020).

Для цитирования: Тарабрина А.А., Огородова Л.М., Самойлова Ю.Г., Федосенко С.В., Федорова О.С., Петров В.А., Подчиненова Д.В., Бойко А.С. Цитокиновый профиль при ожирении и бронхиальной астме у детей. *Бюллетень сибирской медицины.* 2023;22(2):97–103. https://doi.org/10.20538/1682-0363-2023-2-97-103.

INTRODUCTION

Obesity in childhood and adolescence is one of the pressing issues of modern healthcare, as it is associated with a high risk of chronic non-communicable diseases, such as asthma, arterial hypertension, and type 2 diabetes mellitus at an older age [1–4]. According to the World Health Organization (WHO), in 2020, obesity was registered in 4.4 million (7.9%) children under the age of 5 years in the European region [5].

Furthermore, this report states that every eighth child (11.6%) aged 5–9 years is obese, and every third child (29.5%) is overweight [5]. A study conducted in eight (8) federal districts of Russia in 2017 that included 2,000 children showed that the incidence of obesity in boys aged 11 and 15 years was 18.6 and 10%, respectively. In girls aged 11 and 15 years, it was 9.2 and 3.6%, respectively [6].

Currently, special attention is paid to patients with excess visceral adipose tissue (VAT) who have a normal body mass index (BMI) [7]. Iu.G. Samoilova et al. in their work found that the prevalence of visceral obesity in children under the age of 10 years (n = 625) was 2% in girls and 1.6% in boys, and in the group older than 10 years (n = 1,314) – 6.7% in girls and 8.5% in boys [8].

Numerous studies have shown that obesity or overweight is associated with the development of asthma in children [9–11]. At the same time, patients with asthma and obesity had a worse response to the use of budesonide in relation to lung function and also more often required hospitalization for asthma [12, 13]. Additionally, the results of some works indicate a possible role of excess VAT in the development of systemic inflammation and an increase in the subsequent risk of chronic non-communicable diseases, such as asthma [2, 14, 15]. In particular, the mechanism of participation of M1 macrophages, which promote the secretion of non-T2 cytokines (TNFα, IL-17A, IL-21, IFNγ, TGF-β1, IL-6) by activated Th1 and / or Th17 lymphocytes in the adipose tissue, with subsequent accumulation of neutrophils in the target tissues is discussed [15–17].

The work by H.A. Periyalil et al. showed that in adult patients with obesity and asthma, the number of M1 macrophages in the VAT correlates with BMI [18]. On the other hand, studies demonstrate the development of chronic inflammation involving VAT and subcutaneous adipose tissue (SAT) [19].

In general, current research results are miscellaneous and do not provide an insight into the contribution of inflammation initiated by visceral or subcutaneous obesity to the risk of developing asthma in children.

The aim of the study was to determine the features of the cytokine profile in children with diagnosed asthma and those without it, depending on body weight and visceral fat area.

MATERIALS AND METHODS

The present study was carried out in two stages. The first epidemiological stage was a part of a multicenter, prospective epidemiological study "Prevention of Obesity in Children and Adolescents (Clinical, Metabolic, Diagnostic, and Rehabilitation Aspects)" carried out from October 2020 to June 2021 in four schools in Tomsk (approved by the Ethics Committee at Siberian State Medical University, Protocol No. 8459/2 of 28.10.2020). As part of this stage, 506 schoolchildren aged 7–12 years were continuously included in the study, with the exception of children with monogenic obesity, type 1 and 2 diabetes mellitus, and severe or unstable somatic symptom disorder. Before carrying out the prescribed procedures, the legal representative of the child signed an informed consent.

In this group, a set of studies was performed, including measurement of anthropometric parameters (height, weight) in light clothes and without shoes, using scales installed in the InBody 770 analyzer (accuracy 0.1 kg) and the MSK-233 medical stadiometer (accuracy up to 0.1 cm). The Standard Deviation Score for BMI was calculated using the WHO Anthro Plus; a bioimpedance analysis with determination of the visceral fate area was performed using the InBody 770 analyzer.

At the second clinical diagnostic stage, a case-control study was conducted, and all participants from the first phase were offered the opportunity to continue participating in the study. After the first stage, the children were divided into four clinical groups: group 1 consisted of patients with obesity (n = 17); group 2 consisted of patients with normal SDS BMI and visceral obesity according to the bioimpedance analysis (n = 7); group 3 included patients with asthma without excess VAT and obesity (n = 15); and group 4 encompassed healthy children (n = 12). Patients with asthma were recruited from the clinical database of the Children's Clinic of Siberian State Medical University. The children were examined for the serum levels of cytokines (IL-6, IL-8, IL-4, IL-10) on the Magpix and Luminex 200 multiplex analyzers (Luminex Corp., USA) at the "Medical Genomics" Center for Collective Use (Tomsk NRMC).

Statistical data processing was carried out using the Statistica for Windows 10.0 software package. Descriptive statistics were used to process the results of the study. Normality of data distribution was checked using the Shapiro – Wilk test. Normally distributed quantitative data were presented as the arithmetic mean and standard deviation $M \pm SD$. For non-normal distributions, the median and the interquartile range $Me\ (Q_1; Q_3)$ were calculated. The differences in paraclinical parameters between the groups were assessed

using the Mann – Whitney – Wilcoxon test (for quantitative variables). The differences were considered statistically significant at $p < 0.05$.

The statistical analysis was also carried out using the R language (version 4.2.2). Prior to the analysis, cytokine values were normalized using the rank normalization method and converted to units of standard deviation. Then, the sample was analyzed for multivariate outliers. To assess the contribution of the patients' condition and their anthropometric parameters to the variability of cytokine concentration, we used the multivariate analysis of variance for distance matrices with permutations (the adonis2 function in the R vegan package). To do this, we calculated the distance matrix between the cytokine concentrations in patients in Euclidean space (the vegdist function in the R vegan package) and then applied adonis2 with 9999 permutations and calculated the marginal effects for all variables. The model included age, BMI, gender, grouping by clinical parameters, and VAT / VFA. The pairwise.adonis function was used to search for pairwise differences between the groups of patients. For multiple comparisons, the false discovery rate (FDR) was used for *p* values.

RESULTS

The article shows the results of the second clinical diagnostic stage. Fifty-one (51) children were included in the clinical diagnostic phase of the study, 31 of whom (58%) were boys and 20 (36%) were girls. The mean age was 9.3 (9; 10) years. The main anthropometric, gender, and age characteristics, as well as the results of the bioimpedance analysis of kinetic groups are shown in Table 1.

The allergic nature of the diseases was confirmed in all patients of the "Asthma" group by the results of the study of IgE and IL-4, which amounted to 450 IU / ml (151.6; 500) and 76.1 pg / ml (2.61; 428.7), respectively.

The results of assessing the levels of proinflammatory cytokines IL-6, IL-8, and IL-10 are presented in Table 2.

Table 1

Anthropometric, gender, and age characteristics and results of the bioimpedance analysis of the clinical groups

Group	Height, cm, $M \pm SD$	BMI, $M \pm SD$	VFA, cm^2 $M \pm SD$	Gender		Age, years, $Me\ (Q_1; Q_3)$
				boys	girls	
Group 1, $n = 17$	142.3 ± 6,3	24.3 ± 4.11	99.1 ± 48.3	10	7	9 (9; 10)
Group 2, $n = 7$	144.5 ± 4.5	17.2 ± 1.13	46.9 ± 5.7	2	5	10 (9;10)
Group 3, $n = 15$	139.1 ± 6.3	15.4 ± 1.03	24 ± 7.6	11	4	9 (8;10)
Group 4, $n = 12$	138.0 ± 5.9	16.4 ± 0.6	24.7 ± 9.2	8	4	9 (9;10)

Table 2

Variability of IL-6, IL-8, and IL-10 levels in the clinical groups, pg / ml $Me\ (Q_1; Q_3)$

Parameter	Group 1, $n = 17$	Group 2, $n = 7$	Group 3, $n = 15$	Group 4, $n = 12$
IL-10	1.83 (1.10; 3.72)[2]	0.92 (0.43; 1.14)[1, 2]	2.1 (1.15; 3.79)[1]	1.26 (1.09; 2.05)
IL-8	8.9 (5.48; 14.25)[2]	4.36 (2.23; 4.76)[1, 2, 3]	9.6 (6.43; 29.3)[1]	8.9 (7.5; 11.01)[3]
IL-6	1.3 (0.46; 5.39)[2]	0.46 (0.25; 0.46)[1, 2, 3]	5.3 (1.02; 20.6)[1, 4]	0.48 (0.46; 1.49)[3, 4]

Note: significant differences ($p < 0.05$) between the groups: [1] "Asthma" and "Visceral obesity", [2] "Obesity" and "Visceral obesity", [3] "Visceral obesity" and "Healthy Children", [4] "Asthma" and "Healthy Children" (Mann – Whitney *U*-test).

The IL-10 level in the "Asthma" ($p < 0.006$) and "Obesity" ($p < 0.008$) groups was significantly higher than in the "Visceral Obesity" group (Table 2). When evaluating proinflammatory IL-8, significantly higher levels were found in patients with asthma ($p < 0.003$) and obesity ($p < 0.003$) than in patients with visceral obesity. The study of proinflammatory IL-6 demonstrated its higher content in the "Asthma" ($p < 0.001$) and "Obesity" ($p < 0.028$) groups compared to the "Visceral Obesity" group (Table 2).

At the next stage, the overall cytokine profile was assessed using a multivariate analysis of variance, which included such characteristics as age, BMI, gender, clinical group, and VFA. Table 3 shows the correlation between these characteristics and the overall cytokine profile.

Table 3

Correlation between patients' characteristics and the overall cytokine profile (IL-6, IL-8, IL-4, IL-10)

Parameter	R^2	p
Age	0.015	0.353
Gender	0.033	0.059
BMI	0.045	0.018
VFA	0.045	0.019
Clinical groups	0.110	0.028

Note: R^2 – coefficient of determination (here and in Table 4).

The results of the nonparametric analysis of variance showed that the "Clinical groups" parameter explained 11% variability in the cytokine levels ($R^2 = 0.110$, $p = 0.028$), 4% variability in the BMI ($R^2 = 0.045$, $p = 0.018$), and 4% variability in VFA ($R^2 = 0.045$, $p = 0.019$).

After that, the intergroup differences in the overall cytokine profile were analyzed using the pairwise. adonis function (Table 4).

Table 4

Correlation between the cytokine profile and the clinical groups

Clinical groups	R^2	p	p-adjusted
Asthma vs Visceral Obesity	0.247	0.0021	0.0105
Asthma vs Obesity	0.049	0.169	0.241
Asthma vs Healthy Children	0.100	0.031	0.078
Visceral Obesity vs Obesity	0.140	0.007	0.023
Visceral Obesity vs Healthy Children	0.177	0.001	0.005
Obesity vs Healthy Children	0.029	0.545	0.681

Note: achieved significance level with the FDR – p-adjusted.

During the pairwise comparisons of the clinical groups in the overall cytokine concentration, significant differences were found between the following groups: "Asthma" and "Visceral Obesity" ($R^2 = 0.247$, $p = 0.002$); "Visceral Obesity" and "Obesity" ($R^2 = 0.140$, $p = 0.007$); and "Visceral Obesity" and "Healthy Children" ($R^2 = 0.177$, $p = 0.001$). However, no significant differences were found between the "Asthma" and "Obesity" groups (Table 4).

DISCUSSION

Obesity and asthma are included in the group of chronic non-communicable diseases in children and adolescents [20]. Researchers are actively discussing the role of obesity and visceral obesity as possible risk factors for the development of asthma, as well as concomitant diseases that aggravate the course of asthma [4, 20–22]. The results of this study indicate similar upward changes in some non-T2 cytokines (IL-6, IL-8, IL-10) in asthmatic children and obese children without asthma. It is the unidirectionality of proinflammatory changes that can be the fundamental basis for the realization of the risk of developing asthma in obese children. These changes were not confirmed in the group of patients with visceral obesity without an increase in BMI, which may indicate lower proinflammatory activity of VAT in these patients in relation to the production of the studied cytokines and / or the significance of high BMI in the pathogenesis of these abnormalities.

In terms of heterogeneity of clinical manifestations and differences in the immune response, two main endotypes of asthma are distinguished [20]. The T2 endotype (T2-high), which is mediated predominantly through the activity of Th2 lymphocytes, is the main mechanism of childhood allergic asthma, characterized by eosinophilic inflammation and secretion of T2 cytokines (IL-4, -5, -9, and -13) [23, 24]. Indeed, patients with asthma had high levels of IgE and IL-4, reflecting the activity of Th2 inflammation. Along with the basic allergic mechanism, high levels of non-Th2 cytokines (IL-6, IL-8, and IL-10) were also registered in the patients with asthma during the study. The overall cytokine profile in asthma during the multivariate analysis of variance did not show significant differences with the "Obesity" group, but significantly differed from the "Visceral Obesity" group due to lower levels of the studied cytokines.

It is well-known that IL-6 is involved in the development of neutrophilic inflammation [25]. Studies also indicate that the involvement of this cytokine in the development of inflammation in allergic asthma is associated with the ability to regulate differentiation of naive CD4 T lymphocytes to Th2 cells through synthesis of IL-4 [26, 27].

IL-8 shows high levels in children with asthma. This cytokine has chemoattractant activity, mainly in relation to neutrophil chemotaxis in the focus of inflammation [14, 28]. Meanwhile, M. Hodeib et al. (2021) found a correlation between the IL-8 concentration and the IgE level ($r = 0.789$, $p < 0.001$) in the blood serum [29].

On the one hand, published data confirm the role of IL-10 in the regulation of allergic inflammation and IgE synthesis [30, 31]. On the other hand, IL-10 promotes the activation of M2 macrophages in the adipose tissue and exerts a direct effect on adipocytes, reducing their proinflammatory activity, which may explain high levels of this cytokine in obese patients [32].

CONCLUSION

Therefore, the non-Th2 cytokines studied in this work (IL-6, IL-8, IL-10), which are well-known participants of systemic inflammation in obesity, are also involved in the development of inflammation in allergic asthma. Altogether, this similarity of mechanisms may underlie the contribution of obesity as a risk factor for asthma in children, possibly through overproduction of these proinflammatory cytokines that promote allergic Th2-mediated inflammation.

As for visceral obesity, the results of this study do not allow to confirm the independent role of VAT in the implementation of systemic inflammation in the context of the studied proinflammatory cytokines.

REFERENCES

1. Peterkova V.A., Bezlepkina O.B., Bolotova N.V., Bogova E.A., Vasjukova O.V., Girsh Ja.V. et al. Clinical guidelines "Obesity in children". *Endocrinology Problems.* 2021;67 (5):67–83 (in Russ.).
2. Rohm T.V., Meier D.T., Olefsky J.M., Donath M.Y. Inflammation in obesity, diabetes, and related disorders. *Immunity.* 2022;55(1):31–55. DOI: 10.1016/j.immuni.2021.12.013.
3. Suliga E. Visceral adipose tissue in children and adolescents: A review. *Nutr. Res. Rev*. 2009;22(2):137–147. DOI: 10.1017/S0954422409990096.
4. Gaines J., Vgontzas A.N., Fernandez-Mendoza J. et al. Increased inflammation from childhood to adolescence predicts sleep apnea in boys: A preliminary study. *Brain Behav. Immun*. 2017;64:259–265. DOI: 10.1016/j.bbi.2017.04.011.
5. WHO European Regional Obesity Report 2022. Copenhagen: WHO Regional Office for Europe, 2022.
6. Namazova-Baranova L.S., Yeletskaya K.A., Kaytukova E.V., Makarova S.G. Evaluation of the physical development of children of secondary school age: an analysis of the results of a cross-sectional study. *Pediatric Pharmacology*. 2018;15. (4):333–342 (in Russ.). DOI: 10.15690/pf.v15i4.1948.
7. Simoni P., Guglielmi R., Aparisi Gómez M.P. Imaging of body composition in children. *Quant Imaging Med Surg*. 2020;10(8):1661–1671. DOI: 10.21037/qims.2020.04.06.
8. Samoilova Iu.G., Podchinenova D.V., Kudlaj D.A., Olejnik O.A., Matveeva M.V., Kovarenko M.A. et al. Bioimpedance analysis as a promising screening technology in children. *Physician*. 2021;32 (7):32–37 (in Russ.).
9. Deng X., Ma J., Yuan Y., Zhang Z., Niu W. Association between overweight or obesity and the risk for childhood asthma and wheeze: An updated meta-analysis on 18 articles and 73,252 children. *Pediatr. Obes.*2019;14:e12532. DOI: 10.1111/ijpo.12532.
10. Egan K.B., Ettinger A.S., Bracken M.B. Childhood body mass index and subsequent physician-diagnosed asthma: A systematic review and meta-analysis of prospective cohort studies. *BMC Pediatr.* 2013;13:121. DOI: 10.1186/1471-2431-13-121.
11. Black M.H., Smith N., Porter A.H., Jacobsen S.J., Koebnick C. Higher prevalence of obesity among children with Asthma. *Obesity.* 2012;20:1041–1047. DOI: 10.1038/oby.2012.5.
12. Hay C., Henrickson .SE. The impact of obesity on immune function in pediatric asthma. *Curr. Opin. Allergy Clin. Immunol*. 2021;21(2):202–215. DOI: 10.1097/ACI.0000000000000725.
13. Gross E., Lee D.S., Hotz A., Ngo K.C., Rastogi D. Impact of obesity on asthma morbidity during a hospitalization. *Hosp. Pediatr*. 2018;8(9):538–546. DOI: 10.1542/hpeds.2017-0265.
14. Konishheva A.Ju., Gervazieva V.B., Mazurina S.A. Features of inflammatory mediator and autoreactivity profile in bronchial asthma associated with obesity. *Journal of Microbiology, Epidemiology, and Immunobiology.* 2019;(1):59–63 (in Russ.).
15. Kenđel Jovanović G., Mrakovcic-Sutic I., Pavičić Žeželj S., Šuša B., Rahelić D., Klobučar Majanović S. The efficacy of an energy-restricted anti-inflammatory diet for the management of obesity in younger adults. *Nutrients*. 2020;12(11):3583. DOI: 10.3390/nu12113583.
16. Chehimi M., Vidal H., Eljaafari A. Pathogenic role of IL-17-producing immune cells in obesity, and related inflammatory diseases. *J Clin. Med*. 2017;6(7):68. DOI: 10.3390/jcm6070068.
17. Al-Sharif F.M., Abd El-Kader S.M., Neamatallah Z.A., AlKhateeb A.M. Weight reduction improves immune system and inflammatory cytokines in obese asthmatic patients. *Af.r Health Sci*. 2020;20(2):897–902. DOI: 10.4314/ahs.v20i2.44.
18. Periyalil H. A., Wood L.G., Wright T.A., Karihaloo C., Starkey M.R., Miu A.S. et al. Obese asthmatics are characterized by altered adipose tissue macrophage activation. *Clin. Exp. Allergy*. 2018;48(6):641–649. DOI: 10.1111/cea.13109.
19. Girón-Ulloa A., González-Domínguez E., Klimek R.S., Patiño-Martínez E., Vargas-Ayala G., Segovia-Gamboa N.C. et al. Specific macrophage subsets accumulate in human subcutaneous and omental fat depots during obesity. *Immunol. Cell Biol*. 2020;98(10):868–882. DOI: 10.1111/imcb.12380.
20. Hay C., Henrickson S.E. The impact of obesity on immune function in pediatric asthma. *Curr. Opin. Allergy Clin. Immunol*. 2021;21(2):202–215. DOI: 10.1097/ACI.0000000000000725.
21. Osorio-Conles Ó., Vega-Beyhart A., Ibarzabal A., Balibrea J.M., Graupera I., Rimola J. et al. A distinctive NAFLD signature in adipose tissue from women with severe obesity. *Int. J. Mol. Sci.* 2021;22(19):10541. DOI: 10.3390/ijms221910541.
22. Neeland I.J., Marso S.P., Ayers C.R., Lewis B., Oslica R., Francis W. et al. Effects of liraglutide on visceral and ectopic fat in adults with overweight and obesity at high cardiovascular risk: a randomised, double-blind, placebo-controlled, clinical trial. *Lancet Diabetes Endocrinol.* 2021;9(9):595–605. DOI: 10.1016/S2213-8587(21)00179-0.
23. Kuo C.S., Pavlidis S., Loza M., Baribaud F., Rowe A., Pandis I. et al. T-helper cell type 2 (Th2) and non-Th2 molecular phenotypes of asthma using sputum transcriptomics in U-BIOPRED. *Eur. Respir. J.* 2017;49(2):1602135. DOI: 10.1183/13993003.02135-2016.
24. Bantulà M., Roca-Ferrer J., Arismendi E., Picado C. Asthma and obesity: two diseases on the rise and bridged by inflammation. *J. Clin. Med.* 2021;10(2):169. DOI: 10.3390/jcm10020169.

25. Li X., Hastie A.T., Peters M.C., Hawkins G.A., Phipatanakul W., Li H. et al. Investigation of the relationship between IL-6 and type 2 biomarkers in patients with severe asthma. *J. Allergy Clin. Immunol*. 2020;145(1):430–433. DOI: 10.1016/j.jaci.2019.08.031.
26. Rincón M., Anguita J., Nakamura T., Fikrig E., Flavell R.A. Interleukin (IL)-6 directs the differentiation of IL-4-producing CD4+ T cells. *J. Exp. Med*. 1997;185(3):461–469. DOI: 10.1084/jem.185.3.461.
27. Rincon M., Irvin C.G. Role of IL-6 in asthma and other inflammatory pulmonary diseases. *Int. J. Biol. Sci*. 2012;8(9):1281–1290. DOI: 10.7150/ijbs.4874.
28. Bi H., Zhang Y., Wang S., Fang W., He W., Yin L. et al. Interleukin-8 promotes cell migration via CXCR1 and CXCR2 in liver cancer. *Oncol. Lett*. 2019;18(4):4176–4184. DOI: 10.3892/ol.2019.10735.
29. Hodeib M., Taha G., Mohamed M., Maarek E., Doudar N.A. IL-8 gene expression and bronchial asthma phenotypes in children. *The Egyptian Journal of Immunology*. 2021;28(3):138–144.
30. Hussein Y.M., Shalaby S.M., Mohamed R.H., Hassan T.H. Association between genes encoding components of the IL-10/IL-0 receptor pathway and asthma in children. *Ann. Allergy Asthma Immunol.* 2011;106:474–480. DOI: 10.1016/j.anai.2011.02.021.
31. Saraiva M., Vieira P., O'Garra A. Biology and therapeutic potential of interleukin-10. *J. Exp. Med*. 2020;217(1):e20190418. DOI: 10.1084/jem.20190418.
32. Xie L., Fu Q., Ortega T.M., Zhou L., Rasmussen D., O'Keefe J. et al. Overexpression of IL-10 in C2D macrophages promotes a macrophage phenotypic switch in adipose tissue environments. *PloS One.* 2014;9(1):e86541. DOI: 10.1371/journal.pone.0086541.

Authors' information

Tarabrina Anna A. – Post-Graduate Student, Pediatrics Division with a Childhood Disease Course, General Medicine Department, Siberian State Medical University, Tomsk, Aa.tarabrina@mail.ru, http://orcid.org/0000-0003-1945-3600

Ogorodova Ludmila M. – Dr. Sci. (Med.), Professor, RAS Corresponding Member, Honored Worker of Science of the Russian Federation, Professor of the Pediatrics Division with a Childhood Disease Course, General Medicine Department, Siberian State Medical University, Tomsk, lm-ogorodova@mail.ru, http://orcid.org/0000-0002-2962-1076

Samoilova Iuliia G. – Dr. Sci. (Med.), Professor of the Pediatrics Division with an Endocrinology Course, Siberian State Medical University, Tomsk, samoilova_y@inbox.ru, http://orcid.org/0000-0002-2667-4842

Fedosenko Sergey V. – Dr. Sci. (Med.), Associate Professor, General Medical Practice and Outpatient Therapy Division, Siberian State Medical University, Tomsk, s-fedosenko@mail, http://orcid.org/0000-0001-6655-3300

Fedorova Olga S. – Dr. Sci. (Med.), Vice-Rector for Postgraduate Education and Research, Head of the Pediatrics Division with a Childhood Disease Course, Siberian State Medical University, Tomsk, olga.sergeevna.fedorova@gmail.com, http://orcid.org/0000-0002-7130-9609

Petrov Vyacheslav A. – Cand. Sci. (Med.), Junior Researcher, Center for Research in Biology Bioengineering, Central Research Laboratory, Siberian State Medical University, Tomsk, vyacheslav.a.petrov@mail.ru, http://orcid.org/0000-0002-5205-9739

Podchinenova Daria V. – Cand. Sci. (Med.), Associate Professor, Pediatrics Division with an Endocrinology Course, Siberian State Medical University, Tomsk, darvas_42@mail.ru, http://orcid.org/0000-0001-6212-4568

Boyko Anastasiia S. – Cand. Sci. (Med.), Associate Professor, Researcher, Laboratory for Molecular Genetics and Biochemistry, Mental Health Research Institute, Tomsk NRMC of the Russian Academy of Sciences, Tomsk, anastasya-iv@yandex.ru, http://orcid.org/0000-0002-2955-9057

(✉) **Tarabrina Anna A.,** Aa.tarabrina@mail.ru

Received 30.03.23;
approved after peer review 10.04.2023;
accepted 14.04.2023

УДК 616.345-006-092.19-07:577.112
https://doi.org/10.20538/1682-0363-2023-2-104-110

Prognostic value of the levels of CTLA-4 and its ligand B7.2 in patients with colorectal cancer

Chetveryakov A.V., Tsepelev V.L.

Chita State Medical Academy
39a, Gorkogo Str., Chita, 672000, Russian Federation

ABSTRACT

Aim. To develop a computer program to determine the probability of colorectal cancer based on the assessment of the levels of CTLA-4 and its ligand B7.2.

Materials and methods. The study included 44 patients with colorectal cancer (CRC) and 25 patients with benign tumors of the colon. The control group consisted of 25 individuals who had been operated for colon injury. We determined the levels of CTLA-4 and B7.2 in the blood serum and in the supernatants of tumor tissue and lymph node homogenates using flow cytofluorometry.

Results. We found that the level of CTLA-4 in the blood serum increased by 2.77 times in CRC patients compared to the control group ($p < 0.001$). The concentration of CTLA-4 in the tumor tissue in patients with CRC was 2.34 times higher than in the control group ($p = 0.007$). The concentration of the B7.2 ligand in the blood serum of patients with CRC exceeded this parameter in the control group by 2.51 times ($p = 0.002$). The concentration of B7.2 in the tumor tissue of CRC patients was 1.68 times higher ($p = 0.004$) than in the control group. The analysis of the obtained data determined the parameters that have prognostic value in the structure of the diagnostic model. Using these parameters, we developed a computer program to determine the probability of CRC in the patient.

Conclusion. The data obtained demonstrate an increase in the levels of CTLA-4 and its ligand B7.2 in the serum and tumor tissue of patients with CRC.

Keywords: immune checkpoints, CTLA-4, B7.2, colorectal cancer

Conflict of interest. The authors declare the absence of obvious and potential conflicts of interest related to the publication of this article.

Source of financing. The authors state that they received no funding for the study.

Conformity with the principles of ethics. All patients signed an informed consent to participate in the study. The study was approved by the local Ethics Committee at Chita State Medical Academy (Protocol No. 98 of 27.11.2019).

For citation: Chetveryakov A.V., Tsepelev V.L. Prognostic value of the levels of CTLA-4 and its ligand B7.2 in patients with colorectal cancer. *Bulletin of Siberian Medicine.* 2023;22(2):104–110. https://doi.org/10.20538/1682-0363-2023-2-104-110.

✉ *Chetveryakov Andrey V.,* yasnogorsk94@gmail.com

Прогностическое значение уровня белка CTLA-4 и его лиганда B7.2 у больных раком толстого кишечника

Четверяков А.В., Цепелев В.Л.

Читинская государственная медицинская академия (ЧГМА)
Россия, 672000, г. Чита, ул. Горького, 39а

РЕЗЮМЕ

Цель. Разработать программу для определения вероятности онкологической патологии толстого кишечника на основании оценки уровня белка CTLA-4 и его лиганда B7.2.

Материалы и методы. В исследование включены 44 пациента с колоректальным раком (КРР) и 25 больных с доброкачественными опухолями толстого кишечника. Контрольную группу составили 25 пациентов, оперированных в плановом порядке (пластика колостомы), сформированной ранее по поводу травмы толстой кишки. Концентрацию CTLA-4 и B7.2 определяли в сыворотке крови, а также в супернатантах гомогенатов ткани опухоли и лимфатических узлов с помощью метода проточной цитофлуометрии.

Результаты. Установлено, что у пациентов с раком толстой кишки уровень CTLA-4 в сыворотке крови увеличивается в 2,77 раза в сравнении с группой контроля ($p < 0,001$). Концентрация CTLA-4 в ткани новообразования у пациентов с КРР была выше аналогичного показателя группы контроля в 2,34 раза ($p = 0,007$). Концентрация лиганда B7.2 в сыворотке крови у пациентов с КРР превышала данный показатель в группе контроля в 2,51 раза ($p = 0,002$). Концентрация лиганда B7.2 в ткани опухоли у пациентов с КРР превышала таковую в группе контроля в 1,68 раза ($p = 0,004$). При анализе полученных данных определены параметры, которые имеют значимость в структуре диагностической модели. На основании этих параметров разработана компьютерная программа для определения вероятности наличия онкологической патологии толстого кишечника.

Заключение. Полученные данные демонстрируют увеличение уровня CTLA-4 и его лиганда B7.2 в сыворотке крови и ткани опухоли у пациентов с колоректальным раком.

Ключевые слова: иммунные контрольные точки, CTLA-4, B7.2, колоректальный рак

Конфликт интересов. Авторы декларируют отсутствие явных и потенциальных конфликтов интересов, связанных с публикацией настоящей статьи.

Источник финансирования. Авторы заявляют об отсутствии финансирования при проведении исследования.

Соответствие принципам этики. Все пациенты подписали информированное согласие на участие в исследовании. Исследование одобрено локальным этическим комитетом ЧГМА (протокол № 98 от 27.11.2019).

Для цитирования: Четверяков А.В., Цепелев В.Л. Прогностическое значение уровня белка CTLA-4 и его лиганда B7.2 у больных раком толстого кишечника. *Бюллетень сибирской медицины.* 2023;22(2):104–110. https://doi.org/10.20538/1682-0363-2023-2-104-110.

INTRODUCTION

Colorectal cancer (CRC) is one of the late-diagnosed tumors. Moreover, it ranks third worldwide for mortality among malignant neoplasms [1, 2]. Its ability to escape the immune surveillance plays an essential role in the development and growth of the tumor. To escape the immune surveillance, tumor cells use certain molecular pathways, known as immune checkpoints (ICP) [3, 4]. The main function of ICP is to regulate immune processes and prevent the activated immune system from attacking cells indiscriminately [5]. These data made it possible to develop a new type of targeted immunotherapy for cancer based on blocking ICP [6].

Cytotoxic T-lymphocyte-associated protein 4 (CTLA-4, CD152) is an ICP mainly expressed by T cells [7, 8]. B 7.2 (CD86) is CTLA-4 ligand. The interaction between CTLA-4 and this ligand is an important mechanism in the immunosuppressive regulation of T cell activity [9–11]. The mechanism of this regulation is triggered when CTLA-4 captures B 7.2

from the surface of an antigen-presenting cell (APC) or cancer cell and transfers them into the T lymphocyte via transendocytosis [12]. A number of studies devoted to the analysis of the effectiveness of monoclonal antibodies to CTLA-4 demonstrated objective positive responses in cases of breast cancer, melanoma, and kidney cancer [11]. However, studies confirming the effective use of monoclonal antibodies to CTLA-4 in patients with CRC are insufficient.

The aim of our research was to study the level of CTLA-4 and B7.2 in the blood serum and tumor tissue, as well as to assess the diagnostic value of these parameters in patients with CRC.

MATERIALS AND METHODS

A total of 44 patients with CRC were included in the study. The comparison group consisted of 25 patients with benign neoplasms of the colon who were treated at the Regional Oncology Dispensary in Chita from 2019 to 2020. The control group consisted of 25 patients admitted to the Regional Clinical Hospital for elective surgery (reconstruction of colostomy) due to prior colon injuries. All the patients were examined in accordance with the clinical guidelines approved by the Ministry of Healthcare of Russia [13]. In each case, a patient signed an informed consent. The study was approved by the Ethics Committee of Chita State Medical Academy of the Ministry of Healthcare of the Russian Federation and complied with the requirements of the Declaration of Helsinki of the World Medical Association (2013). Inclusion criteria were a patient's consent to participate in the study and a history of colon tumor. Exclusion criteria were HIV-positive status; autoimmune diseases; viral and bacterial infections; chemotherapy or radiation treatment before surgery.

A histologic examination of tumor tissue specimens showed that 39 CRC patients (88.6%) had moderately differentiated adenocarcinoma (G2). Well differentiated adenocarcinoma (G1) was diagnosed in three cases (6.8%). Two CRC patients (4.6%) had poorly differentiated adenocarcinoma (G3). Six patients had stage I of the disease, 24 patients were diagnosed with stage II. Stages III and IV were diagnosed in eight and six patients, respectively.

Blood sampling was carried out in the morning, 2 hours before the surgery. The day before sampling, patients received standard preoperative medication. Biopsies of the tumor tissue, lymph node tissue, and colon specimens in the control group weighing up to 1 gram were homogenized using the Ultra-Turrax T 10 basic homogenizer (IKA, Germany) in phosphate-buffered saline (pH 7.4). Then they were centrifuged at 5,000 rpm for 10 minutes, and a supernatant was selected. The concentration of CTLA-4 and B7.2 in the blood serum and tissue homogenate supernatant was determined by flow cytofluorometry on the CytoFlex LX analyzer (Beckman Coulter, USA) using the LEGENDplex™ HU multiplex immunoassay panel (Immune Checkpoint, USA) in accordance with the manufacturer's instructions.

In the statistical analysis, we followed the recommendations of the International Committee of Medical Journal Editors (ICMJE) and Statistical Analysis and Methods of Published Literature (SAMPL) Guidelines [14, 15]. Nominal data were described in absolute and relative values. The Pearson's chi-square test ($\chi 2$) was used to compare the nominal data of the study, which allowed to assess the significance of differences between the actual number of outcomes or qualitative characteristics of the sample falling into each category and the theoretical number that can be expected in the studied groups if the null hypothesis is valid [16].

As the number of participants in the study groups was less than 50, we used the Shapiro – Wilk test to assess the normality of the distribution of quantitative variables. Taking into account that the distribution of characteristics in all groups was different from normal, the data obtained were presented in as the median and the interquartile range Me [Q_1; Q_3]. The Kruskal – Wallis H test was performed to compare three independent groups in terms of one quantitative characteristic. If there were statistically significant differences, a pairwise comparison was performed using the Mann – Whitney U test with the Bonferroni correction [17]. The Spearman's rank correlation coefficient was used to measure correlations between the studied parameters. The strength of the relationship between the studied parameters was determined by the Chaddock scale [18].

The diagnostic model was constructed by binary logistic regression. To determine the value of the model, we applied the ROC analysis, which made it possible to assess the sensitivity, specificity, and accuracy of the model. Statistical processing of the research results was carried out using the IBM SPSS Statistics Version 25.0 software package (International Business Machines Corporation, USA).

RESULTS

We found that the level of CTLA-4 in the blood serum in CRC patients increased by 2.77 times compared to the control group ($U = 119.0$, $p < 0.001$). There were

no significant differences in the level of CTLA-4 in the blood serum of CRC patients and those with benign tumors of the colon (Table 1). The data obtained indicate that an increase in the concentration of CTLA-4 in the blood serum may be a marker of a colon tumor, but it does not allow to determine its nature.

Table 1

CTLA-4 level in patients with colon tumor, pg / ml, *Me* [Q_1; Q_3]

Parameter	Group			Test statistics, df = 2
	Control group, *n* = 25	Benign tumor, *n* = 25	Colorectal cancer, *n* = 44	
Blood serum	4.88 [4.38; 6.22]	10.48 [10.30; 14.50]	13.50 [13.07; 20.80]	$H = 34.26$, $p < 0.001$
Tumor tissue	6.06 [6.03; 8.40]	9.42 [8.84; 11.37]	14.17 [13.72; 27.28]	$H = 8.82$, $p = 0.012$

Note: *H* – the Kruskal–Wallis *H* test, *p* – the achieved level of significance (here and in Table 2).

Similar changes were observed in the study of the CTLA-4 concentration in the tumor tissue. The level of CTLA-4 in the tumor tissue was 2.34 times higher in CRC patients compared to the control group ($U = 334.0$; $p = 0.007$). This parameter in CRC patients was 1.5 times higher than in patients with benign colon tumors ($U = 371.0$; $p = 0.02$) (Table 1). The results obtained allowed to note that an increase in the CTLA-4 concentration was associated with the nature of the tumor. However, these statistically significant data are of no practical interest, since a histologic examination of the obtained material can determine the nature of a neoplasm.

The concentration of the B7.2 ligand in the blood serum of CRC patients was 2.51 times higher than in the control group ($U = 302.5$; $p = 0.002$). We also found that the levels of B7.2 in the blood serum of patients with colon cancer and patients with benign colon tumors had no statistically significant differences (Table 2).

Table 2

B7.2 level in patients with colon neoplasms, pg / ml, *Me* [Q_1; Q_3]

Parameter	Group			Test statistics, df = 2
	Control group, *n* = 25	Benign tumor, *n* = 25	Colorectal cancer, *n* = 44	
Blood serum	33.00 [30.08; 40.11]	79.00 [78.68; 97.46]	82.93 [76.70; 113.26]	$H = 23.08$, $p < 0.001$
Tumor tissue	37.09 [34.11; 44.34]	40.40 [43.36; 48.90]	62.31 [61.74; 79.93]	$H = 9.96$, $p = 0.007$

The data obtained demonstrate an increase in the concentration of B7.2 in patients with colon tumors. However, it is impossible to differentiate between a benign and a malignant tumor by analyzing the concentration of this biological marker.

A similar increase in the parameters was noted in the tumor tissue. The concentration of the B7.2 ligand in the tissue in CRC patients was 1.68 times higher than in the control group ($U = 319.0$; $p = 0.004$). The level of B7.2 in CRC patients was 1.54 times higher than in patients with benign colon tumor ($U = 387.0$; $p = 0.04$) (Table 2). The concentration of the B7.2 ligand was increased in the tumor tissue, as was the CTLA-4 level in the tissue. The data obtained allow to differentiate between a benign and a malignant neoplasm in the colon.

We determined the concentration of CTLA-4 and B7.2 in the tissue of regional lymph nodes in CRC patients. The level of CTLA-4 in the lymph node tissue was 132.22 [117.36; 174.40] pg / ml; the concentration of B7.2 was 537.35 [466.76; 650.84] pg / ml.

The analysis of the data obtained indicated that the level of CTLA-4 in the blood serum had a moderate correlation with the level of CTLA-4 in the tissue ($\rho = 0.37$; $p < 0.01$). No statistically significant correlations were found for B7.2 ligand. The level of B7.2 in the blood serum did not correlate with its level in the tumor tissue ($\rho = 0.008$; $p = 0.94$). At the same time, a pronounced correlation was revealed between the levels of CTLA-4 and B7.2 in the blood serum ($\rho = 0.57$; $p < 0.01$). At the same time, there was a weak direct correlation between the described membrane molecules in the tissue ($\rho = 0.28$; $p = 0.004$), which confirmed the role of B7.2 as a ligand for CTLA-4, and not as a separate biomarker.

When analyzing the data, we identified parameters that may be essential in the diagnostic model for determining the probability of cancer (Table 3) and obtained the following equation:

Table 3

Value of CTLA-4 and B7.2 in the structure of the diagnostic model

Parameter	B	Root mean square error	Wald test	Degree of freedom, df	Significance, p	Exp (B)	95% CI for Exp B
CTLA-4 in the blood serum	0.42	0.132	9.98	1	0.002	1.52	1.17–1.96
B7.2 in the blood serum	0.03	0.013	3.78	1	0.05	1.03	1.01–1.05
Constant	–3.25	0.968	11.28	1	0.001	0.04	–

Note: CI – confidence interval.

$$C = \frac{1}{1+e^{3,25-0,42*CTLA4ser-0,03*B7.2ser}},$$

where CTLA-4ser is the level of the CTLA-4 protein in the blood serum; B7.2ser is the level of B7.2 in the blood serum; 3.25 is the constant of the logistic regression level; 0.42 and 0.03 are non-standardized B coefficients, e-exponent ~ 2.72. When the coefficient C is ≥ 0.59, the development of a tumor in the colon is diagnosed. In the control group, this parameter (C) was 0.40 [0.36; 0.50], it was 0.86 in the patients with cancer [0.82; 0.87]. The controls were found to have C ≥ 0.59 in 20% of cases (5 / 25), CRC patients had C ≥ 0.59 in 94.2% (65 / 69) of cases (Sensitivity of this conclusion is 0.94, specificity and accuracy are 0.80 and 0.90, respectively (AUC = 0.88 [95% CI 0.79–0.97], $p < 0.001$) (Figure).

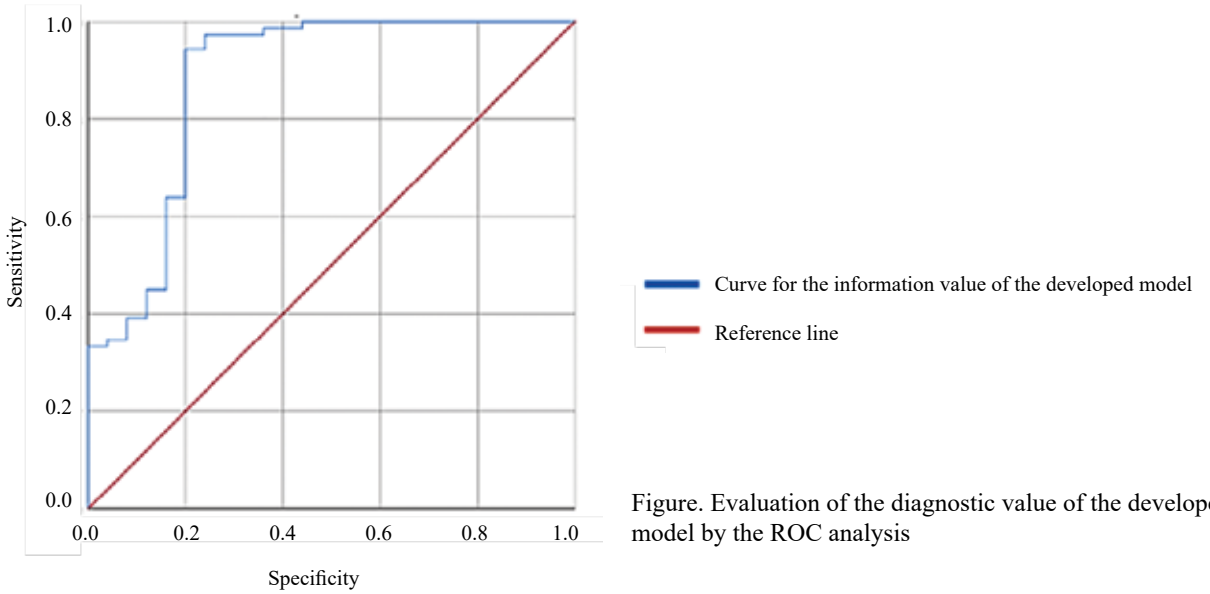

Figure. Evaluation of the diagnostic value of the developed model by the ROC analysis

The described method can be used in both outpatient departments and surgical hospitals to predict the presence of cancer in the colon. We developed a program for the Windows-based Object Pascal development environment (Borland Delphi) to simplify the method when used in clinical practice. A set of actions is created in a special mode of the user window, in which the user gets access to entering data on the level of CTLA-4 (pg / ml) and its B7.2 ligand in the blood serum (pg / ml) in patients with complaints of functional intestinal disorders. The program is applicable and provides an opportunity to determine the probability of cancer in the colon, which makes it possible to identify a risk group and optimize the strategy for their examination and treatment [19].

DISCUSSION

We found that the levels of CTLA-4 and B7.2 increased in the blood serum of CRC patients. There were no significant differences between the concentrations of CTLA-4 and B7.2 in the blood serum of CRC patients and patients with benign intestinal neoplasms. The data obtained demonstrate that an increase in the level of CTLA-4 and B7.2 indicates the presence of a colon tumor, but it is impossible to determine whether it is malignant or benign.

Similar changes in their concentration were observed in the study of these markers in the tumor tissue. The levels of CTLA-4 and B7.2 in the tumor tissue in CRC patients were higher than in the control

group. In addition, the concentration of these markers in CRC patients was increased in comparison with patients with a benign colon tumor.

We also determined cut-off values for CTLA-4 and B7.2 markers in the blood serum, which are significant in the structure of the diagnostic model. The developed computer program makes it possible to suspect a colon tumor, which will allow to form risk groups and optimize the examination strategy.

Similar data on high CTLA-4 expression in the tumor tissue were obtained in patients with breast cancer and cholangiocarcinoma [20, 21]. This fact indicates that the presence of CTLA-4 in the tumor microenvironment is one of the markers of immune suppression development, which contributes to the growth and spread of tumor cells. We believe that the CTLA-4 protein is an important link in the pathogenesis of cancer cells escaping from the immune surveillance. X.J. Guo (2021) discussed the role of the CTLA-4 protein in the activation of regulatory T cells (Treg), which are the strongest inhibitors of the immune response [21]. Therefore, the role of CTLA-4 in the activation of regulatory T cells in malignant neoplasms of various localizations requires further comprehensive studies.

CONCLUSION

The data obtained demonstrate an increase in the levels of CTLA-4 and B7.2 in the blood serum and tumor tissue in CRC patients, as well as their direct correlation with each other. Thus, we suppose that these proteins are essential in the pathogenesis of cancer cells escaping from immune surveillance in colon cancer. Based on the established patterns, we developed a computer program to determine the probability of colon cancer in the patient.

REFERENCES

1. Bray F., Ferlay J., Soerjomataram I., Siegel R.L., Torre L.A., Jemal A. Global cancer statistics 2018: GLOBOCAN estimates of incidence and mortality worldwide for 36 cancers in 185 countries. *CA Cancer J. Clin*. 2018;68(6):394–424. DOI: 10.3322/caac.21492.
2. Siegel R.L., Miller K.D., Fedewa S.A., Ahnen D.J., Meester R.G.S., Barzi A. et al. Colorectal cancer statistics. *CA Cancer J. Clin.* 2017;67(3):177–193. DOI: 10.3322/caac.21395.
3. Zhu Y., Hu Y., Kong X., Xiao Q., Pan Z., Zheng Z. et al. Cohort profile: The National Colorectal Cancer Cohort (NCRCC) study in China. *BMJ Open*. 2021;11(12):e051397. DOI: 10.1136/bmjopen-2021-051397.
4. Zhu S., Yi M., Wu Y., Dong B., Wu K., Zhu S. Roles of tumor-associated macrophages in tumor progression: implications on therapeutic strategies. *Exp. Hematol. Oncol*. 2021;10(1):60. DOI: 10.1186/s40164-021-00252-z.
5. Eptaminitaki G.C., Wolff N., Stellas D., Sifakis K., Baritaki S. Long non-coding RNAs (lncRNAs) in response and resistance to cancer immunosurveillance and immunotherapy. *Cells*. 2021;10(12):3313. DOI: 10.3390/cells10123313.
6. Prakadan S.M., Alvarez-Breckenridge C.A., Markson S.C., Kim A.E., Klein R.H., Nayyar N. et al. Genomic and transcriptomic correlates of immunotherapy response within the tumor microenvironment of leptomeningeal metastases. *Nat. Commun*. 2021;12(1):5955. DOI: 10.1038/s41467-021-25860-5.
7. Feng Y., Liu L., Li J., Huang J., Xie J.H., Menard L. et al. Systematic characterization of the tumor microenvironment in Chinese patients with hepatocellular carcinoma highlights intratumoral B cells as a potential immunotherapy target. *Oncol. Rep*. 2022;47(2):38. DOI: 10.3892/or.2021.8249.
8. Yin J., Wang H., Hong Y., Ren A., Wang H., Liu L. et al. Identification of an at-risk subpopulation with high immune infiltration based on the peroxisome pathway and TIM3 in colorectal cancer. *BMC Cancer.* 2022;22(1):44. DOI: 10.1186/s12885-021-09085-9.
9. Sharma P., Allison J.P. The future of immune checkpoint therapy. *Science*. 2015;348(6230):56–61. DOI: 10.1126/science.aaa8172.
10. Shapoval A.I., Shapoval S.P., Shcherbakova N.S., Shcherbakov D.N. Immune control Molecules of the B7 family. Part 1. General characteristics and first representatives: b7-1, b7-2, b7-h1, b7-h2 and b7-dc. *Russian Journal of Bioorganic Chemistry*. 2019;45(4):348–364. DOI: 10.1134/S1068162019040101.
11. Rowshanravan B., Halliday N., Sansom D.M. CTLA-4: a moving target in immunotherapy. *Blood.* 2018;131(1):58–67. DOI: 10.1182/blood-2017-06-741033.
12. Borrie A.E., Maleki Vareki S. T lymphocyte-based cancer immunotherapeutics. *Int. Rev. Cell. Mol. Biol*. 2018;341:201–276. DOI: 10.1016/bs.ircmb.2018.05.010.
13. All-Russian National Union "Association of Oncologists of Russia". Malignant neoplasms of the colon and rectosigmoid area. Clinical guidelines. Moscow, 2020:70 (in Russ.).
14. Alshogran O.Y., Al-Delaimy W.K. Understanding of international committee of medical journal editor's authorship criteria among faculty members of pharmacy and other health sciences in Jordan. *J. Empir. Res. Hum. Res. Ethics*. 2018;13(3):276–284. DOI: 10.1177/15562646187 64575.
15. Lang T.A., Altman D.G. Basic statistical reporting for articles published in biomedical journals: the "Statistical analyses and methods in the published literature" or the SAMPL guidelines. *Int. J. Nurs. Stud*. 2015;52(1):5–9. DOI: 10.1016/j.ijnurstu.2014.09.006.
16. Mudrov V.A. Statistical analysis algorithms of quantitative features in biomedical research using the SPSS software package. *The Transbaikalian Medical Bulletin*. 2020;1:140–150 (in Russ.). DOI: 10.52485/19986173_2020_1_140.
17. Mudrov V.A. Statistical analysis algorithms of quantitative features in biomedical research using the SPSS software package. *The Transbaikalian Medical Bulletin*. 2020;1:151–163 (in Russ.). DOI: 10.52485/19986173_2020_1_151.
18. Mudrov V.A. Algorithms for correlation analysis of data in biomedical research using the SPSS software package. *The Transbaikalian Medical Bulletin.* 2020;2:169–176 (in Russ.). DOI: 10.52485/19986173_2020_2_169.

19. Chetveryakov A.V., Tsepelev V.L., Kryukova V.V., Mudrov V.A. A program for determining the probability of oncological pathology of the large intestine. Chita State Medical Academy of the Ministry of Healthcare of Russia (in Russ.). URL: https://new.fips.ru/ofpstorage/Doc/PrEVM/RUNWPR /000/002/022/613/721/2022613721-00001/document.pdf.
20. Bagbudar S., Karanlik H., Cabioglu N., Bayram A., Ibis K., Aydin E. et al. Prognostic implications of immune infiltrates in the breast cancer microenvironment: the role of expressions of CTLA-4, PD-1, and LAG-3. *Appl. Immunohistochem. Mol. Morphol.* 2022;30(2): 99–107. DOI: 10.1097/PAI.0000000000000978.
21. Guo X.J., Lu J.C., Zeng H.Y., Zhou R., Sun Q.M., Yang G.H. et al. CTLA-4 synergizes with PD1/PD-L1 in the inhibitory tumor microenvironment of intrahepatic cholangiocarcinoma. *Front. Immunol*. 2021;12:705378. DOI: 10.3389/fimmu.2021.705378.

Authors' information

Chetveryakov Andrey V. – Surgeon, Post-Graduate Student, Department of Hospital Surgery, Chita State Medical Academy, Chita, yasnogorsk94@gmail.com.

Tsepelev Viktor L. – Dr. Sci. (Med.), Professor, Head of the Department of Hospital Surgery, Chita State Medical Academy, Chita, viktorcepelev@mail.ru.

(✉) **Chetveryakov Andrey V.,** yasnogorsk94@gmail.com

Received 04.05.2022;
approved after peer review 24.06.2022;
accepted 08.12.2022

УДК 616.5-002-097:577.112:576.5:576.385.5
https://doi.org/10.20538/1682-0363-2023-2-111-121

Inflammasome as an early pathophysiological phenomenon of inflammation in skin diseases and other pathologies

Klimov V.V.[1], Zagreshenko D.S.[2], Urazova O.I.[1], Klimov A.V.[1], Naidina O.A.[1], Tsyplina E.Yu.[1], Kologrivova E.N.[1], Koshovkina T.V.[1], Koshkarova N.S.[1]

[1] Siberian State Medical University
2, Moscow Trakt, Tomsk, 634050, Russian Federation,

[2] Novokuznetsk State Institute for Advanced Training of Doctors – branch of the Russian Medical Academy for Continuing Professional Education
2, Stroiteley Av., Novokuznetsk, 654005, Russian Federation

ABSTRACT

The review considers the molecular structure of inflammasomes, routes of inflammasome activation, appropriate downstream effects, and their association with autoinflammatory, autoimmune, neurodegenerative, and allergic diseases and malignancies with a focus on the involvement of the skin in these pathologies. Inflammasome activation is interpreted as an early pathophysiological event before the onset of inflammation, and, especially, if inflammasome dysregulation occurs. All research aspects related to the NLRP3 inflammasome are described in detail. The review also considers promising directions for therapeutic interventions in NLRP3-associated diseases.

Keywords: inflammasome, NLRP3, AIM2, myeloid cells, keratinocytes, pattern recognition receptors, signaling, caspases, IL-1β, IL-18, IL-33, pyroptosis, inflammaging, skin diseases

Conflict of interest. The authors declare the absence of obvious and potential conflicts of interest related to the publication of this article.

Source of financing. The authors state that they received no funding for the study.

Для цитирования: Klimov V.V., Zagreshenko D.S., Urazova O.I., Klimov A.V., Naidina O.A., Tsyplina E.Yu., Kologrivova E.N., Koshovkina T.V., Koshkarova N.S. Inflammasome as an early pathophysiological phenomenon of inflammation in skin diseases and other pathologies. *Бюллетень сибирской медицины.* 2023;22(2):111–121. https://doi.org/10.20538/1682-0363-2023-2-111-121.

Инфламмасома как ранний патофизиологический феномен воспалительного процесса при болезнях кожи и других патологиях

Климов В.В.[1], Загрешенко Д.С.[2], Уразова О.И.[1], Климов А.В.[1], Найдина О.А.[1], Цыплина Е.Ю.[1], Кологривова Е.Н.[1], Кошовкина Т.В.[1], Кошкарова Н.С.[1]

[1] Сибирский государственный медицинский университет (СибГМУ)
Россия, 634050, г. Томск, Московский тракт, 2

✉ *Klimov Vladimir V.,* klimov@mail.tomsknet.ru

[2] *Новокузнецкий государственный институт усовершенствования врачей (НГИУВ) – филиал Российской медицинской академии непрерывного профессионального образования (РМАНПО) Россия, 654005, г. Новокузнецк, пр. Строителей, 5*

РЕЗЮМЕ

В обзоре рассмотрены молекулярная структура, последовательность, пути активации инфламмасом, варианты нисходящих эффектов и их связь с аутовоспалительными, аутоиммунными, нейродегенеративными, аллергическими и злокачественными патологиями, с фокусом на вовлечение кожи в патологический процесс. Дана интерпретация инфламмасом как раннего патофизиологического события перед началом воспалительного процесса и возможные варианты нарушения регуляции их функционирования. Более подробно описаны все аспекты исследований, относящихся к инфламмасоме NLRP3. Приведены данные по имеющимся и перспективным направлениям терапевтических интервенций при NLRP3-ассоциированных болезнях.

Ключевые слова: инфламмасома, NLRP3, AIM2, миелоидные клетки, кератиноциты, паттерн-распознающие рецепторы, сигнальная трансдукция, каспазы, IL-1β, IL-18, IL-33, пироптоз, старение клетки в связи с воспалением, кожные болезни

Конфликт интересов. Авторы декларируют отсутствие явных и потенциальных конфликтов интересов, связанных с публикацией настоящей статьи.

Источник финансирования. Авторы заявляют об отсутствии финансирования при проведении исследования.

Для цитирования: Климов В.В., Загрешенко Д.С., Уразова О.И., Климов А.В., Найдина О.А., Цыплина Е.Ю., Кологривова Е.Н., Кошовкина Т.В., Кошкарова Н.С. Инфламмасома как ранний патофизиологический феномен воспалительного процесса при болезнях кожи и других патологиях. *Бюллетень сибирской медицины.* 2023;22(2):111–121. https://doi.org/10.20538/1682-0363-2023-2-111-121.

INTRODUCTION

The skin is the largest barrier organ of the body in the face of environmental microbes, allergens, and multiple dangerous chemical and physical factors [1, 2]. The skin consists of epidermis and dermis, whereas the epidermis is subdivided into cornified, granular, spinous, clear, and basal layers. Some researchers do not differentiate stratum lucidum (a clear layer) as a separate layer of the epidermis. Many skin cells, including keratinocytes, Langerhans cells, intraepithelial CD8αα+ T lymphocytes, NK cells, innate lymphoid cells (ILC), macrophages, mast cells, eosinophils, neutrophils, and memory T cells, are related to the immune system and, in fact, represent its secondary organ [2, 3].

Most of them express pattern recognition receptors, such as Toll-like receptors (TLRs), NOD-like receptors (NLRs), RIG-I-like receptors (RLRs), and AIM2-like receptors (ALRs), to sense pathogen-associated molecular patterns (PAMPs), damage-associated molecular patterns (DAMPs) [1, 4], and allergens [5]. Keratinocytes undergo differentiation during keratinization, which is an essential innate immunity mechanism. Lymphocytes (90%) along with some other cells (10%) are structured in the skin-associated lymphoid tissue (SALT). The skin also contains melanocytes and fibroblasts [3]. Inflamed skin contains a variety of cells (Fig. 1)., including many cells of the immune system. Keratinocytes, dendritic cells, neutrophils, macrophages, and fibroblasts can serve as container cells for inflammasomes. A new transcriptomic technology, single-cell RNA sequencing, described skin cell landscape in some skin diseases [6, 7].

The inflammasome is an early phenomenon of inflammation under a harmful effect and refers to innate immunity mechanisms. Structurally, any inflammasome represents a high-molecular-weight protein complex located in the cytosol and containing pattern recognition receptors, signaling molecules (including ASC Speck [8, 9]), enzymes (including caspases [10]), and other components [1, 2, 11].

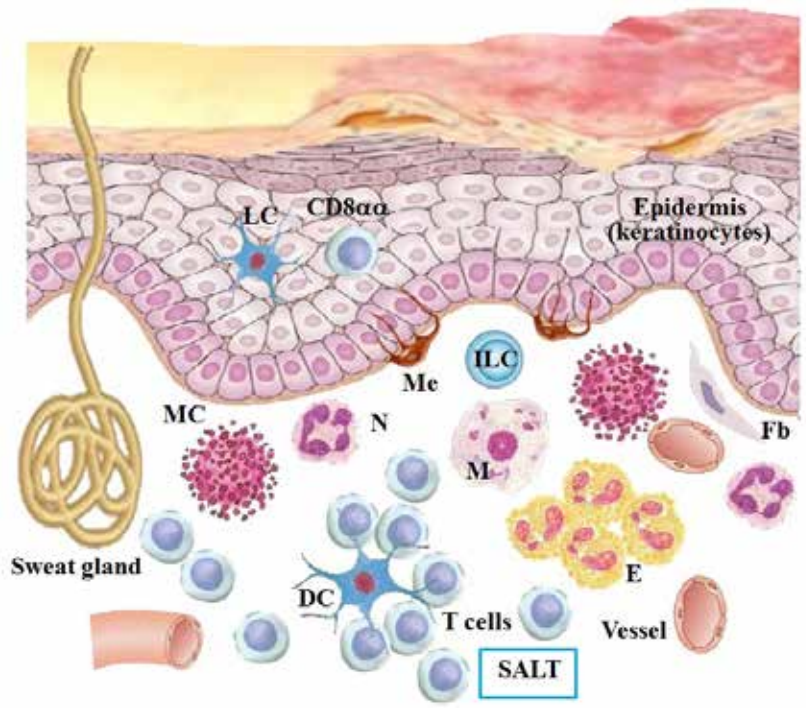

Fig.1. Cells of the inflamed skin: SALT – skin-associated lymphoid tissue, LC – Langerhans cell, CD8αα – γδT cell with CD8αα+ phenotype, ILC – innate lymphoid cell, MC – mast cell, N – neutrophil, Me – melanocyte, M – macrophage, Fb – fibroblast, E – eosinophil, DC – dendritic cell

INFLAMMASOME STRUCTURE, ACTIVATION, FUNCTIONING, AND REGULATION

The inflammasome was first described in 2002 by F. Martinon et al. [12]. Nowadays, about twenty different inflammasomes (NLRP1-NLRP14, NLCR4/NAIP, AIM2, IFI16, CARD8, and PYRIN) have been identified [4, 11]. Their components belong to different families (NLR, ALR, and PYRIN), which recognize different molecular patterns. For example, the NLR family is subdivided into five subfamilies (NLRA, NLRB, NLRC, NLRP, and NLRX) and has up to 23 members in total [4, 13]. In the skin, myeloid cells, keratinocytes, and fibroblasts can serve as main container cells for inflammasomes [4, 14]. Over the past 20 years, inflammasomes in myeloid cells have been characterized in detail, however, inflammasomes contained in non-myeloid cells, such as keratinocytes and fibroblasts, have been described to a lesser extent.

The functioning of inflammasomes implies a downstream effect, such as development of inflammation due to proinflammatory cytokines with or without cell death. For this, an inflammasome has to be activated and assembled. Inflammasome activation proceeds in four key steps [1]:

(1) *priming* – expression of the main inflammasome components and inactive cytokine forms after molecular pattern recognition by TLRs;

(2) *sensing* or recognition of additional activation signals by NLRs or other pattern recognition receptors in the cytosol;

(3) *oligomerization* – assembly of the inflammasome as a high molecular mass multimeric complex;

(4) *final activation* of caspases that results in cytokine secretion through membrane pores and promotion of pyroptosis and possible different types of cell death [15–17].

Depending on the activation route, all inflammasomes are divided into canonical and non-canonical [2, 18–20]. Canonical activation of the LRP3 inflammasome is implemented by two consecutive signal groups. Initially, the first group of impulses go from PAMP / TLR or DAMP / TLR couples and interleukin (IL)-1β, TNF /their receptor couples, which leads to expression of genes encoding inactive pro-IL-1β, pro-IL-18, pro-IL-33, and components of a future inflammasome. After that, the second activation signals arise from many sources and lead to the inflammasome assembly when caspases like caspase-1 enzymatically activate immature forms of IL-1β, IL-

18, and IL-33 before their secretion [11, 20, 21] and promote a cell death mechanism like pyroptosis [18]. A non-canonical activation route is mediated by direct binding of PAMP or DAMP to caspase-4 or caspase-5 [11, 18, 22]. Unfortunately, descriptions of signaling pathways made by various researchers are quite controversial.

In canonical activation, PAMP and DAMP molecular patterns are recognized by TLRs expressed on the cell surfaces or located in endosomes. Next, TLR signaling is triggered which involves adaptor proteins MyD88 and TRIF. Also, external cytokines TNF and IL-1 are sensed by appropriate cytokine receptors to take part in the same pathway. After that, transcription factors AP-1, NF-κB, and IRF-3 stimulate expression of genes encoding components related to a future inflammasome and its proinflammatory cytokines [1, 3, 18, 23].

So, the first step (priming) is over. As a result of the next steps, some upstream signaling events occur, including K+ efflux, Ca++ influx, Cl^- efflux, lysosomal disruption, mitochondrion-derived reactive oxygen species (ROS) generation, and release of oxidized mitochondrial DNA. During oligomerization, the NLRP inflammasome is assembled as a high molecular weight complex. In the fourth step, the formed NLRP inflammasome activates caspase-1 to cleave pro-IL-1β, pro-IL-18, and pro- IL-33, as well as a pore-forming protein gasdermin D that promotes pyroptosis and leads to membrane pore formation. Through the pores, cytokines are released outside [14, 18, 21]. More information about the canonical activation route is presented in Fig. 2.

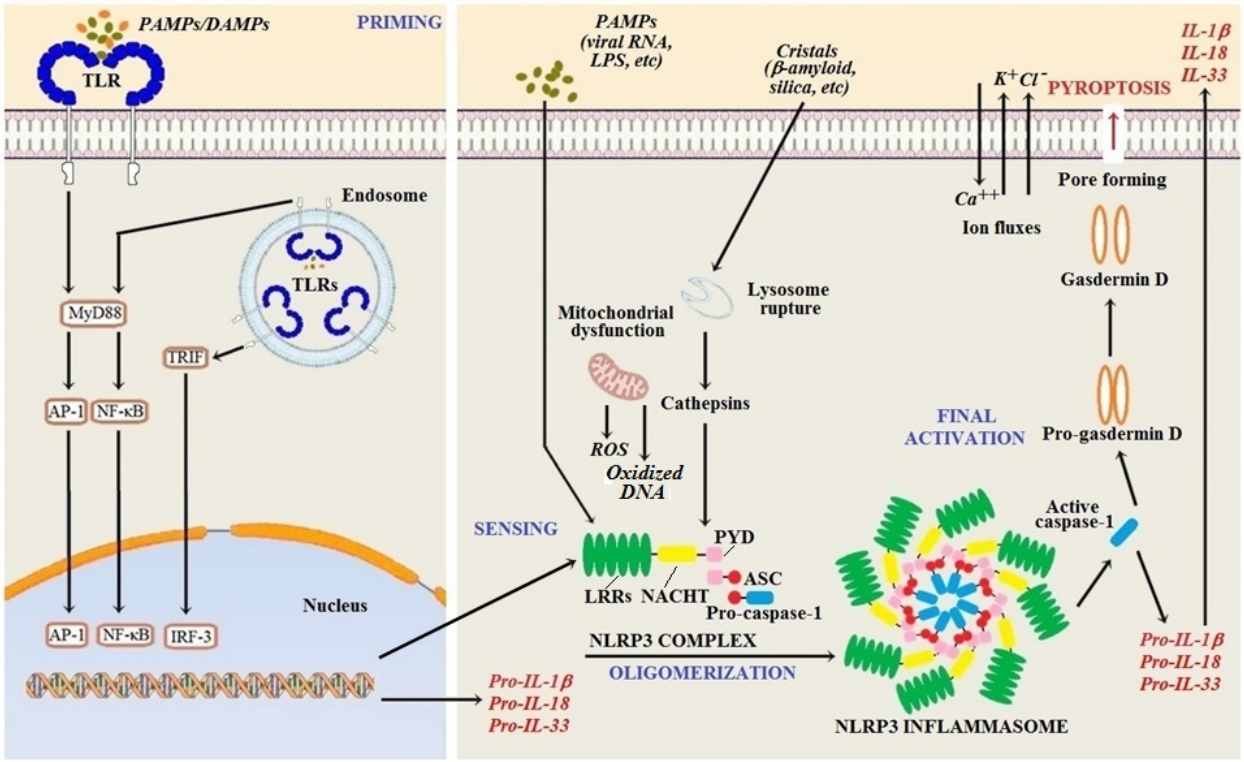

Fig. 2. The canonical inflammasome activation route on the example of NLRP3: TLR – Toll-like receptor, LPS – lipopolysaccharide, MyD88, TRIF, ASC – adaptor proteins, AP-1, NF-κB, IRF-3 – transcription factors, LRR, NACHT, PYD – NLRP3 domains, IL-1β, – interleukin-1β,, IL-18 – interleukin-18, IL-33 – interleukin-33, ROS – reactive oxygen species

Priming, sensing, oligomerization, and final activation are the four steps of the canonical NLRP3 inflammasome activation route. After PAMPs and DAMPs are recognized by TLRs expressed on a container cell, the cell generates immature forms of IL-1β, IL-18, and IL-33, and inactive components of the NLRP3 complex. The NLRP3 complex consists of 1) leucine-rich repeats (LRRs), 2) central NACHT domain, 3) pyrin domain (PYD), 4) apoptosis-associated speck-like (ASC) protein, and 5) pro-caspase-1. The NLRP3 complex is committed to sense signals, including those of PAMPs, cathepsins, ion fluxes, and ROS, required for NLRP3 inflammasome assembly. Eventually, active caspase-1 upregulates the production of membrane pore-forming gasdermin D that leads to pyroptosis. Also, caspase-1 cleaves cyto-

kine pro-forms, which become active secreted IL-1β, IL-18, and IL-33. Here, the early pathophysiological event preceding inflammation completes. Not all the details of the NLRP3 inflammasome activation are presented in Fig. 2.

In non-canonical activation, lipopolysaccharide (LPS) in Gram-negative bacterial infection, is recognized by TLR4 that leads to type I interferon (IFN) upregulation and then expression of GTPases (including IFN-induced GTP-ase IRGB10) and guanylate-binding proteins (GBPs). They destroy intracellular bacteria and promote release of LPS into the cytosol [24]. The cytosolic LPS activates caspase-4 and caspase-5. Subsequently, caspases cleave gasdermin D to induce pyroptosis. In parallel, caspase-1 upregulates the conversion of pro-IL-1β to a secreted IL-1β form [14, 18, 23].

In addition, an alternative inflammasome activation route was described [1, 23, 25] which enables the secretion of cytokines without gasdermin D involvement and pyroptosis induction. In response to LPS that proceeds in the absence of other activation signals, the TRIF-RIPK1-FADD-caspase-8 complex triggers this activation route.

The functioning of any inflammasome is a well-regulated process [4, 18, 20, 26]. It is crucial to establish the optimal balance between inflammasome activation and inhibition. Due to differences in the structures and molecules of inflammasome sensors, different inflammasomes are regulated by different mechanisms [20]. Depending on polarization control, inflammasome can be canonical and non-canonical [11, 18, 20, 23], proinflammatory and anti-inflammatory [4], and protumoral and anti-tumoral [11].

Paradoxically, NLRP10 and NLRP12 inflammasomes downregulate caspase-1, and NLRP6 and NLRP7 inhibit IL-1β, manifesting anti-inflammatory properties. However, NLRP10 and NLRP12 are known to be associated with atopic dermatitis [4]. In cancer, the functioning of various inflammasomes is contradictory. On the one hand, inflammasomes take part in upregulating anti-tumor immunity, but, on the other hand, they can directly contribute to pathological tolerance or promote tumor cell survival, proliferation, and metastasis [11].

Appropriate inflammasome activation is a physiological event for the body to protect against environmental and its own reactivated microbes using innate immunity mechanisms. However, aberrant inflammasome activation can cause uncontrolled cell death and damage to healthy tissues that may contribute to various disorders, particularly autoinflammatory, neurodegenerative, and cardiometabolic diseases, and cancer [20].

PYROPTOSIS, APOPTOSIS, NECROPTOSIS, AND PANOPTOSIS

Nowadays, our understanding of the types and mechanisms of cell death and its effects on the functioning of the whole body has increased significantly; some pathways of programmed cell death have been described in current research: apoptosis [27, 28], pyroptosis [18, 27], necroptosis [16, 27], and PANoptosis [15]. In addition, NETosis and ferroptosis are known [27]. Cell death has both physiological and pathological features. For example, clonal deletion of T lymphocytes in the thymus, selection of B lymphocytes in the bone marrow, and embryonic development are physiological processes required for the body; conversely, death of numerous cells during chronic inflammation and tissue damage is an absolutely pathological event [28].

Apoptosis is commonly a non-inflammatory event, but in case when acute inflammation prolongs and efferocytosis of apoptotic cells is delayed, *late apoptosis*, a lytic form of cell death, occurs [27]. Apoptosis-related conditions and specific features, including wound healing in space and molecular mechanisms of apoptosome assembly in both extrinsic and intrinsic apoptosis, are well-known and described in some review articles [27, 29].

Pyroptosis is described as inflammasome-dependent programmed cell death, which is implemented by gasdermin family members at the last step of inflammasome activation. It is characterized by cell swelling, early cytoplasm membrane rupture, and nuclear condensation. Release of cell content into the extracellular space upregulates both inflammatory and repair processes [18, 27].

Necroptosis is the most unfavorable programmed cell death type for organs and tissues. It contributes to the pathogenesis of many severe disorders (toxic epidermal necrolysis, acute pancreatitis, neurodegenerative diseases, complications of cardiovascular pathologies, etc.). When apoptosis signaling is blocked, necroptotic pathways are activated, and caspase-8, PIP1 / PIP3 kinases, and MLKL pseudokinase are upregulated [16, 28]. So far, the precise mechanism of the necroptosome assembly is not entirely clear.

PANoptosis is a newly described programmed cell death type implemented by a recently identified cytoplasmic multimeric protein complex termed the

PANoptosome. At the same time, the PANoptosome can involve three key modalities of programmed cell death, such as pyroptosis, apoptosis, and necroptosis [15]. Although the PANoptosome incorporates fundamentally distinct mechanisms of cell death, in fact, PANoptosis is a combined inflammatory cell death pathway. Expressed PANoptosome components are associated with autoinflammatory, autoimmune, and neurodegenerative diseases, and many cancer types [15].

INFLAMMAGING

There are many environmental factors affecting the skin and cells of the immune system in the skin and other barrier organs. Some of these factors can be harmful, represent danger signals, and, at least, induce inflammasome formation or skin inflammation.

In an experiment on NLRP1 and NLRP3 inflammasomes, normal human epidermal keratinocytes were exposed to UVB (ultraviolet B) radiation and adenosine triphosphate (ATP), which resulted in release of caspase-1, whereas the bacterial toxin nigericin and urban dust did not exert such an effect [30]. In another experiment, it was described that cigarette smoke extract increased the caspase-1 activity via the NLRP3-independent and TLR4-TRIF-caspase-8-dependent pathway. Simultaneously, it inhibited the expression of the NLRP3 inflammasome and release of IL-1β and IL-18, acting at the transcriptional level [31].

Solar UVB radiation is a major challenge for the skin, which can induce inflammation, cell aging, and even skin cancer. Upon inflammasome activation, the secretion of proinflammatory cytokines and pyroptosis occur. Using the CRISPR / Cas9 protocol with regard to human primary keratinocytes, it was reported that NLRP1 plays a more important role in UVB sensing and subsequent IL-1β and IL-18 secretion than NLRP3 [32]. Other signals apart from pattern recognition receptors are required for NLRP3 formation and caspase-1 activation; they are signals from ATP, nigericin, uric acid crystals, or asbestos. UVB and nigericin are known as inflammasome activators in myeloid cells and keratinocytes, because they both promote IL-1β secretion only in the presence of ASC and NLRP1, whereas knocking out NLRP3 does not impact IL-1β release [33].

In general, the influence of harmful factors on the skin results in development of chronic low-grade subclinical inflammation or *inflammaging* [34]. This phenomenon is associated with a combination of environmental and genetic factors, which can include accumulation of persistent senescent cells and cellular memory formed by epigenetic modifications of the genome [35]. Based on the experiments using cell cultures and laboratory animals, it has been reported that cellular senescence is greatly dependent on the tumor suppressive protein p53 and caspase-4 (caspase-8 in mice) non-canonical pathway triggered by stress and cytoplasmic LPS [22, 36].

If persons already suffer from atopic dermatitis, psoriasis, and acne, exposure to air and contact pollutants and UVB leads to exacerbation of chronic conditions due to an increase in skin inflammation caused by IL-1β and IL-18 [33, 37]. If the exposure lasts for a long time, inflammasome-associated diseases develop. Furthermore, UVB may trigger the development of skin cancer [9, 33].

INFLAMMASOME-ASSOCIATED DISEASES

Inflammation is not a single downstream effect of inflammasomes, since there are other forms of their activity, such as antigen presentation, transcription [4], post-transcriptional and post-translational regulation [18, 19], cell aging and death [37], and tumorigenesis [9]. In case inflammasomes have been overactivated in an uncontrolled manner, their combined downstream effects can result in the development of inflammasome-associated diseases: autoinflammatory [38–40], autoimmune [41, 42], allergic [43, 44] diseases, and cancer [11, 45] (Table). Classical, most common inflammasome-associated disorders are autoinflammatory diseases, such as Familial Mediterranean fever, cryopyrin-associated syndromes, periodic fever, Still's disease, etc. [38, 39].

Table

Association of inflammasomes with pathologies

Inflammasome	Diseases and syndromes	References
NLRP1	Generalized vitiligo, congenital toxoplasmosis, Addison's disease	[2, 4]
	Cutaneous squamous cell carcinoma	[45, 46]
NLRP2	Early-onset childhood atopic dermatitis	[4, 47]
NLRP3	Atopic dermatitis, psoriasis, acne vulgaris, urticaria, bullous pemphigoid, vitiligo	[1, 2, 13, 23, 42, 48–52]
	Allergic contact dermatitis	[53]
	Autoinflammatory, neurodegenerative, and cardiovascular diseases, cancer	[9, 23, 38]
NLRP10, NLRP12	Atopic dermatitis	[4]
	Periodic fever	[38, 39]

Table (continued)

Inflammasome	Diseases and syndromes	References
NAIP-NLRC4	Autoinflammatory syndromes	[1, 38]
NLRC5	Melanoma, fibrous tumors	[4, 54]
AIM-2	Vitiligo, allergic contact dermatitis, aldosterone-induced kidney injury	[1, 2]
IFI16	Cervical cancer	[55]
PYRIN	Autoinflammatory diseases	[1, 38]

The skin is a barrier organ through which invaders enter the body, therefore, it is here that both innate and adaptive immune responses most frequently proceed. Most immune-related skin diseases are affected by genetic and epigenetic mechanisms and environmental factors in different combinations among which inflammasomes occupy a specific place.

As seen from Table, almost all skin diseases were included in the list of inflammasome-associated conditions. In the past 15 years, great progress has been made in identifying new associations of inflammasomes and their components with skin disorders and developing new medications, which enable to regulate inflammasome activity. The canonical NLRP3 and AIM2 inflammasomes were especially well studied [1, 2, 42]. Functional deficiencies in some NLRs and skin colonization with *S. aureus* were observed more frequently in persons with atopic dermatitis than in healthy controls. Higher expression of NLRs was also found in plaque psoriasis [4]. The role of NLRP3 inflammasomes in the pathogenesis and therapy for psoriasis has been demonstrated at different levels, including epigenetic regulation. In particular, researchers reported that miR-155 can trigger psoriasis-like inflammation via activation of the NLRP3 inflammasome [56]. The NLRC5 presence is downregulated in melanoma cells due to a decrease in oncoantigen presentation [54], and, conversely, it is highly upregulated in keloid fibroblasts and skin fibrous tumors [4].

There are new interesting data related to another barrier organ, the unified airway. It has been described that NLRP3 inflammasome activation promotes the development of allergic rhinitis via nasal epitheliocyte and macrophage pyroptosis [57, 58]. It was found that the NLRP3 inflammasome is involved in cytokine shock in a severe course of COVID-19 and acute respiratory distress syndrome due to the fact that SARS-CoV-2 N protein strongly upregulates the binding of NLRP3 to ASC and NLRP3 assembly [59].

PROSPECTS OF THERAPEUTIC INTERVENTIONS

The use of the NLRP3 inflammasome as a target in new therapeutic approaches to disease treatment is rapidly progressing. Some known drugs used in other diseases were tested in NLRP3 inflammasome-associated pathologies [23]. Many new medications, including small molecules, became promising candidates in trials [20]. Depending on inflammasome polarization, current treatment for NLRP3 pathologies focuses on medications with inhibitory or stimulatory effects [18]. More often used inhibitors are directed to NLRP3 activation, signaling molecules, caspases, ASC, and NLRP3-derived proinflammatory cytokines [23]. Approved for clinical use, tranilast, an analog of a tryptophan metabolite, directly binds to the NACHT domain of the NLRP3 complex and downregulates the assembly of the NLRP3 inflammasome by blocking NLRP3 oligomerization step [60].

Over last years, the main approach to treatment for NLRP3-associated pathologies was inhibition of the inflammasome-derived cytokine IL-1β. Three biologicals were approved by the US FDA for many inflammatory (or inflammasome NLRP3-mediated) diseases: canakinumab, an IL-1β inhibitor; anakinra, a recombinant IL-1 receptor antagonist; and rilonacept, a decoy receptor that binds IL-1β and IL-1α [18, 61]. In particular, canakinumab, an anti-IL-1β monoclonal antibody, has been reported to treat a generalized pustular psoriasis patient and resulted in complete remission of skin lesions [62]. Effective anti-TNF therapy by monoclonal antibodies in psoriasis has also been described [49]. However, in some cases, these biologicals displayed side-effects [18].

The second approach directly targeting NLRP3 by small molecules, is specific, cost-effective, and less toxic compared to cytokine blockade [18, 63]. *B. pertussis* bacteria-derived outer membrane vesicles (nanoparticles) are proposed as a new vaccine platform targeted at the NLRP3 inflammasome in macrophages. Bacterial LPS can be delivered by the nanoparticles and transfected into macrophage NLRP3 inflammasome components to trigger the non-canonical activation route and then innate immunity [64].

The novelty of recent years has been the understanding of the association between NLRP3 inflammasome activation and the development of united airway diseases like allergic rhinitis. The NLRP3 inflammasome appears to be a new target in drug therapy to supplement or even replace traditional therapeutic approaches in the future [65].

There are not many medications for the therapy for NLRP3-associated diseases currently approved by the FDA or other agencies. It remains crucial to assess the safety, tolerance, and dose-dependent toxicity of NLRP3 inflammasome modulators to implement them into clinical practice [23]. Nevertheless, novel research data on inflammasome-associated pathogenesis of skin diseases can help to transfer molecular knowledge into clinical therapy in the nearest future.

CONCLUSION

The discovery of the inflammasome as an early event just before the onset of the inflammatory process at the beginning of the XXI century was a starting point for the impressive cellular and molecular research that followed, leading to a new understanding of the mechanisms of inflammation and innate immunity. So far, about 20 inflammasomes have been identified, but only two canonical inflammasomes, NLRP3 and AIM2, have been described in detail. Such container cells for inflammasomes as previously well-known myeloid cells and keratinocytes and fibroblasts, related to the skin have also been studied. Omics technologies made it possible to renew and update our understanding of cell landscape of the skin.

Inflammasome research involved specialists of various specialties: pathologists, histologists, immunologists, molecular biologists, clinicians, etc. As is often the case in science, at the interface of different approaches, new thoughts are born and discoveries are made. At the fundamental level, an understanding of the structure, routes of inflammation activation, signaling pathways, and various downstream effects not limited to the onset of inflammation has been shaped. However, transfer of fundamental knowledge into clinical practice has not yet happened. There is a reason to believe that new therapeutic approaches and drugs with high efficacy and a better adverse effect profile will contribute to modern therapy for autoinflammatory, autoimmune, neurodegenerative, allergic diseases, and cancer in the nearest future.

REFERENCES

1. Lara-Reyna S., Caseley E.A., Topping J., Rodrigues F., Jimenez Macias J., Lawler S.E. et al. Inflammasome activation: from molecular mechanisms to autoinflammation. *Clin. Transl. Immunol*. 2022;11(7):e1404. DOI: 10.1002/cti2.1404.
2. Tang L., Zhou F. Inflammasomes in common immune-related skin diseases. *Front. Immunol*. 2020;11:882. DOI: 10.3389/fimmu.2020.00882.
3. Klimov V.V. Innate immunity. In: From basic to clinical immunology. Cham: Springer, 2019:127–159. DOI: 10.1007/978-3-030-03323-1_3.
4. Danis J., Mellett M. Nod-Like receptors in host defence and disease at the epidermal barrier. *Int. J. Mol. Sci*. 2021;22(9):4677. DOI: 10.3390/ijms22094677.
5. Jacquet A. Characterization of innate immune responses to house dust mite allergens: Pitfalls and limitations. *Front. Allergy*. 2021;2:662378. DOI: 10.3389/falgy.2021.662378.
6. Liu B., Li A., Xu J., Cui Y. Single-cell transcriptional analysis deciphers the inflammatory response of skin-resident stromal cells. *Front. Surg*. 2022;9:935107. DOI: 10.3389/fsurg.2022.935107.
7. Solé-Boldo L., Raddatz G., Schütz S., Mallm J.-P., Rippe K., Lonsdorf A.S. et al. Single-cell transcriptomes of the human skin reveal age-related loss of fibroblast priming. *Commun. Biol*. 2020;3(1):188. DOI: 10.1038/s42003-020-0922-4.
8. Nagar A., Rahman T., Harton J.A. The ASC Speck and NLRP3 inflammasome function are spatially and temporally distinct. *Front. Immunol*. 2021;12:752482. DOI: 10.3389/fimmu.2021.752482.
9. Ciążyńska A., Bednarski I.A., Wódz K., Narbutt J., Lesiak A. NLRP1 and NLRP3 inflammasomes as a new approach to skin carcinogenesis (Review). *Oncol. Letters*. 2020;19(3):1649–1656. DOI: 10.3892/ol.2020.11284.
10. Ross C., Chan A.H., von Pein J.B., Maddugoda M.P., Boucher D., Schroder K. Inflammatory caspases: toward a unified model for caspase activation by inflammasomes. *Annu. Rev. Immunol*. 2022;40:249–269. DOI: 10.1146/annurev-immunol-101220-030653.
11. Lillo S., Saleh M. Inflammasomes in cancer progression and anti-tumor immunity. *Front. Cell Dev. Biol*. 2022;10:839041. DOI: 10.3389/fcell.2022.839041.
12. Martinon F., Burns K., Tschopp J. The inflammasome: a molecular platform triggering activation of inflammatory caspase and processing of proIL-beta. *Mol. Cell*. 2002;10(2):417–426. DOI: 10.1016/s1097-2765(02)00599-3.
13. Tsang M.S.-M., Hou T., Chan B.C.-L., Wong C.K. Immunological roles of NLR in allergic diseases and its underlying mechanisms. *Int. J. Mol. Sci*. 2021;22(4):1507. DOI: 10.3390/ijms22041507.
14. Lachner J., Mlitz V., Tschachler E., Eckhart L. Epidermal cornification is preceded by the expression of a keratinocyte-specific set of pyroptosis-related genes. *Sci. Rep*. 2017;7(1):17446. DOI: 10.1038/s41598-017-17782-4.
15. Samir P., Malireddi R.K.S., Kanneganti T.D. The PANoptosome: A deadly protein complex driving pyroptosis, apoptosis, and necroptosis (PANoptosis). *Front. Cell Infect. Microbiol*. 2020;10:238. DOI: 10.3389/fcimb.2020.00238.
16. Dmitriev Yu.V., Galagudza M.M. Necroptosis and the experience of its targeted modulation in the context of personalized medicine. Rus J Person Med 2022;2(2):33–45 (in Russ.). DOI: 10.18705/2782-3806-2022-2-2-33-45.
17. Li Y., Sun L., Zhang Y. Programmed cell death in the epithelial cells of the nasal mucosa in allergic rhinitis. *Int. Immunopharm*. 2022;112:109252. DOI: 10.1016/j.intimp.2022.109252.

18. Swanson K.V., Deng M., Ting J.P. The NLRP3 inflammasome: molecular activation and regulation to therapeutics. *Nat. Rev. Immunol*. 2019;19(8):477–489. DOI: 10.1038/s41577-019-0165-0.
19. Seok J.K., Kang H.C., Cho Y.Y., Lee H.S., Lee J.Y. Regulation of the NLRP3 inflammasome by post-translational modifications and small molecules. *Front. Immunol.* 2020;11:618231. DOI: 10.3389/fimmu.2020.618231.
20. Zheng D., Liwinski T., Elinav E. Inflammasome activation and regulation: toward a better understanding of complex mechanisms. *Cell Discov*. 2020;6(1):36. DOI: 10.1038/s41421-020-0167-x.
21. Zheng J., Yao L., Zhou Y., Gu X., Wang C., Bao K. et al. A novel function of NLRP3 independent of inflammasome as a key transcription factor of IL-33 in epithelial cells of atopic dermatitis. *Cell Death Dis*. 2021;12(10):871. DOI: 10.1038/s41419-021-04159-9.
22. Fernandez-Duran I., Quintanilla A., Tarrats N., Birch J., Hari P., Millar F.R. et al. Cytoplasmic innate immune sensing by the caspase-4 non-canonical inflammasome promotes cellular senescence. *Cell Death Differ*. 2022;29(6):1267–1282. DOI: 10.1038/s41418-021-00917-6.
23. Seok J.K., Kang H.C., Cho Y.-Y., Lee H.-S., Lee J.Y. Therapeutic regulation of the NLRP3 inflammasome in chronic inflammatory diseases. *Arch. Pharm. Res.* 2021;44(1):16–35. DOI: 10.1007/s12272-021-01307-9.
24. Ha H.J., Chun H.L., Lee S.Y., Park H.H. Molecular basis of IRGB10 oligomerization and membrane association for pathogen membrane disruption. *Commun. Biol.* 2021;4(1):92. DOI: 10.1038/s42003-020-01640-7.
25. Gaidt M.M., Hornung V. Alternative inflammasome activation enables IL-1β release from living cells. *Curr. Opin. Immunol*. 2017;44:7–13. DOI: 10.1016/j.coi.2016.10.007.
26. Christgen S., David E., Place D.E., Kanneganti T.-D. Toward targeting inflammasomes: Insights into their regulation and activation. *Cell Res*. 2020;30(4):315–327. DOI: 10.1038/s41422-020-0295-8.
27. Anderton H., Alqudah S. Cell death in skin function, inflammation, and disease. *Biochem. J*. 2022;479(15):1621–1651. DOI: 10.1042/BCJ20210606.
28. Bertheloot D., Latz E., Franklin B.S. Necroptosis, pyroptosis and apoptosis: An intricate game of cell death. *Cell Mol. Immunol*. 2021;18(5):1106–1121. DOI: 10.1038/s41423-020-00630-3.
29. Riwaldt S., Corydon T.J., Pantalone D., Sahana J., Wise P., Wehland M. et al. Role of apoptosis in wound healing and apoptosis alterations in microgravity. *Front. Bioengin. Biotechnol*. 2021;9:679650. DOI: 10.3389/fbioe.2021.679650.
30. Gruber J.V., Holtz R. *In vitro* expression of NLRP inflammasome-induced active Caspase-1 expression in normal human epidermal keratinocytes (NHEK) by various exogenous threats and subsequent inhibition by naturally derived ingredient blends. *J. Inflam. Res*. 2019;12:219–230. DOI: 10.2147/JIR.S215776.
31. Buscetta M., Di Vincenzo S., Miele M., Badami E., Pace E., Cipollina C. Cigarette smoke inhibits the NLRP3 inflammasome and leads to caspase-1 activation via the TLR4-TRIF-caspase-8 axis in human macrophages. *FASEB J*. 2020;34(1):1819–1832. DOI: 10.1096/fj.201901239R.
32. Fenini G., Grossi S., Contassot E., Biedermann T., Reichmann E., French L.E. et al. Genome editing of human primary keratinocytes by CRISPR/Cas9 reveals an essential role of the NLRP1 inflammasome in UVB sensing. *J. Invest. Dermatol*. 2018;138(12):2644–2652. DOI: 10.1016/j.jid.2018.07.016.
33. Burian M., Yazdi A.S. NLRP1 Is the key inflammasome in primary human keratinocytes. *J. Invest. Dermatol*. 2018;138(12):2507–2510. DOI: 10.1016/j.jid.2018.08.004.
34. Latz E., Duewell P. NLRP3 inflammasome activation in inflammaging. *Sem. Immunol*. 2018;40:61–73. DOI: 10.1016/j.smim.2018.09.001.
35. Nardini C., Moreau J.-F., Gensous N., Ravaioli F., Garagnani P., Bacalini M.G. The epigenetics of inflammaging: The contribution of age-related heterochromatin loss and locus-specific remodelling and the modulation by environmental stimuli. *Sem. Immunol*. 2018;40:49–60. DOI: 10.1016/j.smim.2018.10.009.
36. Cyr B., Hadad R., Keane R.W., Vaccari J.P.R. The role of non-canonical and canonical inflammasomes in inflammaaging. *Front. Mol. Neurosci*. 2022;15:774014. DOI: 10.3389/fnmol.2022.774014.
37. Ferrara F., Prieux R., Woodby B., Valacchi G. Inflammasome activation in pollution-induced skin conditions. *Plast. Reconstr. Surg*. 2021;147(1S-2):15S–24S. DOI: 10.1097/PRS.0000000000007617.
38. Georgin-Lavialle S., Fayand A., Rodrigues F., Bachmeyer C., Savey L., Grateau G. Autoinflammatory diseases: state of the art. *Presse Med*. 2019;48(1Pt2):e25–e48. DOI: 10.1016/j.lpm.2018.12.003.
39. Georgin-Lavialle S., Ducharme-Benard S., Sarrabay G., Savey L., Grateau G., Hentgen V. Systemic autoinflammatory diseases: clinical state of the art. Best practice and research. *Clin. Rheumatology*. 2020;34(4):101529. DOI: ff10.1016/j.berh.2020.101529.Georgin-Lavialle S., Ducharme-Benard S., Sarrabay G., Savey L., Grateau G., Hentgen V. Systemic autoinflammatory diseases: clinical state of the art. Best practice and research. *Clin. Rheumatology*. 2020;34(4):101529. DOI: ff10.1016/j.berh.2020.101529.
40. Pirozhkov S.V., Litvitskiy P.F. Inflammasome-associated diseases. *Immunology*. 2018;39(2-3):158–165 (in Russ.). DOI: 10.18821/0206-4952-2018-39-2-3-158-165.
41. Zhang Y., Yang W., Li W., Zhao Y. NLRP3 inflammasome: Checkpoint connecting innate and adaptive immunity in autoimmune diseases. *Front. Immunol*. 2021;12:732933. DOI: 10.3389/fimmu.2021.732933.
42. Wang D., Duncan B., Li X., Shi J. The role of NLRP3 inflammasome in infection-related, immune-mediated and autoimmune skin diseases. *J. Dermatol. Sci*. 2020;98(3):146–151. DOI: 10.1016/j.jdermsci.2020.03.001.
43. Kazimirsky A.N., Salmasi J.M., Poryadin G.V., Svitich O.A., Bragvadze B.G., Alekseeva A.A., Gankovskaya L.V. The role of epithelial cells in atopy pathogenesis. *Bulletin of Siberian Medicine.* 2019;8(1):201–210 (in Russ.). DOI: 10.20538/1682-0363-2019-1-201–210.
44. Zagreshenko D.S., Klimov V.V., Trofimenko N.A., Dorofeeva M.S. “Skin window” exudate IL-1β and IL-18 in patients

with chronic urticaria. *Medicine in Kuzbass*. 2022;21(3):27–29 (in Russ.). DOI: 10.24412/2687-0053-2022-3-27-29.
45. Di Filippo M., Hennig P., Karakaya T., Slaufova M., Beer H.-D. NLRP1 in cutaneous SCCs: An example of the complex roles of inflammasomes in cancer development. *Int. J. Mol. Sci*. 2022;23(20):12308. DOI: 10.3390/ijms232012308.
46. Zhong F.L., Mamaï O., Sborgi L., Boussofara L., Hopkins R., Robinson K. et al. Germline NLRP1 mutations cause skin inflammatory and cancer susceptibility syndromes via inflammasome activation. *Cell*. 2016;167(1):187–202.e17. DOI: 10.1016/j.cell.2016.09.001.
47. Thürmann L., Grützmann K., Klös M., Bieg M., Winter M., Polte T. et alEarly-onset childhood atopic dermatitis is related to NLRP2 repression. *J. Allergy Clin. Immunol*. 2018;141(4):1482–1485.e16. DOI: 10.1016/j.jaci.2017.11.018.
48. Li S., Kang P., Zhang W., Jian Z., Zhang Q., Yi X. et al. Activated NLR family pyrin domain containing 3 (NLRP3) inflammasome in keratinocytes promotes cutaneous T-cell response in patients with vitiligo. *J. Allergy Clin. Immunol*. 2020;145(2):632–645. DOI: 10.1016/j.jaci.2019.10.036.
49. Deepti V., Shora Z.F., Gunnthorunn S., Cecilia B.E., Charlotta S., Charlotta E. Enhanced inflammasome activity in patients with psoriasis promotes systemic inflammation. *J. Invest. Dermatol*. 2021;141(3):586–595.e5. DOI: 10.1016/j.jid.2020.07.012.
50. Su F., Xia Y., Huang M., Zhang L., Chen L. Expression of NLPR3 in psoriasis is associated with enhancement of interleukin-1b and caspase-1. *Med. Sci. Monit*. 2018;24:7909–7913. DOI: 10.12659/MSM.911347.
51. Tsuji G., Hashimoto-Hachiya A., Yen V.H., Takemura M., Yumine A., Furue K. et al. Metformin inhibits IL-1β secretion via impairment of NLRP3 inflammasome in keratinocytes: implications for preventing the development of psoriasis. *Cell Death Discovery*. 2020;6:11. DOI: 10.1038/s41420-020-0245-8.
52. Yang B.-Y., Cheng Y.-G., Liu Y., Liu Y., Tan J.-Y., Guan W. et al. *Datura Metel L*. ameliorates imiquimod-induced psoriasis-like dermatitis and inhibits inflammatory cytokines production through TLR7/8–MyD88–NF-kB–NLRP3 inflammasome pathway. *Molecules*. 2019;24(11):2157. DOI: 10.3390/molecules24112157.
53. Bonnekoh H., Vera C., Abad-Perez A., Radetzki S., Neuenschwander M., Specker E. et al. Topical inflammasome inhibition with disulfiram prevents irritant contact dermatitis. *Clin. Transl. Allergy*. 2021;11(5):e12045. DOI: 10.1002/clt2.12045.
54. Luo Q., Zeng J., Li W., Lin L., Zhou X., Tian X. et al. Silencing of miR155 suppresses inflammatory responses in psoriasis through inflammasome NLRP3 regulation. *Int. J. Mol. Med*. 2018;42(2):1086–1095. DOI: 10.3892/ijmm.2018.3677.
55. Cai H., Yan L., Liu N., Xu M., Cai H. IFI16 promotes cervical cancer progression by upregulating PD-L1 in immunomicroenvironment through STING-TBK1-NF-kB pathway. *Biomed. Pharmacother*. 2020;123:109790. DOI: 10.1016/j.biopha.2019.109790.
56. Yang Z., Liang C., Wang T., Zou Q., Zhou M., Cheng Y. et al. *Biochem. Biophys. Res. Commun.* 2020;522(1):61–67. DOI: 10.1016/j.bbrc.2019.11.031.
57. Kim H., Kim H., Feng Y., Li Y., Tamiya H., Tocci S. et al. PRMT5 control of cGAS/STING and NLRC5 pathways defines melanoma response to antitumor immunity. *Sci. Transl. Med*. 2020;12(551):eaaz5683. DOI: 10.1126/scitranslmed.aaz5683.
58. Zhou H., Zhang W., Qin D., Liu P., Fan W., Lv H. et al. Activation of NLRP3 inflammasome contributes to the inflammatory response to allergic rhinitis via macrophage pyroptosis. *Int. Immunopharmacol.* 2022;110:109012. DOI: 10.1016/j.intimp.2022.109012.
59. Pan P., Shen M., Yu Z., Ge W., Chen K., Tian M. et al. SARS-CoV-2 N protein promotes NLRP3 inflammasome activation to induce hyperinflammation. *Nat. Commun*. 2021;12(1):4664. DOI: 10.1038/S41467-021-25015-6.
60. Huang Y., Jiang H., Chen Y., Wang X., Yang Y., Tao J. et al. Tranilast directly targets NLRP3 to treat inflammasome-driven diseases. *EMBO Mol. Med*. 2018;10(4):e8689. DOI: 10.15252/emmm.201708689.
61. Nasonov E.L. The role of interleukin 1 in the development of human diseases. *Rheumatology Science and Practice*. 2018;56(Suppl. 4):19–27 (in Russ.). DOI: 10.14412/1995-4484-2018-19-27.
62. Skendros P., Papagoras C., Lefaki I., Giatromanolaki A., Kotsianidis I., Speletas M. et al. Successful response in a case of severe pustular psoriasis after interleukin-1beta inhibition. *Br. J. Dermatol*. 2017;176(1):212–215. DOI: 10.1111/bjd.14685.
63. Sebastian-Valverde M., Wu H., Rahim M.A, Sanchez R., Kumar K., De Vita R.J. et al. Discovery and characterization of small-molecule inhibitors of NLRP3 and NLRC4 inflammasomes. *J. Biol. Chem*. 2021;296:100597. DOI: 10.1016/j.jbc.2021.100597.
64. Elizagaray M.L., Gomes M.T.R., Guimaraes E.S., Rumbo M., Hozbor D.F., Oliveira S.C. et al. Canonical and non-canonical inflammasome activation by outer membrane vesicles derived from Bordetella pertussis. *Front. Immunol*. 2020;11:1879. DOI: 10.3389/fimmu.2020.01879.
65. Leszczyńska K., Jakubczyk D., Górska S. The NLRP3 inflammasome as a new target in respiratory disorders treatment. *Front. Immunol*. 2022;13:1006654. DOI: 10.3389/fimmu.2022.1006654.

Authors' information

Klimov Vladimir V. – Dr. Sci. (Med.), Professor, Head of the Immunology and Allergy Division, Siberian State Medical University, Tomsk, klimov@mail.tomsknet.ru, http://orcid.org/0000-0001-6673-7556

Zagreshenko Denis S. – Cand. Sci. (Med.), Associate Professor, Clinical Lab Diagnostics Division, Novokuznetsk State Institute for Advanced Training of Doctors, Novokuznetsk, zagreshenko@rambler.ru, http://orcid.org/0000-0003-4309- 664X

Urazova Olga I. – Dr. Sci. (Med.), Professor, Corresponding Member of the RAS, Head of the Pathophysiology Division, Siberian State Medical University, Tomsk, http://orcid.org/ 0000-0002-9457-8879

Klimov Andrew V. – Cand. Sci. (Med.), Associate Professor, Immunology and Allergy Division; Teaching Assistant, ENT Division, Siberian State Medical University, Tomsk, klimov.lor@mail.ru, http://orcid.org/0000-0002-2776-5834

Naidina Oxana A. – Cand. Sci. (Med.), Teaching Assistant, Immunology and Allergy Division, Siberian State Medical University, Tomsk, klimov.lor@mail.ru, http://orcid.org/0000-0002-1407-2086

Tsyplina Ekaterina Yu. – Research Lab Assistant, Immunology and Allergy Division, Siberian State Medical University, Tomsk, katyts9917@gmail.com, http://orcid.org/ 0000-0001-9046-6637

Kologrivova Elena N. – Dr. Sci. (Med.), Professor, Immunology and Allergy Division, Siberian State Medical University, Tomsk, enkologrivova@mail.ru, http://orcid.org/0000-0003-1639-4676

Koshovkina Tatiana V. – Cand. Sci. (Med.), Associate Professor, Immunology and Allergy Division, Siberian State Medical University, Tomsk, koshov.tan@yandex.ru, http://orcid.org/0000-0001-7280-1980

Koshkarova Natalia S. – Cand. Sci. (Med.), Associate Professor, Immunology and Allergy Division, Siberian State Medical University, Tomsk, kasy@list.ru, http://orcid.org/0000-0002-6032-2402

(✉) **Klimov Vladimir V.,** klimov@mail.tomsknet.ru

Received 30.12.2022;
approved after peer review 16.01.2023;
accepted 27.02.2023

УДК 618.11-006.6:616.381-008.8—091.8
https://doi.org/10.20538/1682-0363-2023-2-122-133

Stem cell properties of cancer cells in ascitic fluid of patients with ovarian cancer: a key to control over cancer progression

Kovalev O.I.[1, 2], Vtorushin S.V.[1, 2], Kaigorodova E.V.[1, 2]

[1] *Cancer Research Institute, Tomsk National Research Medical Center (NRMC) Russian Academy of Sciences*
5, Kooperativny Str., Tomsk, 634009, Russian Federation

[2] *Siberian State Medical University*
2, Moscow Trakt, Tomsk, 634050, Russian Federation

ABSTRACT

Ovarian cancer is considered to be the most malignant and aggressive tumor of the female reproductive system, which is largely associated with early development of malignant ascites and peritoneal carcinomatosis. Cancer cells representing the primary focus, as well as those contained in the ascitic fluid, are extremely heterogeneous in terms of morphological, immunohistochemical, and molecular genetic aspects. Cancer stem cells play a significant role in tumor self-renewal, differentiation, metastasis, and development of chemoresistance.

This literature review is aimed at summarizing the available data on cancer stem cells in ovarian cancer and their role in tumor progression. A bioinformatic search was carried out in the PubMed, NCBI, Google Scholar, and eLibrary databases using the keywords “cancer stem cells”, “ovarian cancer”, “malignant ascites”, “chemoresistance”, etc.

The data presented in the review make it possible to comprehensively characterize the role of stem cell properties of ovarian cancer cells. The review presents up-to-date information on the molecular and biological parameters of cancer stem cells in ovarian cancer, which are the cellular component of malignant ascites, as well as data from the authors’ studies. Along with this, the article describes modern ideas about the mechanisms of formation of cellular spheroids and their contribution to cancer progression.

Cancer stem cells are an extremely promising target in the development of future therapeutic strategies based on the study of signaling pathways in ovarian cancer stem cells, the mechanisms of spheroid formation, and the contribution of immune cells to the acquisition of cancer stem cell properties.

Keywords: ovarian cancer, cancer stem cells, malignant ascites, tumor spheroids, chemoresistance

Conflict of interest. The authors declare the absence of obvious and potential conflicts of interest related to the publication of this article.

Source of financing. The authors state that they received no funding for the study.

For citation: Kovalev O.I., Vtorushin S.V., Kaigorodova E.V. Stem cell properties of cancer cells in ascitic fluid of patients with ovarian cancer: a key to control over cancer progression. *Bulletin of Siberian Medicine.* 2023;22(2):122–133. https://doi.org/10.20538/1682-0363-2023-2-122-133.

✉ *Vtorushin Sergey V.,* wtorushin@rambler.ru

Стволовые свойства опухолевых клеток асцитической жидкости у больных раком яичника: ключ к управлению распространением процесса

Ковалев О.И.[1, 2], Вторушин С.В.[1, 2], Кайгородова Е.В.[1, 2]

[1] *Научно-исследовательский институт (НИИ) онкологии, Томский национальный исследовательский медицинский центр (НИМЦ) Российской академии наук*
Россия, 634009, г. Томск, пер. Кооперативный, 5

[2] *Сибирский государственный медицинский университет (СибГМУ)*
Россия, 634050, г. Томск, Московский тракт, 2

РЕЗЮМЕ

Рак яичника принято рассматривать как наиболее злокачественную и агрессивную опухоль женской репродуктивной системы, что во многом связано с ранним развитием злокачественного асцита и перитонеального канцероматоза. Опухолевые клетки, представляющие первичный очаг, а также содержащиеся в составе асцитической жидкости, крайне гетерогенны с морфологической, иммуногистохимической и молекулярно-генетической позиций. Значимую роль в процессах самообновления опухоли, ее дифференцировки, метастазирования и развития химиорезистенстности играют опухолевые стволовые клетки.

Настоящий обзор направлен на обобщение имеющихся данных о стволовых опухолевых клетках рака яичников и их роли в опухолевой прогрессии. При написании обзора проведен биоинформационный поиск в универсальных базах данных PubMed, NCBI, Google Scholar и eLibrary с применением следующих ключевых слов для поиска: cancer stem cells, ovarian cancer, malignant ascites, hemoresistance и т.п.

Представленные данные позволяют всесторонне охарактеризовать роль стволовых свойств опухолевых клеток рака яичника. Изложена актуальная информация о молекулярно-биологических параметрах стволовых опухолевых клеток рака яичника, представляющих клеточный компонент злокачественного асцита, с приведением данных собственных исследований. Отражены современные представления о механизмах формирования клеточных сфероидов и их вкладе в прогрессирование опухолевого процесса.

Опухолевые стволовые клетки являются крайне перспективной мишенью в создании будущих терапевтических стратегий, основанных на изучении сигнальных путей в стволовых клетках рака яичников, механизмах образования сфероидов, а также вкладе иммунных клеток в приобретение стволовых свойств опухоли.

Ключевые слова: рак яичника, опухолевые стволовые клетки, злокачественный асцит, опухолевые сфероиды, химиорезистентность

Конфликт интересов. Авторы декларируют отсутствие явных и потенциальных конфликтов интересов, связанных с публикацией настоящей статьи.

Источник финансирования. Авторы заявляют об отсутствии финансирования при проведении исследования.

Для цитирования: Ковалев О.И., Вторушин С.В., Кайгородова Е.В. Стволовые свойства опухолевых клеток асцитической жидкости у больных раком яичника: ключ к управлению распространением процесса. *Бюллетень сибирской медицины.* 2023;22(2):122–133. https://doi.org/10.20538/1682-0363-2023-2-122-133.

INTRODUCTION

Ovarian cancer (OC) is an extremely malignant and the most aggressive tumor among all neoplasms of the female reproductive system. Tumor progression is accompanied by early development of malignant ascites with metastatic spread of the tumor to the abdominal organs [1]. The modern stem cell theory of cancer postulates that cancer stem cells (CSCs) are responsible for self-renewal, differentiation, metastasis, and development of chemotherapy resistance. By their nature, CSCs are capable of symmetric and asymmetric division with subsequent differentiation of tumor subclone(s), which contributes to phenotypic and functional heterogeneity in the hierarchical organization of tumors [2].

CANCER STEM CELL MARKERS IN OVARIAN CANCER

It should be noted that identification of CSC properties in cancer patients is rather challenging due to the lack of a universal marker or panel of markers. Currently, there is a wide variety of proteins whose expression is considered as a sign of stem cell-like properties in these cells (Table 1).

Table 1

Cancer stem cell markers in ovarian cancer

Marker	Description	Reference
CD133 (prominin-1)	Glycosylated transmembrane protein	[3]
CD44	Hyaluronic acid receptor	[4, 5]
CD24	P-selectin ligand	[6]
CD177	Type III tyrosine kinase receptor	[7]
MyD88	TIR domain-containing cytosolic adaptor protein	[8–10]
EpCAM	Calcium-independent homotypic epithelial cell adhesion molecule	[11]
ALDH1	Enzyme catalyzing oxidation of aldehydes to carboxylic acids	[12, 13]
CXCR4	CXCL12 chemokine receptor	[14–16]
Nanog	Transcription factor	[17–19]
SOX2	Transcription factor	[20, 21]
OCT4	Transcription factor	[22]

A number of diagnostic markers proved useful for isolating ovarian CSC subpopulations, including CD133+ [23, 24] CD133+ ALDH+ [25], CD44+ CD117+ [7], EpCAM [26].

EpCAM, a calcium-independent homotypic epithelial cell adhesion molecule, is a type I transmembrane glycoprotein expressed by subpopulations of normal epithelial cells and numerous stem cells, including ovarian CSCs [11, 27]. It was shown *in vivo* that EpCAM-positive tumor cells isolated from the remaining ovarian carcinoma cell population have greater tumorigenic potential in comparison with EpCAM-negative tumor cells [28].

CD133 is a glycosylated transmembrane protein which is encoded by the *PROM1* gene. The physiological function of this protein is not fully understood to date, but it was shown that this receptor is actively involved in modulating tumor spread and developing drug resistance of the tumor. CD133 is one of the most studied CSC markers of ovarian, colon, prostate, and lung cancer [3]. Y.J. Lee et al. (2016) demonstrated a correlation of CD133 expression with tumor differentiation. The CD133 expression score in grade III tumors (high-grade tumors) was significantly higher than in grade I tumors (low-grade tumors) [5].

ALDH1 is a member of the family of enzymes that catalyze oxidation of aldehydes to carboxylic acids. Metabolic activity of this enzyme was detected by the ALDEFLUOR assay in identifying CSCs in a number of solid tumors. High ALDH1 expression is significantly associated with poor clinical outcomes in serous ovarian cancer. Currently, ALDH is used as a CSC marker in ovarian cancer [12, 13].

CD44 is a receptor for hyaluronic acid and many other components of the extracellular matrix. CD44 is responsible for cell – cell interactions, adhesion, and cell migration. The accumulated data indicate that CD44, especially a CD44v isoform, is a CSC marker in various tumors including ovarian carcinomas. CD44 is also involved in the regulation of stem cell-like properties including self-renewal, tumor initiation, metastasis, and chemotherapy and radiotherapy resistance. In addition, there is ample evidence that CD44 expression, especially of the CD44v isoform, correlates with poor patient survival. This is significantly an unfavorable prognostic marker. In turn, the CD44v isoform can be a promising target for targeted therapy [4, 5].

CD24 is a ligand of P-selectin, an adhesion receptor on activated endothelial cells. It is often co-expressed in CD44 and CD133-positive tumor cells in ovarian carcinomas. CD24-positive tumor cells have a higher metastatic potential compared to CD24-negative cell populations. It is important that CD24 induces EMT that leads to the formation of a highly proliferative mesenchymal CSC phenotype as well as the development of drug resistance of the tumor through the activation of the PI3K / Akt, NF-κB, and ERK signaling cascades [29].

Recent studies of ascitic fluid in ovarian cancer patients by multicolor flow cytometry showed that the cellular composition of ascitic fluid is heterogeneous. A big proportion of ascites tumor cells is represented by atypical / hybrid cell forms with stemness traits, as well as Epcam+CD45-CD44+CD24+CD133+/- CSCs both with and without EMT [30]. In addition, we found that the number of ascites tumor cells with Epcam+CD45-CD44-CD24+CD133-Ncadherin+ and Epcam+CD45-CD44-CD24+CD133+Ncadherin+

phenotypes as well as the number of atypical / hybrid Epcam+CD45+CD44+CD24+/-CD133+/-Ncadherin+/- cells have a positive correlation with the carcinomatosis index [31]. It should be noted that these cells are CD24-positive.

MyD88 is a TIR domain-containing cytosolic adaptor protein involved in signal transduction from Toll-like receptors. Activation of the TLR4 / MyD88 / NF-κB signaling pathway enhances the aggressive tumor phenotype and worsens the clinical outcome in patients with ovarian cancer. Expression of this protein is often detected in CSCs [8–10].

CD177 is a type III tyrosine kinase receptor, which activates phosphorylation by initiating transcriptional processes in various cell types. It is involved in the regulation of cell apoptosis, differentiation, proliferation, chemotaxis, and adhesion. The receptor is often expressed in hematopoietic stem cells (HSCs), myeloid progenitor cells, pro-B cells, progenitor cells, as well as in CSCs [7].

CXCR4 is a chemokine receptor. The receptor is involved in cell chemotaxis in response to CXCL12 chemokine binding and is used as one of the markers of ovarian CSCs. It is assumed that CXCR4 is associated with the induction of ovarian cancer metastasis, as well as poor overall survival of patients [14–16].

NANOG as a transcription factor is one of the most important markers used to identify CSCs. It is reported that NANOG mRNA was detected in pluripotent mouse and human stem cells, but not in differentiated cells (Chambers et al., 2003). Nanog expression is known to be statistically higher in CSCs compared to tumor cells without stemness traits. NANOG is responsible for morphofunctional plasticity and self-renewal of embryonic stem cells through interaction with other transcription factors, such as SOX-2 and Oct-4. These genes attach to Octamer / SOX elements in the NANOG promoter, which leads to activation of NANOG transcription (Rodda et al., 2005). NANOG was found to maintain CSC traits through activation of various signaling pathways, including TGIF-β, Wnt / β-catenin, JAK / STAT, Notch, and Hedgehog (Alemohammad et al., 2020). NANOG overexpression was found in tumors from embryonic cells, which correlates with cell proliferation, tumor recurrence, clonal tumor evolution, oncogenicity, invasiveness, and resistance to treatment, such as chemotherapy and radiotherapy [17–19].

SOX2 is a member of the SOXB1 transcription factor family, and its three main domains are the N-terminal domain, the high mobility group (HMG) domain, and the transactivation domain. SOX2 is an important marker of CSCs. It was observed that SOX2 is overexpressed in spheroids as well as in subsequent generations of cancer cell spheroids. SOX2 expression is closely associated with chemoresistance and a poor prognosis in patients with ovarian cancer [20, 21].

Oct4 transcription factor is expressed in embryonic stem cells as well as in ovarian CSCs [22].

The analysis of the key stemness-related genes in CSC subpopulations found new promising markers closely related to the development of ovarian carcinoma including LCP2, FCGR3A, COL1A1, COL1A2, MT-CYB, CCT5, and PAPPA [32].

REGULATION OF STEM CELL-LIKE PROPERTIES OF OVARIAN CANCER CELLS

To date, many mechanisms of regulation of ovarian stem cell-like properties have been described. S. Bai et al. (2021) showed that epidermal growth factor-like protein 6 (EGFL6) acts as a stem cell regulatory factor, promotes asymmetric division of ALDH-positive ovarian CSCs, and thereby increases tumor cell proliferation *in vitro* and tumor growth *in vivo* [33]. EIF5A2 factor positively regulates ovarian cancer cell stemness through the E2F1 / KLF4 pathway [34]. The L1CAM / FGFR1 / SRC / STAT3 signaling pathway is considered as a new driver of stemness in ovarian cancer. L1CAM was shown to potentiate several stemness-related properties in ovarian cancer cells, including spheroid formation and tumor initiation *in vivo* [35]. FOXK2-driven activation of IRE1α leads to unconventional splicing of XBP1 and activation of SOX2, OCT4, NANOG, and ALDH1A1 stemness pathways [36].

Interestingly, the CSC phenotype is regulated in particular by the tumor microenvironment. It has been shown that activation of NF-κB signaling leads to increased activity of the Wnt signaling pathway, which leads to dedifferentiation of tumor cells from non-stem cells into CSCs [37]. Heterospheroids including polarized CD206+ M2 macrophages showed increased aldehyde dehydrogenase (ALDH) activity, which suggests an interaction between CSCs and macrophages promoting tumor cell activation and self-renewal of CSCs [38].

Cells of the tumor microenvironment secrete factors that contribute to the acquisition of stemness traits in tumor cells, such as KIT ligand and R-spondin as ligands for CD117 [39] and LGR5 [40], respectively.

INDIVIDUAL CELLS WITH STEM CELL-LIKE PROPERTIES IN ASCITIC FLUID IN OVARIAN CANCER

A study by S.O. Genning et al. (2021), which examined stem cell populations in ascites, showed that 95.5% of CSCs had a CD44+ / CD133- phenotype and 4.5% had a CD44- / CD133+ phenotype. The population of CD44+ / CD133+ cells was minor (0.2%) [41]. In other studies, ascites cells with a high level of CD44 and CD133 expression, which were obtained from ovarian cancer patients, had a great potential for self-renewal and long-term proliferation [42–45].

The co-expression of CD133 and CD44, as well as the expression of each marker individually was the highest in tumor cells that were present in ascitic fluid of primary human ovarian cancer. In addition, the expression of CD97, CD104, CD107a, CD121a, and CD307c was significantly higher in CD133+CD44+ tumor cells of malignant ascites than in primary tumor cells or metastatic ovarian tumors [5]. In studies by M. Jäger et al. (2012) double staining of ascites cells in samples obtained by cytospin revealed the presence of CD133+ / EpCAM+ cells in 100% of the studied patients [46].

Stemness-related markers can be expressed not only by classical tumor cells, but also hybrid cells found in ascitic fluid. Their presence is characteristic of ovarian carcinoma. M.Z. Akhter et al. (2018) state that the entire EpCAM+CD45+ population is highly invasive and consists of ovarian CSCs (CD133+ and CD117+CD44+) [47]. Another striking finding of this study is that CSC phenotypes are primarily restricted to the EpCAM+CD45+ compartment. This does not allow to deny the existing hypothesis that CSCs arise due to dysregulation of tissue-specific stem cells [48].

Similar results were obtained in the studies by E.V. Kaigorodova et al. (2020) that showed high heterogeneity of EpCAM+ cells in ascitic fluid of ovarian cancer patients. A high concentration of these cells was represented by atypical and hybrid forms of EpCAM+CD45+ cells with stemness traits [30, 49]. In addition, another study demonstrated a positive correlation between the number of EpCAM+CD45+ cells with stemness traits in ascitic fluid and the carcinomatosis prevalence index in ovarian cancer patients [31]. It was also revealed that the number of atypical / hybrid EpCAM+CD45+ cells in ascitic fluid in patients with borderline ovarian tumors was significantly lower than in patients with serous ovarian carcinomas ($p = 0.02$) [50]. A review by E.V. Kaigorodova et al. (2022) suggests theories of hybrid tumor cell formation, their varieties and characteristics and shows the role of cancer-associated macrophage-like cells (CAMLs) and circulating hybrid cells (CHCs) as tumor biomarkers [51].

The most comprehensive and complex study of ascites cells in patients with ovarian cancer was performed by B. Izar et al. (2020) [52]. The authors conducted RNA sequencing (scRNA-seq) of individual cells (approximately 11,000 cells) from 22 ascites samples obtained from 11 ovarian cancer patients, while they comprehensively characterized the ascites ecosystem in high-grade serous ovarian cancer (HGSOC). Eighteen different cell clusters were annotated, encompassing epithelial cells (5 clusters labeled by EPCAM, cytokeratins, kallikreins), macrophages (4 clusters labeled by CD14, AIF1, CSF1R, CD163) cancer-associated fibroblasts (CAFs) (4 clusters labeled by PDPN, DCN, and THY1), dendritic cells (2 clusters labeled by CD1C, CD1E, CCR7, CD83), B cells (CD19, CD79A/B), T cells (CD2, CD3D/E/G), and red blood cells (GATA1, hemoglobin). Signaling pathways that differed in malignant cells of each patient were identified among the five tumor clusters. One cluster of cells contained distinct markers of stem (ALDH1A3 and CD133 / PROM1) and mesenchymal (FN1, ACTA2, and MYL9) cells, as well as AXL and its only known ligand GAS6, which is associated with drug therapy resistance [53].

COMPLEXES OF CELLS WITH STEM CELL-LIKE PROPERTIES IN ASCITIC FLUID IN OVARIAN CANCER

There is limited information about the study of stem cell-like properties of individual cells. At the same time, complexes of cells found in ascites, which also have stemness traits, are widely described. Indeed, it is common to distinguish single tumor cells, cell aggregates, and cell spheroids among the cellular component of malignant ascites in ovarian cancer [54].

Moreover, formation of essential spheroids is considered as a stemness trait. The process of spheroid formation can be easily observed when cells are cultured *in vitro*. In patients, however, it is not always possible to establish whether they were formed from a single detached cell due to its proliferation, following aggregation of individual cells or a release of cell complexes from the primary tumor.

S.A. Bapat et al. (2005) isolated two tumorigenic

clones (A2 and A4-T) of CD44+ ovarian stem-like cancer cells that were capable of forming spheroids in ascitic fluid. When these cell lines were further cultured, NESTIN and NANOG were overexpressed in A2 and A4-T monolayers, while a decrease in the level of spheroid expression from these cell lines was noted. The described phenomenon gave the authors a reason to believe that the formation of spheroids represents an event of differentiation. In addition, the spheroids showed expression of markers that may indicate differentiation into the ovarian surface epithelium (cytokeratin 18 and vimentin), granulosa (cytokeratin 18 and E-cadherin), or germ cells (alkaline phosphatase, etc.). The differentiation into germ cells was aberrant [55].

In contrast to the results obtained during the study of CD44+ / CD24- breast cancer stem cells, the data obtained by H. Jiang et al. (2012) show that in ascites transformation of CSCs occurs with formation of a tumor subclone, referred to as side population (SP) cells. This cell population is more differentiated and does not correspond to primary cancer cells (non-SP cells), which is probably due to epithelial – mesenchymal transition (EMT) [27]. In addition, the authors showed that SP ovarian cancer cells showed a lower invasive potential. In contrast, non-SP ovarian cancer cells presumably have greater migration and invasive properties. The authors of the study made a reasonable assumption that SP cells can be responsible for the interaction between the tumor and tumor microenvironment, which is also determined by their lateral / edge localization in the tumor focus [28].

A number of questions remain, including whether the metastatic potential of single cells and spheroids is the same.

MECHANISMS OF SPHEROID FORMATION IN ASCITIC FLUID IN OVARIAN CANCER

One hypothesis suggests that multicellular spheroids arise from single cells that aggregate in the abdominal cavity [56]. It can be assumed that not all cells have the ability to aggregate and, perhaps, aggregation occurs only among cells with certain properties. For example, CD44 expression through homotypic interactions is known to mediate tumor cell aggregation and polyclonal metastasis in patient-derived xenograft models of breast cancer [57]. The intercellular adhesion molecule E-cadherin appears to play a crucial role in spheroid formation. Indeed, higher expression of E-cadherin was generally associated with denser and more compact spheroids [58]. MUC16 and integrin β1were also shown to be involved in spheroid formation [59]. The role of endogenous fibronectin (FN1) in the process of metastasis was previously demonstrated in experimental models of ovarian cancer. Using *in vitro* model, H.A. Kenny et al. [60] and M.P. Iwanicki et al. [61] showed that FN1, which is either secreted by mesothelial cells or ovarian cancer cells, is necessary for tumor spheroids formed by ovarian cancer cells to survive in the absence of fixation and in an unsuitable metabolic environment.

An alternative mechanism of spheroid formation discussed by some authors is that cells separate from the primary tumor in whole groups (layers of cells), subsequently forming spheroids [62–64]. The authors report that spheroids predominantly form as a result of multicellular detachment from the primary tumor and are responsible for the development of peritoneal carcinomatosis. In addition, it was shown that detached spheroids after implantation and proliferation of tumor cells form morphological structures corresponding or similar to the patterns of the primary tumor, while possessing immunophenotypic heterogeneity.

The proportion of tumor cells in spheroids is poorly understood. Indeed, ascites spheroids in ovarian cancer are usually described as heterogeneous cell complexes consisting of a small number of tumor cells and various types of non-tumor cells [65–68]. In addition, the proportion of cancer cells in the entire ascites varies in patients and is reported to range from 1% [69] to approximately 8% [52] of the total cellular component of malignant ascites.

The role of fibroblasts and macrophages in the formation of tumor spheroids is described in sufficient detail in the review by M. Rakina et al., which also discusses the specific functions of fibroblasts, macrophages, and T cells in tumor proliferation and implantation in the peritoneum [70].

In Fig. 1, we presented our own scheme of the way tumor spheroids, which are a part of malignant ascites in ovarian cancer, are formed. On the basis of the literature data and our own studies, we can assume two main mechanisms of tumor spheroid formation. The first mechanism is due to the proliferation of single CSCs followed by the formation of a spherical structure. The second mechanism involves the detachment of a cell layer containing stem cells from the primary tumor (Fig. 1). Subsequently, tumor fibroblasts and M2 macrophages are attached to the spheroid, and adhesion of non-stem cells to the formed structure occurs, followed by the dissemination through the abdominal cavity.

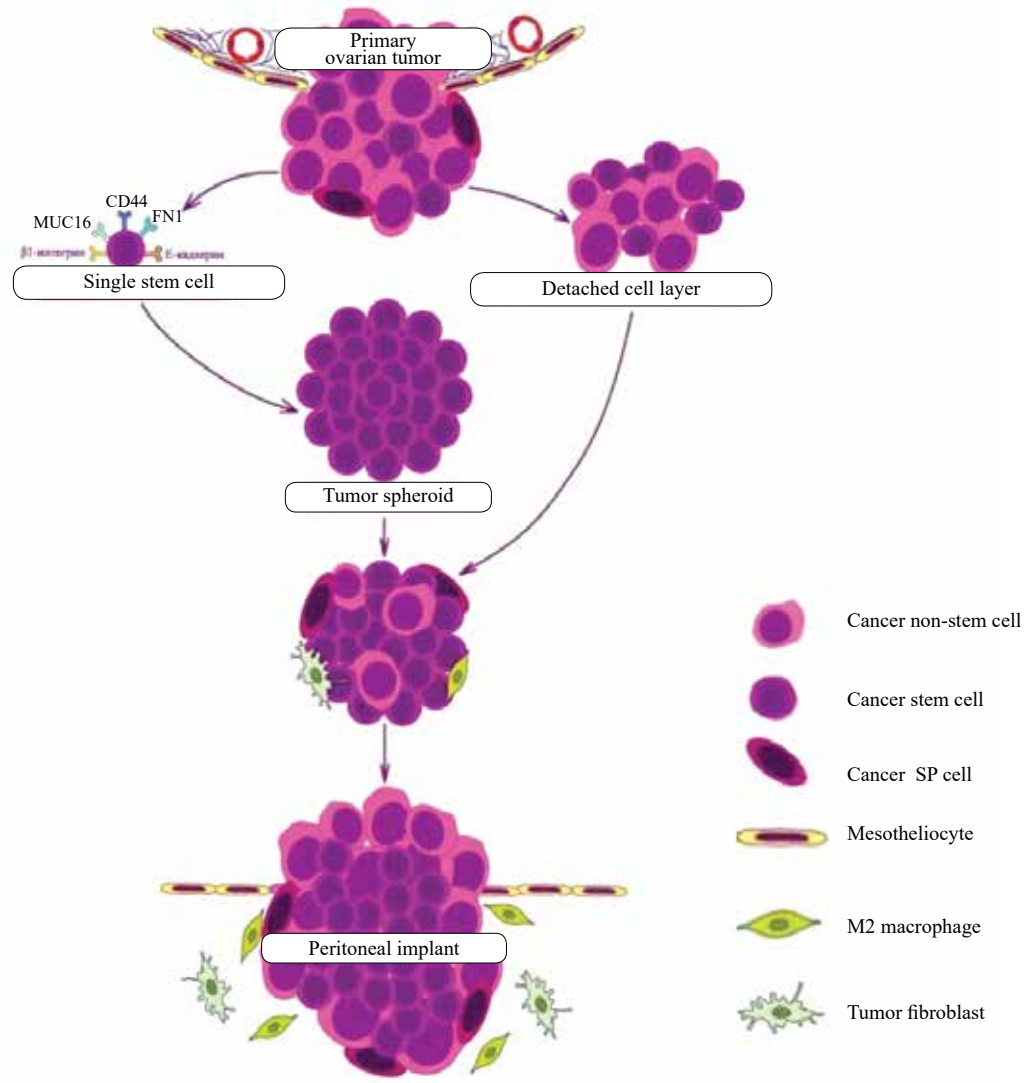

Fig. 1. A contemporary view on the formation of tumor spheroids as a part of malignant ascites in ovarian cancer

CHEMORESISTANCE OF CSCS AND STRATEGIES TO OVERCOME IT IN OVARIAN CANCER

The property of excreting cytotoxic substances from their cytoplasm is characteristic of CSCs, and on the basis of this property it is possible to identify them. This property was used in the isolation of CSCs by fluorescence-assisted cell sorting (FACS). In *in vitro* and *in vivo* experimental models, cells were incubated with a dye and separated into different fractions using FACS based on their ability to retain the dye. It was shown that cells that excreted most of the dye had more pronounced stemness traits compared to the rest of the cells. This method was first used to isolate tumor-initiating cells in acute myeloid leukemia [71]. Resistance to cisplatin, topotecan, and docetaxel was described in tumor cells forming spheroids [72].

Stimulation of CSC differentiation can be a rather promising approach to ovarian cancer therapy. Chemotherapy regimens targeting CSCs may be ineffective since the possibility of proliferation and dedifferentiation of daughter CSCs can replace the population of eradicated therapy-sensitive CSCs. Currently, there are developed approaches to differentiation therapy, for example, using all-trans-retinoic acid in the treatment of acute promyelocytic leukemia [73]. Similar strategies using bone morphogenetic proteins proved effective in experimental therapy of gliomas, which led to a decrease in the number of CSCs [74].

Some studies discussed that fasudil treatment for lateral osteosarcoma in murine models induced de-differentiation of some CSCs caused by the implantation of a cell-line with an inhibited *c-Myc* gene (osteosarcoma-mimicking cells). These cells were capable of trilinear differentiation (into osteocytes, chondrocytes, and adipocytes). Some of the resistant tumor cells with stem cell-like properties were transformed into adipocytes under the effect of chemotherapy, thereby contributing to tumor pathomorphosis [75]. In the literature, there are no data on differentiating agents for ovarian CSCs, but it was shown that mullerian inhibitory substance (MIS) or its mimetic SP600125 specifically inhibit CD44+CD24+Epcam+ CSCs in ovarian cancer cell lines derived from ascites cells [27].

The point of impact for systemic therapy for ovarian cancer, which is aimed at suppressing stem cell-like properties can be various signaling pathways regulating stemness. For example, one of the mechanisms for the development of chemoresistance of spheroids derived from the culture of tumor cells in malignant ascites was demonstrated *in vitro*. It consists in the transition of these cellular structures into the quiescent stage (G0 phase) by reducing the synthesis of B-protein kinases due to inhibition of *AKT* (alpha serine / threonine-protein kinase) gene, which led to increased expression of p130/ RBL2 and p27Kip1 and a decreased SKP2 level. Subsequently, it was shown that after spheroid adhesion on the surface optimal for implantation, activation of the AKT signaling pathway occurs, thereby triggering tumor cell invasion and proliferation [76]. Two AKT inhibitors, capivasertib and ipatasertib, are currently undergoing phase III clinical trials for cancer treatment [77].

A strategy based on destroying or preventing spheroid formation also seems quite promising. Inhibition of another known Hedgehog signaling pathway by cyclopamine resulted in the induction of a 10-fold decrease in spheroid formation in ovarian cancer cell lines [78]. Nectin-4 peptide 10 (N4-P10) is known to lead to rapid disruption of spheroid formation in ovarian cancer [78]. The study by S. Rafehi et al. showed that spheroid formation from cells isolated from ascites of ovarian cancer patients was impaired by SB-431542, which made the cells susceptible to carboplatin-induced cell death [79].

Interaction of tumor and non-tumor cells within spheroids could be another possible application point for therapy. Paracrine activation of Wnt during the interaction of CSCs and M2 macrophages represents a positive feedback loop, which probably contributes to the formation of a more aggressive tumor cell phenotype [38], which makes the Wnt pathway a potential target for CSC suppression. In addition, studies showed that catumaxomab eliminates CD133+ / EpCAM+ CSCs by activating T cells in ascites in advanced ovarian cancer [80].

In Figure 2, we presented a scheme describing several strategies to overcome CSC chemoresistance in ovarian cancer.

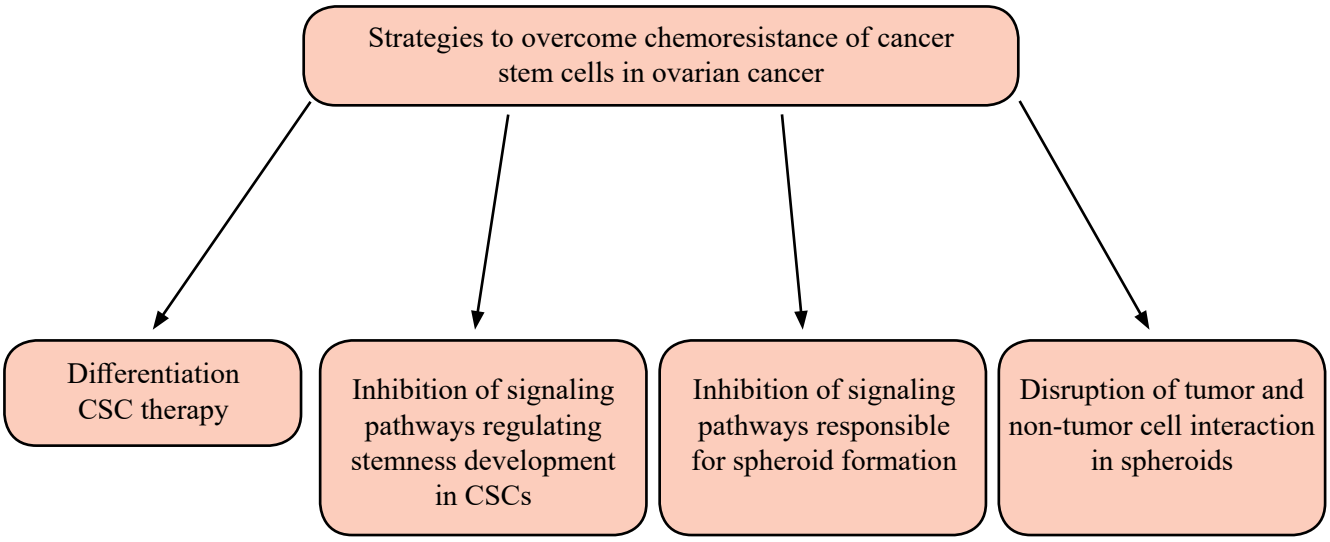

Fig. 2. Strategies to overcome chemoresistance of cancer stem cells in ovarian cancer

CONCLUSION

Future ovarian cancer treatment strategies will be based on the study of signaling pathways in ovarian CSCs, mechanisms of spheroid formation, as well as the contribution of immune cells to the acquisition of stem cell-like properties by tumor cells. It is also important to highlight the possibility of using prognostic biomarkers based on the determination of CSCs. This can be extremely promising in modifying approaches to predict ovarian cancer outcomes and individualize chemotherapy with current treatment regimens.

Considering that CSCs can mediate chemoresistance in ovarian cancer, evaluation of the stem cell-like properties of tumor cells in ascites will allow to quickly predict the efficacy of ongoing therapy in patients. However, identification of CSCs remains the main challenge. Numerous studies show that subpopulations of ovarian cancer cells were found to express stemness markers at very different levels in various combinations, with none of these markers being obligatory. These data confirm the phenomenon of tumor plasticity, which researchers have begun to be study recently, and which requires further research in clinical practice.

REFERENCES

1. Motohara T., Masuda K., Morotti M., Zheng Y., El-Sahhar S., Chong K.Y. et al. An evolving story of the metastatic voyage of ovarian cancer cells: Cellular and molecular orchestration of the adipose-rich metastatic microenvironment. *Oncogene*. 2019;38(16):2885–2898. DOI: 10.1038/s41388-018-0637-x.
2. Ahmed N., Abubaker K., Findlay J.K. Ovarian cancer stem cells: Molecular concepts and relevance as therapeutic targets. *Mol. Asp. Med.* 2014;39:110–125. DOI: 10.1016/j.mam.2013.06.002.
3. Horst D., Kriegl L., Engel J., Kirchner T., Jung A. Prognostic significance of the cancer stem cell markers CD133, CD44, and CD166 in colorectal cancer. *Cancer Investigation.* 2009;27(8):844–850. DOI: 10.1080/07357900902744502.
4. Yan Y., Zuo X., Wei D. Concise Review: Emerging Role of CD44 in Cancer Stem Cells: A Promising Biomarker and Therapeutic Target. *Stem Cells Translational Medicine.* 2015;4(9):1033–1043. DOI: 10.5966/sctm.2015-0048.
5. Lee Y.J., Wu C.C., Li J.W., Ou C.C., Hsu S.C., Tseng H.H. et al. A rational approach for cancer stem-like cell isolation and characterization using CD44 and prominin-1(CD133) as selection markers. *Oncotarget.* 2016;7(48):78499–78515. DOI: 10.18632/oncotarget.12100.
6. Gao M.Q., Choi Y.P., Kang S., Youn J.H., Cho N.H. CD24+ cells from hierarchically organized ovarian cancer are enriched in cancer stem cells. *Oncogene.* 2010;29(18):2672–2680. DOI: 10.1038/onc.2010.35.
7. Zhang S., Balch C., Chan M.W., Lai H.C., Matei D., Schilder J.M. et al. Identification and characterization of ovarian cancer-initiating cells from primary human tumors. *Cancer Res.* 2008;68(11):4311–4320. DOI: 10.1158/0008-5472.CAN-08-0364.
8. Li Z., Block M.S., Vierkant R.A., Fogarty Z.C., Winham S.J., Visscher D.W. et al. The inflammatory microenvironment in epithelial ovarian cancer: a role for TLR4 and MyD88 and related proteins. *Tumour Biology: the Journal of the International Society for Oncodevelopmental Biology and Medicine*. 2016;37(10):13279–13286. DOI: 10.1007/s13277-016-5163-2.
9. Burns K., Clatworthy J., Martin L., Martinon F., Plumpton C., Maschera B. et al. Tollip, a new component of the IL-1RI pathway, links IRAK to the IL-1 receptor. *Nature Cell Biology*. 2000;2(6):346–351. DOI: 10.1038/35014038.
10. López J., Valdez-Morales F.J., Benítez-Bribiesca L., Cerbón M., Carrancá A.G. Normal and cancer stem cells of the human female reproductive system. *Reproductive Biology and Endocrinology*. 2013;11:53. DOI: 10.1186/1477-7827-11-53.
11. Spizzo G., Went P., Dirnhofer S., Obrist P., Moch H., Baeuerle P.A. et al. Overexpression of epithelial cell adhesion molecule (Ep-CAM) is an independent prognostic marker for reduced survival of patients with epithelial ovarian cancer. *Gynecologic Oncology*. 2006;103(2):483–488. DOI: 10.1016/j.ygyno.2006.03.035.
12. Chang B., Liu G., Xue F., Rosen D.G., Xiao L., Wang X. et al. ALDH1 expression correlates with favorable prognosis in ovarian cancers. *Modern Pathology: an Official Journal of the United States and Canadian Academy of Pathology.* 2009;22(6):817–823. DOI: 10.1038/modpathol.2009.35.
13. Deng S., Yang X., Lassus H., Liang S., Kaur S., Ye Q. et al. Distinct expression levels and patterns of stem cell marker, aldehyde dehydrogenase isoform 1 (ALDH1), in human epithelial cancers. *PLoS One*. 2010;5(4):e10277. DOI: 10.1371/journal.pone.0010277.
14. Cioffi M., D'Alterio C., Camerlingo R., Tirino V., Consales C., Riccio A. et al. Identification of a distinct population of CD133(+)CXCR4(+) cancer stem cells in ovarian cancer. *Sci. Report*. 2015;5:10357. DOI: 10.1038/srep10357.
15. Kajiyama H., Shibata K., Terauchi M., Ino K., Nawa A., Kikkawa F. Involvement of SDF-1alpha/CXCR4 axis in the enhanced peritoneal metastasis of epithelial ovarian carcinoma. *International Journal of Cancer.* 2008;122(1):91–99. DOI: 10.1002/ijc.23083.
16. Krohn A., Song Y.H., Muehlberg F., Droll L., Beckmann C., Alt E. CXCR4 receptor positive spheroid forming cells are responsible for tumor invasion *in vitro. Cancer Letters.* 2009;280(1):65–71. DOI: 10.1016/j.canlet.2009.02.005.
17. Rodda D.J., Chew J.L., Lim L.H., Loh Y.H., Wang B., Ng H.H. et al. Transcriptional regulation of nanog by OCT4 and SOX2. *J. Biol. Chem.* 2005;280(26):247317. DOI: 10.1074/jbc.M502573200.
18. Alemohammad H., Asadzadeh Z., Motafakker Azad R., Hemmat N., Najafzadeh B., Vasefifar P. et al. Signaling pathways and microRNAs, the orchestrators of NANOG activity during cancer induction. *Life Sci*. 2020;260:118337. DOI: 10.1016/j.lfs.2020.118337.
19. Lin F.K., Chui Y.L. Generation of induced pluripotent stem cells from mouse cancer cells. *Cancer Biother. Radiopharm*. 2012;27(10):694–700. DOI: 10.1089/cbr.2012.1227.

20. Kaufhold S., Garbán H., Bonavida B. Yin Yang 1 is associated with cancer stem cell transcription factors (SOX2, OCT4, BMI1) and clinical implication. *J. Exp. Clin. Cancer Res.* 2016;35:84. DOI: 10.1186/s13046-016-0359-2.
21. Stevanovic M., Zuffardi O., Collignon J., Lovell-Badge R., Goodfellow P. The cDNA sequence and chromosomal location of the human SOX2 gene. *Mamm. Genome.* 1994;5(10):640–642. DOI: 10.1007/BF00411460.
22. Peng S., Maihle N.J., Huang Y. Pluripotency factors Lin28 and Oct4 identify a sub-population of stem cell-like cells in ovarian cancer. *Oncogene.* 2010;29(14):2153–2159. DOI: 10.1038/onc.2009.500.
23. Baba T., Convery P.A., Matsumura N., Whitaker R.S., Kondoh E., Perry T. et al. Epigenetic regulation of CD133 and tumorigenicity of CD133+ ovarian cancer cells. *Oncogene.* 2009;28(2):209–218. DOI: 10.1038/onc.2008.374.
24. Curley M.D., Therrien V.A., Cummings C.L., Sergent P.A., Koulouris C.R., Friel A.M. et al. CD133 expression defines a tumor initiating cell population in primary human ovarian cancer. *Stem Cells*. 2009;27(12):2875–2883. DOI: 10.1002/stem.236.
25. Silva I.A., Bai S., McLean K., Yang K., Griffith K., Thomas D. et al. Aldehyde dehydrogenase in combination with CD133 defines angiogenic ovarian cancer stem cells that portend poor patient survival. *Cancer Res*. 2011;71(11):3991–4001. DOI: 10.1158/0008-5472.CAN-10-3175.
26. Wei X., Dombkowski D., Meirelles K., Pieretti-Vanmarcke R., Szotek P.P., Chang H.L. et al. Mullerian inhibiting substance preferentially inhibits stem/progenitors in human ovarian cancer cell lines compared with chemotherapeutics. *Proc. Natl. Acad. Sci. U S A.* 2010;107(44):18874–18879. DOI: 10.1073/pnas.1012667107.
27. Jiang H., Lin X., Liu Y., Gong W., Ma X., Yu Y. et al. Transformation of epithelial ovarian cancer stemlike cells into mesenchymal lineage via EMT results in cellular heterogeneity and supports tumor engraftment. *Mol. Med*. 2012;18(1):1197–1208. DOI: 10.2119/molmed.2012.00075.
28. Motohara T., Masuko S., Ishimoto T., Yae T., Onishi N., Muraguchi T. et al. Transient depletion of p53 followed by transduction of c-Myc and K-Ras converts ovarian stem-like cells into tumor-initiating cells. *Carcinogenesis*. 2011;32(11):1597–1606. DOI: 10.1093/carcin/bgr183.
29. Gao M.Q., Choi Y.P., Kang S., Youn J.H., Cho N.H. CD24+ cells from hierarchically organized ovarian cancer are enriched in cancer stem cells. *Oncogene.* 2010;29(18):2672–2680. DOI: 10.1038/onc.2010.35.
30. Kaigorodova E.V., Fedulova N.V., Ochirov M.O., Dyakov D.A., Molchanov S.V., Chasovskikh N.Yu. Dissimilar tumor cell populations in ascitic fluid of ovarian cancer patients. *Bulletin of Siberian Medicine*. 2020;19(1):50–58 (in Russ.). DOI: 10.20538/1682-0363-2020-1-50-58.
31. Kaigorodova E.V., Ochirov M.O., Molchanov S.V., Rogachev R.R., Dyakov D.D., Chernyshova A.L., et al. Dissimilar populations of EpCam-positive cells in ascitic fluid of ovarian cancer patients: a relationship with the degree of carcinomatosis. *Bulletin of Siberian Medicine.* 2021;20(2):44–53 (in Russ.). DOI: 10.20538/1682-0363-2021-2-44-53.
32. Wang Z., Yang L., Huang Z., Li X., Xiao J., Qu Y. et al. Identification of prognosis biomarkers for high-grade serous ovarian cancer based on stemness. *Front. Genet*. 2022;13:861954. DOI: 10.3389/fgene.2022.861954.
33. Bai S., Ingram P., Chen Y.C., Deng N., Pearson A., Niknafs Y.S. et al. EGFL6 regulates the asymmetric division, maintenance, and metastasis of ALDH+ ovarian cancer cells. *Cancer Res.* 2016;76(21):6396–6409. DOI: 10.1158/0008-5472.CAN-16-0225.
34. Wang K., Wang Y., Wang Y., Liu S., Wang C., Zhang S. et al. EIF5A2 enhances stemness of epithelial ovarian cancer cells via a E2F1/KLF4 axis. *Stem Cell Res. Ther*. 2021;12(1):186. DOI: 10.1186/s13287-021-02256-2.
35. Giordano M., Decio A., Battistini C., Baronio M., Bianchi F., Villa A. et al. L1CAM promotes ovarian cancer stemness and tumor initiation via FGFR1/SRC/STAT3 signaling. *J. Exp. Clin. Cancer Res*. 2021;40(1):319. DOI: 10.1186/s13046-021-02117-z.
36. Zhang Y., Wang Y., Zhao G., Tanner E.J., Adli M., Matei D. FOXK2 promotes ovarian cancer stemness by regulating the unfolded protein response pathway. *J. Clin. Invest*. 2022;132(10):151591. DOI: 10.1172/JCI151591.
37. Schwitalla S., Fingerle A.A., Cammareri P., Nebelsiek T., Göktuna S.I., Ziegler P.K. et al. Intestinal tumorigenesis initiated by dedifferentiation and acquisition of stem-cell-like properties. *Cell.* 2013;152(1-2):25–38. DOI: 10.1016/j.cell.2012.12.012.
38. Raghavan S., Mehta P., Xie Y., Lei Y.L., Mehta G. Ovarian cancer stem cells and macrophages reciprocally interact through the WNT pathway to promote pro-tumoral and malignant phenotypes in 3D engineered microenvironments. *J. Immunother. Cancer*. 2019;7(1):190. DOI: 10.1186/s40425-019-0666-1.
39. Zhang S., Balch C., Chan M.W., Lai H.C., Matei D., Schilder J.M. et al. Identification and characterization of ovarian cancer-initiating cells from primary human tumors. *Cancer Res.* 2008;68(11):4311–4320. DOI: 10.1158/0008-5472.CAN-08-0364.
40. Lau W., Peng W.C., Gros P., Clevers H. The R-spondin/Lgr5/Rnf43 module: regulator of Wnt signal strength. *Genes Dev.* 2014;28(4):305–316. DOI: 10.1101/gad.235473.113.
41. Gening S.O., Abakumova T.V., Antoneeva I.I., Rizvanov A.A., Gening T.P., Gufurbayeva D.U. Stem-like tumor cells and proinflammatory cytokines in the ascitic fluid of patients with ovarian cancer. *Russian Clinical Laboratory Diagnostics*. 2021;66(5):297–303 (in Russ.). DOI: 10.51620/0869-2084-2021-66-5-297-303.
42. Meirelles K., Benedict L.A., Dombkowski D., Pepin D., Preffer F.I., Teixeira J. et al. Human ovarian cancer stem/progenitor cells are stimulated by doxorubicin but inhibited by Mullerian inhibiting substance. *Proceedings of the National Academy of Sciences of the United States of America.* 2012;109(7):2358–2363. DOI: 10.1073/pnas.1120733109.
43. Bourguignon L.Y., Peyrollier K., Xia W., Gilad E. Hyaluronan-CD44 interaction activates stem cell marker Nanog, Stat- 3-mediated MDR1 gene expression, and ankyrin-regulated multidrug efflux in breast and ovarian tumor cells. *The Journal of Biological Chemistry.* 2008;283(25):17635–17651. DOI: 10.1074/jbc.M800109200.

44. Xia M., Overman M.J., Rashid A., Chatterjee D., Wang H., Katz M.H. et al. Expression and clinical significance of epidermal growth factor receptor and insulin-like growth factor receptor 1 in patients with ampullary adenocarcinoma. *Human Pathology*. 2015;46(9):1315–1322. DOI: 10.1016/j.humpath.2015.05.012.
45. Garson K., Vanderhyden B.C. Epithelial ovarian cancer stem cells: underlying complexity of a simple paradigm. *Reproduction*. 2015;149(2):59–70. DOI: 10.1530/REP-14-0234.
46. Jäger M., Schoberth A., Ruf P., Hess J., Hennig M., Schmalfeldt B. et al. Immunomonitoring results of a phase II/III study of malignant ascites patients treated with the trifunctional antibody catumaxomab (anti-EpCAM x anti-CD3). *Cancer Res*. 2012;72(1):24–32. DOI: 10.1158/0008-5472.CAN-11-2235.
47. Akhter M.Z., Sharawat S.K., Kumar V., Kochat V., Equbal Z., Ramakrishnan M. et al. Aggressive serous epithelial ovarian cancer is potentially propagated by EpCAM+CD45+ phenotype. *Oncogene*. 2018;37(16):2089–2103. DOI: 10.1038/s41388-017-0106-y.
48. Wicha M.S., Liu S., Dontu G. Cancer stem cells: an old idea – a paradigm shift. *Cancer Res.* 2006;66(4):1883–1890. DOI: 10.1158/0008-5472.CAN-05-3153.
49. Kaigorodova E.V., Kovalev O.V., Chernyshova A.L., Vtorushin S.V., Shpileva O.V. Heterogeneity of EpCAM-positive cells in low-grade serous ovarian carcinoma ascitic fluid: a clinical case. *Tumors of Female Reproductive System.* 2021;17(4):90–95 (in Russ.). DOI: 10.17650/1994-4098-2021-17-4-90-95.
50. Kozik A.V., Kaigorodova E.V., Grishchenko M.Yu., Vtorushin S.V., Chernyshova A.L. EPCAM+CD45+ cells in ascitic fluid of patients with ovarian cancer: a relationship with tumor marker levels and tumor grade. *Siberian Journal of Oncology.* 2022;21(5):44–51 (in Russ.). DOI: 10.21294/1814-4861-2022-21-5-44-51.
51. Kaigorodova E.V., Kozik A.V., Zavaruev I.S. Grishchenko M.Y. Hybrid/atypical forms of circulating tumor cells: current state of the art. *Biochemistry Moscow.* 2022;87(4):380–390. DOI: 10.1134/S0006297922040071.
52. Izar B., Tirosh I., Stover E.H., Wakiro I., Cuoco M.S., Alter I. et al. A single-cell landscape of high-grade serous ovarian cancer. *Nature Medicine.* 2020;26(8):1271–1279. DOI: 10.1038/s41591-020-0926-0.
53. Wu X., Liu X., Koul S., Lee C.Y., Zhang Z., Halmos B. AXL kinase as a novel target for cancer therapy. *Oncotarget.* 2014;5(20):9546–9563. DOI: 10.18632/oncotarget.2542.
54. Shield K., Ackland M.L., Ahmed N., Rice G.E. Multicellular spheroids in ovarian cancer metastases: Biology and pathology. *Gynecologic Oncology.* 2009;113(1):143–148. DOI: 10.1016/j.ygyno.2008.11.032.
55. Bapat S.A., Mali A.M., Koppikar C.B., Kurrey N.K. Stem and progenitor-like cells contribute to the aggressive behavior of human epithelial ovarian cancer. *Cancer Res.* 2005;65(8):3025–3029. DOI: 10.1158/0008-5472.CAN-04-3931.
56. Shield K., Ackland M.L., Ahmed N., Rice G.E. Multicellular spheroids in ovarian cancer metastases: biology and pathology. *Gynecol. Oncol.* 2009;113(1):143–148. DOI: 10.1016/j.ygyno.2008.11.032.
57. Liu X., Taftaf R., Kawaguchi M., Chang Y.F., Chen W., Entenberg D. et al. Homophilic CD44 interactions mediate tumor cell aggregation and polyclonal metastasis in patient-derived breast cancer models. *Cancer Discov*. 2019;9(1):96–113. DOI: 10.1158/2159-8290.CD-18-0065.
58. Xu S., Yang Y., Dong L., Qiu W., Yang L., Wang X. et al. Construction and characteristics of an E-cadherin-related three-dimensional suspension growth model of ovarian cancer. *Scientific Reports.* 2014;4:5646. DOI: 10.1038/srep05646.
59. Sodek K.L., Ringuette M.J., Brown T.J. Compact spheroid formation by ovarian cancer cells is associated with contractile behavior and an invasive phenotype. *International Journal of Cancer.* 2009;124(9):2060–2070. DOI: 10.1002/ijc.24188.
60. Kenny H.A., Chiang C.Y., White E.A., Schryver E.M., Habis M., Romero I.L. et al. Mesothelial cells promote early ovarian cancer metastasis through fibronectin secretion. *The Journal of Clinical Investigation.* 2014;124(10):4614–4628. DOI: 10.1172/JCI74778.
61. Iwanicki M.P., Chen H.Y., Iavarone C., Zervantonakis I. K., Muranen T., Novak M. et al. Mutant p53 regulates ovarian cancer transformed phenotypes through autocrine matrix deposition. *JCI Insight.* 2016;1(10):e86829. DOI: 10.1172/jci.insight.86829.
62. Lengyel E. Ovarian cancer development and metastasis. *Am. J. Pathol.* 2010;177(3):1053–1064. DOI: 10.2353/ajpath.2010.100105.
63. Elloul S., Elstrand M.B., Nesland J.M., Tropé C.G., Kvalheim G., Goldberg I. et al. Snail, slug, and smad-interacting protein 1 as novel parameters of disease aggressiveness in metastatic ovarian and breast carcinoma. *Cancer.* 2005;103(8):1631–1643. DOI: 10.1002/cncr.20946.
64. Veatch A.L., Carson L.F., Ramakrishnan S. Differential expression of the cell-cell adhesion molecule E-cadherin in ascites and solid human ovarian tumor cells. *International Journal of Cancer*. 1994;58(3):393–399. DOI: 10.1002/ijc.2910580315.
65. Latifi A., Luwor R.B., Bilandzic M., Nazaretian S., Stenvers K., Pyman J. et al. Isolation and characterization of tumor cells from the ascites of ovarian cancer patients: molecular phenotype of chemoresistant ovarian tumors. *PloS One.* 2012;7(10):e46858. DOI: 10.1371/journal.pone.0046858.
66. Fritz J.L., Collins O., Saxena P., Buensuceso A., Ramos Valdes Y., Francis K. E. et al. A novel role for NUAK1 in promoting ovarian cancer metastasis through regulation of fibronectin production in spheroids. *Cancers.* 2020;12(5):1250. DOI: 10.3390/cancers12051250.
67. Ojasalu K., Brehm C., Hartung K., Nischak M., Finkernagel F., Rexin P. et al. Upregulation of mesothelial genes in ovarian carcinoma cells is associated with an unfavorable clinical outcome and the promotion of cancer cell adhesion. *Molecular Oncology*. 2020;14(9):2142–2162. DOI: 10.1002/1878-0261.12749.
68. Reinartz S., Lieber S., Pesek J., Brandt D.T., Asafova A., Finkernagel F. et al. Cell type-selective pathways and clinical associations of lysophosphatidic acid biosynthesis and signaling in the ovarian cancer microenvironment. *Molecular Oncology*. 2019;13(2):185–201. DOI: 10.1002/1878-0261.12396.
69. Kipps E., Tan D.S., Kaye S.B. Meeting the challenge of ascites in ovarian cancer: new avenues for therapy and research. Nature reviews. *Cancer.* 2013;13(4):273–282. DOI: 10.1038/nrc3432.

70. Rakina M., Kazakova A., Villert A., Kolomiets L., Larionova I. Spheroid formation and peritoneal metastasis in ovarian cancer: the role of stromal and immune components. *International Journal of Molecular Sciences*. 2022;23(11):6215. DOI: 10.3390/ijms23116215.
71. Dick J.E., Bhatia M., Gan O., Kapp U., Wang J.C. Assay of human stem cells by repopulation of NOD/SCID mice. *Stem Cells*. 1997;15Suppl.1:199–203;discussion 204–197. DOI: 10.1002/stem.5530150826.
72. Wang L., Mezencev R., Bowen N.J., Matyunina L.V., McDonald J.F. Isolation and characterization of stem-like cells from a human ovarian cancer cell line. *Molecular and Cellular Biochemistry*. 2012;363(1-2):257–268. DOI: 10.1007/s11010-011-1178-6.
73. De Thé H. Differentiation therapy revisited. *Nat. Rev. Cancer.* 2018;18(2):117–127 DOI: 10.1038/nrc.2017.103.
74. Nayak S., Mahenthiran A., Yang Y., McClendon M., Mania-Farnell B., James C.D. et al. Bone morphogenetic protein 4 targeting glioma stem-like cells for malignant glioma treatment: latest advances and implications for clinical application. *Cancers (Basel).* 2020;12(2):516. DOI: 10.3390/cancers12020516.
75. Arima Y., Nobusue H., Saya H. Targeting of cancer stem cells by differentiation therapy. *Cancer Sci*. 2020;111(8):2689–2695. DOI: 10.1111/cas.14504.
76. Correa R.J., Peart T., Valdes Y.R., DiMattia G.E., Shepherd T.G. Modulation of AKT activity is associated with reversible dormancy in ascites-derived epithelial ovarian cancer spheroids. *Carcinogenesis.* 2012;33(1):49–58. DOI: 10.1093/carcin/bgr241.
77. Hua H., Zhang H., Chen J., Wang J., Liu J., Jiang Y. Targeting Akt in cancer for precision therapy. *Journal of Hematology & Oncology*. 2021;4(1):128. DOI: 10.1186/s13045-021-01137-8.
78. Emami K.H., Nguyen C., Ma H., Kim D.H., Jeong K.W., Eguchi M. et al. A small molecule inhibitor of beta-catenin/CREB-binding protein transcription [corrected]. *Proceedings of the National Academy of Sciences of the United States of America*. 2004;101(34):12682–12687. DOI: 10.1073/pnas.0404875101.
79. Rafehi S., Ramos Valdes Y., Bertrand M., McGee J., Préfontaine M., Sugimoto A. et al. TGFβ signaling regulates epithelial-mesenchymal plasticity in ovarian cancer ascites-derived spheroids. *Endocrine-related cancer.* 2016;23(3):147–159. DOI: 10.1530/ERC-15-0383.
80. Jäger M., Schoberth A., Ruf P., Hess J., Hennig M., Schmalfeldt B. et al. Immunomonitoring results of a phase II/III study of malignant ascites patients treated with the trifunctional antibody catumaxomab (anti-EpCAM x anti-CD3). *Cancer Research*. 2012;72(1):24–32. DOI: 10.1158/0008-5472.CAN-11-2235.

Authors' information

Kovalev Oleg I. – Post-Graduate Student, Pathological Anatomy Division, Siberian State Medical University, Tomsk, oleg.kovalev8284@gmail.com, http://orcid.org/0000-0002-6826-725X

Vtorushin Sergey V. – Head of the Department of General and Molecular Pathology, Cancer Research Institute, Tomsk NRMC; Dr. Sci. (Med.), Professor, Pathological Anatomy Division, Siberian State Medical University, Tomsk, wtorushin@rambler.ru, http://orcid.org/0000-0002-1195-4008

Kaigorodova Evgeniya V. – Dr. Sci. (Med.), Associate Professor, Leading Researcher, Department of General and Molecular Pathology, Cancer Research Institute, Tomsk NRMC; Professor, Biochemistry and Molecular Biology Division with Clinical Laboratory Diagnostics Course, Siberian State Medical University, Tomsk, zlobinae@mail.ru, http://orcid.org/0000-0003-4378-6915https://orcid.org/0000-0003-4378-6915?lang=ru

(✉) **Vtorushin Sergey V.,** wtorushin@rambler.ru

Received 08.02.2023;
approved after peer review 15.02.2023;
accepted 27.02.2023

УДК 616.98:578.834.1]-036.21-06:616.36-002.17-02
https://doi.org/10.20538/1682-0363-2023-2-134-144

Factors affecting the development of liver fibrosis in patients who experienced COVID-19

Kruchinina M.V.[1, 2], Pershina N.E.[1], Svetlova I.O.[1, 2], Kruchinina E.V.[2]

[1] *Research Institute of Internal and Preventive Medicine – branch of the Institute of Cytology and Genetics, SB RAS 175/1, B. Bogatkova Str., Novosibirsk, 630089, Russian Federation*

[2] *Novosibirsk State Medical University 52, Krasny Av., Novosibirsk, 630091, Russian Federation*

ABSTRACT

The aim of the review is to highlight the main factors affecting the development of liver fibrosis and possible mechanisms of liver damage in patients who have experienced COVID-19. A search was carried out using keywords in the Scopus, Web of Science, and PubMed databases in literary sources of the last three years on factors associated with fibrogenesis in novel coronavirus infection.

The review presents the main mechanisms of liver damage in COVID-19: direct effects on hepatocytes and cholangiocytes, hypoxia, and immune-mediated and drug-induced damage. We analyzed the significance of factors affecting fibrosis development in patients with COVID-19: chronic diffuse liver diseases, against which COVID-19 occurs, such as non-alcoholic fatty liver disease, alcohol-associated liver disease, chronic hepatitis B, C, and cirrhosis of the liver.

Damage to the liver in coronavirus infection develops by several mechanisms. The development of COVID-19 against the background of diffuse liver pathology of various genesis is associated with progression of these diseases (increased fibrogenesis) and a poorer prognosis.

Keywords: factors, liver fibrosis, COVID-19

Conflict of interest. The authors declare the absence of obvious and potential conflicts of interest related to the publication of this article.

Source of financing. The study was carried pit within the topic of the state assignment “Epidemiological monitoring of the population health and study of molecular genetic and biological mechanisms of development of common internal diseases in Siberia to improve their diagnosis, prevention, and treatment” (No. 122031700094-5).

For citation: Kruchinina M.V., Pershina N.E., Svetlova I.O., Kruchinina E.V. Factors affecting the development of liver fibrosis in patients who experienced COVID-19. *Bulletin of Siberian Medicine.* 2023;22(2):134–144. https://doi.org/10.20538/1682-0363-2023-2-134-144.

✉ *Kruchinina Margarita V.,* kruchmargo@yandex.ru

Факторы, влияющие на развитие фиброза печени, у пациентов, перенесших COVID-19

Кручинина М.В.[1, 2], Першина Н.Е.[1], Светлова И.О.[1, 2], Кручинина Э.В.[2]

[1] Научно-исследовательский институт терапии и профилактической медицины (НИИТПМ) – филиал «Федеральный исследовательский центр Институт цитологии и генетики Сибирского отделения Российской академии наук» (ИЦиГ СО РАН)
Россия, 630089, г. Новосибирск, Б. Богаткова 175/1

[2] Новосибирский государственный медицинский университет (НГМУ)
Россия, 630091, г. Новосибирск, Красный проспект, 52

РЕЗЮМЕ

Цель обзора – осветить основные факторы, влияющие на развитие фиброза печени, и возможные механизмы повреждения печени у пациентов, перенесших COVID-19. Проведен поиск с использованием ключевых слов в текстовых базах данных Scopus, Web of Science, PubMed по литературным источникам последних 3 лет о факторах, ассоциированных с фиброгенезом, при коронавирусной инфекции.

Представлены основные механизмы повреждения печени при COVID-19: прямое воздействие на гепатоциты, холангиоциты, гипоксическое, иммуноопосредованное, лекарственно-индуцированное повреждение. Проведен анализ значимости факторов развития фиброза у пациентов, перенесших коронавирусную инфекцию: хронические диффузные заболевания печени, на фоне которых протекает COVID-19: неалкогольная жировая болезнь печени, алкоголь-ассоциированная болезнь печени, хронические вирусные гепатиты B, C, цирроз печени.

Поражение печени при коронавирусной инфекции развивается по нескольким механизмам. Развитие COVID-19 на фоне диффузной патологии печени различного генеза ассоциировано с прогрессированием этих заболеваний (усиление фиброгенеза), худшим прогнозом.

Ключевые слова: факторы, фиброз печени, COVID-19

Конфликт интересов. Авторы декларируют отсутствие явных и потенциальных конфликтов интересов, связанных с публикацией настоящей статьи.

Источник финансирования. Работа выполнена в рамках темы госзадания «Эпидемиологический мониторинг состояния здоровья населения и изучение молекулярно-генетических и молекулярно-биологических механизмов развития распространенных терапевтических заболеваний в Сибири для совершенствования подходов к их диагностике, профилактике и лечению» (№ 122031700094-5).

Для цитирования: Кручинина М.В., Першина Н.Е., Светлова И.О., Кручинина Э.В. Факторы, влияющие на развитие фиброза печени, у пациентов, перенесших COVID-19. *Бюллетень сибирской медицины.* 2023;22(2):134–144. https://doi.org/10.20538/1682-0363-2023-2-134-144.

INTRODUCTION

A new coronavirus outbreak with an epicentre in the City of Wuhan, Hubei province, is known to have occurred in the People's Republic of China (PRC) in late 2019. On February 11 2020, the World Health Organization (WHO) defined the official name of the infection caused by the new coronavirus – COVID-19 (Coronavirus disease 2019) [1]. Within several months the coronavirus infection swept the globe, and it continues to spread. According to the available data as of March 2022, 436,520,897 cases were registered worldwide, of which 16,398,036 cases were confirmed in the Russian Federation.

People of all ages and with any health condition are at risk of contracting SARS-CoV-2. Risk factors for severe disease and mortality have been identified. They include old age, coexisting chronic pathologies, such as diabetes mellitus, cancer, obesity, cardiopulmonary disease, and chronic kidney disease, as well as features of the living conditions (e.g. residents of long-term care facilities) [2].

SARS-CoV-2 is an enveloped virus with a positive-sense single-stranded RNA belonging to the Coronaviridae family, *Betacoronavirus* genus, *Sarbecovirus* subgenus. This name is associated with the structure of the virus: large thorny spikes in the form of a mace, which resemble a crown, exit the supercapsid. The nucleocapsid is a flexible spiral consisting of a positive strand of RNA and a large number of nucleoprotein N molecules. The supercapsid contains spike (S) glycoprotein, membrane (M) protein, small envelope (E) protein, and hemagglutinin esterase (HEs) (Fig. 1) [1, 3].

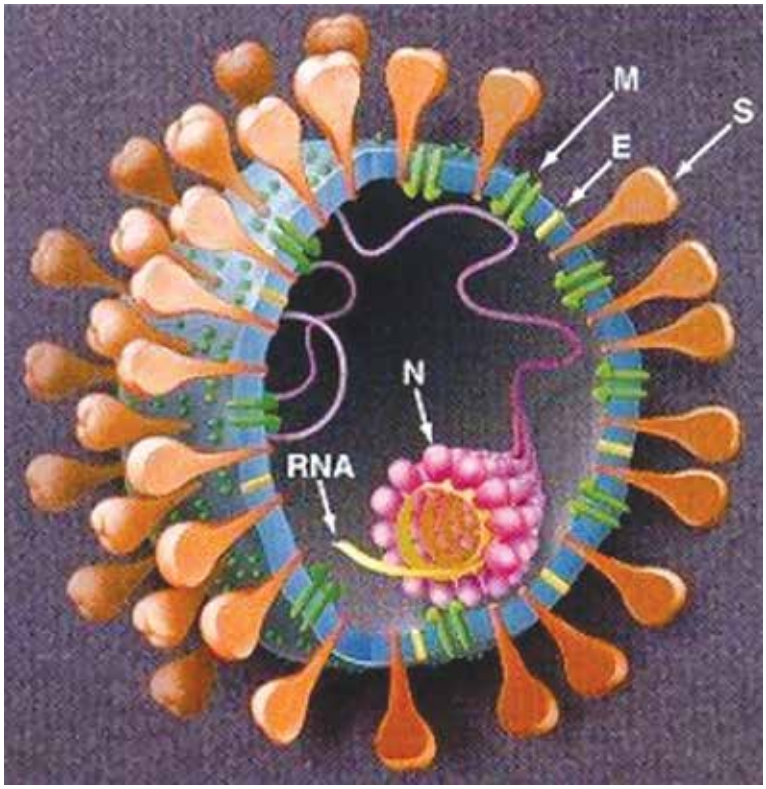

Fig. 1. A model of the coronavirus structure, showing the location of spikes (S), membrane glycoproteins (M), and the envelope (E). The RNA is protected by a spiral capsid of protein (N) monomers [4]

The entry gateway of infection is the epithelium of the upper respiratory tract and epithelial cells of the stomach and intestines [1]. The clinical presentation includes fever and symptoms of acute respiratory infections (nasal congestion, sore throat, dry cough, anosmia, myalgia), as well as cardiovascular and hemostatic disorders, and damage to the gastrointestinal tract (decreased appetite, vomiting, nausea, diarrhoea) [5].

The assessment of the course of the disease in 74 patients with COVID-19 who had gastrointestinal complaints showed that severe and critical infections occurred significantly more frequently (22.97 and 31.08%, respectively) than in individuals without such symptoms (8.14 and 20.45%, respectively) [6].

The liver is the second most frequently affected internal organ in COVID-19 after the lungs [7]. With increasing numbers of cases and further studies, biochemical parameters, such as serum alanine aminotransferase (ALT), aspartate aminotransferase (AST), gamma-glutamyl transferase (GGT), and alkaline phosphatase (ALP), have been shown to be significantly elevated in many patients with COVID-19, indicating hepatocellular and cholangiocellular damage [8].

Although hepatic disease does not appear to occur in the absence of pre-existing liver disease, liver damage in COVID-19 may correlate with the overall disease severity and serve as a prognostic factor for the development of acute respiratory distress syndrome (ARDS) [9].

The aim of the review was to highlight the main factors affecting the development of liver fibrosis and possible mechanisms of liver damage in patients who have experienced COVID-19.

COVID-19 INVASION PROCESS

According to W. Tai et al. (2020), the key virulence factor is the interaction of the receptor-binding domain of protein S located on the outer membrane of SARS-CoV-2 with the receptor of angiotensin-converting enzyme 2 (ACE2) activated by human transmembrane serine proteases (TMPRSS2) [10]. The ACE2 receptor, an important part of the renin – angiotensin – aldosterone system, is the entry gateway for the penetration of SARS-CoV-2 into host cells. ACE2 is located in the cytoplasmic membrane of many types of human cells, including alveolar type II epithelial cells in the lungs, enterocytes in the small intestine, endothelial cells in arteries and veins, smooth muscle cells in arteries, and macrophages. ACE2 and TMPRSS2 have been found in the tissue cells of the respiratory organs, esophagus, intestines, heart, adrenal glands, bladder, brain, etc. [1].

As airborne transmission is the main transmission route for the infection, the respiratory tract is most often affected. Therefore, with a large amount of replication of SARS-CoV-2 and accumulation of various proinflammatory cytokines and chemokines, alveolar epithelial cells can be damaged, and the integrity of the air – blood barrier can be compromised. The virus diffuses from damaged alveoli into capillaries and spreads to organs and tissues [11]. Since the liver has dual blood supply, it can be easily exposed to COVID-19. Another way of SARS-CoV-2 penetrating into the liver is also possible. After penetration of SARS-CoV-2 into the intestinal tract, it can damage the intestinal epithelium and the vascular barrier and enter the liver through the portal vein. Then SARS-CoV-2 can enter the bile via bile capillaries after the virus infects hepatocytes [8].

The mechanism of liver damage in COVID-19. Several mechanisms for the damaging effects of the novel coronavirus infection on the liver are being currently considered, such as the direct effect of SARS-CoV-2 on the liver (direct cytotoxicity due to active viral replication in liver cells), immune-mediated liver injury in the light of hyperinflammatory syndrome with cytokine storm, hypoxia (associated with lung damage), multiple organ failure, use of hepatotoxic drugs, vascular changes due to coagulopathy, endotheliitis or right ventricular heart failure, and exacerbation of the underlying liver disease, although the ultimate cause is likely to be multifactorial [9].

Hepatic damage in COVID-19 manifests itself as a moderate increase in serum AST and ALT levels, accompanied by a moderate increase in total bilirubin [10, 12, 13]. Having analyzed 79 medical histories of patients who died of coronavirus infection, J.B. Ibrayeva et al. found that a 4-fold increase in ALT and AST levels was revealed in 28 and 16% of cases, respectively. The total bilirubin level in 96.0% of patients remained within the normal range [14].

Direct effects of COVID-19 on the liver. X. Chai et al. found low expression of ACE2 in hepatocytes (2.6%), with an average expression level being 20 times lower than that in cholangiocytes [15]. Although the level of ACE2 expression in the liver is very low, the distribution of the ACE2 receptor does not correspond to the level of infection of the organ [8]. It has been shown that the virus can bind directly to ACE2-positive cholangiocytes, but not necessarily to hepatocytes [15].

Y. Wang et al. performed a liver biopsy in two deceased COVID-19 patients with elevated transaminase levels. Using transmission electron microscopy, immunohistochemistry, and postmortem studies, they found large numbers of SARS-CoV-2 particles in the cytoplasm of the liver cells in these patients [16]. The authors suggested that liver injury caused by SARS-CoV-2 is more associated with the biliary system, and to a lesser extent – with the impact of the virus on ACE2 hepatocytes. The post-mortem biopsies also revealed massive hepatic apoptosis and binuclear hepatocytes in the histologic sections, mitochondrial swelling, and dilation of the endoplasmic reticulum on transmission electron microscopy [2]. These findings suggest that liver injury in patients with SARS-CoV-2 and SARS pneumonia may be due to cholangiocyte dysfunction and other causes, such as drug-induced injury and systemic inflammation [15].

Hypoxic damage. The liver has high metabolic activity and active blood supply, which makes it particularly vulnerable to circulatory disorders [17]. The liver is sufficiently protected against ischemic damage by the dual circulatory system (almost 25% of the cardiac output that the liver receives is distributed between the portal vein and the hepatic artery). It has highly permeable sinusoids (which allows for increased diffusion of oxygen to hepatocytes) and is also able to respond to decreased cardiac blood flow by releasing adenosine and dilating the hepatic vasculature to increase hepatic blood flow [18].

As is known, COVID-19 most commonly affects the lungs; therefore, it can cause the development of respiratory failure (RF). Hypoxemia is the main hemodynamic factor in the development of hypoxic hep-

atitis in RF. Associated with RF, a very low level of oxygen partial pressure can be noted. Cardiac output and hepatic blood flow in this condition are within the normal range or even increased [19]. In addition to hypoxia, coronavirus infection can cause a number of complications, such as systemic inflammatory response syndrome and multiple organ dysfunction, which can lead to reperfusion injury [19, 20]. These two processes lead to a decrease in the oxygen content and accumulation of lipids in hepatocytes [21], which results in cell death. A subsequent increase in reactive oxygen species (ROS) and their peroxidation products can act as a secondary mediator, further enhancing the release of multiple proinflammatory factors and liver injury [17].

In addition, there is evidence that SARS-CoV-2 is capable of secreting non-structural proteins orf1ab, ORF10, and ORF3a, which easily penetrate the erythrocyte cell membrane and displace a divalent Fe atom from the porphyrin nucleus of the beta chain in hemoglobin molecules. One Fe atom is capable of transporting four oxygen molecules. Thus, hemoglobin is destroyed inside the erythrocyte. The released iron ion contributes to further oxidation of organic molecules. Hemolytic and microhemolytic anemia occurs. The authors attribute the occurrence of respiratory failure primarily to the resulting hemoglobin deficiency and the oxidative damage initiated by iron ions and haemolysis [22]. Such exposure can lead to increased inflammatory processes in the lungs, development of oxidative stress, hypoxemia, hypoxia, symptoms of acute respiratory distress syndrome, and multiple organ failure due to oxygen deficiency [23].

Immune-mediated liver injury. The spectrum of potential pathophysiological mechanisms of liver damage in COVID-19 is extensive, including immune-mediated liver damage due to a severe inflammatory response [9]. The occurrence of multiple organ failure in critically ill COVID-19 patients is mainly associated with the sudden onset of an inflammatory storm.

The so-called inflammatory (cytokine) storm, or systemic inflammatory response syndrome (SIRS), is closely linked to the activation of both humoral and cellular immunity triggered by COVID-19 infection. [12] The term “cytokine storm” refers to an immunopathological condition characterized by elevated levels of proinflammatory cytokines in the blood, such as tumour necrosis factor (TNF) , interleukin (IL)-2, IL-6, IL-7, IL-18, granulocyte colony-stimulating factor (G-CSF), granulocyte-macrophage colony-stimulating factor (GM-CSF), interferon (IFN)γ, and ferritin, as well as by impaired immune defence mechanisms, and development of life-threatening systemic reactions [17, 24].

SARS-CoV-2 binds to lung epithelial cells and induces multiple proinflammatory signals via Toll-like receptors (TLRs), as well as activation of cytotoxic T cells. After infection with SARS-CoV-2, cytotoxic T cells are rapidly activated, producing GM-CSF, IL-6, and other proinflammatory cytokines. Later, GM-CSF activates CD14+ / CD16+ inflammatory monocytes, which produce more IL-6 and other proinflammatory cytokines. Activated T lymphocytes attack infected cells of the body, leading to their apoptosis and necrosis, until the T lymphocytes are shrivelled [7].

Drug-induced liver injury. Liver injury that occurs in some patients with coronavirus infection depends on age, geographical region, severity of COVID-19 in general, and a number of other circumstances. The liver is the main organ serving as a metabolic and detoxification tool; thus, maintaining healthy liver function is crucial for the efficacy and tolerability of different COVID-19 treatment regimens [25].

Many medicines have been tested to fight against the novel coronavirus infection. Some pharmaceuticals or their combinations can cause exacerbations of chronic liver disease (CLD) and drug-induced hepatotoxicity and can interact with other medicines to increase their toxic effects on the liver.

Earlier clinical guidelines recommended the use of lopinavir / ritonavir, ribavirin, chloroquine, and hydroxychloroquine for etiotropic drug therapy for COVID-19. Currently, it is recommended to prescribe such drugs as favipiravir, molnupiravir, remdesivir, umifenovir, and interferon alpha. In addition to antiviral drugs, antipyretics, antibiotics, glucocorticoids, and genetically-engineered biological drugs (GEBD) are used [1].

It was shown that the increase in serum enzyme levels during treatment with hydroxychloroquine was low and similar to that in patients receiving placebo or reference listed drugs [26]. But in one of the cases described, a patient with severe COVID-19 pneumonia, who received hydroxychloroquine, was shown to have a 10-fold increase in the transaminase levels; these levels quickly regressed after withdrawal of this drug [27]. Tocilizumab may be the cause of the elevated transaminase level and acute liver damage in patients with COVID-19 [28]. The mechanism of drug-induced hepatotoxicity mainly includes mitochondrial dysfunction, oxidative stress, endoplasmic reticulum stress, lipodystrophy, and insulin resistance [8, 29].

Favipiravir is a synthetic antiviral l drug, a selective RNA polymerase inhibitor, which acts against RNA-containing viruses. In a study including 200 men and women with COVID-19 aged 18–80 years, L.A. Balykova et al. investigated the hepatotoxicity of favipiravir. The favipiravir group included 53 (50.96%) men and 51 (49.04%) women, and the standard therapy group encompassed 47 (49.02%) men and 55 (50.98%) women. Both groups showed an increase in both ALT (17.3 and 18.6% for the experimental and control groups, respectively) and AST (12.5 and 12.7%, respectively). Thus, favipiravir itself does not lead to an increase in the level of transaminases, and their increase is most likely due to other factors [1, 30].

Lopinavir / ritonavir is a combination antiviral medication, a protease inhibitor of human immunodeficiency virus. This drug is mainly metabolized in the liver, first of all through cytochrome P450 (CYP). This pathway produces a toxic intermediate product that can cause drug-induced liver injuries. [29] Moderate to severe elevation of serum aminotransferase levels can be found (> 5 times higher than the upper limit of the normal range) in 3–10% of patients taking lopinavir / ritonavir [12]. Remdesivir (RDV), originally used to treat Ebola disease, also shows antiviral activity against SARS-CoV-2. Studies have shown that the use of RDV is associated with an increase in the AST and ALT levels [29]. In most cases, the increase in enzymes did not reflect severe liver damage. [31]. However, cases of acute liver failure, presumably caused by the use of RDV, have been reported. Two patients have been described who had a significant increase in transaminase levels between days 3 and 10 of RDV therapy, accompanied by coagulopathy and encephalopathy [31]. Therefore, hepatotoxic drugs should be used with caution in patients with reduced liver function.

S. Gao et al. performed a retrospective, multicenter study that included 4,010 patients treated for coronavirus infection between December 19, 2019 and April 26, 2020. 395 patients (9.85%) developed acute liver failure during hospitalization. Acute liver failure was diagnosed with an increase in ALT or AST ≥ 3 × upper limit of normal (ULN), alkaline phosphatase or total bilirubin ≥ 2 × ULN. Drug therapy for hospitalized patients with COVID-19 mainly included antiviral drugs, antibacterial, antifungal drugs, hydroxychloroquine / chloroquine, corticosteroids, traditional Chinese medicine (TCM), immunotherapy, and diet therapy. Among the patients who developed acute liver failure, 293 (12.71%) patients were treated with antibiotics and 25 (35.71%) patients received antifungal medicines. Regarding antiviral drugs, 52 (18.18%), 200 (19.92%), 252 (7.23%), 88 (23.78%), and 80 (19.42%) patients were treated with ribavirin, corticosteroids, TCM drugs, parenteral nutrition (PN), and enteral nutrition (EN), respectively. There was a significant difference in the incidence of drug-induced hepatotoxicity between the patients who used and those who did not use these drugs ($p < 0.05$). Patients who received hydroxychloroquine / chloroquine (362 (95.26%)) and TCM drugs (3,234 (92.77%)) were less likely to develop acute liver failure [25].

DEFINITION AND PATHOGENESIS OF LIVER FIBROSIS

Liver fibrosis (LF) is accumulation of major extracellular matrix components (collagen, non-collagenous glycoproteins, glycosaminoglycans, proteoglycans, and elastin) in the liver tissue. Development of septal and perisinusoidal fibrosis is a universal mechanism of progression of chronic hepatitis and cirrhosis of the liver [32].

Hepatitis B and hepatitis C viruses, immune and metabolic disorders in the liver, oxidative stress accompanied by activation of free radical lipid peroxidation, various hepatotoxins, and hypoxia act as triggers for the development of liver fibrosis [32]. Fibrotic changes in the liver also occur in diseases, such as primary sclerosing cholangitis, hereditary hemochromatosis, alpha-1 antitrypsin deficiency, Wilson's disease, primary biliary cholangitis, and chronic heart failure [33].

In the era of the coronavirus pandemic, triggers for the development and progression of liver fibrosis can be hypoxia, cytokine storm, the effects of medications, as well as the direct effect of SARS-CoV-2 on hepatocytes. This, in turn, leads to damage to hepatocytes, which begin to release various substances, including peroxides and proteases. As a result, these biologically active substances (BAS) activate macrophages. Activated macrophages, in turn, begin to secrete BAS, causing activation of stellate cells. The main inducers of their activity include proinflammatory cytokines (IL-1), TNFα, peroxides, nitric oxide, endothelin, but the main role in stellate cell activation is attributed to the platelet-derived growth factor (PDGF), plasminogen activator, and transforming growth factor beta 1 (TGFβ1). Under their influence, stellate cells come out of a state of rest and undergo a number of transformations. Along with this, the number of cytokine

receptors stimulating proliferation and fibrogenesis increases [34].

In the first step, the resting stellate cell, under the influence of the macrophage and endothelial cell products listed above, loses its retinoid depot and starts secreting TGFβ1, which plays a key role in the development of subsequent stellate cell autoactivation. Under its influence, stellate cells not only continue to activate themselves, but also acquire the ability to migrate to areas of inflammation.

The next stage is accompanied by transformation of stellate cells into myofibroblasts, which are elongated cells containing alpha actins (which gives them some ability to contract). These cells continue to secrete TGFß1 and are also capable of producing the hepatic extracellular matrix. Myofibroblasts acquire the ability to actively divide in areas of inflammation. Liver fibrosis is a reversible process, but only if the etiological and / or pathogenetic factor is timely removed [34].

CHRONIC LIVER DISEASES AND CORONAVIRUS INFECTION

Individuals with chronic liver diseases, especially those having cirrhosis of the liver, are more susceptible to the novel coronavirus infection due to weakened immunity [35]. Therefore, it is likely that they are more susceptible to a more severe course of COVID-19 with a potential for liver fibrosis progression. The most common diseases are non-alcoholic fatty liver disease (NAFLD), alcohol-related liver disease (ARLD), chronic viral hepatitis B and C (CHB, CHC), and the outcome of these diseases is the cirrhosis of the liver.

Non-alcoholic fatty liver disease. Non–alcoholic fatty liver disease (NAFLD) is a chronic liver disease of metabolic genesis in individuals with no exogenous factors of toxic damage caused by accumulation of lipids in the cellular elements that make up the liver lobule. According to histologic signs, steatosis, non-alcoholic steatohepatitis (NASH), and cirrhosis of the liver are distinguished as the outcome of NAFLD. The prevalence of NAFLD in the general population worldwide ranges from 6.3 to 33.0%. The disease affects all age groups but is significantly more frequent in obese individuals (up to 62–93%) [36].

The level of ACE2 expression in the adipose tissue is higher than in the lung tissue. This conclusion may explain vulnerability of the adipose tissue to COVID-19 invasion [37]. A retrospective study conducted by M.F. Fondevila et al. showed that in the liver of obese patients, SARS-CoV-2 penetration factors depend differently on type 2 diabetes and NAFLD. At the same time, in obese women suffering from type 2 diabetes, the levels of ACE2 and TMPRSS2 are unexpectedly lower than in obese women with normoglycaemia, whereas in obese patients with steatohepatitis, the expression of these genes is noticeably higher. Consequently, late stages of NAFLD may predispose to COVID-19 [38].

It is worth noting that the risk of developing severe COVID-19 is significantly higher in patients with NAFLD who have been diagnosed with liver steatosis by computed tomography (CT) (odds ratio (OR) 4.32; 95% confidence interval (CI) 1.94–9.59) or in individuals with intermediate-risk and high-risk of fibrosis according to the FIB-4 scoring system (OR 5.73; 95% CI 1.84–17.9), regardless of metabolic comorbidities, compared to patients with NAFLD with a low FIB-4 index or persons without NAFLD [39].

However, a two-sample Mendelian Randomisation Study (TSMR) showed that NAFLD (OR 0.97, p = 0.61), the ALT level (OR 1.03, p = 0.47), the degree of steatosis (OR 1.08, p = 0.41), the degree of NAFLD intensity (OR 1.02, p = 0.39), and fibrosis stage (OR 1.01, p = 0.87) were not associated with severe COVID-19. Among all the associated NAFLD factors, the risk of severe COVID-19 was associated only with body mass index (BMI) (OR 1.73, $p = 7.65 \times 10^{-9}$), waist circumference (WC) (OR 1.76, $p = 2.58 \times 10^{-5}$), and hip circumference (HC) (OR 1.33, $p = 7.26 \times 10^{-3}$).

Currently, it seems likely that general obesity (indexed by BMI, WC, and HC), rather than NAFLD, plays a causal role in the development of severe COVID-19 symptoms. The potential mechanism underlying the increased risk of developing severe COVID-19 with an increase in BMI remains unclear. Preliminary hypotheses explaining this phenomenon included lower cardiopulmonary reserve and immune dysregulation in patients with high BMI, which exacerbate the symptoms of COVID-19. In general, weight control may be the most important modifiable risk factor for preventing the development of severe COVID-19 [40].

Alcohol-related liver disease. Alcohol consumption is one of the leading risk factors for the development of pathology of internal organs. Alcohol-related diseases are associated with almost 10% of deaths in the world among the population aged 15–49 years [41]. According to the National Research Center of Narcology in Moscow, alcohol consumption has increased in the context of the COVID-19 pandemic.

Alcohol-related liver disease (ARLD) is independently associated with a 1.8-fold increased risk of mortality in patients with COVID-19 [39].

There are many reasons why alcohol consumption can predispose to worsening of COVID-19 outcomes. Firstly, alcohol consumption and concomitant liver disease disrupt the innate and adaptive immunity, affecting the functioning of immune cells important for protection against viral infections [42].

Secondly, chronic alcohol consumption is associated with increased susceptibility to acute respiratory distress syndrome [43]. This may be due to the direct effect of alcohol on immune function in addition to the dysfunction of the alveolar epithelium and a decrease in the concentration of pulmonary antioxidants in people with chronic alcohol abuse [43].

Thirdly, patients with excessive alcohol consumption often have other concomitant diseases, including metabolic syndrome, chronic kidney disease, and tobacco smoking, which were independently associated with severe outcomes of COVID-19 [43].

Coinfection of SARS-CoV-2 and viral hepatitis B. Currently, hepatitis B virus (HBV) remains the main cause of cirrhosis of the liver, liver failure, and hepatocellular carcinoma [44]. L. Chen et al. showed in their study that among 326 confirmed COVID-19 patients, of whom 20 (6.1%) were coinfected with HBV, there was no difference in the length of hospital stay between the two groups. According to the authors, HBV coinfection did not affect the course and prognosis of COVID-19 [45].

Yu. Rentao et al. observed 67 patients who were divided into HBsAg+ (n = 7) and HBsAg- (n = 60) groups with an assessment of the levels of AST and HBV markers (HBsAg, HBsAb, HBeAg, HBeAb, HBcAb, and HBV-DNA) at admission and discharge. There were no significant differences between the groups of patients with positive and negative HBsAg. The authors suggested that SARS-CoV-2 infection was not associated with HBV reactivation in the examined patients. On the other hand, the presence of HBV also did not affect the severity of SARS-CoV-2 [46].

From a virological point of view, coinfection with HBV did not increase the cycle of virus spread or the incubation period of SARS-CoV-2 infection. From a clinical point of view, HBV coinfection did not intensify the severity of diseases or the duration of hospitalization in patients with COVID-19 [46]. HBV can also cause immunological exhaustion, in which stimulated T cells cannot produce such a strong cytokine response to SARS-COV2 infection, resulting in a less severe course of the disease [2].

For patients with severe COVID-19 and HBV coinfection, there is a risk of HBV reactivation. This is usually associated with immunosuppressive therapy, such as treatment with IL-6 receptor antagonists (tocilizumab and siltuximab), IL-1 receptor antagonists (anakinra), and high doses of corticosteroids. These drugs are used to control cytokine storm, thereby reducing immune-mediated multiple organ dysfunction [44].

J. Liu et al. observed 21 patients with SARS-CoV-2 and HBV coinfection in a retrospective study. 19 patients were tested for HBV DNA viral load at least twice during hospitalization. Three of the 19 patients developed HBV reactivation, which manifested itself by a rapid increase in the viral load of HBV DNA. These three patients were negative for the hepatitis B antigen and had not received any treatment against HBV prior to hospitalization. During hospitalization, two out of three patients received methylprednisolone, which may explain the reactivation, and one patient did not receive corticosteroids [47].

Coinfection of SARS-CoV-2 and hepatitis C virus. Chronic hepatitis C virus (HCV) is a chronic inflammatory disease lasting more than 6 months with predominant lesion of the liver tissue due to infection with HCV. Globally, an estimated 1% of the population (about 71 million people) have HCV antibodies (anti-HCV), of whom 2/3 are chronically infected and 1/3 have recovered or have been cured [48].

B. Cerbu et al. conducted a study that included 1,057 patients infected with HCV, in 126 (11.9%) individuals COVID-19 was verified. Of these, 95 patients (75.4%) were treated according to the SOF / VEL regimen or achieved a stable virological response, while the remaining 31 (24.6%) patients showed active HCV replication. The proportion of severe COVID-19 cases in the active HCV group was significantly higher compared to the inactive HCV group (32.2 vs. 7.3%, $p < 0.001$). It was also shown that the length of stay in the hospital and intensive care unit for COVID-19 was significantly greater in patients with active HCV infection [49]. Currently, data on the effect of coronavirus infection on the course of HCV, as well as its prognosis, are insufficient.

Cirrhosis of the liver. Cirrhosis is a late stage of liver fibrosis caused mainly by NAFLD / NASH, ARLD, and chronic viral hepatitis [39]. In a study conducted in New York, only 0.4% of patients with a novel coronavirus infection had pre-existing cirrhosis.

The effect of cirrhosis on the course of COVID-19 is not fully known yet. Liver cirrhosis has been found to be associated with increased mortality in patients with acute respiratory distress syndrome [50]. ACE2 levels are known to increase (a 97-fold increase in the parenchyma) in cirrhosis [51]. Therefore, patients with cirrhosis may be more vulnerable to SARS-CoV2 infection.

CONCLUSION

COVID-19 is a multisystem disorder. Damage to the liver can occur in several ways: via direct impact of SARS-CoV-2 on hepatocytes, immune-mediated damage due to a severe inflammatory response, hypoxia, and drug use.

Particular attention is paid to diffuse chronic liver diseases, such as NAFLD, ARLD, viral hepatitis, and cirrhosis of the liver. Coronavirus infection, apparently, can contribute to the progression of these diseases, as well as have a worse outcome in these conditions.

Data on the follow-up of patients with chronic liver disease who have experienced SARS-CoV-2 are currently insufficient for definite conclusions, and this situation requires further research.

REFERENCES

1. Prevention, diagnosis and treatment of novel coronavirus infection (COVID-19). Temporary guidelines. Version 15 (22.02.2022). Moscow: Ministry of Health of the Russian Federation, 2022 (in Russ.). URL: https://static-0.minzdrav.gov.ru/system/attachments/attaches/000/059/392/original/BMP_COVID-19_V15.pdf (date of access: 10.06.2022).
2. Driggers K.E., Sadowski B.W., Shagla E., Kwok R.M. Care of the hepatology patient in the COVID-19 era. *Current Hepatology Reports*. 2022;21(2):9–20. DOI: 10.1007/s11901-021-00581-x.
3. Nikiforov V.V., Suranova T.G., Mironov A.Yu., Zaboz-laev F.G. Novel coronavirus infection (COVID-19): etiology, epidemiology, clinical presentation, diagnosis, treatment, and prevention. M., 2020: 48 (in Russ.).
4. Holmes K.V., Enjuanes L. The SARS coronavirus: a post-genomic era. *Science*. 2003;300(5624):1377–1378. DOI: 10.1126/science.1086418.
5. Mnatsakanyan M.G., Pogromov A.P., Lishuta A.S., Fomin V.V., Tashchyan O.V., Kuprina I.V. et al. Liver and COVID-19: possible mechanisms of damage. *Therapeutic Archives.* 2021;93(4):427–430 (in Russ.). DOI: 10.26442/00403660.2021.04.200733.
6. Jin X., Lian J.S., Hu J.H., Gao J., Zheng L., Zhang Y.M. et al. Epidemiological, clinical and virological characteristics of 74 cases of coronavirus-infected disease 2019 (COVID-19) with gastrointestinal symptoms. *Gut*. 2020;69(6):1002–1009. DOI: 10.1136/gutjnl-2020-320926.
7. Idalsoaga F., Ayares G., Arab J.P., Díaz L.A. COVID-19 and indirect liver injury: a narrative synthesis of the evidence. *J. Clin. Transl. Hepatol*. 2021;9(5):760–768. DOI: 10.14218/JCTH.2020.00140.
8. Zhang X.T., Yu Y., Zhang C. Wang H., Zhao L., Wang H. et al. Mechanism of SARS-CoV-2 invasion into the liver and hepatic injury in patients with COVID-19. *Mediterr. J. Hematol. Infect. Dis.* 2022;14(1):e2022003. DOI: 10.4084/MJHID.2022.003.
9. Nardo A.D., Schneeweiss-Gleixner M., Bakail M., Dixon E.D., Lax S.F., Trauner M. Pathophysiological mechanisms of liver injury in COVID-19. *Liver Int.* 2021;41(1):20–32. DOI: 10.1111/liv.14730.
10. Sabirov I.S., Murkamilov I.T., Fomin V.V. Hepatobiliary system and novel coronavirus infection (COVID-19). *The Scientific Heritage.* 2020;49:49–58 (in Russ.).
11. Xiaohong Y., Tingyuan L., Zhicheng H., Yifang P., Huawen L., Shicang Y. et al. A pathological report of three COVID-19 cases by minimal invasive autopsies. *Chinese Journal of Pathology.* 2020;49(5):411–417. DOI: 10.3760/cma.j.cn112151-20200312-00193.
12. Vinokurov A.S., Nikiforova M.V., Oganesyan A.A., Vinokurova O.O., Yudin A.L., Yumatova E.A. COVID-19. Liver damage – visualization features and possible causes. *Medical Imaging*. 2020;24(3):26–36 (in Russ.). DOI: 10.24835/1607-0763-2020-3-26-36.
13. Il'chenko L.Yu., Nikitin I.G., Fedorov I.G. COVID-19 and liver damage. *Archives of Internal Medicine.* 2020;10(3):188–197 (in Russ.). DOI: 10.20514/2226-6704-2020-10-3-188-197.
14. Ibraeva Zh.B., Aitkuluev N.S., Makembaeva Zh.I., Suranbaeva G.S., Murzakulova A.B., Anarbaeva A.A. et al. COVID-19 and liver damage. *International Journal of Applied and Basic Research*. 2021;9:17–21 (in Russ.). DOI: 10.17513/mjpfi.13266.
15. Chai X., Hu L., Zhang Y., Han W., Lu Z., Ke A. et al. Specific ACE2 expression in cholangiocytes may cause liver damage after 2019-nCoV infection. *BioRxiv.* 2020. DOI: 10.1101/2020.02.03.931766.
16. Wang Y., Liu S., Liu H., Li W., Lin F., Jiang L. et al. SARS-CoV-2 infection of the liver directly contributes to hepatic impairment in patients with COVID-19. *Journal of Hepatology*. 2020;73:807–816. DOI: 10.1016/j.jhep.2020.05.002.
17. Surkova E.Yu., Mosina L.M., Esina M.V. To the question about some pathogenetic features of liver damage in COVID-19. *Modern Problems of Science and Education*. 2021;3 (in Russ.). DOI: 10.17513/spno.30880.
18. Waseemand N., Chen P.H. Hypoxic Hepatitis: A Review and Clinical Update. *J. Clin. Transl. Hepatol*. 2016;4(3):263–268. DOI: 10.14218/JCTH.2016.00022.
19. Storozhakov G.I, Oskanova R.S., Il'chenko L.Yu., Kosyura S.D., Fedorov I.G. Hypoxic hepatitis. *Archives of Internal Medicine.* 2014;6(20):42–47 (in Russ.). DOI: 10.20514/2226-6704-2014-0-6-42-47.
20. Petrov V.I., Ponomareva A.V., Ivakhnenko I.V., Razvalyaeva O.V., Meshrki B.A., Statsenko V.I. Etiopathogenetic aspects of liver injury in patients with COVID-19. *Bulletin of VolgGMU*. 2020;4(76):9–15 (in Russ.). DOI: 10.19163/1994-9480-2020-4(76)-9-15.
21. Feng G., Zheng K.I., Yan Q.Q., Rios R.S., Targher G., Byrne C.D. et al. COVID-19 and liver dysfunction: Current

insights and emergent therapeutic strategies. *J. Clin. Transl. Hepatol.* 2020;8(1):18–24. DOI: 10.14218/JCTH.2020.00018.
22. Wenzhong L., Hualan L. COVID-19: Attacks the 1-beta chain of hemoglobin and captures the porphyrin to inhibit human heme metabolism. *ChemRxiv.* 2020. DOI: 10.26434/chemrxiv.11938173.v5.
23. Sandler Yu.G., Vinnitska E.V., Khaimenova T.Yu., Bordin D.S. Clinical aspects of liver damage in COVID-19. *Effective Pharmacotherapy*. 2020;16(15):18–23 (in Russ.). DOI: 10.33978/2307-3586-2020-16-15-18-23.
24. Potapnev M.P. Cytokine storm: causes and consequences. *Immunology.* 2021;42(2):175–188 (in Russ.). DOI: 10.33029/0206-4952-2021-42-2-175-188.
25. Gao S., Yang Q., Wang X., Hu W., Lu Y., Yang K. et al. Association between drug treatments and the incidence of liver injury in hospitalized patients with COVID-19. *Front Pharmacol*. 2022;13:799338. DOI: 10.3389/fphar.2022.799338.
26. LiverTox: Clinical and research information on druginduced liver injury [Internet]. Bethesda (MD): National Institute of Diabetes and Digestive and Kidney Diseases; 2012–Hydroxychloroquine. URL: https://www.ncbi.nlm.nih.gov/books/ (date of access: 15.04. 2021).
27. Falcao M.B., Pamplona de Goes Cavalcanti L., Filgueiras Filho N.M., Antunes de Brito C.A. Case Report: Hepatotoxicity Associated with the Use of Hydroxychloroquine in a Patient with COVID-19. *Am. J. Trop. Med. Hyg*. 2020;102(6):1214–1216. DOI: 10.4269/ajtmh.20-0276.
28. Muhovic D., Bojovic J., Bulatovic A., Vukcevic B., Ratkovic M., Lazovic R. et al. First case of drug-induced liver injury associated with the use of tocilizumab in a patient with COVID-19. *Liver International*. 2020;40(8):1901–1905. DOI: 10.1111/liv.14516.
29. Satsangi S., Gupta N., Kodan P. Current and new drugs for COVID-19 treatment and its effects on the liver. *J. Clin. Transl. Hepatol.* 2021;9(3):436–446. DOI: 10.14218/JCTH.2020.00174.
30. Balykova L.A., Granovskaya M.V., Zaslavskaya K.Ya., Simakina E.N., Agaf'ina A.S., Ivanova A.Yu. et al. New possibilities for targeted antiviral therapy for COVID-19. Results of a multicenter clinical study of the efficacy and safety of the drug Areplivir. *Infectious Diseases: News, Opinions, Training.* 2020;9(3):16–29 (in Russ.). DOI: 10.33029/2305-3496-2020-9-3-16-29.
31. Carothers C., Birrer K., Vo M. Acetylcysteine for the treatment of suspected remdesivir-associated acute liver failure in COVID-19: A case series. *Pharmacotherapy*. 2020;40(11):1166–1171. DOI: 10.1002/phar.2464.
32. Tsimmerman Ya.S. Liver fibrosis: pathogenesis, diagnosis, and treatment. *Clinical Pharmacology and Therapy*. 2017;26(1):54–58 (in Russ.).
33. Pavlov Ch.S., Shul'pekova Yu.O., Zolotarevskii V.B., Ivashkin V.T. Current views on the pathogenesis, diagnosis, and treatment of liver fibrosis. *Russian Journal of Gastroenterology, Hepatology, Coloproctology.* 2005;2:13–20 (in Russ.).
34. Gubergrits N.B., Lukashevich G.M., Fomenko P.G., Belyaeva N.V. Liver fibrosis: from fatalism to optimism. Moscow: Prima Print, 2015: 48 (in Russ.).
35. Vranić L., Radovan A., Poropat G., Mikolašević I., Milić S. Non-alcoholic fatty liver disease and COVID-19-two pandemics hitting at the same time. *Medicina (Kaunas).* 2021;57(10):1057. DOI: 10.3390/medicina57101057.
36. Lazebnik L.B., Golovanova E.V., Turkina S.V., Raikhel'son K.L., Okovityi S.V., Drapkina O.M. et al. Non-alcoholic fatty liver disease in adults: clinical presentation, diagnosis, and treatment. Guidelines for therapists, third version. *Experimental and Clinical Gastroenterology*. 2021;185(1):4–52 (in Russ.). DOI: 10.31146/1682-8658-ecg-185-1-4-52.
37. Metawea M.I., Yousif W.I., Moheb I. COVID 19 and liver: An A–Z literature review. *J. Digestive and Liver Disease.* 2021;53(2): 46–152. DOI: 10.1016/j.dld.2020.09.010.
38. Fondevila M.F., Mercado-Gomez M., Rodriguez A., Gonzalez-Rellan M.J., Iruzubieta P., Valentí V. et al. Obese patients with NASH have increased hepatic expression of SARS-CoV-2 critical entry points. *Journal of Hepatology*. 2021;74(2):469–471. DOI: 10.1016/j.jhep.2020.09.027.
39. Martinez M.A., Franco S. Impact of COVID-19 in liver disease progression. *Hepatology Communications.* 2021;5(7):1138–1150. DOI: 10.1002/hep4.1745.
40. Li J., Tian A., Zhu H., Chen L., Wen J., Liu W. et al. Mendelian randomization analysis reveals no causal relationship between nonalcoholic fatty liver disease and severe COVID-19. *Clin. Gastroenterol. Hepatol.* 2022;20(7):1553–1560.e78. DOI: 10.1016/j.cgh.2022.01.045.
41. Lazebnik L.B., Golovanova E.V., Tarasova L.V., Krivosheev A.B., Sas E.I., Eremina E.Yu. et al. Adult alcoholi-related liver disease. *Experimental and Clinical Gastroenterology*. 2020;174(2):4–28 (in Russ.). DOI: 10.31146/1682-8658-ecg-174-2-4-28.
42. Szabo G., Saha B. Alcohol's effect on host Defense. *Alcohol Res.* 2015;37(2):159–170.
43. Moon M., Curtis B., Mandrekar P., Ashwani K, Singal A.K., Verna E.C. et al. Alcohol-associated liver disease before and after COVID-19 – an overview and call for ongoing investigation. *Hepatol. Commun*. 2021;5(9):1616–1621. DOI: 10.1002/hep4.1747.
44. Xiang T.D., Zheng X. Interaction between hepatitis B virus and SARS-CoV-2 infections. *World J. Gastroenterol.* 2021;27(9):782–793. DOI: 10.3748/wjg.v27.i9.782.
45. Chen L., Huang S., Yang J., Cheng X., Shang Z., Lu H. et al. . Clinical characteristics in patients with SARS-CoV-2/HBV co-infection. *J. Viral Hepat.* 2020;27(12):1504–1507. DOI: 10.1111/jvh.13362.
46. Yu R., Tan S., Dan Y., Lu Y., Zhang J., Tan Z. et al. Effect of SARS-CoV-2 coinfection was not apparent on the dynamics of chronic hepatitis B infection. *Virology*. 2021;553:131–134. DOI: 10.1016/j.virol.2020.11.012.
47. Liu J., Wang T., Cai Q., Sun L., Huang D., Zhou G. et al. Longitudinal changes of liver function and hepatitis B reactivation in COVID 19 patients with preexisting chronic hepatitis B virus infection. *Hepatology Research*. 2020;50 (11):1211–1221. DOI: 10.1111/hepr.13553.
48. Chronic viral hepatitis C. Clinical guidelines. M.: Ministry of Health of the Russian Federation, 2021 (in Russ.). URL: https://cr.minzdrav.gov.ru/schema/516_2 (date of access: 10.06.2022).

49 Cerbu B., Pantea S., Bratosin F. Vidican, I.. Turaiche M., Frent S. et al. Liver Impairment and Hematological Changes in Patients with Chronic Hepatitis C and COVID-19: A Retrospective Study after One Year of Pandemic. *Medicina.* 2021;57(6):597. DOI: 10.3390/medicina57060597.

50. Pinchuk T.V., Orlova N.V., Suranova T.G., Bonkalo T.I. Mechanisms of liver damage in COVID-19. *Medical Alphabet*. 2020;19:39–46 (in Russ.). DOI: 10.33667/2078-5631-2020-19-39-46.

51. Lizardo-Thiebaud M., Cervantes-Alvarez E., Limon-de la Rosa N., Tejeda-Dominguez F., Palacios-Jimenez M., Méndez-Guerrero O. et al. Direct or collateral liver damage in SARS-CoV-2–Infected patients. *Semin. Liver Dis*. 2020;40(3):321–330. DOI: 10.1055/s-0040-1715108.

Authors' information

Kruchinina Margarita V. – Dr. Sci. (Med.), Associate Professor; Leading Researcher, Head of Gastroenterology Laboratory, Research Institute of Internal and Preventive Medicine – Branch of the Institute of Cytology and Genetics, SB RAS; Professor, Department for Propaedeutics of Internal Medicine, Novosibirsk, kruchmargo@yandex.ru, http://orcid.org/0000-0003-0077-3823

Pershina Natalia E. – Resident, Gastroenterology Laboratory, Research Institute of Internal and Preventive Medicine – Branch of the Institute of Cytology and Genetics, SB RAS, Novosibirsk, 16041997nata@mail.ru

Svetlova Irina O. – Cand. Sci. (Med.), Associate Professor, Department for Therapy, Hematology and Transfusiology (Faculty of Continuing Education and Retraining of Doctors), Novosibirsk State Medical University; Gastroenterologist, Research Institute of Internal and Preventive Medicine – Branch of the Institute of Cytology and Genetics, SB RAS, Novosibirsk, iosvetlova@yandex.ru

Kruchinina Elina V. – 6th-year Student, Novosibirsk State Medical University, Novosibirsk, linakruchininaaa1998@gmail.com

(✉) **Kruchinina Margarita V.,** kruchmargo@yandex.ru

Received 20.07.2022;
approved after peer review 05.09.2022;
accepted 08.12.2022

УДК 618.146-006.6
https://doi.org/10.20538/1682-0363-2023-2-145-155

Modern concepts in cervical carcinogenesis

Naumova L.A., Starodumova V.A.

Surgut State University
1, Lenina Str., Surgut, Khanty-Mansiysk Autonomous Area – Yugra, 628412, Russian Federation

ABSTRACT

The article discusses modern ideas about cervical carcinogenesis as a multi-stage process of multifactorial genesis. Currently, ideas about the pathogenesis of cervical cancer (CC) are based not only on understanding the role of high-risk oncogenic human papillomavirus (HPV) in this process and accumulation of genetic changes caused by it, but also on formation of a complex HPV interactome, or a network of intermolecular interactions of HPV oncoproteins with host cell proteins. Carcinogenesis also involves a wide range of epigenetic events and, above all, impairment of the regulatory function of miRNAs. An important role in cervical carcinogenesis is attributed to the concept of cancer stem cells (CSCs) formulated in recent years, which is closely related to the explanation of disease recurrence and treatment resistance, as well as to new approaches to treatment. The cervicovaginal microbiome and cervical microenvironment, which are responsible for natural clearance of HPV, regression of epithelial lesions, and modeling of the immune response, are becoming promising objects for research.

The aim of the review was to present up-to-date information on the most important mechanisms of cervical carcinogenesis, as well as on new approaches to the treatment of CC, based, in particular, on the use of knowledge about regulatory miRNAs, CSC markers, and the state of the cervicovaginal microbiota.

Keywords: cervical carcinogenesis, cervical cancer genomics, miRNA, cancer stem cells, microbiota

Conflict of interest. The authors declare the absence of obvious and potential conflicts of interest related to the publication of this article.

Source of financing. The authors state that they received no funding for the study.

For citation: Naumova L.A., Starodumova V.A. Modern concepts in cervical carcinogenesis. *Bulletin of Siberian Medicine.* 2023;22(2):145–155. https://doi.org/10.20538/1682-0363-2023-2-145-155.

Современные представления о цервикальном канцерогенезе

Наумова Л.А., Стародумова В.А.

Сургутский государственный университет (СурГУ)
Россия, 628412, Ханты-Мансийский автономный округ (ХМАО) – Югра, г. Сургут, ул. Ленина, 1

РЕЗЮМЕ

Рассматриваются современные представления о цервикальном канцерогенезе как многостадийном процессе мультифакторного генеза. В настоящее время представления о патогенезе рака шейки матки (РШМ) базируются не только на понимании роли в этом процессе вируса папилломы человека (ВПЧ) высокого онкогенного риска и накоплении обусловленных им генетических изменений, но и формировании сложного интерактома ВПЧ, или сети межмолекулярных взаимодействий онкобелков ВПЧ с белками клетки-хозяина. Также в процессе канцерогенеза принимают участие эпигенетические модификации широкого спектра и, прежде всего, нарушения регуляторной функции микроРНК. Важное место в пред-

✉ *Naumova Lyudmila A.,* naumovala@yandex.ru

ставлениях о цервикальном канцерогенезе занимает сформулированная в последние годы концепция раковых стволовых клеток (CSCs), с которой тесно связано объяснение рецидивов заболевания и устойчивости к лечению, а также понимание новых подходов к лечению. Перспективным объектом для исследования становится также цервиковагинальный микробиом и цервикальное микроокружение, ответственные за естественный клиренс ВПЧ, регрессию эпителиальных повреждений и моделирование иммунного ответа.

Цель обзора – изложение актуальной информации о важнейших механизмах цервикального канцерогенеза, а также новых подходах к лечению РШМ, базирующихся в частности на использовании знаний о регуляторных микроРНК, маркерах CSCs и состоянии цервиковагинальной микробиоты.

Ключевые слова: цервикальный канцерогенез, геномика рака шейки матки, микроРНК, раковые стволовые клетки, микробиота

Конфликт интересов. Авторы декларируют отсутствие явных и потенциальных конфликтов интересов, связанных с публикацией настоящей статьи.

Источник финансирования. Авторы заявляют об отсутствии финансирования при проведении исследования.

Для цитирования: Наумова Л.А., Стародумова В.А. Современные представления о цервикальном канцерогенезе. *Бюллетень сибирской медицины.* 2023;22(2):145–155. https://doi.org/10.20538/1682-0363-2023-2-145-155.

INTRODUCTION

All over the world, cervical cancer (CC) is one of the most common malignant gynecological diseases, for which morbidity and mortality rates tend to worsen. In 2020, more than 600,000 new CC cases were detected globally and 342,000 deaths were registered [1]. CC ranks fourth among cancer types in women after breast cancer, colorectal cancer, and lung cancer [2–4] and is the second cause of death from cancer in women aged 20–39 years [1, 5–7]. In underdeveloped countries, with high CC prevalence (ranks second in cancer incidence in women) and late diagnosis, the 5-year survival rate of patients with CC is less than 50% [2–4]. Despite existing screening programs (human papillomavirus (HPV) tests, cytology, colposcopy) and vaccination leading to a decrease in mortality from CC, there is a growing need for screening for precancer and CC at early stages, allowing for the use of organ preserving therapy that ensures fertility preservation [5, 6, 8].

Ideas about cervical carcinogenesis are closely related to the modern understanding of the features of the transition zone between the endo- and exocervix, which is known as the squamo-columnar junction of the cervix (SCJ) and is characterized by the presence of cervical stem cells (SCs) [2, 4, 5, 9]. The discovery of SCs provides an understanding of not only the mechanisms of physiological and reparative regeneration of cervical epithelium, but also of the appearance of cancer stem cells (CSCs) that are the origin of carcinogenesis [2, 4, 5, 9, 10].

CSCs determine the malignant potency of the tumor that is the rate of development and metastasis and the degree of regression during treatment [4, 5, 9, 11].

Although persistent high-risk HPV infection (HR-HPV) is of particular importance in tumor transformation [1, 5], CC is a multifactorial disease caused not only by the accumulation of genetic changes, but also by a wide range of epigenetic changes: impaired DNA methylation and modification of histones and non-coding RNA (ncRNA) [6, 12–15]. The oncogenic potency of HPV infection is determined by a large number of additional factors including the influence of hormones, multiple sexual partners, obesity, smoking, alcohol abuse, poor nutrition, immunosuppressive cervical microenvironment, abnormal vaginal microbiota, coinfections with *Chlamydia trachomatis* or human immunodeficiency virus [1, 5, 7, 16–19].

Lactobacillus spp. are the main representatives of the vaginal flora and the first line of defense against pathogenic microflora in HPV infection, and as the severity of cervical intraepithelial neoplasia (CIN) increases, the prevalence of an increasingly toxic flora including *Fusobacterium, Sneathia,* and *Streptococcus* is diagnosed [5, 16, 20]. Researchers are accumulating more and more data on the critical role of the cervicovaginal microbiome (CVM) in the dynamics of HPV infection: the natural clearance of HPV, CIN regression, and the immune response modeled by the CVM [1, 5, 7, 16].

The study of molecular mechanisms of CC pathogenesis based on the methods of systems biology (genomics, transcriptomics, proteomics, metabolomics of CC) is crucial for obtaining a large amount of data on prognostic and important for treatment CC biomarkers and for developing effective CC therapies [3, 21].

ONCOGENIC HPV STRAINS AND MOLECULAR GENETIC MECHANISMS OF CERVICAL CANCER PATHOGENESIS

Currently, more than 200 HPV and animal genotypes have been described and sequenced, of which approximately 30 types affect the anogenital tract, 15 of these types (HPV 16, 18, 31, 33, 35, 39, 45, 51, 52, 56, 58, 59, 68, 73 and 82) were classified as HR-HPVs associated with CIN2/3 and cancer *in situ* or high-grade intraepithelial lesion (HSIL) and invasive cervical cancer. HPV 16 and 18 cause about 70% of squamous cell carcinomas and more than 90% of adenocarcinomas [2, 12–14, 22, 23].

At the same time, it was proven that in almost 90% of HPV-infected women the virus is no longer detected (transient infection) 6–18 months after infection, in one tenth of infected women the infection persists (persistent infection), and precancerous cervical lesions may develop [2, 14, 22] which progress to invasive cervical cancer in 0.3–1.2% of cases. The question of the possibility of complete elimination of the virus, with it remaining latent in basal cells with the preservation of the reactivation potential is still to be discussed. Persistent HPV infection is diagnosed in the presence of viral DNA of the same type upon re-examination after 6–12 months [2, 22, 23].

The life cycle of HPV penetrating through a microtrauma into basal cells of the exocervical epithelium is closely related to the differentiation of epitheliocytes, depends on a number of cellular factors and sequentially expressed viral proteins, and is described in detail in numerous reviews [4, 5, 12, 14, 15]. The virus can exist in an episomal, integrated, or mixed (cooccurrence of an integrated and episomal form) forms in infected cells [14, 24].

Integration of viral DNA into the host cell genome can have different signatures (more than 3,500 breakpoints have been described) and cause amplification of oncogenes, inactivation of tumor suppressor genes, inter- or intrachromosomal rearrangements, and genomic instability [14, 24]. Changes are more often detected in the *PIK3CA, TP53, KRAS*, and *PTEN* genes, often in STK*11, POU5F1B, FHIT, KLF12, KLF5, LRP1B, LEPREL1*, etc. [3, 6, 24, 25]. The integration of viral DNA into the host genome is accompanied by the destruction of the *E2* viral gene, which regulates the E6 and E7 oncoproteins, which leads to their overexpression [14].

During integration, the viral genome incorporates into the host cell genome at sites of damage or double-strand breaks in DNA due to the deactivation of the normal DNA damage response (DDR) by oncoproteins E6 and E7, which consists of ATR and P53 activation [3, 12]. The E7 protein affects the ATR protein kinase and inactivates Rb, disrupting the cell cycle inhibitors p21, p27.The E6 protein inhibits DNA repair, causes uncontrolled proliferation of infected cells through disruption of apoptosis (ubiquitin – proteasome degradation of the p53 tumor suppressor and binding to procaspase-8), and suppresses the response of many genes to interferon [3, 12, 14]. The E6 protein activates the PI3K / Akt pathway, promotes the degradation of the transcriptional repressor NFX1, and induces the activation of hTERT (human telomerase reverse-transcriptase), leading to the immortalization of transformed cells [3, 5, 12, 14].

Currently, the existence of a complex HPV interactome or a network of E6 and E7 intermolecular interactions with host cell proteins has been established [12, 14, 15]. The E6 and E7 proteins can modulate the gene expression profile, host cell proteome, and intracellular signaling pathways, including MAPK-, Wnt-, Akt-, Notch-, mTORC-, and STAT-dependent cascades, which leads to changes in the epithelial phenotype [12, 14].

Integration of viral DNA into the genome of basal cells with stem-like properties in the transformation zone leads to their transformation into CSCs [2, 5, 15], the population of which is maintained by activation of Wnt/β-catenin, Notch, and Hedgehog [3, 12, 14], Oct3/4, NANOG, and SOX2 signaling pathways by oncoproteins [26]. A study of CC (whole exome sequencing) carried out as a part of the Cancer Genome Atlas (TCGA) revealed a huge number of mutations. So, 192 “tumor – control” pairs in the aggregate contained 43,324 somatic mutations; 11 samples containing more than 600 mutations per sample were identified as hypermutated [25].

Integrative clustering of CC samples using data from the analysis of the genome (DNA), transcriptome (mRNA), DNA methylation, microRNA expression (miRNA), and copy number variations (CNV) of genes revealed pronounced molecular heterogeneity of CC. In particular, three clusters of CC were identified: clusters of squamous CC with high and low expression of keratin genes and a cluster that includes predominantly adenocarcinomas. The three clusters identified were associated with features of CC histology, HPV types, HPV integration status, UCEC-like status, APOBEC mutagenesis level, evaluation of the epithelial – mesenchymal transition (EMT) and mRNA, expression of KRAS, ERBB3, and HLA-A. The isolated clusters differed not only in the expression of the *SPRR* and *TMPRSS* genes involved in keratinization, but also of *SMGs, ARID1A, NFE2L2*, and *PIK3CA* genes responsible for various metabolic pathways in the cell [25, 27].

For the first time, mutations in ERBB3, CASP8, HLA-A, SHKBP1, and TGFBR2 were identified in CC, and ERBB3 (HER3) was immediately identified as a

therapeutic target due to aberrant signaling between mutant HER3 and activated HER2. Mutations of HLA-A, HLA-B, NFE2L2, MAPK1, CASP-8, SHKBP1, and TGFBR2 have been found exclusively in squamous CC [25]. The detected amplifications of CD274 (PD-L1) and PDCD1LG2 (PD-L2), which significantly correlate with the expression of granzyme A and perforin, key genes of cytolytic effector cells, do not exclude the effectiveness of immunotherapy in some types of CC [25].

Also, 1,026 epigenetically silent genes were identified including zinc-metalloproteinases ADAM and ADAMATS modeling the extracellular matrix and collagen genes (COL), which were methylated to a greater extent in CC than in the control samples [25].

In the *PIK3CA* gene, there were mainly activating mutations of the helical domain E542K and E545K, in which the main nucleotide substitution pattern was associated with the mutagenesis of APOBEC, a family of cytidine deaminases that play the main role in the deamination of cytidine to uridine in DNA and RNA and control various biological processes (embryogenesis, innate immunity, regulation of protein expression). Currently, APOBEC mutagenesis, which causes tumor mutations due to the aberrant DNA editing mechanism, is considered as a molecular driver of CC pathogenesis [23, 25]. In HPV-negative CC, a lower rate of APOBEC mutagenesis and high expression of miRNAs responsible for EMT were noted [27].

In general, the differences were found in CC pathogenesis in the presence and absence of its association with HPV in terms of three important characteristics including cancer driver genes, the severity of genomic instability, and mitotic pathways in cancer pathogenesis [28]. It is the features of molecular mechanisms and genetic disorders that underlie cancer pathogenesis in each specific case that determine various outcomes of CC [28, 29].

EPIGENETIC MODIFICATIONS IN CERVICAL CARCINOGENESIS

Recent studies have shown that the integration of the viral genome into the host cell genome is not enough for the development of CC [12–14]. CC pathogenesis is a multi-stage process associated not only with the accumulation of genetic changes, but, above all, with the accumulation of a wide range of epigenetic modifications in the viral and host cell genomes. These modifications are associated with impaired DNA methylation and modification of histones and ncRNA [12–15, 30]. Epigenetic changes referring to reversible modifications of gene function are natural mechanisms of cellular adaptation and occur under the influence of a wide range of factors including age, lifestyle, endocrine profile, chronic inflammation, and cellular stress. These factors, in turn, form a cellular microenvironment with a complex network of interactions of cytokines, chemokines, free radicals, growth factors, and enzymes, which determines the effect on critical signaling pathways involved in maintaining cellular homeostasis [12–14, 17, 18, 30, 31].

In CC, cytosine methylation (the replacement of a hydrogen atom by a methyl group) catalyzed by DNA methyltransferases (DNMTs) is predominantly observed in the CpG motif. Methylation of the gene promoter usually leads to gene silence, while demethylation causes an increase in its expression, and it is also possible when oncogenes are expressed due to demethylation of their promoters (shown on the example of serine / threonine kinase 31 (STK31)), as well as variation in the effects of DNA methylation depending on ethnicity [13, 14].

The E6 and E7 oncoproteins can induce the expression of DNMTs and histone-modifying enzymes, including histone deacetylases (HDACs), acetyltransferases (HATs), methyltransferases (HMTS), and demethylases. They can also alter the activity of proteins associated with chromatin remodeling complex and miRNA processing [13]. The E6 oncoprotein activates *DNMT1* expression through degradation of p53 and release of transcription factors Sp1, which bind to the *DNMT1* gene promoter, while the E7 oncoprotein activates the expression of a stable complex with pRB and the release of the transcription factor E2F [12–14]. In CC, *CADM1, CDH1, DAPK1, EPB41L3, FAM1A4, MAL, PAX1,* and *hTER* are the most frequently methylated genes [13]. At the early stage of CC pathogenesis, the retinoic acid receptor β (*RARβ*) gene associated with cell differentiation and the Wnt/β inhibitory factor gene, the product of which inhibits the Wnt/β-catenin signaling pathway, are often methylated [14].

The HPV genome also undergoes epigenetic modification, as during the virus life cycle, methylation of late L1 and L2 oncoproteins and the LCR regulatory region changes [12, 13]. LCR hypermethylation prevents the E2 protein from regulating the expression of viral *E6* and *E7* oncogenes, causing its overexpression [14].

Post-translational modifications of histones (acetylation, methylation, phosphorylation, SUMOylation, and ubiquitination) affecting the structural state and transcriptional activity of chromatin are crucial in the regulation of the cell cycle, cell differentiation, maintenance of SCs, and epigenetic inheritance of transcriptional programs [14]. In normal cells, the balance between HDACs and HATS ensures the control over cell proliferation and death; E6 and E7 oncoproteins disrupt this balance, causing uncontrolled proliferation of cancer cells [12, 14]. Inhibition of HDACs, which reduce the level of histone acetylation and cause the silence of tumor suppressor

genes, is becoming a promising approach in cancer therapy. So, the inhibitor of HDAC all-trans retinoic acid (ATRA) in combination with suberoylanilide hydroxamic acid (SAHA) increases the content of acetylated histones in the promoter of the tumor suppressor genes *RARβ2*, E-cadherin and β-catenin, the deacetylation of promoters of which is reduced or absent in CC. The combination of valproic acid (VPA) and ATRA demonstrates additional antitumor effects due to reactivation of the expression of RARβ2, E-cadherin, P21CIP1, and P53 and a decrease in the expression of the *STAT3* gene, which activates transcription of genes responsible for proliferation. These results do not exclude the use of HDAC inhibitors and RARβ2 agonists as a new approach to the CC treatment [14].

Due to advances in biotechnology and high-throughput sequencing, the leading role of the aberrant expression of ncRNAs, single-stranded RNA transcripts, which include miRNAs, long ncRNAs (lncRNAs), and circular ncRNAs (circRNAs) in cancer pathogenesis has become clear. MiRNAs are of particular importance in this process, since they can participate in the regulation of both the most important biological processes (proliferation, differentiation, apoptosis) and molecular pathways of cancer pathogenesis (cell cycle, Wnt / β-catenin pathway, P53, E6-p53, E7 -pRb, PI3K-Akt, Notch) [3, 12–15, 30, 32–34]. MiRNA dysregulation may be a consequence of genomic mutations, abnormal modification of DNA methylation at miRNA gene loci or single-nucleotide polymorphisms (SNPs), as well as dysregulation of proteins involved in miRNA biogenesis [15, 32, 35].

Based on their effect on proto-oncogenes and oncosuppressors, miRNAs are respectively divided into oncomiRNAs and tumor suppressor miRNAs (TSMIRs); the content of the latter is significantly reduced in most types of cancer [15]. MiRNAs can also affect viral DNA replication; in turn, E6 and E7 oncoproteins can catalyze aberrant methylation of genes encoding miRNAs through the induction of DNMT overexpression [32]. Continuous E6 / E7 expression is associated with a decrease in intracellular concentrations of miR-23a, miR-23b, miR-206, miR-143, miR-15, and miR-16, all of which are associated with antitumor activity [12, 14].

Almost every stage of CC development has its own miRNA signature, which theoretically can be of great importance for the diagnosis, treatment, and monitoring of the process [15, 33, 36]. So, increased expression of miR-16, miR-21, miR-34a, and miR-143 was found in LSIL. In HSIL, increased expression of miR-21 and a decrease in expression of miR-143 were found [36] along with an increase in miR-205-5p, miR-130a-3p, and miR-3136-3p expression and suppression of miR-381-3p and miR-4531, while miRNA expression patterns did not depend on HR-HPV infection [33]. MiR-499 and miR-18a are described as markers of invasive CC; miR-125, which suppresses VEGF and migration and invasion of tumor cells (already used as TSMIR in the treatment of CC), and miR-375, acting through regulation of MELK and increased apoptosis, are described as oncosuppressors [15].

Downregulation of let-7c, miR-124, miR-126, miR-143, and miR-145 regulates oncogene expression. Destabilization of p53 by the E6 oncoprotein leads to suppression of miR-34a expression, which affects several components of the cell cycle, including CDK4, cyclin E2, E2F-1, hepatocyte growth factor MET receptor, and Bcl-2 [14]. Overexpression of miR-21 and downregulation of miR-29 were found useful for the diagnosis of invasive CC [15]. Activation of miR-31 and miR-9 expression and overexpression of miRNA-21 under the influence of E6 / E7 are associated with the progression of CC and poor prognosis [14].

Currently, several hundred miRNAs have been identified that are differentially expressed in CC [15, 34, 36]. Participation of ncRNAs in cancer pathogenesis significantly complicates the understanding of the molecular biology of cancer and makes these transcripts the subject of numerous studies aimed at revealing their diagnostic and prognostic value [14]. Their use in diagnosis has not yet been successful due to methodological problems and pronounced variability in the composition of miRNAs in different patients with the same type of cancer. In treatment based on miRNAs, it is also necessary to overcome the problem of their degradation by nucleases, inaccurate delivery to target cells, and side effects in the form of activation of immune responses [15].

CANCER STEM CELLS

In accordance with the hypothesis on cancer stem cells (**CSCs**), a tumor is characterized by a special hierarchy of cells, in which a small part of the subpopulation, called CSCs, has stem cell-like properties, including the ability to undergo asymmetric division, self-renewal, oncogenesis, and resistance to chemo- and radiation therapy due to the presence of detoxification or elimination systems [4, 5, 8, 9, 30, 37]. As a result of asymmetric division of CSCs, one daughter cell remains a stem cell, while another one losing its stemness gives rise to descendants that form the bulk of tumor cells of various degrees of differentiation [9]. The CSC paradigm allows to approach the understanding of the genesis of cancer, including CC, the explanation of the mechanisms of its metastasis, relapses, and resistance to chemo- and radiation therapy [4, 9, 11, 30, 38].

There are several theories on the origin of CSCs. Mutations leading to the appearance of CSCs can occur

in SCs and in already transformed (tumor) cells, causing the selection of cells with high oncogenic activity [5, 30]. Researchers cannot rule out the presence of a subpopulation of resident CSCs that ensure the development and maintenance of the initial tumor and are dormant in the niches of CSCs [4, 5, 8, 30], as well as circulating in the blood and disseminating CSCs responsible for metastasis. The CSC niche is a microenvironment of cells formed by the extracellular matrix and stromal cells (fibroblasts, macrophages, etc.) and which, through call – cell and cell – matrix interactions involving a large number of various signaling molecules (cytokines, miRNAs, hormones), determines the regulation of the dormant state of CSCs, activation of CSCs in response to stress (hypoxia, chemotherapy), as well as proliferation and differentiation of their descendants [4, 39]. Cancer cells are able to transit stochastically between these states, which also supports the hierarchy of differentiation and occurs, in particular, during treatment [9].

The existence of CSCs determines the heterogeneity of most tumors, including CC, which is manifested both through intertumor heterogeneity that refers to different aggressiveness and different clinical outcomes in the same type of tumor and through intratumor heterogeneity which is manifested by biological and molecular differences between tumor cells in the same tumor in one patient. The tumor is a combination of CSCs with mixed mesenchymal / epithelial phenotypes and cancer non-stem cells, which can acquire stem cell-like properties when exposed to EMT [4, 9]. EMT characterized by the induction of transcription factors SNAI1, SNAI2, TWIST1, and BMI1 is considered as the main source of CSCs [4, 5]. CSCs are capable of transdifferentiating into vascular endothelial cells, as well as into other tumor-associated stromal cells, which can also contribute to tumor heterogeneity [4, 9].

CIN and subsequent events of CC pathogenesis develop in the cells of the transition zone between the endo- and exocervix, which is known as SCJ of the cervix or the transformation zone [4, 5]. The cells at the cervical SCJ have unique morphology and their specific markers include keratin 7 (Krt7), anterior gradient 2 (AGR2), CD63, matrix metalloproteinase 7 (MMP7), and guanine deaminase (GDA). The persistence of the SCJ genetic profile in CIN and CC cells indicates the origin of numerous CC subtypes from the cells at cervical SCJ and suggests that SCJ may be a niche for cervical CSCs [4, 9, 26].

Existing methods of treatment (chemo- and radiation therapy) eliminate only cancer non-stem cells, CSCs survive in niches that protect them and lead to cancer relapse [4, 5, 8, 9, 39], which allows them to be considered as a core of the malignant tumor [39] and the most likely target for treatment [8, 9, 39]. The molecular mechanisms that determine the future of CSCs, cell – cell interactions, and the molecular profile of the cervical CSC niche are still largely unclear, and laboratory protocols have not been developed to isolate CSCs in a sufficient amount, which makes their identification a difficult task [9, 11].

Currently, there is no set of universal markers for the identification and isolation of CSCs. The main source of material for studying CSCs is the so-called side population, which is a small (up to 20%) subpopulation of cells inside the tumor, exhibiting the properties of CSCs [4, 5]. Identification of multipotent CSCs can be based on the ability of these cells to secrete the Hoechst fluorescent dye and under certain conditions to form spheroids that are cells of the epithelial / mesenchymal phenotype. The existing method of isolating CSCs is based on determining the expression of surface markers using fluorescence-activated cell sorting (FACS), confocal microscopy, immunohistochemistry, reverse transcription polymerase chain reaction (RT-qPCR), as well as subsequent testing of the oncogenic efficiency of the obtained cells in an animal experiment and analyzing the resulting tumor subpopulation [5].

A number of cytokeratins (CK-5, 8, 13, 17, 18 and 19) of CSCs and SCs of the cervix have common expression, but only CK-19 and CK-17 are considered as possible CSC markers, since their high expression in CC is associated with high malignancy and metastasis, while the side population of cells expressing CK-19 and CK-17 demonstrates high oncogenicity [5, 11]. Np63, a key protein of the Sonic-Hg signaling pathway, is also considered as a putative CSC marker, and it may be responsible for stemness through the induction of the Bmi-1 protein required for SC proliferation [11].

Common CSC markers in cancers of various body locations include high expression of CD44, CD90, CD44, CD133, CD271, CD49f, ALL+ [4, 5, 26] and OCT4, NANOG, β-catenin, and aldehyde dehydrogenase (ALDH1). ALDH1 is associated with detoxification of chemicals through the oxidation of aldehydes and protection from high concentrations of reactive oxygen species. Expression of ALDH1 correlates with high tumor activity and radioresistance [3–5, 11, 26]. The resistance of CSCs to death is provided by active repair of DNA damage through phosphorylation of ATM and CHK1 / CHK2 or activation of anti-apoptotic WNT / β-catenin, PI3K / Akt, and Notch signaling pathways [4]. The development of therapies that prevent DNA repair in cancer cells or target anti-apoptotic proteins of the Bcl-2 family has proven to be more difficult than expected; studies of PARPi inhibitors (poly(ADP-ribose)

polymerase), which is involved in DNA repair, mainly concern ovarian cancer [15].

The SOX2-positive cell population in CC demonstrates radioresistance and expresses higher levels of genes related to stemness (OCT4 and ALDH1) and EMT, which confirms that SOX2 is a marker for cervical CSCs. As a key transcription factor, SOX2 plays an important role in SCs and may be involved in the initiation of the tumor process [9, 26, 40].

The resistance of CSCs to treatment and the occurrence of relapses are associated with increased activity in CSCs in carrier proteins, including MDR1 (ABCB1), ABCC1 (MRP1,) and ABCG2. ABCG2 is an ATP-binding cassette transporter that blocks absorption, pumps a wide range of chemical compounds out of cells, and plays an important role in the development of multiple drug resistance in a number of cancer types [4, 5, 9, 11, 26]. ABCG2 activity is also associated with an increase in the expression of HIF-2α, a transcription factor induced by hypoxia 2, which, in turn, is associated with the expression of Oct4, a transcription factor that maintains CSC stemness [11]. In CC, the Nrf2 transcription factor plays an important role in regulating the expression of some endogenous antioxidants and detoxification enzymes [9].

Osteopontin (OPN), a chemokine-like protein of the extracellular matrix, which is secreted by tumor and stromal cells, is also considered as a potential CSC marker. Overexpression of OPN in CC correlates with resistance to hypoxic cell injury during radiation exposure and poor survival rate. OPN also induces tumor angiogenesis by modulating HIF1α-dependent VEGF expression in response to hypoxia, regulates CD44-mediated p38 phosphorylation, affects the nuclear factor kappa-B (NF-kB) in activated B cells and NF-kB-dependent furin expression, which are involved in the response to HPV. The self-renewal ability of CSCs mediated by OPN can be suppressed by a decrease in NF-κB expression [9].

More and more data are accumulated on epigenetic programming of stemness, in particular, the involvement of miRNAs in the regulation of the cell cycle of both SCs and CSCs by direct or indirect influence on its various components (*RB*, p53, p21, *LATS2, PTEN*, cyclins, CDKs, and CDKIs) [4, 30], while differences in the transcription level of individual miRNAs in resident SCs and CSCs were revealed [30]. In CSCs of various tumors, a decrease in the expression of the let-7 miRNA family with oncosuppressive properties was revealed, which leads to overexpression of the MYC, RAS, HMGA2, and BLIMP oncogenes. Members of the let-7 family also downregulate PTEN, cause inactivation of the PI3K / AKT / MTOR pathway, and suppress EMT [30].

Therapeutic strategies targeting CSC signaling pathways and the niche of CSCs are under development [4]. As a component of the CC treatment, DNMT inhibitors, which are anti-CSC compounds, are already used. The use of a dual delivery system with sequential release of drugs suppressing tumor cell proliferation can be potentially effective. The use of drugs (antibodies) that affect CSCs can be also effective along with targeting molecular mechanisms that maintain the dormant state of CSCs indefinitely or eliminate a subpopulation of such cells, in particular, ablation of cytosolic phospholipase A2 alpha (CPLA2a). CPLA2a is a key mediator of inflammation and the pathophysiology of cancer. It markedly improves the sensitivity of CSCs to chemotherapy by suppressing β-signaling catenin. Targeting CSCs using nanoparticles can be an effective approach [4].

EPITHELIAL – MESENCHYMAL TRANSITION

Mortality in CC is largely determined by the recurrence of the tumor process. At the same time, EMT plays the most important role in invasion, metastasis, and metastatic recurrence of a tumor [4, 41]. EMT is characterized by transdifferentiation, or the acquisition of a mesenchymal phenotype by an epithelial cell due to a loss of expression of epithelial markers (E-cadherin, β-catenin, occludin, claudin, plakophilin, cytokeratins, desmoplakins) and increased expression of mesenchymal markers (N-cadherin, vimentin, fibronectin) [30, 41–43].

EMT can be initiated by dysregulation of various signaling pathways, which include transcriptional regulators of oncogenes and oncosuppressors, miRNAs, and growth factors [30, 41]. The transcriptional regulators of EMT in CC include Snail / Slug / Smug; Zeb1 / Zeb2; Twist1 / Twist2; E47; among growth factors – TGF, EGF; among oncogenes – HVP16; E6 / E7; Sam68; AEG1; FTS, among oncosuppressors – Klotho, SFRPs; and a wide range of miRNAs – miR200, the miR-155 and miR361-5p family [25, 41], as well as a number of other molecular factors – β1-integrin receptors, MMPs7 / 9, IL-6, TNF-α, etc. [41]. EMT is also determined by the regulatory function of the chemokine network, in particular, by the level of CXCL6. In CC, a decrease in the level of miR-101-5p was found, which normally suppresses cancer progression through inhibition of CXCL6 promoting EMT [32]. Twist1 / Twist2 are the main regulators of EMT; they are responsible for the activation of the AKT and β-catenin pathways and the preservation of CSCs [41]. EMT-exposed CSCs can enter a dormant state, evading traditional therapies that target actively dividing cells [4].

In the EMT cluster in CC, studies revealed high immunoreactivity of the stroma with high expression of caveolin-1, MYH11, and RAB11, as well as YAP and

ZEB1 dysregulation, which may be associated with lower levels of miR-200A-3p expression in this cluster. These data suggest a potential role of YAP and stromal reactivity in the regulation of EMT and progression of CC [25]. Understanding the molecular aberrations characteristic of EMT and the underlying cellular signaling of EMT is important for the development of treatment leading to reduction of mortality from CC [4, 41].

VAGINAL MICROBIOTA AND CERVICAL MICROENVIRONMENT

In recent years, studies have accumulated data on the significant role of the cervicovaginal microbiome (CVM) in the dynamics of HPV infection, including the natural clearance of HPV, CIN regression, and the immune response modeled by the CVM [7, 16, 19]. The protective role of the normal vaginal microbiota is associated with certain types of lactobacilli: *Lactobacillus (L.) crispatus*, *L. gasseri*, *L. jensenii*, *L. iners*, which produce a number of antimicrobial compounds and lactic acid, providing low vaginal pH (≤ 4.5) necessary to suppress colonization by pathogenic species (*Chlamydia trachomatis, Neisseria gonorrhoeae, and G. Vaginalis)* and maintain vaginal homeostasis [2, 7, 16, 19, 22, 44–46].

In dysbiosis, or bacterial vaginosis, lactobacilli are depleted and replaced by a polymicrobial consortium of microaerophilic and anaerobic bacteria [2, 7, 22, 44, 47]. HPV infection is more often associated with non-lactobacillus dominance in the CVM, when *Atopobium*, *Mycoplasma hominis, Haemophilus, Gardnerella, Sneathia and Megasphaera, Prevotella* dominate. The development of CIN is caused by the presence *of Sneathia, Atopobium, Parvimonas, Fusobacterium, Anaerococcus, Peptostreptococcus, Mycoplasmateles, Pseudomanales* [7, 19, 22]. CC is associated with an increase in aerobic bacterial flora and the presence of *Corynobacterium spp.* and *Staphylococcus spp*. [20]. A high risk of HR-HPV infection and the development of CIN is associated with a small number of *L. crispatus* producing peptidoglycans that activate Langerhans cells, which are the most important antigen-presenting cells in the cervical epithelium. A strong relationship was established *in vivo* between Langerhans cell activity and the clearance of HPV, while *L. crispatus* was the most common *Lactobacillus* species in individuals with the natural clearance of HPV [7, 5, 46]. The clearance of HPV is also associated with *L. gasseri* [22].

Vaginal dysbiosis is accompanied by an alteration of the epithelial barrier due to the production of sialidase by anaerobes, alters immune and metabolic signaling, supporting the production of proinflammatory cytokines and chemokines, activating a number of cell signaling pathways, in particular the NF-κB pathway. It also induces genomic instability of epithelial cells, angiogenesis, impaired proliferation, and apoptosis [16, 22, 46]. It also plays an active role in the progression of the tumor process in both CC, endometrial and ovarian cancer, including through participation in the modulation of estrogen metabolism [22].

A comprehensive analysis revealed signatures associated with the development of the tumor process and the composition of the cervicovaginal microbiota and identified features of the cervicovaginal microenvironment (immune mediators, vaginal pH), which may contribute to the persistence of HPV, the development of precancerous lesions, and cancer progression [16, 19, 22, 47–50]. A number of studies demonstrated the critical role of CVM in the modulation of cervicovaginal immune responses and even host susceptibility to HIV [7]. Potencies of LSIL (low-grade squamous intraepithelial lesion) and HSIL are closely correlated with the functional state of the immune system, in particular T- and B lymphocytes, dendritic cells, NK cells, and macrophages [6, 46]. The depletion of T cells that helps tumors escape the host immune system is phenotypically characterized by co-expression of immune inhibitory receptors or immune checkpoints, a gradual loss of proliferation, cytokine secretion, and cytolytic activity.

In CC, the most promising immune checkpoints are PD-1 (programmed cell death protein 1) and CTLA-4 (cytotoxic T lymphocyte antigen-4) [6]. In HSIL, the immune microenvironment is characterized by the absence of intraepithelial CD3+, CD4+, and CD8+ T cell infiltrates and Langerhans cells compared to normal epithelium and an increase in CD25+FoxP3+ regulatory T cells (Tregs) and CD163+ M2 macrophages. Spontaneous regression of HSIL is associated with a low Treg count, an increasing number of intraepithelial CD8+ T cells, and a high ratio of CD4+/CD25+ T cells [46].

L. crispatus can suppress anaerobic growth and activate Langerhans cells by lowering factors associated with epithelial barrier disruption (sialidase and anaerobic biopellicle) and immune suppression through the effect on Treg, Th2, Th17 cells, IL-10, IL-17, and TGFß. At the same time, the expression of biomarkers of activated Langerhans cells, which include antigen-binding langerin and TLR9, antigen-presenting CD1a and MHC-I, co-stimulatory CD80 / 86 and CD40 molecules, and CMI-associated molecules (cytotoxic T lymphocytes, Th1, IFNγ, TNFα), increases [7].

In general, the effect of CVM on the CC pathogenesis is a complex and not yet fully clear process. It is probably associated with the implementation of various enzymatic mechanisms and metabolic pathways involved in protecting the epithelium, removing toxins, and stimulating and regulating the immune system, which makes

CVM a target for the development of innovative therapeutic approaches based on the use of microbial products as immune activators, in particular in HPV infection [7, 16, 44, 46].

CONCLUSION

Knowledge obtained in the field of cancer biology suggests that, despite the close relationship between CC and HR-HPV, a variety of epigenetic events play an important role in CC pathogenesis, as they regulate the cell cycle, determine chromosome stability, and activate telomeres and apoptosis. These epigenetic events are functionally closely related to the state of the cervicovaginal microbiota and immunity. Expanding the understanding of the most important mechanisms of CC pathogenesis determines both the variety of diagnostic and prognostic markers and potentially possible ways of treating CC, in particular, based on the use of knowledge about regulatory miRNAs, CSC markers, and the state of the cervicovaginal microbiota.

REFERENCES

1. Wilailak S., Kengsakil M., Kehoe S. Worldwide initiatives to eliminate cervical cancer. *Int. J. Gynecol. Obstet*. 2021;155(1):102–106. DOI: 10.1002/ijgo.13879.
2. Bhatla N., Aoki D., Sharma D.N., Sankaranarayanan R. Cancer of the cervix uteri. *Int. J. Gynaecol. Obstet*. 2018;143(2):22–36. DOI: 10.1002/ijgo.12611.
3. Lin M., Ye M., Zhu X. Recent advances on the molecular mechanism of cervical carcinogenesis based on systems biology technologies. *Comput. Struct. Biotechnol. J.* 2019;17:241–250. DOI: 10.1016/j.csbj.2019.02.001.
4. Fiore R.D., Suleiman S., Drago-Ferrante R., Subbannayya Y., Pentimalli F., Giordano A. et al. Cancer Stem Cells and Their Possible Implications in Cervical Cancer: A Short Review. *Int. J. Mol. Sci.* 2022;23(9):5167. DOI: 10.3390/ijms23095167.
5. Mendoza-Almanza G., Ortíz-Sánchez E., Rocha-Zavaleta L., Rivas-Santiago C., Esparza-Ibarra E., Olmos J. Cervical cancer stem cells and other leading factors associated with cervical cancer development. *Oncol. Lett*. 2019;18(4):3423–3432. DOI: 10.3892/ol.2019.10718.
6. Guo L., Hua K. Cervical cancer: emerging immune landscape and treatment. *Onco. Targets Ther.* 2020;12(13):8037–8047. DOI: 10.2147/OTT.S264312.
7. Dai W., Du H., Li S., Wu R. Cervicovaginal microbiome factors in clearance of human papillomavirus Infection. *Front. Oncol.* 2021;11:722639. DOI: 10.3389/fonc.2021.722639.
8. Chhabra R. Cervical cancer stem cells: opportunities and challenges. *J. Cancer Res. Clin. Oncol.* 2015;141(11):1889–1897. DOI: 10.1007/s00432-014-1905-y.
9. Huang R., Rofstad E.K. Cancer stem cells (CSCs), cervical CSCs and targeted therapies. *Oncotarget.* 2017;8(21):35351–35367. DOI: 10.18632/oncotarget.10169
10. Zhao Z., Wang Y., Wu Y., Li D., Zhang T., Ma Y. et al. Single-cell analysis defines the lineage plasticity of stem cells in cervix epithelium. *Cell Regen.* 2021;10(1):36. DOI: 10.1186/s13619-021-00096-2.
11. Ortiz-Sánchez E., Santiago-López L., Cruz-Domínguez V.B., Toledo-Guzmán M.E., Hernandez-Gueto D., Muñiz-Hernández S. et al. Characterization of cervical cancer stem cell-like cells: phenotiping, stemness, and human papilloma virus co-receptor expression. *Oncotarget.* 2016;7(22):31943–31954. DOI: 10.18632/oncotarget.8218.
12. Senapati R., Senapati N.N., Dwibedi B. Molecular mechanisms of HPV mediated neoplastic progression. *Infect. Agent. Cancer*. 2016;11(1):59. DOI: 10.1186/s13027-016-0107-4.
13. Soto D., Song C., McLaughlin-Drubin M.E. Epigenetic alterations in human papillomavirus-associated cancers. *Viruses.* 2017;9(9):248. DOI: 10.3390/v9090248.
14. Da Silva M.L.R., De Albuquerque B.H.D.R., Allyrio T.A.M.F., De Almeida V.D., Cobucci R.N.O., Bezerra F.L. et al. The role of HPV-induced epigenetic changes in cervical carcinogenesis (Review). *Biomed. Rep*. 202115(1):60. DOI: 10.3892/br.2021.1436.
15. Bañuelos-Villegas E.G., Pérez-yPérez M.F., Alvarez-Salas L.M. Cervical cancer, papillomavirus, and miRNA dysfunction. *Front. Mol. Biosci*. 2021;8:758337. DOI: 10.3389/fmolb.2021.758337.
16. Castanheira C.P., Sallas M.L., Nunes R.A.L., Lorenzi N.P.C., Termini L. Microbiome and cervical cancer. *Pathobiology.* 2021;88(2):187–197. DOI: 10.1159/000511477.
17. Lee S.A., Baik S., Chung S.H. Functional roles of female sex hormones and their nuclear receptors in cervical cancer. *Essays Biochem*. 2021;65(6):941–950. DOI: 10.1042/EBC20200175.
18. Baik S., Mehta F.F., Unsal E., Park Y., Chung S.H. Estrogen inhibits epithelial progesterone receptor-dependent progestin therapy efficacy in a mouse model of cervical cancer. *Am. J. Pathol.* 2022;192(2):353–360. DOI: 10.1016/j.ajpath.2021.10.008.
19. Klein C., Gonzalez D., Samwel K., Kahesa C., Mwaiselage J., Aluthge N. et al. Relationship between the Cervical Microbiome, HIV Status, and Precancerous Lesions. *mBio*. 2019;10(1):e02785-18. DOI: 10.1128/mBio.02785-18.
20. Manzanares-Leal G.L., Coronel-Martínez J.A., Rodríguez-Morales M., Rangel-Cuevas I., Bustamante-Montes L.P., Sandoval-Trujillo H. et al. Preliminary identification of the aerobic cervicovaginal microbiota in Mexican women with cervical cancer as the first step towards metagenomic studies. *Front. Cell Infect. Microbiol*. 2022;12:838491. DOI: 10.3389/fcimb.2022.838491.
21. Martinez-Rodriduez F., Limones-Gonzalez J.E., Mendoza-Almanza B., Esparza-Ibarra El., Gallegos-Flores P.I., Ayla-Lujan J.A. et al. Understanding cervical cancer trough proteomics. *Cells.* 2021;10(8):1854. DOI: 10.3390/cells10081854.
22. Łaniewski P., Ilhan Z.E., Herbst-Kralovetz M.M. The microbiome and gynaecological cancer development, prevention and therapy. *Nat. Rev. Urol*. 2020;17(4):232–250. DOI: 10.1038/s41585-020-0286-z.
23. Revathidevi S., Murugan A.K., Nakaoka H., Inoue I., Munirajan A.K. APOBEC: A molecular driver in cervical cancer pathogenesis. *Cancer Lett.* 2021;496:104–116. DOI: 10.1016/j.canlet.2020.10.004.

24. Kamal M., Lameiras S., Deloger M., Morel A., Vacher S., Lecerf C. et al. Human papilloma virus (HPV) integration signature in Cervical Cancer: identification of MACROD2 gene as HPV hot spot integration site. *Br. J. Cancer*. 2021;124(4):777–785. DOI: 10.1038/s41416-020-01153-4.
25. Salvesen H.B. The cancer genome atlas research network. Integrated genomic and molecular characterization of cervical cancer. *Nature*. 2017;543(7645):378–384. DOI: 10.1038/nature21386.
26. Organista-Nava J., Gómez-Gómez Y., Garibay-Cerdenares O.L., Leyva-Vázquez M.A., Illades-Aguiar B. Cervical cancer stem cell-associated genes: prognostic implications in cervical cancer. *Oncol. Lett.* 2019;18(1):7–14. DOI: 10.3892/ol.2019.10307.
27. Kecheryukova M.M., Snezhko A.V., Verenikina E.V., Mensheninina A.P., Adamyan M.L., Arja A.Yu., et al. Complex molecular characterization of cervical cancer: metastatic markers. *Modern Problems of Science and Education.* 2020.2 (in Russ.). URL:https://science–education.ru/ru/article/view?id=29769 (accessed 23.09.2021).
28. Yu X., Xu J., Xu D., Bi X., Wang H., Lu Y. et al. Comprehensive analysis of the carcinogenic process, tumor microenvironment, and drug response in HPV-positive cancers. *Front. Oncol*. 2022;12:842060. DOI: 10.3389/fonc.2022.842060.
29. Olusola P., Banerjee H.N., Philley J.V., Santanu Dasgupta S. Human papilloma virus-associated cervical cancer and health disparities. *Cells.* 2019;8(6):622. DOI: 10.3390/cells8060622.
30. Mens M.M.J., Ghanbari M. Cell cycle regulation of stem cells by microRNAs. *Stem. Cell Rev. Rep*. 2018;14(3):309–322. DOI: 10.1007/s12015-018-9808-y.
31. Li Y., Tollefsbol T.O. Age-related epigenetic drift and phenotypic plasticity loss: implications in prevention of age-related human diseases. *Epigenomics.* 2016;8(12):1637–1651. DOI: 10.2217/epi-2016-0078.
32. Shen S., Zhang S., Liu P., Wang J., Du H. Potential role of microRNAs in the treatment and diagnosis of cervical cancer. *Cancer Genet.* 2020;248–249:25–30. DOI: 10.1016/j.cancergen.2020.09.003.
33. Causin R.L., Silva L.S., Evangelista A.F., Leal L.F., Souza K.C.B., Pessôa-Pereira D. et al. MicroRNA biomarkers of high-grade cervical intraepithelial neoplasia in liquid biopsy. *Biomed Res. Int*. 2021;2021:6650966. DOI: 10.1155/2021/6650966.
34. Zheng M., Hou L., Ma Y., Zhou L., Wang F., Cheng B. et al. Exosomal let-7d-3p and miR-30d-5p as diagnostic biomarkers for non-invasive screening of cervical cancer and its precursors. *Mol. Cancer.* 2019;18(1):76. DOI: 10.1186/s12943-019-0999-x.
35. Babion I., Jaspers A., van Splunter A.P., van der Hoorn I.A.E., Wilting S.M., Steenbergen R.D.M. miR-9-5p exerts a dual role in cervical cancer and targets transcription factor TWIST1. *Cells.* 2019;9(1):65. DOI: 10.3390/cells9010065.
36. Babion I., Miok V., Jaspers A., Huseinovic A., Steenbergen R.D.M., van Wieringen W.N., Wilting S.M. Identification of deregulated pathways, key regulators, and novel miRNA-mRNA interactions in HPV-mediated transformation. *Cancers (Basel).* 2020;12(3):700. DOI: 10.3390/cancers12030700.
37. Zhao Z., Wang Y., Wu Y., Li D., Zhang T., Ma Y. et al. Single-cell analysis defines the lineage plasticity of stem cells in cervix epithelium. *Cell Regen*. 2021;10(1):36. DOI: 10.1186/s13619-021-00096-2.
38. Lim J.R., Mouawad J., Gorton O.K., Bubb W.A., Kwan A.H. Cancer stem cell characteristics and their potential as therapeutic targets. *Med. Oncol.* 2021;38(7):76. DOI: 10.1007/s12032-021-01524-8.
39. Oshimori N. Cancer stem cells and their niche in the progression of squamous cell carcinoma. *Cancer Sci.* 2020;111(11):3985–3992. DOI: 10.1111/cas.14639.
40. Sudhalkar N., Rathod N.P., Mathews A., Chopra S., Sriram H., Shrivastava S.K. et al. Potential role of cancer stem cells as biomarkers and therapeutic targets in cervical cancer. *Stem. Cell Rev. Rep*. 2018;14(3):309–322. DOI: 10.1007/s12015-018-9808-y.
41. Campo L., Zhang C., Breuer E.-K. EMT-inducing molecular factors in gynecological cancer. *Biomad. Res. Int*. 2015;2015:420891. DOI: 10.1155/2015/420891.
42. Gonzalez D.M., Medici D. Signaling mechanisms of the epithelial–mesenchymal transition. *Science Signaling*. 2014;7(344):re8. DOI: 10.1126/scisignal.2005189.
43. Ye X., Weinberg R.A. Epithelial–mesenchymal plasticity: a central regulator of cancer progression. *Trends Cell Biol.* 2015;25(11):675–686. DOI: 10.1016/j.tcb.2015.07.012.
44. Tango C.N., Seo S.S., Kwon M. et al. Taxonomic and functional differences in cervical microbiome associated with cervical cancer development. *Scic. Rep.* 2020;10(1):9720. DOI: 10.1038/s41598-020-66607-4.
45. Kaelin E.A., Skidmore P.T., Łaniewski P., Holland L.A., Chase D.M., Herbst-Kralovetz M.M. et al. Cervicovaginal DNA virome alterations are associated with genital inflammation and microbiota composition. *mSystems*. 2022;7(2):e0006422. DOI: 10.1128/msystems.00064-22.
46. Muntinga C.L.P., Vos van Steenwijk P.J., Bekkers R.L.M., van Esch E.M.G. Importance of the immune microenvironment in the spontaneous regression of cervical squamous intraepithelial lesions (CSIL) and implications for immunotherapy. *J. Clin. Med*. 2022;11(5):1432. DOI: 10.3390/jcm11051432.
47. Lin W., Zhang Q., Chen Y., Dong B., Xue H., Lei H. et al. Changes of the vaginal microbiota in HPV infection and cervical intraepithelial neoplasia: a cross-sectional analysis. *Sci. Rep.* 2022;12(1):2812. DOI: 10.1038/s41598-022-06731-5.
48. Bokulich N.A., Łaniewski P., Adamov A., Chase D.M., Caporaso J.G., Herbst-Kralovetz M.M. Multi-omics data integration reveals metabolome as the top predictor of the cervicovaginal microenvironment. *PLoS Comput. Biol.* 2022;18(2):e1009876. DOI: 10.1371/journal.pcbi.1009876.
49. Curty G., de Carvalho P.S., Soares M.A. The role of the cervicovaginal microbiome on the genesis and as a biomarker of premalignant cervical intraepithelial neoplasia and invasive cervical cancer. *Int. J. Mol. Sci*. 2019;21(1):222. DOI: 10.3390/ijms21010222.
50. Yang L., Yang Y., Meng M., Wang W., He S., Zhao Y. et al. Identification of prognosis-related genes in the cervical cancer immune microenvironment. *Gene.* 2021;766:145119. DOI: 10.1016/j.gene.2020.145119.

Authors' information

Naumova Lyudmila A. – Dr. Sci. (Med.), Professor, Department of Pathophysiology and General Pathology, Medical Institute, Surgut State University, Khanty-Mansiysk Autonomous District – Yugra, Surgut, naumovala@yandex.ru, https://orcid.org/0000-0003-1145-3710

Starodumova Valentina A. – Post-Graduate Student, Department of Pathophysiology and General Pathology, Medical Institute, Surgut State University, Khanty-Mansiysk Autonomous District – Yugra, Surgut, starodumovav@list.ru, https://orcid.org/0000-0001-8362-0608

(✉) **Naumova Lyudmila A.,** naumovala@yandex.ru

Received 07.06.2022;
approved after peer review 30.08.2022;
accepted 08.12.2022

УДК 616.132.2-089.86-06-055.2
https://doi.org/10.20538/1682-0363-2023-2-156-164

Surgical revascularization in women: focus on factors worsening the prognosis

Serebryakova V.N., Kaveshnikov V.S., Kuzmichkina M.A.

Cardiology Research Institute, Tomsk National Research Medical Center (NRMC), Russian Academy of Sciences
111a, Kievskaya Str., Tomsk, 634012, Russian Federation

ABSTRACT

In recent years, there has been an increase in the number of women undergoing coronary artery bypass grafting (CABG). Although the evidence of gender effects on outcomes is controversial, a number of publications have reported less favorable outcomes of CABG in women. The aim of this paper was to review the literature regarding factors that worsen short- and long-term prognosis in women undergoing surgical myocardial revascularization.

Gender differences in early outcomes of CABG are largely explained by gender distribution of baseline clinical characteristics. Women, compared to men, undergo CABG at an older age and have a worse profile of cardiovascular disease (CVD) risk factors (RF), comorbidity burden, structural and functional cardiac pathology, and coronary lesions. In women, complete myocardial revascularization is less frequent than in men, venous shunts are used more frequently, and the left internal mammary artery is less frequently used as a conduit. In addition to the baseline characteristics, higher incidence of perioperative myocardial infarction (MI), higher prevalence of anxiety and depression, lower quality of life and social adaptation after CABG, and lower involvement of women in rehabilitation programs, compared to men, may contribute to a less favorable long-term prognosis after CABG in women.

There is a need for more information for physicians about the specifics of CVDs and anatomical and surgical aspects of CABG in women. It is also necessary to raise patients' awareness of RF correction and to involve them in educational technologies. Recommendations for diagnosis and treatment of CVDs should be developed taking into account gender. Further research is also required to develop and implement sex-specific models for predicting surgical risks. Long-term follow-up is appropriate in women with recent MI and a history of diabetes mellitus. To further improve clinical outcomes of CABG in women, development of approaches that facilitate more complete revascularization and reduce the incidence of perioperative complications, such as MI and pneumonia, is needed. More answers to questions regarding gender differences in long-term outcomes of CABG may be obtained by analyzing further studies involving a larger number of female patients.

Keywords: coronary artery bypass grafting, female sex, women, complications, predictors, prognosis

Conflict of interest. The authors declare the absence of obvious and potential conflicts of interest related to the publication of this article.

Source of financing. The authors state that they received no funding for the study.

For citation: Serebryakova V.N., Kaveshnikov V.S., Kuzmichkina M.A. Surgical revascularization in women: focus on factors worsening the prognosis. *Bulletin of Siberian Medicine.* 2023;22(2):156–164. https://doi.org/10.20538/1682-0363-2023-2-156-164.

✉ *Kuzmichkina Maria A.,* kuzmariakuz@gmail.com

Хирургическая реваскуляризация у женщин: фокус на факторы, ухудшающие прогноз

Серебрякова В.Н., Кавешников В.С., Кузьмичкина М.А.

Научно-исследовательский институт (НИИ) кардиологии, Томский национальный исследовательский медицинский центр (НИМЦ) Российской академии наук
Россия, 634012, Томск, ул. Киевская, 111а

РЕЗЮМЕ

В прошедшие годы отмечается рост количества женщин, перенесших операцию коронарного шунтирования (КШ). Хотя данные о влиянии пола на исходы операции неоднозначны, в ряде публикаций сообщается о менее благоприятных результатах КШ у женщин. Целью данной работы явился анализ литературы в отношении факторов, ухудшающих краткосрочный и долгосрочный прогнозы у женщин, подвергнутых хирургической реваскуляризации миокарда.

Гендерные различия в ранних исходах КШ в значительной мере объясняются особенностями распределения между полами исходных клинических характеристик. У женщин, по сравнению с мужчинами, КШ осуществляется в более старшем возрасте, и они имеют более отягощенный профиль факторов риска (ФР) сердечно-сосудистых заболеваний (ССЗ), коморбидной нагруженности, структурно-функциональной патологии сердца и поражения коронарных артерий (КА). В отдельных случаях у женщин реже, чем у мужчин, осуществляется полная реваскуляризация миокарда, чаще используются венозные шунты, реже в качестве кондуита используется левая маммарная артерия. Кроме исходных клинических характеристик менее благоприятному отдаленному прогнозу после КШ у женщин могут способствовать более высокая частота периоперационного инфаркта миокарда (ИМ), более высокая распространенность тревоги и депрессии, менее высокий уровень качества жизни и социальной адаптации, а также меньшая вовлеченность женщин в реабилитационные программы по сравнению с мужчинами.

Существует потребность в дополнительном информировании врачей относительно особенностей течения ССЗ и анатомо-хирургических аспектов КШ у женщин. Также необходимо повышение осведомленности пациентов в вопросах коррекции ФР, привлечение их к участию в обучающих технологиях. Рекомендации по диагностике и лечению ССЗ целесообразно разрабатывать с учетом пола. Также необходимы дальнейшие исследования, направленные на разработку и практическое внедрение поло-специфических моделей прогнозирования хирургического риска. Долгосрочное наблюдение целесообразно у женщин с недавним ИМ и сахарным диабетом в анамнезе. Существенное значение имеет компенсация коморбидных состояний. Для улучшения клинических результатов КШ у женщин необходимо дальнейшее развитие подходов, способствующих осуществлению более полной реваскуляризации, а также снижению частоты периоперационных осложнений, таких как ИМ и пневмония. Больше ответов на вопросы относительно гендерных различий в отдаленных исходах КШ может быть получено при анализе дальнейших исследований с участием большего числа пациентов женского пола.

Ключевые слова: коронарное шунтирование, женский пол, женщины, осложнения, предикторы, прогноз

Конфликт интересов. Авторы заявляют об отсутствии конфликта интересов.

Источник финансирования. Авторы заявляют об отсутствии финансирования при проведении исследования.

Для цитирования: Серебрякова В.Н., Кавешников В.С., Кузьмичкина М.А. Хирургическая реваскуляризация у женщин: фокус на факторы, ухудшающие прогноз. *Бюллетень сибирской медицины.* 2023;22(2):156–164. https://doi.org/10.20538/1682-0363-2023-2-156-164.

INTRODUCTION

It is well known that cardiovascular diseases (CVDs) are one of the leading causes of death, in particular among women, and they continue to be the subject of close attention of scientists. Understanding the potential influence of gender on the development of not only CVDs but also their complications is currently of paramount importance to eliminate gender differences in approaches to the diagnosis and treatment of this group of diseases. A characteristic feature of coronary artery disease (CAD) is that this patholo-

gy has clinical manifestations mainly in patients over the age of 40 years. Development of many chronic diseases (multimorbidity) with age is explained by involutionary processes, and the deterministic possibility of their combination (comorbidity) remains a very urgent problem for scientific research, both among men and women [1–3].

One of the most effective methods for improving long-term prognosis and quality of life (QoL) in patients with severe CAD is coronary artery bypass grafting (CABG) [4]. About a million CABGs are performed annually in the world among patients with chronic CAD. Attention is drawn to repeated reports of a less favorable immediate and long-term prognosis after CABG in women [5–7]. Predictors that affect the immediate and long-term outcome of CABG have been actively studied over the past decades. At the same time, the factors explaining the gender difference in the outcome of surgical treatment for CAD have not been fully determined yet. The aim of this work was to review the literature regarding factors that explain gender differences in the immediate and long-term prognosis after CABG.

According to research data, the mortality rate from CAD among women is higher than among men and amounts to 23 and 21%, respectively [8]. According to the US Society of Thoracic Surgeons, a study of 344,913 patients who underwent CABG showed a higher rate of operative mortality among women (4.5 vs. 2.6% in men, $p < 0.001$) [9]. The results of other studies also support this standpoint. Thus, in a large meta-analysis, it was noted that postoperative mortality was significantly higher in women than in men (relative risk (RR) = 1.77; 95% confidence interval (CI): 1.67–1.88) [10].

When CABG is performed with the aid of cardiopulmonary bypass (CPB), in-hospital mortality among women is also higher than among men. M. Alam et al. revealed higher mortality among women compared to men, not only in the short term, but also in the medium and long term after CABG [10]. A less favorable long-term prognosis in women after CABG is also confirmed by other works [6, 11–13]. At the same time, the analysis of CABG cases in the period from 2003 to 2015 showed that the 30-day survival rate in women (average age 67 years) was lower, but the long-term survival, on the contrary, was higher than in operated men (average age 64 years) [14]. J.F. ter Woorst et al. noted lower rates of long-term mortality (120 days) in women after CABG performed without the use of CPB compared to the traditional revascularization method. No such difference was found in men [15]. A similar pattern was previously identified in the work by S.P. Fu et al. [16].

Despite the fact that criteria for selecting patients for surgery have been developed, hospital-acquired complications remain relevant in cardiac surgery practice. The most common complications are perioperative myocardial infarction (MI), neurological and infectious complications, systemic inflammatory response, as well as development of renal failure and various arrhythmias [17–20]. A number of studies have noted that in-hospital mortality and a higher proportion of severe complications (MI, stroke, acute kidney injury with the development of renal failure) after the intervention are more characteristic of women [21–23]. In women, angina pectoris recurs more often, there is higher incidence of intraoperative MI, acute heart failure, or chronic decompensation, respectively [24, 25]. In the long term after CABG, women were more likely to have repeated hospitalizations for MI and congestive heart failure than men, but survival did not differ between the genders [26].

However, in the available literature there are data that do not confirm the prognostic value of gender. For example, in a study by C.R. Herman et al. [27] that evaluated immediate outcomes of cardiac surgery, no gender effect on the development of a composite end point (infection, stroke, acute renal failure, death) was revealed. Among age-matched patients under 65 years, gender-specific mortality did not show statistically significant differences [28]. Other authors note that perioperative mortality among women was no higher than among men, and differences in the immediate CABG outcomes related only to infectious wounds, neurological complications, the frequency of resternotomy, and the duration of inpatient treatment [29]. A number of studies have shown that gender did not have a significant impact on the long-term prognosis [30, 31]. Thus, the data on the effect of gender on the immediate and long-term prognosis after CABG are ambiguous: in some studies, prognostic parameters in women do not differ from those in men, in others, they show less favorable trends.

Of the factors potentially influencing gender differences in the outcomes of CABG we should first of all consider the effect of age. According to the results of numerous studies, it has been established that men are 3 times more likely to undergo CABG than women, which is due to an earlier onset of CAD [9]. However, the situation changes with age: among candidates for CABG over the age of 65 years, women prevail

[32]. According to domestic and foreign researchers, women are admitted for surgical treatment for CAD at an older age than men [33–35]. It is also worth noting that the maximum gender differences in the incidence of MI and other cardiovascular complications in most studies are detected at a relatively early age and significantly decrease after the age of 65 years.

A study conducted in Germany showed the relationship between gender, age, and early mortality after CABG. It was found that in the group of young women under the age of 50 years, postoperative mortality was 2.4 times higher than in men, while in 80-year-old women, mortality was similar to that of men of the same age [36]. In another study, however, the largest gender difference in early mortality after CABG (180 days) was noted in the age group of 70–79 years, with higher mortality rates in women [5]. At the same time, the difference between the genders in relation to the risk of in-hospital mortality was leveled after adjusting for gender differences in the distribution of preoperative risk factors. A similar age pattern was revealed in the study by American researchers, who showed that in-hospital mortality was higher in women than in men in all age groups, but it was most pronounced among patients under 50 years of age (3.4 vs. 1.1%) [37].

Similar differences were noted among patients aged 50–59 years – the probability of death among women was 2.4 times higher (2.6 vs. 1.1%) [37]. In older age groups, these differences were less pronounced ($p < 0.001$). There were also no gender differences in early prognosis after CABG among 70–84-year-old patients in an observational study presented by Turkish cardiologists that included 223 patients [38]. Thus, the severity of gender differences in relation to the immediate prognosis after CABG largely depends on age. The reported age limits for the maximum gender effect are controversial, but there is a trend toward the most pronounced gender differences among relatively young patients and toward a gradual decrease in the differences as the age approaches 80 years and older.

A characteristic feature of the clinical manifestations of CAD in women is significant severity of symptoms of the disease [39, 40]. Women who subsequently undergo CABG seek surgery with more severe symptoms of CAD and higher urgency for cardiac surgery [6]. The possibility of systematic delays in recognizing and diagnosing the severity of CAD in women, resulting in a less favorable outcome of CABG, cannot be ruled out [6, 41]. This, in turn, can be facilitated by a number of factors: in women, an atypical course of CAD is detected more often, the sensitivity of non-invasive methods for diagnosing this disease is lower, diagnostic angiography is performed less frequently, stenosing coronary atherosclerosis is detected less often, and CAD develops 7–10 years later than in men [42]. However, American researchers showed that if women are admitted for CABG sufficiently early, this improves both the immediate outcomes of the surgery and patients' QoL later after the surgery [43].

It should also be noted that until 2013, the classical anatomical EuroSCORE (European System for Cardiac Operative Risk Evaluation) risk scale was used. Undoubtedly, this scale helped in choosing the optimal method of revascularization, since it made it possible to identify patients with a high risk of adverse events after percutaneous intervention. This scale had a significant drawback – it did not take into account clinical parameters and gender. This drawback was corrected when a new scale had been developed – EuroSCORE II, which made it possible to assess the surgical risk of CABG with account of gender-associated comorbidities [13].

Less favorable outcomes of CABG in women are partly explained by gender differences in the prevalence of major CVD risk factors. It is known that the prevalence of risk factors leading to the development of CVD also differs among men and women. Thus, according to the epidemiological analysis, gender differences are found both in the cardiovascular mortality and in the prevalence of the leading risk factors for CVD, such as smoking, obesity, diabetes mellitus (DM) [44]. In men, the predominant risk factors for CAD are smoking, age, arterial hypertension, high levels of low-density lipoproteins; in women – age, overweight, diabetes, and high triglycerides, respectively. Women with a high triglyceride level have worse long-term survival rates (HR = 1.5; 95% CI: 1.1–2.1) compared to men with high triglyceride concentration (HR = 1.1; 95% CI: 0.9–1.3) [45]. A number of studies report higher prevalence of obesity, DM, and arterial hypertension in women undergoing CABG [6, 46].

Higher incidence of complications after CABG in women is largely due to greater comorbidity burden compared to men [33, 43, 47]. Important factors of early mortality after CABG in women are previous MI and acute cerebrovascular accident (ACV) [36]. Higher incidence of stroke in history in women is predictable, since it has been found that a cerebrovascular event (stroke and transient ischemic attack) in women marked the onset of CVD 1.5–2 times more

often than in men [9, 48]. In a study by V. Vaccarino et al. it was noted that women who were referred for CABG more often had a history of unstable angina and congestive heart failure in the preoperative period [35]. Several studies reported significantly higher prevalence of comorbidities in women, such as DM, chronic kidney disease, and chronic lung disease [46]. According to the American group of researchers, among women who underwent CABG, unstable angina and a higher grade of angina pectoris were more common, they more often suffered from congestive heart failure, although left ventricular ejection fraction (LVEF) did not significantly differ depending on gender [35].

It is believed that a number of perioperative risks in women come from the mechanisms of hormonal regulation, which are different in men and women. Before menopause in women, estrogen plays a protective role in preventing the development of CAD, which has a cardioprotective effect through specific estrogen receptors [49]. With the onset of menopause, a loss of this protective component leads to a cascade of pathological processes, such as deterioration of endothelial function, increased systemic vascular resistance, activation of the platelet link of hemostasis, and a trend toward platelet aggregation [50, 51]. Estrogen deficiency in young women increases the risk of CAD by 7 times. Estrogen replacement therapy in the postmenopausal period does not show a protective effect. Operated women have more frequent microcirculation disorders, which is associated with hormonal deficiency and higher prevalence of DM compared to men [52]. Also, females are characterized by vascular hypersensitivity to serotonin, which is also considered as a causal factor in the development of adverse events after CABG [53].

An important role among the predictors of an immediate and long-term prognosis after CABG is attributed to baseline parameters reflecting the structural and functional state of the heart and coronary bed. Traditionally, predictors of early postoperative complications include LVEF < 50% and the degree of CA stenosis > 70% [9]. Compared to men, women undergoing CABG are more likely to have low LVEF [35] and more pronounced changes in the coronary bed [36].

The prognosis after CABG may be influenced by anatomical and operative factors. In particular, compared to men, CAs in women have a smaller diameter and are more often tortuous, which can make it difficult to perform more complete revascularization. In their work, O'Connor et al. found that anterior descending artery diameter less than 1.5 mm increased the risk of in-hospital mortality [36]. It is reported that in women during CABG surgery, fewer distal anastomoses are applied, venous bypasses are used more often, and the left mammary artery is less commonly used as a conduit. At the same time, there are no differences between the genders in the remote patency of arterial bypasses, while lower rates are reported for venous bypasses in women. The reasons for these patterns continue to be the subject of discussion, in particular, the anatomical aspects already mentioned above are actively discussed. Another characteristic of the female population is insufficient development of the collateral circulation in severe stenosis or occlusion of the CA, especially in DM and postmenopausal women. The combination of these factors can affect both the duration of the surgery and its immediate outcomes [5, 6, 39, 40, 52].

Among the factors complicating the prognosis after surgical myocardial revascularization in women, one cannot but note psychosocial variables and QoL. Compared to men, women who underwent CABG had both more pronounced depression and a lower level of social adaptation. Since there is more pronounced comorbidity burden in operated women, they have lower QoL compared to men, both at baseline and six months after the intervention [35, 54].

Summarizing the above, we can conclude that a significant proportion of gender differences in terms of an early prognosis after CABG is explained by differences between men and women in baseline clinical characteristics, such as age, prevalence of risk factors for CVD and comorbid conditions, structural and functional state of the heart, and severity of CAD. Also, the gender effect can be influenced by anatomical and operative factors, in some cases limiting the possibility of complete myocardial revascularization in women.

As has been repeatedly noted, the gender difference in hospital outcomes of CABG is largely due to gender differences in baseline clinical characteristics. However, the situation changes in the longer term, in particular 3–6 months after the intervention. At this time, according to a number of studies, there is a discrepancy between the incident curves for clinically significant outcomes with less favorable trends observed in the female population [6, 10–12]. In these terms, the impact of operative factors on the further prognosis gradually decreases, and the most important issue in terms of long-term outcomes after

CABG is the effectiveness of secondary prevention of CVD [45].

One of the key approaches to improve the effectiveness of secondary prevention of CVD after CABG is cardiac rehabilitation. Participation in rehabilitation programs improves survival regardless of age, gender, program type, and intensity of moderate physical activity [45]. At the same time, along with the elderly and people with low socioeconomic status, women belong to a specific population which is less frequently referred for cardiac rehabilitation [55]. Subjectively, women tolerate CABG surgery relatively worse [24], it is more difficult for them to self-organize in the treatment of CAD due to fatigue, anxiety, depression, and the need to deal with household chores [56]. Another problem is that, in the long term, women are less committed to physical activity than men. Thus, 35% of women stop physical training 3 months after the end of the cardiac rehabilitation program [57]. These features can serve as potential barriers that reduce the effectiveness of secondary prevention of CVD in women after CABG.

Thus, apart from baseline clinical, structural, and functional variables, the long-term prognosis after CABG is largely influenced by the effectiveness of secondary prevention of CVD. A less favorable course of the late postoperative period in the female population may be due to higher incidence of perioperative MI, higher prevalence of anxiety and depression, lower QoL and social adaptation, and less active participation in rehabilitation programs compared to men.

CONCLUSION

In recent years, there has been an increase in the number of women undergoing CABG. At the same time, a number of publications report less favorable outcomes of CABG in women. In the course of this work, the review of the literature was carried out on factors explaining such gender differences. It was established that gender differences in early outcomes of CABG are largely explained by the peculiarities of the distribution of the baseline clinical characteristics between the genders. Compared to men, women undergo CABG at an older age, which largely explains a more burdened profile of CVD risk factors, comorbidity burden, structural and functional pathology of the heart, and CAD observed in them. In some cases, women are less likely than men to undergo complete myocardial revascularization, venous shunts are used more often, and the left mammary artery is less commonly used as a conduit. In addition to the baseline clinical characteristics, a less favorable long-term prognosis after CABG in women may be contributed by higher incidence of perioperative MI, higher prevalence of anxiety and depression, lower QoL and social adaptation level after CABG, as well as less active involvement of women in rehabilitation programs, compared to men.

Thus, there is a need for raising doctors' awareness about the characteristics of the CVD course and the anatomical and surgical aspects of CABG in women. It is also necessary to increase the awareness of patients about RF correction and to involve them in educational technologies. Recommendations for the diagnosis and treatment of CVD should be developed taking into account gender. Further research is required to develop and implement gender-specific models for predicting surgical risks. Long-term follow-up is reasonable in women with a history of recent MI and DM. Correction of comorbidities is also essential. To further improve the clinical outcomes of CABG in women, it is necessary to develop approaches that promote more complete revascularization and reduce the incidence of perioperative complications, such as MI and pneumonia. More answers to questions about gender differences in long-term outcomes of CABG may be obtained by analyzing further studies with more female patients.

REFERENCES

1. Boytsov S.A., Zayratyants O.V., Andreev E.M., Samorodskaya I.V. Comparison of mortality from ischemic heart disease among men and women over 50 years in Russian and the USA. *Russian Journal of Cardiology*. 2017;22(6):100–107 (in Russ.). DOI: 10.15829/1560-4071-2017-6-100-107.
2. Prados-Torres A., Calderon-Larranaga A., Hancco-Saavedra J., Poblador-Plou B., van den Akker M. Multimorbidity patterns: a systematic review. *J. Clin. Epidemiol.* 2014;67(3):254–66. DOI: 10.1016/j.jclinepi.2013.09.021.
3. Garganeeva A.A., Tukish O.V., Kuzheleva E.A., Okrugin S.A., Kuzmichkina M.A. A portrait of a myocardial infarction patient over the period of 30 years. *Clinical Medicine.* 2018;96(7):641–647 (in Russ.). DOI: 10.18821/0023-2149-2018-96-7-641-647.
4. Gaughan J., Kobel C. Coronary artery bypass grafts and diagnosis related groups: patient classification and hospital reimbursement in 10 European countries. *Health. Econ. Rev*. 2014;4:4. DOI: 10.1186/s13561-014-0004-8.
5. Arif R., Farag M., Gertner V., Szabo G., Weymann A., Veres G., Ruhparwar A. et al. Female gender and differences in outcome after isolated coronary artery bypass graft surgery: Does age play a role? *PLoS. One*. 2016;11(2):e0145371. DOI: 10.1371/journal.pone.0145371.
6. Hassan A., Chiasson M., Buth K., Hirsch G. Women have worse long-term outcomes after coronary artery bypass grafting than men. *Can. J. Cardiol*. 2005;21(9):757–762.

7. Den Ruijter H.M., Haitjema S., van der Meer M.G., van der Harst P., Rouleau J.L., Asselbergs F.W. et al. Long-term outcome in men and women after CABG; results from the IMAGINE trial. *Atherosclerosis.* 2015;241(1):284–288. DOI: 10.1016/j.atherosclerosis.2015.02.039.
8. Crea F., Battipaglia I., Andreotti F. Sex differences in mechanisms, presentation and management of ischaemic heart disease. *Atherosclerosis.* 2015;241(1):157–168. DOI: 10.1016/j.atherosclerosis.2015.04.802.
9. George J., Rapsomaniki E., Pujades-Rodriguez M., Shah A.D., Denaxas S., Herrett E. et al. How does cardiovascular disease first present in women and men? Incidence of 12 cardiovascular diseases in a contemporary cohort of 1,937,360 people. *Circulation.* 2015;132(14):1320–1328. DOI: 10.1161/CIRCULATIONAHA.114.013797.
10. Alam M., Bandeali S.J., Kayani W.T., Ahmad W., Shahzad S.A., Jneid H. et al. Comparison by meta-analysis of mortality after isolated coronary artery bypass grafting in women versus men. *Am. J. Cardiol.* 2013;112(3):309–17. DOI: 10.1016/j.amjcard.2013.03.034.
11. Efros L.A., Samorodskaya I.V. Factors affecting long-term survival after coronary artery bypass grafting (review). *Siberian Medical Journal (Tomsk)*. 2013;28(2):7–14 (in Russ.).
12. Enger T.B., Pleym H., Stenseth R., Greiff G., Wahba A., Videm V. Reduced Long-Term Relative Survival in Females and Younger Adults Undergoing Cardiac Surgery: A Prospective Cohort Study. *PLoS. One.* 2016;11(9): 0163754. DOI: 10.1371/journal.pone.0163754.
13. Johnston A., Mesana T.G., Lee D.S., Eddeen A.B., Sun L.Y. Sex Differences in Long-Term Survival After Major Cardiac Surgery: A Population-Based Cohort Study. *J. Am. Heart. Assoc*. 2019;8(17):e013260. DOI: 10.1161/JAHA.119.013260.
14. Nuru A., Weltzien J.A.H., Sandvik L., Tonnessen T., Bjornstad J.L. Short- and long-term survival after isolated coronary artery bypass grafting, the impact of gender and age. *Scand. Cardiovasc. J.* 2019;53(6):342–347. DOI: 10.1080/14017431.2019.1646430.
15. Ter Woorst J.F., Hoff A.H.T., Haanschoten M.C., Houterman S., van Straten A.H.M., Soliman-Hamad M.A. Do women benefit more than men from off-pump coronary artery bypass grafting? *Neth. Heart. J.* 2019;27(12): 629–635. DOI: 10.1007/s12471–019–01333–9.
16. Fu S.P., Zheng Z., Yuan X., Zhang S.J., Gao H.W., Li Y. et al. Impact of off-pump techniques on sex differences in early and late outcomes after isolated coronary artery bypass grafts. *Ann. Thorac. Surg*. 2009;87(4):1090–1096. DOI: 10.1016/j.athoracsur.2009.01.039.
17. Grigoryev E.V., Geize A.V., Sizova I.N., Plotnikov G.P., Sumin A.N., Ivanov S.V. et al. Preparing patients with ischemic heart disease and low left ventricular ejection fraction for CABG. *Cardiology and Cardiovascular Surgery.* 2012; 5(1): 88–93 (in Russ.).
18. Ter Woorst J.F., van Straten A.H.M., Houterman S., Soliman-Hamad M.A. Sex difference in coronary artery bypass grafting: preoperative profile and early outcome. *J. Cardiothorac. Vasc. Anesth.* 2019;33(10):2679–2684. DOI: 10.1053/j.jvca.2019.02.040.
19. Gurram A., Krishna N., Vasudevan A., Baquero L.A., Jayant A., Varma P.K. Female gender is not a risk factor for early mortality after coronary artery bypass grafting. *Ann. Card. Anaesth*. 2019;22(2): 187–193. DOI: 10.4103/aca.ACA_27_18.
20. Perry A., Chung M.J., Novak E., Krone R., Brown D.L. Development of a risk score to identify patients with type 2 diabetes mellitus and multivessel coronary artery disease who can defer bypass surgery. Diagn. Progn. Res. 2019; 3: 3. DOI: 10.1186/s41512-019-0048-7.
21. Kuzmichkina M.A., Serebryakova V.N. Disability and returning to work in patients after surgical myocardial revascularization. *Siberian Medical Journal (Tomsk)*. 2020;35(2):44–49. DOI: 10.29001/2073-8552-2020-35-2-44-49.
22. Kuzmichkina M.A., Serebryakova V.N. Rehabilitation for patients after CABG in terms of working capacity restoration. *Clinical Medicine*. 2020; 98(4):266–274 (in Russ.). DOI: 10.30629/0023-2149-2020-98-4-266-274.
23. Zhong J., Gao J., Luo J.C., Zheng J.L., Tu G.W., Xue Y. Serum creatinine as a predictor of mortality in patients readmitted to the intensive care unit after cardiac surgery: a retrospective cohort study in China. *J. Thorac. Dis.* 2021;13(3):1728–1736. DOI: 10.21037/jtd-20–3205.
24. Zimmerman L., Barnason S., Hertzog M., Young L., Nieveen J., Schulz P. et al. Gender differences in recovery outcomes after an early recovery symptom management intervention. *Heart. Lung*. 2011;40(5):429–439. DOI: 10.1016/j.hrtlng.2010.07.018.
25. Gaudino M., Samadashvili Z., Hameed I., Chikwe J., Girardi L.N., Hannan E.L. Differences in long-term outcomes after coronary artery bypass grafting using single vs multiple arterial grafts and the association with sex. *JAMA. Cardiol*. 2020:6(4):401–409. DOI: 10.1001/jamacardio.2020.6585.
26. Nicolini F., Vezzani A., Fortuna D., Contini G.A., Pacini D., Gabbieri D. et al. Gender differences in outcomes following isolated coronary artery bypass grafting: long-term results. *J. Cardiothorac. Surg.* 2016;11(1):144. DOI: 10.1186/s13019-016-0538-4.
27. Herman C.R., Buth K.J., Legare J.F., Levy A.R., Baskett R. Development of a predictive model for major adverse cardiac events in a coronary artery bypass and valve population. *J. Cardiothorac. Surg.* 2013;8:177. DOI: 10.1186/1749–8090–8–177.
28. Bhatt D.L., Eagle K.A., Ohman E.M., Hirsch A.T., Goto S., Mahoney E.M. et al. Comparative determinants of 4-year cardiovascular event rates in stable outpatients at risk of or with atherothrombosis. *JAMA.* 2010;304(12):1350–1357. DOI: 10.1001/jama.2010.1322.
29. Al-Alao B.S., Parissis H., McGovern E., Tolan M., Young V.K. Gender influence in isolated coronary artery bypass graft surgery: a propensity match score analysis of early outcomes. *Gen. Thorac. Cardiovasc. Surg.* 2012;60(7):417–424. DOI: 10.1007/s11748-012-0082-7.
30. Altarev S.S., Podaneva Yu.E., Malyshenko E.S., Ivanov S.V., Barbarash O.L. Risk factors for an unfavorable long-term prognosis in patients after CABG. *Heart: Journal for Practicing Physicians*. 2015;14(5(85)):263–272 (in Russ.). DOI: 10.18087/rhj.2015.5.2098

31. Karim M.N., Reid C.M., Huq M., Brilleman S.L., Cochrane A., Tran L. et al. Predicting long-term survival after coronary artery bypass graft surgery. *Interact. Cardiovasc. Thorac. Surg*. 2018;26(2):257–263. DOI: 10.1093/icvts/ivx330.
32. Albrektsen G., Heuch I., Lochen M.L., Thelle D.S., Wilsgaard T., Njolstad I. et al. Lifelong Gender Gap in Risk of Incident Myocardial Infarction: The Tromso Study. *JAMA. Intern. Med.* 2016;176(11):1673–1679. DOI: 10.1001/jamainternmed.2016.5451.
33. Duenas M., Ramirez C., Arana R., Failde I. Gender differences and determinants of health related quality of life in coronary patients: a follow-up study. BMC. *Cardiovasc. Disord*. 2011;11:24. DOI: 10.1186/1471-2261-11-24.
34. Efros L.A., Samorodskaya I.V. Structural features and the effect of comorbidities on the long-term prognosis after CABG. *Bulletin of Bakulev NCCVS. Cardiovascular Diseases.* 2013;14(1):33–41 (in Russ.).
35. Vaccarino V., Lin Z.Q., Kasl S.V., Mattera J.A., Roumanis S.A., Abramson J.L. et al. Krumholz H.M. Gender differences in recovery after coronary artery bypass surgery. *J. Am. Coll. Cardiol.* 2003;41(2):307–314. DOI: 10.1016/s0735-1097(02)02698-0.
36. Regitz-Zagrosek V., Lehmkuhl E., Hocher B., Goesmann D., Lehmkuhl H.B., Hausmann H. et al. Gender as a risk factor in young, not in old, women undergoing coronary artery bypass grafting. *J. Am. Coll. Cardiol.* 2004;44(12):2413–2414. DOI:10.1016/j.jacc.2004.09.031.
37. Vaccarino V., Abramson J.L., Veledar E., Weintraub W.S. Sex differences in hospital mortality after coronary artery bypass surgery: evidence for a higher mortality in younger women. *Circulation.* 2002;105(10):1176–1181. DOI: 10.1161/hc1002.105133.
38. Yuksel A., Kan I.I., Yolgosteren A., Velioglu Y., Cayr M.C., Gurbuz O. et al. Are the early postoperative outcomes of coronary artery bypass grafting surgery in elderly women worse compared to men's? *Braz. J. Cardiovasc. Surg.* 2016;32(3):191–196. DOI: 10.21470/1678-9741-2016-0071.
39. Norheim A., Segadal L. Relative survival after CABG surgery is poorer in women and in patients younger than 70 years at surgery. *Scand. Cardiovasc. J.* 2011;45(4):247–251. DOI: 10.3109/14017431.2011.582139.
40. Saxena A., Dinh D., Smith J.A., Shardey G., Reid C.M., Newcomb A.E. Sex differences in outcomes following isolated coronary artery bypass graft surgery in Australian patients: analysis of the Australasian Society of Cardiac and Thoracic Surgeons cardiac surgery database. *Eur. J. Cardiothorac. Surg.* 2012;41(4):755–762. DOI: 10.1093/ejcts/ezr039.
41. Schuchalter Ludmir S., Bental T., Itzhaki Ben Zadok O., Eisen A., Shochat T., Heruti I. et al. Report from a large and comprehensive single-center Women's Health Cardiology Clinic. *Womens. Health (London)*. 2021;17:17455065211013767. DOI: 10.1177/17455065211013767.
42. Duda-Pyszny D., Trzeciak P., Gasior M. Coronary artery disease in women. *Kardiochir. Torakochirurgia. Pol.* 2018;15(1):44–48. DOI: 10.5114/kitp.2018.74675.
43. Guzelhan Y., Ugurlucan M., Oztas D.M., Beyaz M.O., Unal O., Bektas N. et al. Anxiety and health-related quality of life after cardiac surgery. *Arch. Med. Sci. Atheroscler. Dis.* 2020;5:e27–e35. DOI: 10.5114/amsad.2020.94376.
44. European Cardiovascular Disease Statistics 2012. Løgstrup S., O'Kelly S., ed. European heart network and European Society of Cardiology; 2012:125.
45. Kulik A., Ruel M., Jneid H., Ferguson T.B., Hiratzka L.F., Ikonomidis J.S. et al. Secondary prevention after coronary artery bypass graft surgery: a scientific statement from the American Heart Association. *Circulation.* 2015;131(10):927–964. DOI: 10.1161/CIR.0000000000000182.
46. Ergunes K., Yilik L., Yetkin U., Lafc B., Bayrak S., Ozpak B., Gurbuz A. Early and mid-term outcomes in female patients undergoing isolated conventional coronary surgery. *J. Cardiovasc. Thorac. Res.* 2014;6(2):105–110. DOI: 10.5681/jcvtr.2014.023.
47. Humphries K.H., Izadnegahdar M., Sedlak T., Saw J., Johnston N., Schenck-Gustafsson K. et al. Sex differences in cardiovascular disease – Impact on care and outcomes. *Front. Neuroendocrinol*. 2017;46:46–70. DOI: 10.1016/j.yfrne.2017.04.001.
48. Neumann F., Sousauva M., Ahlsson A., Alfonso F., Banning A.P., Benedettol U., Byrne R.A. et al. Рекомендации ESC/EACTS по реваскуляризации миокарда 2018. *Российский кардиологический журнал*. 2019;24(8):151–226. DOI: 10.15829/1560-4071-2019-8-151-226.
49. Puglisi R., Mattia G., Care A., Marano G., Malorni W., Matarrese P. Non-genomic effects of estrogen on cell homeostasis and remodeling with special focus on cardiac ischemia/reperfusion injury. *Front. Endocrinol. (LaUSAnne*). 2019;10:733. DOI: 10.3389/fendo.2019.00733.
50. Roshan T.M., Normah J., Rehman A., Naing L. Effect of menopause on platelet activation markers determined by flow cytometry. *Am. J. Hematol*. 2005;80(4):257–261. DOI: 10.1002/ajh.20472.
51. Bobbert P., Stellbaum C., Steffens D., Schutte C., Bobbert T., Schultheiss H.P. et al. Postmenopausal women have an increased maximal platelet reactivity compared to men despite dual antiplatelet therapy. *Blood Coagul. Fibrinolysis*. 2012;23(8):723–728. DOI: 10.1097/MBC.0b013e 32835824b3.
52. Di Mauro M., Totaro A., Foschi M., Calafiore A.M. Gender and surgical revascularization: there is a light at the end of the tunnel? *J. Thorac. Dis.* 2018;10(18):S2202–S2205. DOI: 10.21037/jtd.2018.06.145.
53. Lamin V., Jaghoori A., Jakobczak R., Stafford I., Heresztyn T., Worthington M. et al. Mechanisms responsible for serotonin vascular reactivity sex differences in the internal mammary artery. *J. Am. Heart. Assoc.* 2018;7(14):e007126. DOI: 10.1161/JAHA.117.007126.
54. Dvoretskiy L.I., Gibradze N.T., Cherkasova N.A. Ischemic heart disease in women. *Russian Medical Journal.* 2011;19(2):79–83 (in Russ.).
55. Leon A.S., Franklin B.A., Costa F., Balady G.J., Berra K.A., Stewart K.J. et al. Cardiac rehabilitation and secondary prevention of coronary heart disease: an American Heart Association scientific statement from the Council on Clinical Cardiology (Subcommittee on Exercise, Cardiac Rehabilitation, and Prevention) and the Council on Nutrition, Physical Activity, and Metabolism (Subcommittee on Physical Activity), in collabo-

ration with the American Association of Cardiovascular and Pulmonary Rehabilitation. *Circulation.* 2005;111(3):369–376. DOI: 10.1161/01.CIR.0000151788.08740.5C.
56. Beckie T.M. A behavior change intervention for women in cardiac rehabilitation. *J. Cardiovasc. Nurs.* 2006;21(2):146–153. DOI: 10.1097/00005082–200603000–00013.
57. Moore S.M., Dolansky M.A., Ruland C.M., Pashkow F.J., Blackburn G.G. Predictors of women's exercise maintenance after cardiac rehabilitation. *J. Cardiopulm. Rehabil*. 2003;23(1): 409. DOI: 10.1097/00008483-200301000-00008.

Authors' information

Serebryakova Victoria N. – Cand. Sci. (Med.), Head of the Laboratory for Registries of Cardiovascular Diseases, High-Tech Interventions and Telemedicine, Cardiology Research Institute, Tomsk NRMC, Russian Academy of Sciences, Tomsk, vsk75@yandex.ru, https://orcid.org/0000-0002-9265-708X

Kaveshnikov Vladimir S. – Cand. Sci. (Med.), Leading Researcher, Laboratory for Registries of Cardiovascular Diseases, High-Tech Interventions and Telemedicine, Cardiology Research Institute, Tomsk NRMC, Russian Academy of Sciences, Tomsk, kave@ngs.ru, https://orcid.org/ 0000-0002-0211-4525

Kuzmichkina Maria A. – Cand. Sci. (Med.), Researcher, Laboratory for Registries of Cardiovascular Diseases, High-Tech Interventions and Telemedicine, Cardiology Research Institute, Tomsk NRMC, Russian Academy of Sciences, Tomsk, kuzmariakuz@gmail.com, https://orcid.org/0000-0002-5587-3947

(✉) **Kuzmichkina Maria A.,** kuzmariakuz@gmail.com

Received 10.06.2022;
approved after peer review 27.06.2022;
accepted 08.12.2022.

УДК 616.132.2-007-089-073.43-8
https://doi.org/10.20538/1682-0363-2023-2-165-169

A clinical case of the retroaortal course of the circumflex artery from the right coronary artery

Zakharyan E.A.[1], Grigoriev P.E.[2], Shatov D.V.[1], Soldatova O.A.[1], Fedorets A.V.[1], Kapitanova L.E.[1]

[1] Medical Academy named after S.I. Georgievsky, Vernadsky Crimean Federal University
5/7, Lenina Av., Simferopol, 295006, Republic of Crimea, Russian Federation

[2] Sevastopol State University
33, Universitetskaya Str., Sevastopol, 299053, Russian Federation

ABSTRACT

An anomalous course of coronary arteries is fairly rare pathology, which, however, may underlie clinical manifestations of coronary artery disease. Expanding the possibilities of diagnostic coronary angiography makes it possible to detect numerous types of congenital anomalies of the coronary arteries.

However, if earlier they were considered as angiographic findings and were characterized as benign, now this attitude has been changed due to reports of cases of syncope, angina pectoris, and sudden cardiac death associated with their presence. In this regard, a trend emerged to consider such anomalies as "potentially malignant", which explains special caution at their detection. The article presents a clinical case of an anomalous retroaortic course of the circumflex artery from the right coronary artery.

Keywords: coronary angiography, stenting, coronary artery anomaly

Conflict of interest. The authors declare the absence of obvious and potential conflicts of interest related to the publication of this article.

Source of financing. The authors state that they received no funding for the study.

For citation: Zakharyan E.A., Grigoriev P.E., Shatov D.V., Soldatova O.A., Fedorets A.V., Kapitanova L.E. A clinical case of the retroaortal course of the circumflex artery from the right coronary artery. *Bulletin of Siberian Medicine.* 2023;22(2):165–169. https://doi.org/10.20538/1682-0363-2023-2-165-169.

Клинический случай ретроаортального хода огибающей ветви, отходящей от правой коронарной артерии

Захарьян Е.А.[1], Григорьев П.Е.[2], Шатов Д.В.[1], Солдатова О.В.[1], Федорец А.В.[1], Капитанова Л.Э.[1]

[1] Медицинская академия им. С.И. Георгиевского, Крымский федеральный университет (КФУ) им. В.И. Вернадского
Россия, Республика Крым, 295006, г. Симферополь, бульвар Ленина, 5/7

[2] Севастопольский государственный университет (СевГУ)
Россия, 299053, г. Севастополь, ул. Университетская, 33

✉ *Shatov Dmitry V.,* e-mail: dmitrii_shatov@mail.ru

РЕЗЮМЕ

Аномалии отхождения коронарных артерий являются достаточно редко встречающейся патологией, которая, однако, может лежать в основе клинической манифестации ишемической болезни сердца. Расширение возможностей проведения диагностической коронароангиографии позволяет обнаружить многочисленные виды врожденных аномалий коронарных артерий.

Однако если ранее они считались ангиографическими находками и характеризовались как доброкачественные, то в дальнейшем такое отношение было изменено сообщениями о случаях синкопальных состояний, стенокардии и внезапной смерти, связанных с их наличием. В связи с этим сформировалась тенденция рассматривать такого рода аномалии как «потенциально злокачественные», что диктует особую настороженность при их обнаружении. Представлен клинический случай аномалии ретроаортального хода огибающей ветви от правой коронарной артерии.

Ключевые слова: коронароангиография, стентирование, аномалия коронарной артерии

Конфликт интересов. Авторы декларируют отсутствие явных и потенциальных конфликтов интересов, связанных с публикацией настоящей статьи.

Источник финансирования. Авторы заявляют об отсутствии финансирования при проведении исследования.

Для цитирования: Захарьян Е.А., Григорьев П.Е., Шатов Д.В., Солдатова О.В., Федорец А.В., Капитанова Л.Э. Клинический случай ретроаортального хода огибающей ветви, отходящей от правой коронарной артерии. *Бюллетень сибирской медицины.* 2023;22(2):165–169. https://doi.org/10.20538/1682-0363-2023-2-165-169.

INTRODUCTION

According to various data, the frequency of congenital anomalies of the coronary arteries (CAs) ranges from 0.6 to 1.8% [1, 2]. There are various types of dispositions of the CAs: anomalous origin of the left anterior descending artery (LAD) from the right coronary artery (RCA) (absence of the left CA trunk); an increase in the number of CAs branching from the aorta (absence of the right CA trunk); anomalous origin of the circumflex artery (Cx) from the 2nd or 1st sinuses of the aorta or from the RCA.

Pathological origin of the Cx is the most common anomaly of the CA origin, that is why in 1970 D. Effler recommended to call it a 'normal variant" [3, 4]. The location of the anomalous Cx is always the same: from its origin it runs back and to the left, bending around the aorta from behind, then passes between the posterior wall of the aorta and the anterior wall of the right and left atria until it reaches the left part of the atrioventricular sulcus, where it is covered by the left atrial appendage and has the usual location [5].

Despite the fact that this anomaly is still considered to be benign, cases of its association with sudden cardiac death and angina pectoris have been reported [6]. These phenomena may be due to repeated compression of this vessel due to dilation of the aortic root or curvature following its retro-aortic position, followed by compression of the coronary ostium in the sulcus with the formation of an obstacle to the blood flow. It is also necessary to mention recent studies suggesting that the anomalous origin of the CAs may increase the risk of atherosclerotic changes due to their acute angle of inclination [7]. The anomalous origin of the Cx from the right coronary sinus with the retroaortic course has been thoroughly studied and is not considered to be malignant because in this case the artery does not pass between two arterial structures [8].

CLINICAL CASE

A female patient Ch., aged 75 years, was admitted to the Regional Vascular Disease Center for patients with acute coronary syndrome with complaints of attacks of burning sensations behind the sternum lasting 3–10 minutes, arising from habitual physical activity and at rest. The patient had had a history of angina pectoris for more than 20 years with 3–5 attacks per week. During the last month, the patient noted a decrease in exercise tolerance and the fact that anginal attacks occurred at rest.

Upon admission, troponin I, myoglobin, and creatine phosphokinase-MB were negative. Other laboratory parameters were within the reference values. The ECG showed a normal sinus rhythm, heart rate of 64 beats per minute, and disrupted repolarization of the myocardium in the anterior, septal, and apical regions of the left ventricle (Fig. 1).

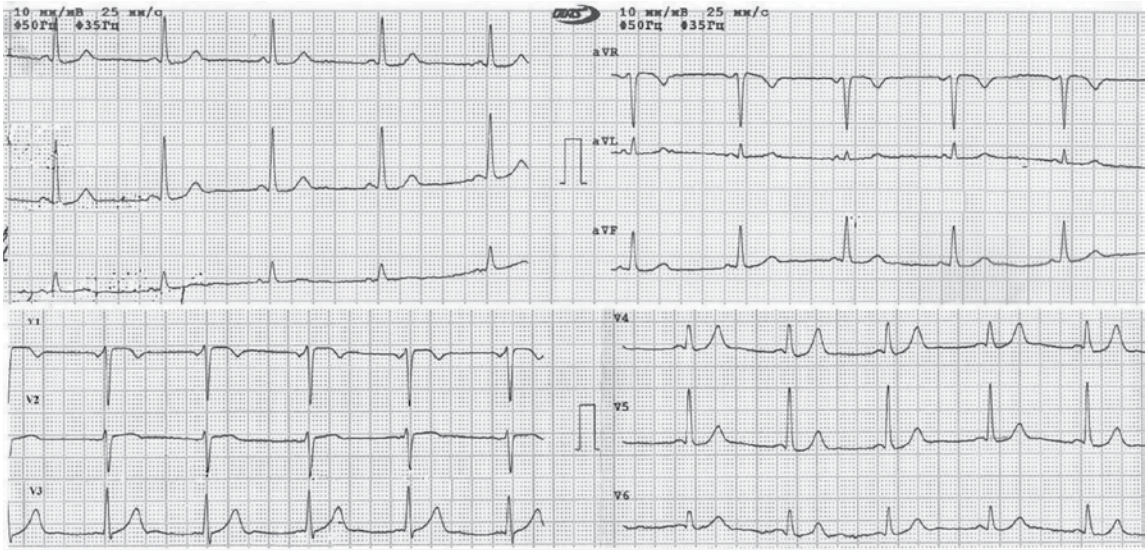

Fig. 1. Electrocardiogram before percutaneous transluminal coronary angioplasty. Speed 25 mm / s, voltage 10 mm / mV.

The results of Holter monitoring were the following: single (93) and paired (6) polytopic supraventricular extrasystoles; paroxysms (3) of unstable supraventricular tachycardia; single (97) and paired (4) polymorphic ventricular extrasystoles; paroxysms (4) of wide QRS complex tachycardia; the total duration of episodes of ischemic ST-segment displacement was 52 minutes; no significant changes in the QT interval were noted.

Echocardiography revealed type I left ventricular diastolic dysfunction (E/A= 0.7), ejection fraction (EF) 60%, slight left atrial dilatation (47 mm), and basal septal hypertrophy (12 mm). Hypokinetic and akinetic zones were not revealed.

The patient underwent coronary angiography, which revealed: atherosclerosis of the CAs, proximal LAD artery stenosis of the left CA of more than 70% with angiographic signs of plaque instability, stenosis of the middle segment of the RCA of about 50%; the origin of Cx from the RCA. At the end of the coronary angiography, percutaneous transluminal coronary angioplasty (PTCA) was performed for proximal LAD artery stenosis: a 3.0 × 20 mm REBEL stent deployed at 14 atm, optimization with a 3.5 x 12 mm balloon at 20 atm (Fig. 2–5).

The patient had no complications in the postoperative period. Positive dynamics were noted. The patient had no angina attacks, dyspnea at rest and when walking. The patient could move actively in the ward, and then she was able to walk around the department. The patient was discharged on the 9th day in a satisfactory condition for the cardiology follow-up care in a clinic at the place of residence. Confirmation Holter monitoring and echocardiography were to be performed after 6 months.

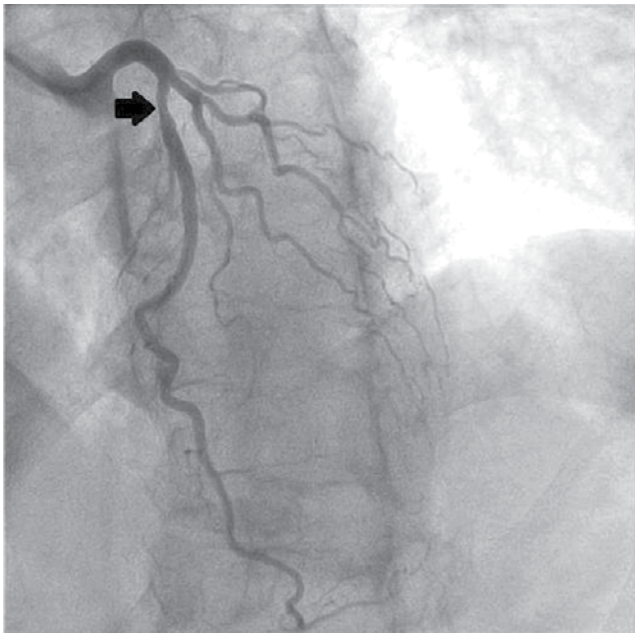

Fig. 2. Coronary angiography view of the LCA branches. The arrow marks stenosis with angiographic signs of atherosclerotic plaque instability

DISCUSSION

The anomalous origin of Cx from the RCA may be asymptomatic until adulthood, as a result it is often diagnosed accidentally or even goes unnoticed. Late diagnosis can lead to poor health and limited physical activity due to impaired myocardial perfusion.

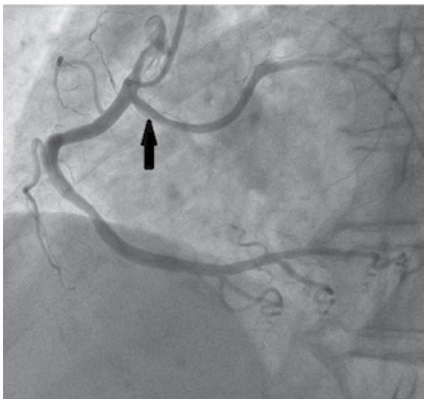

Fig. 3. Coronary angiography view of the RCA branches. The arrow marks the origin of the Cx from the RCA

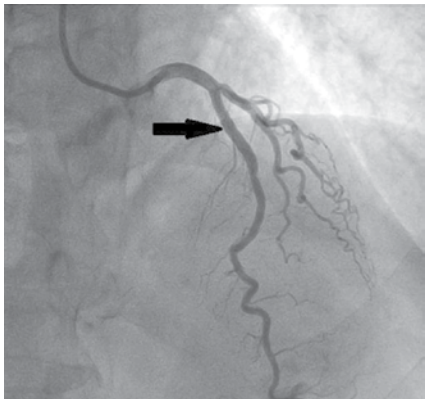

Fig. 4. Image of the LCA branches after PCI. The arrow marks the site of stent implantation

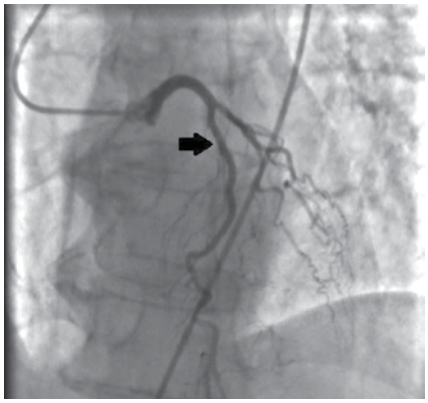

Fig. 5. Coronary angiography view of the LCA branches after 19 months. The arrow marks the site of stent implantation

This anomaly can be identified with the help of coronary angiography, which is sometimes crucial in establishing the final diagnosis. However, the presence of anomalies causes difficulties in conducting selective coronary angiography, since with conventional approaches, the results may not always have the diagnostic value. Moreover, this method is quite invasive, requires more items of specialized equipment, and cannot give an accurate spatial location of the anomalous Cx. These negative aspects can be eliminated by performing multidetector computed tomography of the CAs, which is a kind of mainstay for detecting coronary anomalies before the elective surgical intervention [9].

In this patient, the detected anomaly of the branch of the CA was an accidental finding. The severity of the stenotic lesion of the LAD artery served as an indication for endovascular intervention (stenting) with a subsequent positive clinical effect. It should be noted that the lesion localization in the ostium or proximal RCA can be a significant obstacle for the formation of an adequate blood supply to the posterior diaphragmatic surface of the heart, including the sinus node. The peculiarities of coronary blood flow depending on the cardiac cycle should also be taken into consideration: from the LCA basin – during the diastole, from the RCA basin – during the ventricular diastole and systole.

An increase in the scope of cardiac surgeries and X-ray-guided surgeries on the aortic valve also makes it necessary to focus on exclusion of anomalies in the origin of the CAs in the preoperative period. Thus, after aortic valve replacement, compression by a prosthetic valve ring or ligation of anomalous Cx are considered the main causes of myocardial ischemia; thorough and complete mobilization of the CAs is necessary to prevent this [10]. Also, a well-balanced approach to the surgical maneuver with preservation of coronary blood flow in the Cx should be considered when performing the Bentall procedure [11]. In some cases, balloon aortic valvuloplasty with subsequent transcatheter aortic valve replacement is more controlled, since it is possible to perform selective angiography of the anomalous Cx to confirm impaired blood flow in it early [12].

The presented clinical case confirms the importance of timely diagnosis of congenital anomalies of the origin of the CAs, since their presence can cause ischemia and arrhythmias and may also be associated with a risk of sudden cardiac death. Coronary angiography in combination with multidetector computed tomography of the CAs are complementary methods for diagnosing this pathology.

REFERENCES

1. Bagmanova Z.A. Anomalies of the coronary arteries. *Cardiology.* 2010;8:48–55 (in Russ.).
2. Ghanim D., Kusniec F., Kinany W., Qarawani D., Meerkin D., Taha K. et al. Left circumflex coronary artery as the culprit vessel in st-segment-elevation myocardial infarction. *Texas Heart Institute Journal.* 2017;44(5):320–325. DOI: 10.14503/THIJ-16-5905.
3. Lanjewar C.P., Kumar D., Sabnis G.R., Jare M., Phutane M., Shah H. et al. Anomalous origin of coronary artery from the opposite aortic sinus of Valsalva-a single center experience with a therapeutic conundrum. *Indian Heart Journal.* 2021;73(3):289–294. DOI: 10.1016/j.ihj.2021.03.012.
4. McCord C. Surgical treatment of coronary arteriosclerosis. *JAMA.* 1971;16(10):1650. DOI: 10.1001/jama.1971.03180360096030.
5. Seok O., Ju H.K., Min C.K., Young J.H., Youngkeun A., Myung H.J. Posterior myocardial infarction caused by

superdominant circumflex occlusion over an absent right coronary artery: Case report and review of literature. *MD Journal.* 2021;100(27):e26604. DOI: 10.1097/MD.0000000000026604.
6. Yan G.W., Bhetuwal A., Yang G.Q., Fu Q.S., Hu N., Zhao L.W. et al. Congenital absence of the right coronary artery: A case report and literature review. *Medicine (Baltimore).* 2018;97(12):e0187. DOI: 10.1097/MD.0000000000010187.
7. Tomanek R., Angelini P. Embryology of coronary arteries and anatomy/pathophysiology of coronary anomalies. *A comprehensive Update. International Journal of Cardiology*. 2019;281:28–34. DOI: 10.1016/j.ijcard.2018.11.135.
8. Harky A., Hof A., Ahmad M.U., Uppal R. Incidental finding of anomalous circumflex coronary artery from right coronary sinus prior to aortic valve surgery. *BMJ Case Reports*. 2017;2017:bcr2017219265. DOI: 10.1136/bcr-2017-219265.
9. Rosseel L., Bonnier H., Sonck J. Anomalous right coronary artery in a middle-aged patient: a case report and review of the literature. *Medicine (Baltimore)*. 2016;95(49):e5508. DOI: 10.1097/MD.0000000000005508.
10. Botta L., Amodio C., Pagano V., Di Marco L., Leone A., Loforte A. et al. AVR in patients with anomalous course of the circumflex artery without prosthetic downsizing. *Journal of Cardiac Surgery*. 2020;35(11):125–3127. DOI: 10.1111/jocs.14927.
11. Gasparovic I., Artemiou P., Kiss M., Hulman M. Bentall operation in a patient with an anomalous left circumflex artery: case report and review. *Journal of Saudi Heart Association.* 2017;29(4):305–307. DOI: 10.1016/j.jsha.2017.03.003.
12. Tabachnick D., Obokhae B., Harrington K., Brown D.L. Assessing the risk of an anomalous circumflex artery using balloon aortic valvuloplasty prior to transcatheter aortic valve replacement. *Catheter Cardiovascular Intervention*. 2020;96(2):497–499. DOI: 10.1002/ccd.28695.

Authors' information

Zakharyan Elena A. – Cand. Sci. (Med.), Associate Professor, Department of Internal Medicine No. 1, Medical Academy named after S.I. Georgievsky, Vernadsky Crimean Federal University, Simferopol, locren@yandex.ru, http://orcid.org/0000-0002-7384-9705

Grigoriev Pavel E. – Dr. Sci. (Biology), Associate Professor, Professor, Department of Psychology, Sevastopol State University, Sevastopol, mhnty@yandex.ru, http://orcid.org/0000-0001-7390-9109

Shatov Dmitry V. – Cand. Sci. (Med.), Associate Professor, Department of General Surgery, Anesthesiology, Resuscitation and Emergency Medicine, Medical Academy named after S.I. Georgievsky, Vernadsky Crimean Federal University, Simferopol, dmitrii_shatov@mail.ru , http://orcid.org/0000-0003-2248-5400

Soldatova Olga V. – Cand. Sci. (Med.), Teaching Assistant, Department of Internal Medicine No. 1, Medical Academy named after S.I. Georgievsky, Vernadsky Crimean Federal University, Simferopol, olgasolda@mail.ru, http://orcid.org/0000-0002-6310-9199

Fedorets Alina V. – Student, Medical Academy named after S.I. Georgievsky, Vernadsky Crimean Federal University, Simferopol, alinka_fedorec96@mail.ru, http://orcid.org/0000-0001-6079-1527

Kapitanova Leila E. – Student, Medical Academy named after S.I. Georgievsky, Vernadsky Crimean Federal University, Simferopol, leila-namazova@mail.ru, http://orcid.org/0000-0001-5663-8765

(✉) **Shatov Dmitry V.,** e-mail: dmitrii_shatov@mail.ru

Received 30.08.2022;
approved after peer review 07.09.2022;
accepted 08.12.2022

УДК 616-002-039.42-02:575.224
https://doi.org/10.20538/1682-0363-2023-2-170-175

A family case of a rare autoinflammatory disease associated with mutations in the *NLRP3* and *TNFRSF1A* genes in the practice of a rheumatologist

Kurochkina Yu.D.[1], Korolev M.A.[1], Letyagina E.A.[1], Fishman V.S.[2], Gridina M.M.[2], Valeeva E.S.[2]

[1] *Research Institute of Clinical and Experimental Lymphology – branch of the Institute of Cytology and Genetics, Siberian Branch of the Russian Academy of Sciences*
4, Timakova Str., Novosibirsk, 630060, Russian Federation

[2] *Institute of Cytology and Genetics, Siberian Branch of the Russian Academy of Sciences*
10, Akademika Lavrentyeva Av., Novosibirsk, 630090, Russian Federation

ABSTRACT

The article presents a clinical case of a rare autoinflammatory disease – a family case of Muckle – Wells syndrome. The diversity of clinical manifestations and the impossibility of confirming the diagnosis without a genetic study by DNA sequencing determine the complexity of and delay in the diagnosis. The development of severe complications and, as a consequence, a fatal outcome necessitates early diagnosis. The described clinical case demonstrates the importance of DNA sequencing for the timely diagnosis of the disease, the features of the disease course, and the familial nature of the disease. The diagnosis of Mackle – Wells syndrome in young family members before the development of severe complications will allow to start adequate and timely treatment and prevent the development of amyloidosis.

Keywords: autoinflammatory diseases, DNA sequencing, Muckle – Wells syndrome

Conflict of interest. The authors declare the absence of obvious and potential conflicts of interest related to the publication of this article.

Source of financing. The authors state that they received no funding for the study.

For citation: Kurochkina Yu.D., Korolev M.A., Letyagina E.A., Fishman V.S. , Gridina M.M. , Valeeva E.S. A family case of a rare autoinflammatory disease associated with mutations in the NLRP3 and TNFRSF1A genes in the practice of a rheumatologist. *Bulletin of Siberian Medicine.* 2023;22(2):170–175. https://doi.org/10.20538/1682-0363-2023-2-170-175.

Семейный случай редкого аутовоспалительного заболевания, ассоциированного с мутациями в генах *NLRP3* и *TNFRSF1A*, в практике ревматолога

Курочкина Ю.Д.[1], Королев М.А.[1], Летягина Е.А.[1], Фишман В.С.[2], Гридина М.М.[2], Валеева Э.С.[2]

[1] *Научно-исследовательский институт клинической и экспериментальной лимфологии – филиал Федерального исследовательского центра «Институт цитологии и генетики Сибирского отделения Российской академии наук» (НИИКЭЛ – филиал ИЦиГ СО РАН)*
Россия, 630060, г. Новосибирск, ул. Тимакова, 2

✉ *Kurochkina Yulia D.,* juli_k@bk.ru

[2] *Федеральный исследовательский центр «Институт цитологии и генетики Сибирского отделения Российской академии наук» (ИЦиГ СО РАН)*
Россия, 630090, г. Новосибирск, пр. Академика Лаврентьева, 10

РЕЗЮМЕ

Представлен случай из клинической практики редкого аутовоспалительного заболевания – семейного случая синдрома Макла – Уэллса. Разнообразность клинических проявлений и невозможность подтверждения диагноза без проведения генетического исследования методом секвенирования ДНК определяет сложность и несвоевременность диагностики. Развитие тяжелых осложнений и, как следствие, летального исхода обусловливает необходимость ранней постановки диагноза. Описанный клинический случай демонстрирует как важность проведения секвенирования ДНК для своевременной диагностики заболевания, так и особенности течения болезни и семейный характер заболевания. Постановка диагноза синдрома Макла – Уэллса у членов семьи молодого возраста до развития тяжелых осложнений позволят начать адекватное своевременное лечение и предотвратить развитие амилоидоза.

Ключевые слова: аутовоспалительные заболевания, секвенирование ДНК, синдром Макла – Уэллса

Конфликт интересов. Авторы заявляют об отсутствии конфликта интересов.

Источник финансирования. Авторы заявляют об отсутствии финансирования при проведении исследования. Работа выполнена в рамках государственного задания НИИКЭЛ – филиал ИЦиГ СО РАН (тема № FWNR-2023-0009).

Для цитирования: Курочкина Ю.Д., Королев М.А., Летягина Е.А., Фишман В.С., Гридина М.М., Валеева Э.С. Семейный случай редкого аутовоспалительного заболевания, ассоциированного с мутациями в генах *NLRP3* и *TNFRSF1A*, в практике ревматолога. *Бюллетень сибирской медицины.* 2023;22(2):170–175. https://doi.org/10.20538/1682-0363-2023-2-170-175.

INTRODUCTION

Autoinflammatory diseases (AID) refer to a group of rare monogenic and polygenic diseases characterized by innate immunity activation in response to endogenic and exogenic stimuli without the production of autoantibodies[1]. Nowadays almost 32 nosological forms of diseases are registered in the Eurofever registry with definite clinical presentatiton, the common feature of all these forms is recurrent episodes of periodic fever. The main variants of monogenic periodic fevers involve cryopyrin–associated periodic syndrome (CAPS), familial Mediterranean fever, tumor necrosis factor receptor-associated periodic syndrome (TRAPS), mevalonate kinase deficiency, etc. CAPS includes a group of diseases caused by variants of cryopyrin-encoding *NLRP3* gene leading to inflammasome activation and interleukin (IL)-1 overproduction [2].

Diversity of clinical features (fever, hives, iridocyclitis, sensorineural hearing loss, elevated inflammation markers) and confirmation of the diagnosis exclusively by genetic testing (DNA sequencing) make the diagnosis challenging [3]resulting in excessive inflammasome activation with subsequent overproduction of interleukin (IL. To date, early diagnostic criteria have been developed to help suspect AID [4]. The need for timely diagnosis is due to the development of fatal complications, usually amyloidosis. Successful treatment for CAPS is directly associated with early administration of IL-1 inhibitors. Nowadays two monoclonal antibody drugs blocking IL-1 have been registered in the Russian Federation: canakinumab and anakinra. Also, there is some experience of using IL-6 and tumor necrosis factor (TNF)α inhibitors, but the greatest clinical effect is achieved using IL-1 inhibitors [5]efficacy and tolerability of biological disease-modifying antirheumatic drugs (bDMARDs. The main limitation associated with routine use of IL-1 inhibitors is high cost of the drug. We would like to present a clinical case of diagnosing familial CAPS in the practice of a rheumatologist.

CLINICAL CASE

The study was carried out in accordance with ethical standards developed in accordance with the Declaration of Helsinki of the World Medical Association “Ethical principles for medical research involving human subjects” as amended in 2000 and Rules of Clinical Practice in the Russian Federation approved by

the Order of the Ministry of Healthcare of the Russian Federation No. 266 of 19.06.2003.

Female patient X., proband (Fig. 1), aged 28 years, sought a consultation with a rheumatologist at the Research Institute of Clinical and Experimental Lymphology, branch of the Institute of Cytology and Genetics SB RAS, Novosibirsk, in October 2021. The patient complained of recurrent hives on the body and limbs, inflammatory pain in small wrist joints, and episodes of hyperthermia up to 37.5 °C.

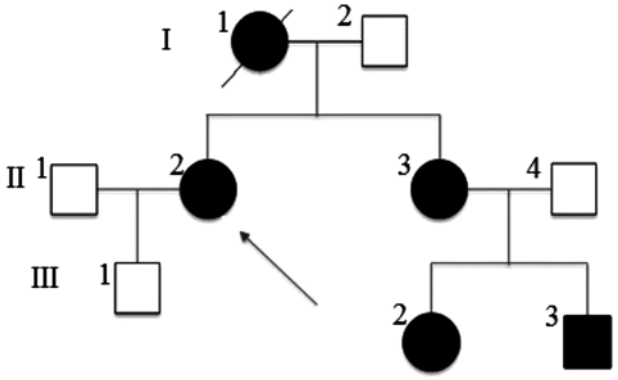

Fig. 1. Family tree

According to the medical history, since infancy, the proband has had relapses of hives on the body and limbs that do not respond to antihistamines and glucocorticoids. For that reason, the patient was repeatedly examined by an allergist and was followed-up with a diagnosis of chronic urticaria. In 2014, the proband turned to a rheumatologist for the first time with complaints of pain and swelling of wrist joints. Inflammation markers were elevated, rheumatoid factor (RF) and anti-cyclic citrullinated peptides (ACCP) were negative. The patient was diagnosed with rheumatoid arthritis and prescribed methotrexate 15 mg which showed a good clinical response, joint syndrome became minimal (DAS28 = 3.08).

In May 2020, the patient discontinued methotrexate due to pregnancy planning. No exacerbation of joint syndrome was recorded during pregnancy and after childbirth. When taking a family history, it was revealed that patient's mother (born in 1966) had the same recurrent hives, sensorineural hearing loss, arthritis, and chronic kidney disease which caused her death at the age of 55. Also, proband's sibling (born in 1989) has manifestations of hives, arthralgia in wrist joints, and episodes of hyperthermia up to 37.5 °C. Sibling's children (boy and girl) were observed by a rheumatologist with juvenile arthritis. After genetic testing, which revealed a pathogenic variant of the *NLRP3* gene, in 2018, their diagnosis was changed to cryopyrin-associated periodic syndrome, Muckle – Wells syndrome. Both children receive canakinumab with a good clinical response. The sibling also underwent a genetic testing in 2019 and the pathogenic variant *chr1:247587529C>T [hg19], NM_004895.4:c.784C>T, P_004886.3:p.(Arg262Ter) (R262X), dbSNP:rs121908150* in the *NLRP3* gene and the pathogenic variant *chr12:6442643C>T [hg19], NM_001065.3:c.362G>A, NP_001056.1:p.(Arg121Gln) (R121Q), HGMD:CM012483, dbSNP:rs4149584* in the *TNFRSF1A* gene were identified (Table 1, 2). According to clinical data and genetic testing results, the diagnosis of Muckle – Wells syndrome was established.

Table 1

Characteristics of the pathogenic variant of the *NLRP3* gene: Arg262Ter, found in the *NLRP3* gene

Parameter	Value
Genomic coordinates [hg19]	chr1:247587529C>T
dbSNP identifier	rs121908150
Transcript	NM_004895.4:c.784C>T
Protein	NP_004886.3:p.(Arg262Ter)
Gene	NP_004886.3:p.(Arg262Ter)
Exon	4/10
Pathogenicity	Pathogenic
Pathogenicity criteria	
PVS1	The nonsense variant of a gene, for which LoF variants are the known cause of pathology
PM2	The variant is absent in the control (or occurs with extremely low frequency). The highest known frequency in the population is 0.0004% (TOPMED).
PM1	The variant is located in an important functional protein domain that does not have known benign changes. According to InterPro Domain, protein NACHT domain is located here.
PP5	Reliable sources indicate the variant pathogenicity. According to CLINVAR, the variant is considered pathogenic (CV000004622.5, RCV000004623.6, RCV000221297.4, RCV001067187.1, RCV001285973.1)

Table 2

Characteristics of the pathogenic variant of the *TNFRSF1A* gene: Arg121Gln, found in the *TNFRSF1A* gene

Parameter	Value
Genomic coordinates [hg19]	chr12:6442643C>T
dbSNP identifier	rs4149584
Transcript	NM_001065.3:c.362G>A
Protein	NP_001056.1:p.(Arg121Gln)

Table 2 (continued)

Parameter	Value
Gene	TNFRSF1A
Exon	4/10
Pathogenicity	Variant of uncertain clinical significance
Pathogenicity criteria	
BS1	The allele frequency is higher than expected for the disease. The highest frequency is 2.7% (population of Northern Sweden).
PM1	The variant is located in an important functional protein domain that does not have known benign changes. According to InterPro Domain, TNFR / NGFR cysteine-rich region is located here.
PP5	Reliable sources indicate the variant pathogenicity. According to HGMD, the variant is considered pathogenic (HGMD: CM012483)

The proband examination revealed the following: erythema on cheeks, hives on the body and limbs. There were vesicular breath sounds in the lungs. The heart sounds were clear and rhythmic. The patient did not feel pain in joints which were also not swollen. As for laboratory tests, ESR was elevated up to 45 ml / h, CRP 49 mg / l, creatinine 76 μmol / l, RF was negative (8 U / ml with the reference value 20 U / ml), ACCP was slightly positive (32 U / ml with the reference value 25 U / ml). Wrist and foot X-ray revealed no joint space narrowing, periarticular osteoporosis or erosive arthritis.

Taking into account that the proband and her relatives have the variant of the *NLRP3* gene with typical manifestations of Muckle – Wells syndrome, Sanger sequencing of all exons of the *TNFRSF1A* and *NLRP3* genes was performed in the proband in October 2021. As a result, pathogenic gene variants previously found in the patient's sibling were revealed in both genes: the pathogenic variant *chr1:247587529C>T [hg19]* in the *NLRP3* gene and the pathogenic variant *chr12:6442643C>T [hg19]* in the *TNFRSF1A* gene (Fig. 2).

Based on the clinical data and the results of molecular genetic testing, the diagnosis of cryopyrin-associated periodic syndrome: Muckle – Wells syndrome was verified. According to ACR / EULAR 2010 criteria, the proband did not match with the diagnosis of rheumatoid arthritis, and joint syndrome was most likely caused by CAPS. Special attention should be paid to the examination of ACCP which was slightly increased in the patient, as its significant increase allows to diagnose rheumatoid arthritis by the ACR / EULAR criteria (symmetric polyarthritis of small wrist joints accompanied by elevated CRP). The combination of AID and rheumatoid arthritis is a rare and difficult to differentiate case. The proband's sibling and mother were invited to the clinic of the Research Institute of Clinical and Experimental Lymphology, branch of the Institute of Cytology and Genetics SB RAS for further examination (Table 3).

Table 3

Clinical manifestations of the family case of Muckle–Wells syndrome

Parameter	Proband, 28 years old	Proband's mother, 54 years old	Sibling, 32 years old	Sibling's son, 11 years old	Sibling's daughter, 9 years old
Hives	+	+	+	–	–
Fever	+	+	+	–	–
Arthritis / arthralgia of small wrist joints	+	+	+	+	+
Conjunctivitis	–	–	+	–	–
Sensorineural hearing loss	–	+	–	–	–
Renal lesion (chronic kidney disease most likely due to amyloidosis)	–	+	–	–	–
Uveitis	–	–	–	+	+
Elevated acute phase reactants (ESR, CRP)	+	+	+	+	+

According to Table 3, all family members had typical clinical manifestations of Muckle – Wells syndrome including fever, recurrent hives, joint syndrome, and elevated inflammation markers. All family members, with the exception of the proband's mother, underwent a molecular genetic testing, which revealed the pathogenic variant of the *NLRP3* gene. A proband's child did not undergo genetic testing due to the absolute absence of any clinical manifestations of the disease. However, it is planned to conduct genetic testing later as the disease is likely to manifest itself not in early childhood.

The proband's mother had the most severe course of the disease with sensorineural hearing loss and chronic kidney disease that possibly caused her death in 2021. The presence of verified Muckle – Wells syn-

drome with clear clinical manifestations and elevated inflammation markers was an indication for the use of genetically engineered biologicals. Also, the presence of a pathogenic variant of the *TNFRFS1A* gene is associated with a high level of TNFα, which may also determine the choice of genetically engineered biologicals. Currently, the patient and her sibling are undergoing safety screening to assess the possibility of prescribing genetically engineered biologicals, including canakinumab.

According to the literature, the severity of Muckle – Wells syndrome can be divided into mild, moderate, and severe[6]. As can be seen in the clinical case described, there are both severe manifestations of the disease among family members (in the proband's mother) and a moderate phenotype. It remains unclear whether the presence of a pathogenic variant of the *TNFRFS1A* gene affects the severity of Muckle – Wells syndrome phenotype. More and more studies are aimed at studying the effect of digenic mutations on the severity of the disease [7]. So, A. Blaschek et al. described the combination of genetic variants of *MEFV* and *TNFRSF1A* genes that led to the onset of multiple sclerosis in childhood [8]. Other authors discussed the digenic inheritance of *MEFV* and *NLRP3* genes or *MEFV* and *TNFRSF1A* genes [9]. We could not find any data in the literature on the combination of genetic variants of *TNFRSF1A* and *NLRP3* genes, but it may determine a more severe course of Muckle – Wells syndrome.

CONCLUSION

This clinical case demonstrates the complexity of differential diagnosis between autoimmune and autoinflammatory diseases. As can be seen, even if a case formally meets the criteria of rheumatoid arthritis and there are clinical manifestations that do not correspond to definite nosological forms, physicians should consider other causes of joint syndrome, hives, fever, etc. So, it is necessary for rheumatologists, clinical geneticists, and molecular diagnosis specialists to cooperate in such cases.

This clinical case represents an example of a rare monogenic disease, the diagnosis of which is highly difficult and impossible without DNA sequencing. The disease severity and the development of severe complications, which are the main cause of patient mortality, require early diagnosis and treatment. Patients should be timely referred to a clinical geneticist in order to identify indications for molecular genetic testing, so that the diagnosis of an autoinflammatory disease is confirmed and proper disease-modifying drug therapy is initiated. Also, testing of a larger number of genes may determine the treatment strategy and the choice of the drug.

REFERENCES

1. Masters S.L., Simon A., Aksentijevich I., Kastner D.L. Horror autoinflammaticus: the molecular pathophysiology of autoinflammatory disease. *Annu. Rev. Immunol.* 2009;27:621–668. DOI: 10.1146/annurev.immunol.25.022106.141627.
2. Kelley N., Jeltema D., Duan Y., He Y. The NLRP3 inflammasome: an overview of mechanisms of activation and regulation. *Int. J. Mol. Sci*. 2019;20(13):3328. DOI: 10.3390/ijms20133328.
3. Welzel T., Kuemmerle-Deschner J.B. Diagnosis and management of the cryopyrin-associated periodic syndromes (CAPS): What do we know today? *J. Clin. Med.* 2021;10(1):128. DOI: 10.3390/jcm10010128.
4. Gattorno M., Hofer M., Federici S., Vanoni F., Bovis F., Aksentijevich I. et al. Classification criteria for autoinflammatory recurrent fevers. *Ann. Rheum. Dis.* 2019;78(8):1025–1032. DOI: 10.1136/annrheumdis-2019-215048/
5. Salugina S.O., Fedorov E.S. Biologic disease-modifying antirheumatic drugs in the treatment of major monogenic autoinflammatory diseases: literature review and clinical observation. *Modern Rheumatology Journal*. 2021;15(6):95–100 (in Russ.). DOI: 10.14412/1996-7012-2021-6-95-100.
6. Ben-Chetrit E., Gattorno M., Gul A., Kastner D.L., Lachmann H.J., Touitou I. et al. Consensus proposal for taxonomy and definition of the autoinflammatory diseases (AIDs): a Delphi study. *Ann. Rheum. Dis*. 2018;77(11):1558–1565. DOI: 10.1136/annrheumdis-2017-212515.
7. Ozyilmaz B., Kirbiyik O., Koc A., Ozdemir T.R., Kaya Ozer O., Kutbay Y.B. et al. Molecular genetic evaluation of NLRP 3, MVK and TNFRSF 1A associated periodic fever syndromes. *Int. J. Immunogenet.* 2019;46(4):232–240. DOI: 10.1111/iji.12431.
8. Blaschek A., Kries R., Lohse P., Huss K., Vill K., Belohradsky B.H. et al. TNFRSF1A and MEFV mutations in childhood onset multiple sclerosis. *Eur. J. Paediatr. Neurol.* 2018;22(1):72–81. DOI: 10.1016/j.ejpn.2017.08.007.
9. Neocleous V., Byrou S., Toumba M., Costi C., Shammas C., Kyriakou C. et al. Evidence of digenic inheritance in autoinflammation-associated genes. *J. Genet.* 2016;95(4):761–6. DOI: 10.1007/s12041-016-0691-5.

Authors' contribution

Kurochkina Yu.D., Korolev M.A., Letyagina E.A. – drafting of the manuscript. Korolev M.A. – final approval of the manuscript for publication. Fishman V.S., Gridina M.M., Valeeva E.S. – carrying out of the genetic study.

Authors' information

Kurochkina Yulia D. – Cand. Sci. (Med.), Rheumatologist, Department of Rheumatology; Researcher, Laboratory for Connective Tissue Pathology, Research Institute of Clinical and Experimental Lymphology – branch of the Institute of Cytology and Genetics SB RAS, Novosibirsk, juli_k@bk.ru, https://orcid.org/0000-0002-7080-777X

Korolev Maxim A. – Cand. Sci. (Med.), Rheumatologist, Head of the Laboratory for Connective Tissue Pathology, Deputy Head of the Research Institute of Clinical and Experimental Lymphology – branch of the Institute of Cytology and Genetics SB RAS, Chief Freelance Rheumatologist of the Ministry of Healthcare of the Novosibirsk Region, Novosibirsk, kormax@bk.ru, https://orcid.org/0 000-0002-4890-0847

Letyagina Elena A. – Cand. Sci. (Med.), Senior Researcher, Laboratory for Connective Tissue Pathology, Head of the Department of Rheumatology, Research Institute of Clinical and Experimental Lymphology – branch of the Institute of Cytology and Genetics SB RAS, Novosibirsk, elena_letyagina@list.ru, https://orcid.org/0000-0002-6275-2924

Fishman Veniamin S. – Cand. Sci. (Biology), Leading Researcher, Head of the Sector of Genomic Mechanisms of Ontogenesis, Institute of Cytology and Genetics SB RAS, Novosibirsk, minja- f@ya.ru, https://orcid.org/0000-0002-5573-3100

Gridina Maria M. – Cand. Sci. (Biology), Senior Researcher, Sector of Genomic Mechanisms of Ontogenesis, Institute of Cytology and Genetics SB RAS, Novosibirsk, gridinam@gmail.com, https://orcid.org/0000-0002-7972-5949

Valeeva Emil S. – Laboratory Assistant, Laboratory for Developmental Genetics, Institute of Cytology and Genetics SB RAS, Novosibirsk, emil@bionet.nsc.ru, https://orcid.org/0000-0003-3480-3963

(✉) **Kurochkina Yulia D.,** juli_k@bk.ru

Received 04.05.2022;
approved after peer review 27.06.2022;
accepted 08.12.2022

УДК 616.831-005.1-02:616.857-06
https://doi.org/10.20538/1682-0363-2023-2-176-181

A clinical case of migrainous stroke

Plotnikov D.M.[1], Alifirova V.M.[1], Mosienko E.S.[2]

[1] *Siberian State Medical University (SSMU)*
2, Moscow Trakt, Tomsk, 634050, Russian Federation

[2] *Tomsk Regional Clinical Hospital*
96, I. Chenykh Str., Tomsk, 634063, Russian Federation

ABSTRACT

Migrainous stroke is a rare combination of frequently occurring diseases; only a few cases have been described in the domestic literature. The complexity of differential diagnosis is due to the fact that at the stage of initial manifestations, these two conditions can mimic each other. Treatment strategy and further prevention for each of these diseases is different, so timely and convincing early diagnosis is crucial. The presented clinical case describes a case of ischemic stroke in a young woman who had been suffering from migraine for a long time, which did not fully meet the criteria for migrainous infarction. The patient was treated at the regional vascular center of the Tomsk Regional Clinical Hospital, there was a positive trend in the neurological status. The catamnesis of the disease was tracked. It was suggested that endothelial dysfunction is the main pathogenetic factor in the formation of an ischemic focus against the background of a protracted migraine attack.

Keywords: migraine, ischemic stroke, migrainous infarction

Conflict of interest. The authors declare the absence of obvious or potential conflicts of interest related to the publication of this article.

Source of financing. The authors state that they received no funding for the study.

Conformity with the principles of ethics. The patient signed an informed consent to the publication of this clinical case.

For citation: Plotnikov D.M., Alifirova V.M., Mosienko E.S. A clinical case of migrainous stroke. *Bulletin of Siberian Medicine.* 2023;22(2):176–181. https://doi.org/10.20538/1682-0363-2023-2-176-181.

Мигренозный инсульт: клиническое наблюдение

Плотников Д.М.[1], Алифирова В.М.[1], Мосиенко Е.С.[2]

[1] *Сибирский государственный медицинский университет (СибГМУ)*
Россия, 634050, г. Томск, Московский тракт, 2

[2] *Томская областная клиническая больница (ТОКБ)*
Россия, 634063, г. Томск, ул. И. Черных, 96

РЕЗЮМЕ

Мигренозный инсульт – это редкое сочетание часто встречающихся заболеваний, в отечественной литературе описаны лишь единичные наблюдения. Сложность дифференциальной диагностики связана с тем,

✉ *Plotnikov Denis M.,* dmarkych@gmail.com

что на этапе начальных проявлений эти два состояния могут имитировать друг друга. Лечебная тактика и дальнейшая профилактика при каждом из этих заболеваний различны, поэтому так важна своевременная и убедительная диагностика на ранних этапах.
В представленном клиническом наблюдении описан случай ишемического инсульта у молодой женщины, длительное время страдающей мигренью, который не вполне соответствовал критериям мигренозного инфаркта. Пациентка лечилась в региональном сосудистом центре Томской областной клинической больницы, отмечена положительная динамика в неврологическом статусе. Отслежен катамнез заболевания. Высказано предположение о том, что эндотелиальная дисфункция – основный патогенетический фактор формирования ишемического очага на фоне затянувшегося мигренозного приступа.

Ключевые слова: мигрень, ишемический инсульт, мигренозный инфаркт

Конфликт интересов. Авторы декларируют отсутствие явных и потенциальных конфликтов интересов, связанных с публикацией настоящей статьи.

Источник финансирования. Авторы заявляют об отсутствии финансирования при проведении исследования.

Соответствие принципам этики. Пациент подписал информированное согласие на участие в исследовании.

Для цитирования: Плотников Д.М., Алифирова В.М., Мосиенко Е.С. Мигренозный инсульт: клиническое наблюдение. *Бюллетень сибирской медицины.* 2023;22(2):176–181. https://doi.org/10.20538/1682-0363-2023-2-176-181.

INTRODUCTION

Migrainous ischemic stroke or migrainous infarction (MI) is a rare disease that occurs in the population with a frequency of 1.4–3.4 / 100,000, which is only 0.2–0.5% of all cases of ischemic strokes [1]. According to the brief version of the International Classification of Headache Disorders (ICHD-3 beta, 2013, revised in 2018), this disease under code 1.4.3 refers to complications of migraine [2]. Each of these diseases separately is quite common in the population [1], however, the study of the epidemiology of their combination is quite difficult. This is explained by the fact that before the introduction of clear diagnostic criteria, the diagnosis of MI was vague. Even after their introduction, the establishment of this diagnosis largely depends on the traditions of the clinic and its technical equipment.

The diagnostic criteria for MI are as follows:

A. Migraine attack meets criteria B and C.

B. It occurs in a patient with migraine with aura and a typical previous attack when one or more aura symptoms last > 60 minutes.

C. Neuroimaging shows the presence of ischemic infarction in the corresponding area of the brain.

D. It does not correspond to another diagnosis largely [2].

In other words, MI can be diagnosed only in case of ischemic stroke without another proven cause in patients suffering from migraine with aura at the time of the attack in case of persistent focal neurological symptoms lasting more than an hour and similar to one or more manifestations of the aura, with manifestations characteristic of ischemia on CT or MRI in the corresponding area of the brain. The influence of the following factors on the incidence of MI was proven: female gender, frequency of attacks, smoking, and oral contraceptives with a high content of estrogen [1, 3]. Strokes in patients with migraine that do not occur during an attack are considered only as an associated disease, and not as MI [2]. In real clinical practice, timely and robust diagnosis of MI is still challenging.

CLINICAL CASE

Female patient F., born in 1969 (50 years old) presented to the Regional Stroke Center (RSC) of the Regional Clinical Hospital on November 27, 2019. She had complaints of tension throbbing headaches (5 points on the Visual Analogue Scale (VAS)) without clear lateralization, nausea, periodic vomiting, awkwardness and left arm numbness. The day before, she was taken to the RSC by an ambulance with complaints of tension throbbing headache (9 points according to the VAS) in the right temporoparietal region, nausea and vomiting, difficulty speaking, which she had for three days. No convincing focal symptoms were found during the neurological exam, computed tomography (CT) of the brain showed no focal changes (Fig. 1).

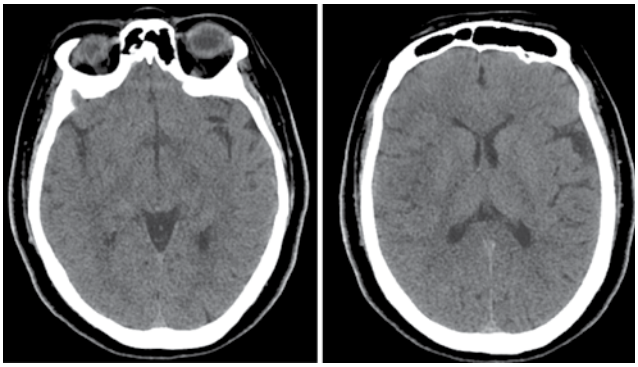

Fig. 1. CT of the brain of patient F. One day before admission to the RSC

With the diagnosis of a protracted migraine attack (simple form), she was referred to a therapeutic hospital on duty. There, the administration of an analgesic (baralgin) eased headache a bit, and the patient was discharged for outpatient follow-up. The next day, moderate diffuse headache and nausea persisted. After sleep, the patient felt left arm numbness and weakness, which was mainly in the hand. Due to her condition, patient's relatives brought her to the RSC again. From the history of present illness, the patient was diagnosed with migraine more than 15 years ago, for 9 years she has been taking sumatriptan (amigrenin), pentalgin, and nise during attacks.

Attacks had the same pattern: a throbbing headache in the right temporoparietal region with nausea and vomiting, a feeling of pressure in the left eye that the patient suffered from 1–2 times a month. The symptoms lasted from several hours to 3 days and could begin spontaneously or be provoked by psycho-emotional stress or odors. When the attack was provoked by odors, the patient had a burning sensation in her nose prior to it. The patient told that drugs, including sumatriptan, did not completely stop the attacks, but sleeping for several hours helped to ease the attack. According to the patient's health history, she suffered from periodic spontaneous vomiting in childhood. The patient had no chronic diseases, except for migraine. She sometimes checked blood pressure, which was not increased. She did not take any medications regularly.

The patient had one pregnancy and one childbirth. Ten years ago, she was operated on for uterine fibroids. For several months, the patient had irregular period. Before admission, she had no period for two months and suspected the onset of menopause. She has not turned not turn to a gynecologist lately and has not taken any hormonal medications. The patient did not smoke. The patient had no family health history of vascular pathology, but her father had similar headaches in his youth.

Upon admission, the neurological examination revealed a slight monoparesis of the left arm; strength was reduced to 4 points, in the hand – up to 3 points, as well as left-sided hemihypesthesia, including the face. A CT scan of the brain on the right in the deep parts of the frontal lobe revealed an ischemic focus 5.0 x 5.0 x 3.5 cm (Fig. 2). With the diagnosis of ischemic stroke in the right middle cerebral artery (unspecified subtype), the patient was hospitalized in the RSC, where an examination was carried out in accordance with the current regulatory documentation (procedure, standard and clinical guidelines).

The results of complete blood count and urinalysis, biochemical blood test, electrolyte test, coagulation test, and lipid profile test were all within the normal range. ECG: sinus rhythm, heart rate 75 beats per minute. The electrical heart axis was horizontal; anterior rotation of the left ventricle around the longitudinal axis of the heart. Daily monitoring of blood pressure revealed no pathology. Echocardiography only revealed minor tricuspid regurgitation. Ultrasound

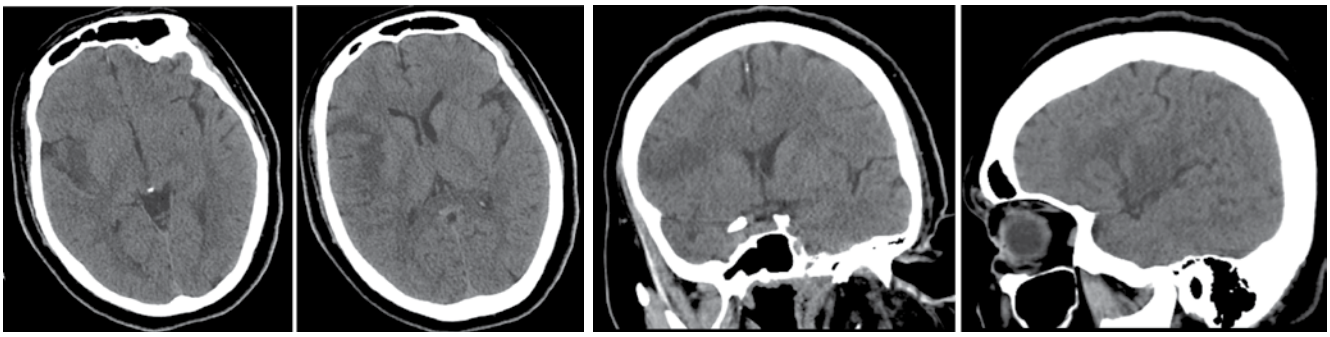

Fig. 2. CT scan of the brain of patient F. at the time of admission to the RSC

examination of extracranial vessels showed asymmetry of the blood flow distribution in the carotid and vertebral arteries. Blood flow deficiency was detected in the right carotid artery and in the left vertebral artery. There was increased peripheral resistance in the system of carotid arteries on the right and vertebral arteries on both sides. Left vertebral artery had a small diameter. Examination of the fundus revealed slight optic disc swelling in both eyes. Retinal angioplasty in both eyes was of hypertonic type. A dynamic CT scan of the brain was conducted 7 days after admission and revealed the focus of subacute ischemia 5.7 x 3.4 x 3.0 cm on the right in the frontal lobe, in the external capsule (Fig. 3). MRI of the brain on day 10 after admission revealed foci of subacute ischemia on the right (increased T2 signal, T2-FLAIR, DWI): a focus of 51 × 11 mm in the subcortical regions of the frontal and parietal lobes and a focus of 11 × 12 mm in the periventricular (medial) regions of the parietal and occipital lobes. Pathology of intracranial vessels was not revealed (Fig. 4). After the examination, the patient was diagnosed with migrainous ischemic stroke in the right middle cerebral artery, left-sided upper mild monoparesis, hemihypesthesia.

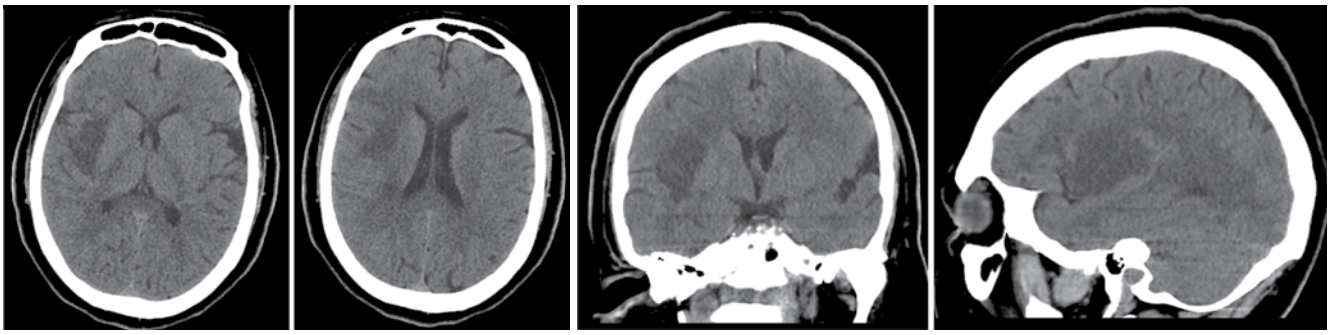

Fig. 3. CT scan of the brain of patient F. 7 days after admission to the RSC

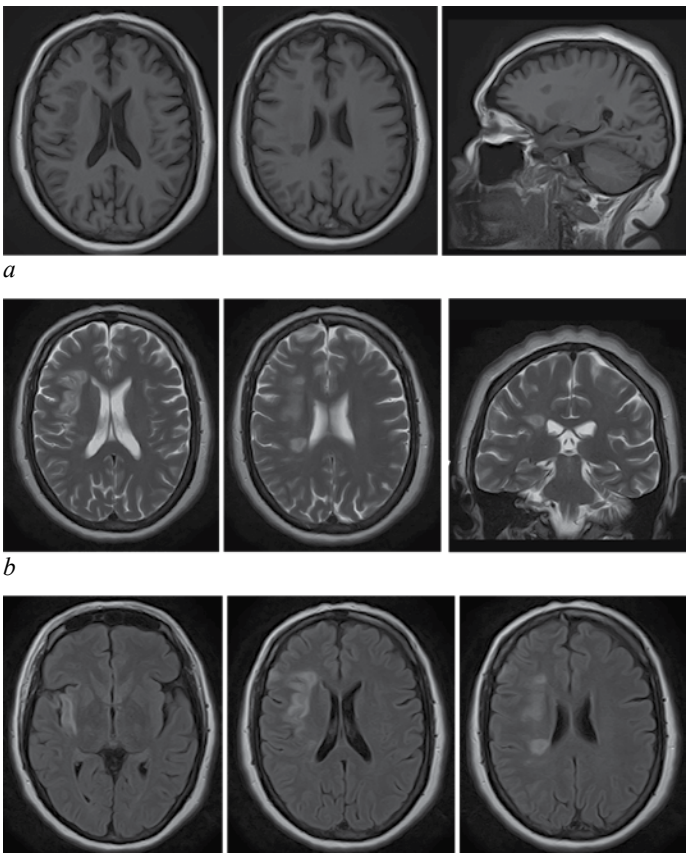

a

b

c

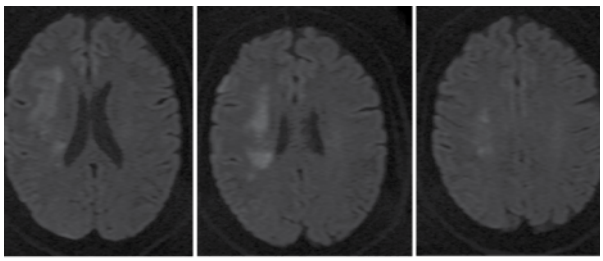

d

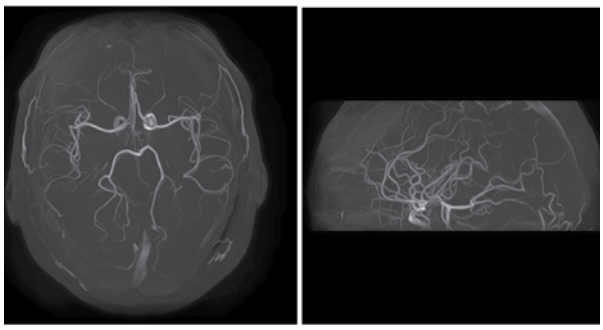

e

Fig. 4. MRI of the brain of patient F. 10 days after admission to the RSC. Modes: *a* – T1, *b* – T2, *c* – FLAIR, *d* – DWI, *e* – 3D-TOF

The patient received the following treatment: infusion therapy, citicoline, sulpiride, amitriptyline, acetylsalicylic acid, exercise therapy, physiotherapy, and occupational therapy, and within a few days, strength was restored in the left hand up to 5 points, but awkwardness when moving fingers and hemihypesthesia remained. After the end of treatment, the patient was discharged with positive dynamics in a satisfactory condition for the second stage of rehabilitation at the rehabilitation center. She was recommended to receive a long course of aspirin cardio 100 mg and amitriptyline, a course of citicoline, and sumatriptan for migraine attacks.

Catamnesis was followed up by phone after 2.5 years. After a course of rehabilitation treatment, the neurologic deficit regressed almost completely: sensory disturbances recovered within 8 months, but some awkwardness in the left hand persisted. She also noted some memory loss, which did not affect daily activity. With the onset of menopause and a change of job (she left a managerial position), headaches changed. They became less frequent, no more than once a month, and less intense (5–6 points according to the VAS). The patient did not need to take sumatriptan, as headaches were usually eased by combined NSAIDs (pentalgin) and glycine. She did not take drugs regularly.

DISCUSSION

The presented clinical case does not fully meet the diagnostic criteria for MI [2]: the patient had no aura. These criteria were formulated based on several meta-analyses, which showed an association of its occurrence with female gender, young age, frequency of attacks, the presence of aura, and the use of oral contraceptives [1, 4–6]. No statistically significant relationship was found between migraine without aura and the risk of ischemic stroke, although such cases were described in both foreign and Russian literature [7]. In addition, it was proven that ischemic foci are more often detected in the posterior circulation and often in the cerebellum [8], while in this case, the ischemic focus was formed in the middle cerebral artery.

According to modern concepts, the activation of serotonergic neurons of the raphe nuclei plays an important role in the onset of a migraine attack. It may initiate a wave of functional inactivation of cortical neurons. This wave of neuronal depolarization, followed by a wave of oligemia, is referred to as “cortical spreading depression”, coincides with the aura phase, and is probably its pathophysiological basis [1].

Endothelial dysfunction may be a common risk factor for both stroke and migraine. The neurovascular effects of endothelial dysfunction ultimately lead to impaired vascular reactivity. Moreover, this is a proven trigger for the activation of procoagulant, proinflammatory, and proliferative mechanisms. In patients with migraine, there is an increase in the activity of key endothelial dysfunction biomarkers: von Willebrand factor, C-reactive protein, nitrate / nitrite levels, as well as circulating endothelial progenitor cells, which correlates with a longer duration of the disease [9]. During a migraine attack, there is an increase in the level of platelet-activating factor, which is released from cerebral endothelial cells, platelets, and mast cells in response to hypoxia possibly induced by cortical spreading depression [10]. It is important that this was found in a study of patients with migraine attacks without aura. Thus, during migraine attacks, a procoagulant state appears which can cause the formation of an ischemic focus.

Probably, in the given clinical case, this was the cause of ischemic stroke in the patient, since its association with a migraine attack is beyond doubt.

CONCLUSION

The above clinical observation describes a case of migrainous stroke in the deep parts of the cerebral hemisphere in the patient suffering from migraine without aura for a long time during a protracted attack of hemicrania. This does not fully meet the criteria for migrainous infarction because they occur more frequently in women suffering from migraine with aura in the posterior circulation. In this case, we do not have any doubts that migraine caused stroke, while endothelial dysfunction with activation of procoagulant systems during a protracted attack of hemicrania most likely caused the formation of an ischemic focus.

REFERENCES

1. Tabeeva G.R. Migraine-associated cerebrovascular disorders. *Medical Council.* 2017;(10):32–35. The international classification of headache; 3rd edition. *Cephalalgia.* 2018;38(1) 1–211 (in Russ.). DOI: 10.1177/0333102417738202.
2. The international classification of headache; 3rd ed. *Cephalalgia.* 2018;38(1):1–211. DOI: 10.1177/0333102417738202.
3. Gryglas A., Smigiel R. Migraine and Stroke: What’s the Link? What to do? *Curr. Neurol. Neurosci. Rep.* 2017;17(3):22. DOI: 10.1007/s11910-017-0729-y.
4. Etminan M., Takkouche B., Isorna F.C., Samii A. Risk of ischaemic stroke in people with migraine: systematic review and meta-analysis of observational studies. *BMJ.* 2005;330(7482):63–65. DOI: 10.1136/bmj.38302.504063.8F.

5. Schurks M., Rist P.M., Bigal M.E., Buring J.E., Lipton R.B., Kurth T. Migraine and cardiovascular disease: systematic review and meta-analysis. *BMJ.* 2009;339:b3914. DOI: 10.1136/bmj.b3914.
6. Spector J.T., Kahn S.R., Jones M.R., Jayakumar M., Dalal D., Nazarian S. Migraine headache and ischemic stroke risk: an updated meta-analysis. *Am. J. Med.* 2010;123(7):612–624. DOI: 10.1016/j.amjmed.2009.12.021.
7. Dubenko O.E., Gavryushin A.Yu., Zubkov A.V., Ekimova S.V., Kovtunov O.V. Complications of migraine. Migraine stroke: analysis of clinical cases. *International Neurological Journal.* 2020;16(6):60–66 (in Russ.). DOI:10.22141/2224-0713.16.6.2020.215142.
8. Kruit M.C., van Buchem M.A., Launer L.J., Terwindt G.M., Ferrari M.D. Migraine is associated with an increased risk of deep white matter lesions, subclinical posterior circulation infarcts and brain iron accumulation: the population-based MRI camera study. *Cephalalgia.* 2010;30(2):129–136. DOI: 10.1111/j.1468-2982.2009.01904.x.
9. Tietjen G.E., Herial N.A., White L., Utley C., Kosmyna J.M., Khuder S.A. Migraine and biomarkers of endothelial activation in young women. *Stroke.* 2009;40(9):2977–2982. DOI: 10.1161/STROKEAHA.109.547901.
10. Sarchielli P., Alberti A., Coppola F., Baldi A., Gallai B., Floridi A. et al. Platelet-activating factor (PAF) in internal jugular venous blood of migraine without aura patients assessed during migraine attacks. *Cephalalgia*. 2004;24(8):623–630. DOI: 10.1111/j.1468-2982.2003.00717.x.

Authors' information

Plotnikov Denis M. – Cand. Sci. (Med.), Associate Professor, Neurology and Neurosurgery Division, Siberian State Medical University, Tomsk, dmarkych@gmail.com, https://orcid.org/0000-0002-5528-1634

Alifirova Valentina M. – Dr. Sci. (Med.), Professor, Head of the Neurology and Neurosurgery Division, Siberian State Medical University; Chief External Expert – Chief Neurologist of the Department of Health of the Tomsk Region, Tomsk, v_alifirova@mail.ru, https://orcid.org/0000-0 0 02-4140-3223

Mosienko Elizaveta S. – Neurologist, Neurological Department, Tomsk Regional Clinical Hospital, Tomsk, mrs.lobanova5@mail.ru

(✉) **Plotnikov Denis M.,** dmarkych@gmail.com

https://doi.org/10.20538/1682-0363-2023-2-182-184

Russian-language open clinical data repository “SibMED Clinical Data Repository”

Kulikov E.S., Fedorova O.S., Tolmachev I.V., Ryazantseva U.V., Vrazhnov D.A., Gubanov A.V., Nesterovich S.V., Shmyrina A.A.

Siberian State Medical University
2, Moscow Trakt, Tomsk, 634050, Russian Federation

ABSTRACT

Global digitalization has become one of the most significant challenges in the field of medicine and healthcare. Rapid development of digital technologies determines a growing demand for constant access to real-time big data. Their use is in need for research and technological projects in the field of artificial intelligence technologies. Siberian State Medical University developed the first Russian-language clinical data repository “SibMed Clinical Data Repository” in Russia (https://dataset.ssmu.ru/). The article describes the structure and functions of the repository as well as features of its potential use.

Keywords: open clinical data repository, open data, medical information systems, digital health, artificial intelligence, machine learning, open science

Conflict of interest. The authors declare the absence of obvious or potential conflicts of interest related to the publication of this article.

Source of financing. The authors state that they received no funding for the study

For citation: Kulikov E.S., Fedorova O.S., Tolmachev I.V., Ryazantseva U.V., Vrazhnov D.A., Gubanov A.V., Nesterovich S.V., Shmyrina A.A. Russian-language open clinical data repository “SibMED Clinical Data Repository”. *Bulletin of Siberian Medicine.* 2023;22(2):176–181. https://doi.org/10.20538/1682-0363-2023-2-176-181.

Русскоязычный репозиторий открытых клинических данных SibMED Data Clinical Repository

Куликов Е.С., Федорова О.С., Толмачев И.В., Рязанцева У.В., Вражнов Д.А., Губанов А.В., Нестерович С.В., Шмырина А.А.

Сибирский государственный медицинский университет
Россия, 634050, г. Томск, Московский тракт, 2

РЕЗЮМЕ

В эпоху глобальной цифровизации отрасли здравоохранения, благодаря развитию медицинских информационных систем, все большую актуальность и значимость приобретают открытые медицинские данные. Их использование востребовано для научных исследований и технологических проектов в сфере искусственного интеллекта. ФГБОУ ВО СибГМУ Минздрава России впервые в России инициировал создание первого

✉ *Fedorova Olga S.,* dmarkych@gmail.com

русскоязычного репозитория клинических данных SibMED Data Clinical Repository (https://dataset.ssmu.ru/). В статье описывается структура, функции репозитория, а также перспективы его использования.

Ключевые слова: репозиторий открытых клинических данных, открытые данные, медицинские информационные системы, цифровые технологии в клинической медицине, искусственный интеллект, машинное обучение, открытая наука

Конфликт интересов. Авторы декларируют отсутствие явных и потенциальных конфликтов интересов, связанных с публикацией настоящей статьи.

Источник финансирования. Авторы заявляют об отсутствии финансирования при проведении исследования.

Для цитирования: Куликов Е.С., Федорова О.С., Толмачев И.В., Рязанцева У.В., Вражнов Д.А., Губанов А.В., Нестерович С.В., Шмырина А.А. Русскоязычный репозиторий открытых клинических данных SibMED Data Clinical Repository . *Бюллетень сибирской медицины.* 2023;22(2):176–181. https://doi.org/10.20538/1682-0363-2023-2-176-181.

Digitalization has become one of the most significant challenges in the field of medicine and healthcare in the XXI century. The introduction of digital solutions in modern clinical practice makes it possible to improve the quality and effectiveness of medical care, reduce healthcare costs, and achieve patient safety. The rapid development of telemedicine and artificial intelligence technologies determine the growing demand for constant access to real-time big data [1, 2].

The Institute for Statistical Studies and Economics of Knowledge of Higher School of Economics, using the iFORA big data analysis system, has identified digital technologies that are the most in demand in medicine and healthcare. Thus, among the leading technologies are open health data / electronic medical records [3]. Big data accumulated in medical databases are actively used for the development of IT technologies [4-6].

One of the large-scale projects that develops such algorithms is the MIMIC-IV open database of clinical data. The database was developed in collaboration with Beth Israel Deaconess Medical Center and the Massachusetts Institute of Technology [7]. Such data are in great demand, however, due to the divergence of health systems in different countries, the use of MIMIC is limited [8].

The development of open health data sources requires formalized algorithms for aggregation and storage of datasets, ensuring information security [9, 10].

Siberian State Medical University developed the first Russian-language clinical data repository "SibMed Clinical Data Repository" (https://dataset.ssmu.ru /). The SibMed Clinical Data Repository project includes the formation of a digital infrastructure for storing and quick access to health data and a training program focused on the work with structured and unstructured biomedical data to solve research and technological problems.

The repository combines datasets of outpatient and inpatient services of multidisciplinary SibMed clinics, contains anonymized health information, and is continuously updated. The data are depersonalized in accordance with the legal requirements.

SibMed Clinical Data Repository is recommended for use both for researchers, specialists in the field of data science, machine learning, and healthcare management, entrepreneurs, and for organizations developing digital solutions in healthcare. The tasks that SibMed Clinical Data Repository solves include: development and testing of new digital products for healthcare and business, data analytics in diagnosis and treatment, implementation of artificial intelligence technologies, development of treatment and diagnostic programs.

The openness of health data within this project will contribute to the creation of new solutions for medicine and healthcare, improve the quality of life of the population, and provide more affordable medical care.

REFERENCES

1. Kong H.J. Managing Unstructured Big Data in Healthcare System. *Healthcare Informatics Research.* 2019;25 (1):1–2. DOI: 10.4258/hir. 2019.25.1.1.
2. Mokhnacheva T., Monogarova Yu., Varakina Zh. Involvement of healthcare organizers in the process of digitalization of healthcare. *Social Aspects of Public Health.* 2023;(1):2–20 (in Russ.). DOI: 10.21045/2071-5021-2023-69-1-11.

3. Grebenyuk A.Yu. Top 10 digital solutions in medicine and healthcare (in Russ.). URL: https://issek.hse.ru/news/691544400.html
4. Karpov O.E., Subbotin S.A., Shishkanov D.V. Using medical data to create medical decision support systems. *Physician and Information Technology.* 2019;(2) (in Russ.).
5. Avetisyan M.S., Egorov K.S., Kokh V.N. et al. Development of an algorithm for searching for clinically homogeneous patients using semi-structured text data of an electronic medical record of cancer patients. *Physician and Information Technology.* 2019;(3) (in Russ.).
6. Gusev A.V., Zingerman B.V., Tyufilin D.S., Zinchenko V.V. Electronic medical records as a source of data from real clinical practice. *MyRWD*. 2022;(2):8–20 (in Russ.).
7. Johnson A.E.W., Bulgarelli L., Shen L. et al. MIMIC-IV, a freely accessible electronic health record dataset. *Sci. Data.* 2023;10(1):1. DOI: 10.1038/s41597-022-01899-x.
8. Giesa N., Heeren P., Klopfenstein S., Flint A., Agha-Mir-Salim L., Poncette A. et al. MIMIC-IV as a clinical data schema. *Stud. Health Technol. Inf.* 2022;294:559–560. DOI: 10.3233/SHTI220522.
9. Zhang J., Symons J., Agapow P., Teo J.T., Paxton C.A., Abdi J. et al. Best practices in the real-world data life cycle. *PLOS Digit. Health*. 2022;1(1). DOI: 10.1371/journal.pdig.0000003.
10. Burov V., Begtin I., Ganeeva E. Working with open data: features of publication and use in the Russian legal field 18.11.2020 [Analytical report]. *Information Culture* (in Russ.). URL: https://www.infoculture.ru/wp-content/uploads/2020/11/OpenDataReview.pdf

Authors' information

Kulikov Evgeniy S. – Dr. Sci. (Med.), Associate Professor, Rector, Siberian State Medical University, Tomsk, kulikov.es@ssmu.ru, https://orcid.org/0000-0002-0088-9204.

Fedorova Olga S. – Dr. Sci. (Med.), Associate Professor, Head of the Intermediate-Level Pediatrics Division, Siberian State Medical University, Tomsk, fedorova.os@ssmu.ru, http://orcid.org/0000-0002-7130-9609.

Tolmachev Ivan V. – Cand. Sci. (Med.), Leading Researcher, Research and Education Laboratory "Bionic Digital Platforms", Siberian State Medical University, Tomsk, ivantolm@mail.ru. http://orcid.org/0000-0002-2888-5539.

Ryazantseva Ulyana V. – Analyst, Scientific Department, Siberian State Medical University, Tomsk, ryazantseva.uv@ssmu.ru, https://orcid.org/0000-0001-9292-3969.

Vrazhnov Denis A. – Researcher, Research and Education Laboratory "Bionic Digital Platforms", Siberian State Medical University, Tomsk, vrazhnov.da@ssmu.ru, https://orcid.org/0000-0002-6915-6156.

Gubanov Alexander V. – Assistant, Research and Education Laboratory "Bionic Digital Platforms", Siberian State Medical University, Tomsk, derzhiabuz@yandex.ru, https://orcid.org/0000-0001-7465-6238.

Nesterovich Sofia V. – Cand. Sci. (Med.), Chief Physician, Clinics of Siberian State Medical University, Tomsk, nesterovich.sv@ssmu.ru, http://orcid.org/0000-0003-2098-2964.

Shmyrina Alexandra A. – Head of the Department of Digital Technologies, Siberian State Medical University, Tomsk, shmyrina.aa@ssmu.ru, http://orcid.org/0009-0002-6549-1608.

(✉) **Fedorova Olga S.,** fedorova.os@ssmu.ru

Received 10.05.2023;
accepted 25.05.2023

ЖУРНАЛ «БЮЛЛЕТЕНЬ СИБИРСКОЙ МЕДИЦИНЫ» ПРЕДСТАВЛЕН НА СЛЕДУЮЩИХ РЕСУРСАХ

unpaywall	Unpaywall – браузерное расширение. Оно находит бесплатные копии научных статей, оригиналы которых находятся под paywall. В открытой базе данных сервиса есть более 31 миллиона научных публикаций
Baidu 学术	Baidu – китайская компания, предоставляющая веб-сервисы, основным из которых является поисковая система с таким же названием – лидер среди китайских поисковых систем
Scilit	Scilit – это всеобъемлющая бесплатная база данных для ученых, использующая новый метод сопоставления данных и индексирования научных материалов. Наши сканеры ежедневно извлекают последние данные из CrossRef и PubMed
CNKI 学术搜索 scholar WORLD OF CNKI CNKI OF WORLD	Регулярно обновляемая коллекция периодических изданий Китая по широкому кругу дисциплин
WIKIDATA	Викиданные – это бесплатная и открытая база знаний, которую могут читать и редактировать как люди, так и машины
SJR SCImago Journal & Country Rank	SCImago Journal & Country Rank – это общедоступный портал, который включает научные показатели журналов и стран, разработанные на основе информации, содержащейся в базе данных Scopus® (Elsevier B.V.). Эти показатели можно использовать для оценки и анализа научных областей.
INTERNET ARCHIVE SCHOLAR	Данный сервис обеспечивает полнотекстовый поиск по всем исследовательским публикациям, заархивированным в различных коллекциях Архива Интернета.
НейроАссистент	НейроАссистент – сервер научного издательства предназначен для авторов, редакторов и рецензентов научных журналов. Сервис позволяет автоматизировать работу с текстами научных статей с помощью искусственного интеллекта

bulletin.ssmu.ru

bulletin.ssmu.ru

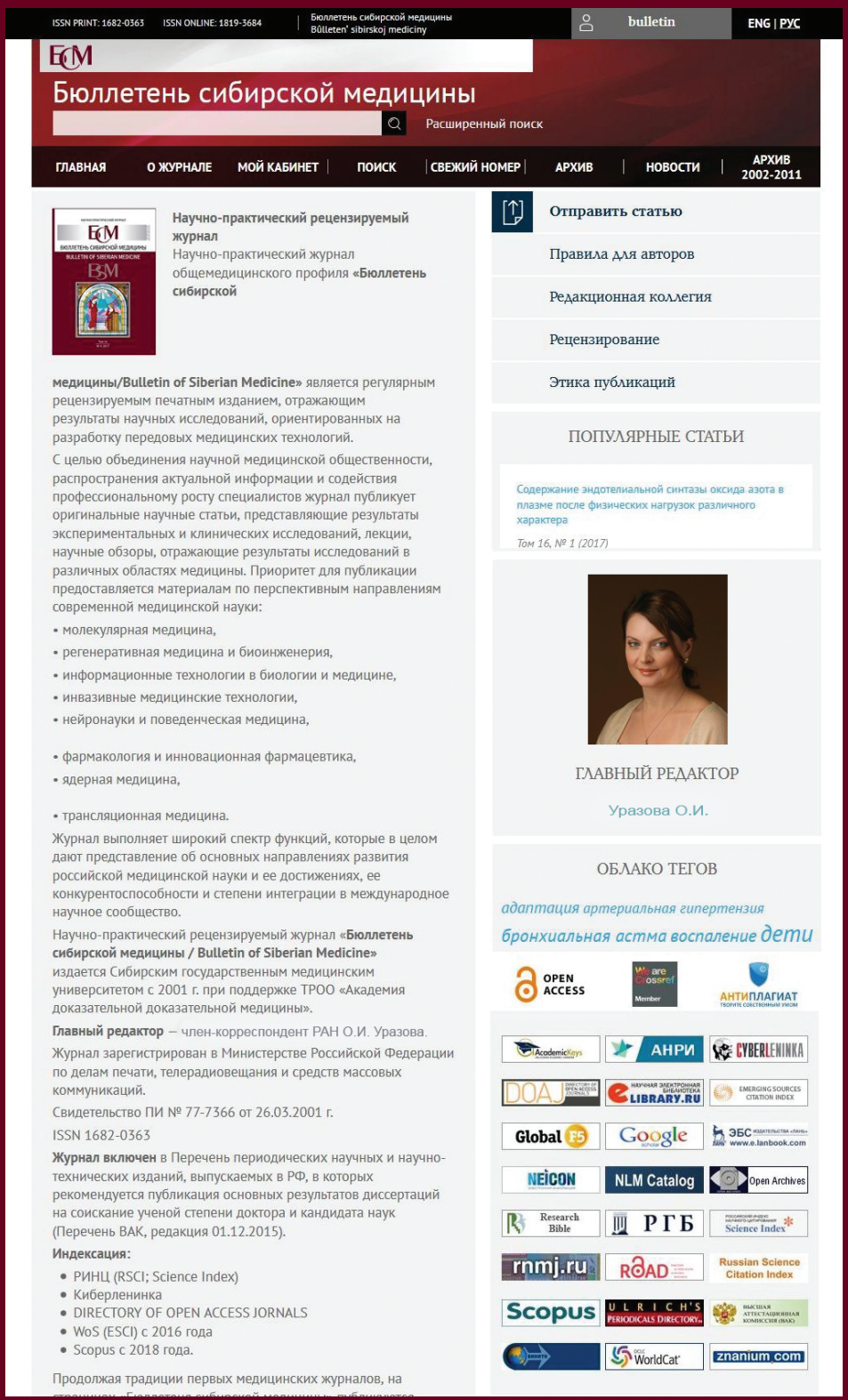

ISSN 1682-0363 (print)
ISSN 1819-3684 (online)
БЮЛЛЕТЕНЬ СИБИРСКОЙ МЕДИЦИНЫ
2023. Т. 22. № 2. 1–184